UNIVERSITÀ DEGLI STUDI DI UDINE
hic sunt futura

www.uniud.it

Corso di dottorato di ricerca in:

Scienze Biomediche e Biotecnologiche

in convenzione con Consiglio Nazionale delle Ricerche

Ciclo 34°

Titolo della tesi

MITOCHONDRIAL MEMORY AT SKELETAL MUSCLE LEVEL

in co-tutela con professor Simone Porcelli

Dottorando
Andrea Pilotto

Supervisore
Bruno Grassi

Co-supervisore
Simone Porcelli

Anno 2022

MITOCHONDRIAL MEMORY AT SKELETAL MUSCLE LEVEL

Andrea Pilotto

Department of Medicine
University of Udine

2022

Mitochondrial Memory at Skeletal Muscle Level

THESIS FOR DOCTORAL DEGREE (Ph.D.)

by

Andrea Pilotto

Principal Supervisor:

Professor Bruno Grassi
Department of Medicine
University of Udine

Co-supervisors:

Professor Simone Porcelli
Institute of Physiology
Department of Molecular Medicine
University of Pavia

LIST OF SCIENTIFIC PAPERS

Pilotto AM, Adami A, Mazzolari R, Brocca L, Crea E, Zuccarelli L, Pellegrino MA, Bottinelli R, Grassi B, Rossiter HB, Porcelli S. Near-infrared spectroscopy estimation of combined skeletal muscle oxidative capacity and O_2 diffusion capacity in humans.
J Physiol. 2022 Sep;600(18):4153-4168. doi: 10.1113/JP283267. Epub 2022 Aug 23. PMID: 35930524; PMCID: PMC9481735.

Baldassarre G, Zuccarelli L, Manferdelli G, Manfredini V, Marzorati M, **Pilotto A**, Porcelli S, Rasica L, Šimunič B, Pišot R, Narici M, Grassi B.
Decrease in work rate in order to keep a constant heart rate: biomarker of exercise intolerance following a 10-day bed rest.
J Appl Physiol (1985). 2022 Jun 1;132(6):1569-1579. doi: 10.1152/japplphysiol.00052.2022. Epub 2022 May 5. PMID: 35511721.

Zuccarelli L, Baldassarre G, Magnesa B, Degano C, Comelli M, Gasparini M, Manferdelli G, Marzorati M, Mavelli I, **Pilotto A**, Porcelli S, Rasica L, Šimunič B, Pišot R, Narici M, Grassi B.
Peripheral impairments of oxidative metabolism after a 10-day bed rest are upstream of mitochondrial respiration.
J Physiol. 2021 Nov;599(21):4813-4829. doi: 10.1113/JP281800. Epub 2021 Sep 28. PMID: 34505290; PMCID: PMC9293208.

Bertozzi F, Porcelli S, Marzorati M, **Pilotto AM**, Galli M, Sforza C, Zago M.
Whole-body kinematics during a simulated sprint in flat-water kayakers.
Eur J Sport Sci. 2022 Jun;22(6):817-825. doi: 10.1080/17461391.2021.1930190. Epub 2021 Jun 13. PMID: 33980124.

Pilotto AM, Rasica L, Scalise G, Annoni S, La Torre A, Marzorati M, Porcelli S.
New On-Water Test for the Assessment of Blood Lactate Response to Exercise in Elite Kayakers.
Med Sci Sports Exerc. 2019 Dec;51(12):2595-2602. doi: 10.1249/MSS.0000000000002077. PMID: 31246717.

ABSTRACT

Mitochondria are key components of skeletal muscles as they provide the energy required for almost all cellular activities. Different forms of exercise training have been associated with mitochondrial adaptations, such as increased mitochondrial content and function, and enhanced mitochondrial biogenesis, as well as improved endurance performance. High-intensity interval training and sprint interval training have been demonstrated to be the most effective training modalities to induce mitochondrial adaptations. However, surprisingly, greater changes in mitochondrial content and biogenesis were also observed after repeated resistance training interventions separated by prolonged detraining. This mechanism, defined muscle memory, has been well established for hypertrophy and skeletal muscle growth in response to resistance training and it has been related to the retention of acquired myonuclei or epigenetic modifications. Thereby, even mitochondrial adaptations might be influenced by muscle memory, but it remains to be explored whether repeated endurance training interventions can rely on the same mechanism. Therefore, the overarching aim of the present thesis was to investigate the potential presence of mitochondrial memory in response to repeated high-intensity endurance training interventions. An experimental design composed of two periods of 8 weeks of interval training interspersed by 3 months of detraining was conducted on murine model and humans. In mice, maximal running velocity (Vmax) by graded exercise test (GXT) on a rodent treadmill. In addition, biomarkers of mitochondrial biogenesis and content, and fusion-fission mitochondrial key factors were analyzed on gastrocnemius muscle by western Blot. Results revealed that endurance performance improved to a greater extent after retraining than training. This functional adaptation was supported by a larger mitochondrial content resulting from a more pronounced mitochondrial biogenesis response after retraining. Mitochondrial dynamics were shifted mainly towards fusion, suggesting larger and more elongated mitochondria and finally, the retraining period elicited increased mitophagic flux, which, associated with a smaller increment in the amount of respiratory chain complexes, suggests an improvement in clearance of damaged mitochondria in order to ensure healthier mitochondria and more efficient respiratory function. In humans, maximal aerobic capacity and peak power output were measured and muscle sample from *vastus lateralis* was used for mitochondrial respiration and epigenetic analysis. Mitochondrial function resulted in a greater improvement after high intensity aerobic stimulus when previous exposure to an identical stimulus has been occurred separated by long-term period of stimulus cessation. The underlying mechanism could reside in epigenetic modifications induced by interval training which led to DNA hypomethylation. Two memory profiles were highlighted at epigenetic level characterized by retention of hypomethylation even during the prolonged detraining period and involving differentially

methylated regions related with genes implicated in skeletal muscle metabolic pathways. Overall, these studies provided evidence for a skeletal muscle memory mechanism, specifically at mitochondrial level, elicited by high-intensity aerobic training that affects muscle aerobic phenotype initiating at the epigenetic level and extends upstream to affect mitochondrial function and endurance performance.

In addition, a methodological project was carried out to assess a novel *in vivo* approach to estimate muscle oxygen diffusion capacity (DmO_2). DmO_2 is indeed a crucial component in the O_2 cascade during exercise along with the microvascular-to-intramyocyte PO_2 difference. Non-invasive methods to determine DmO_2 in humans are currently unavailable. Muscle oxygen uptake ($m\dot{V}O_2$) recovery rate constant (k), measured by near-infrared spectroscopy (NIRS) in well-oxygenated muscle, is associated with muscle oxidative capacity *in vivo*. We reasoned that k would be limited by DmO_2 when muscle oxygenation is low providing an experimental condition to estimate DmO_2 using specific arterial occlusions NIRS protocol. We measured $m\dot{V}O_2$ k in limiting and not-limiting O_2 conditions and muscle sample were obtained from biopsy to measure *ex vivo* muscle oxidative capacity by respirometry and capillary-to-fiber ratio. Results showed that $m\dot{V}O_2$ k reflects muscle oxidative capacity only in well-oxygenated muscle. Δk, the difference in k between well- and poorly-oxygenated muscle, was associated with capillary-to-fiber ratio, a mediator of DmO_2. Assessment of muscle k and Δk using NIRS provides a non-invasive window on both muscle oxidative capacity and O_2 diffusing capacity.

TABLE OF CONTENTS

ABSTRACT ..... **I**
TABLE OF CONTENTS ..... **III**
LISTS OF FIGURES ..... **V**
LISTS OF TABLES ..... **VII**
LISTS OF ABBREVIATIONS ..... **VIII**
INTRODUCTION **1**
MITOCHONDRIA **4**
Mitochondrial Morphology **4**
Intrafibrillar and Peripheral Mitochondria **5**
Mitochondrial Function **9**
Mitochondrial Biogenesis **10**
Mitochondrial Dynamics **13**
PHYSIOLOGICAL RESPONSES TO EXERCISE AND TRAINING ADAPTATIONS **17**
Physiological bases of cardio-respiratory and metabolic responses to exercise **18**
Training modalities and Interval Training **20**
Training Adaptations **21**
Molecular bases of Skeletal Muscle Adaptations **23**
Contraction-Induced Signal Transduction Pathways in Skeletal Muscle **26**
Mitochondrial Adaptations and Endurance Training **30**
Summary **32**
DETRAINING **33**
Cardiovascular and metabolic responses to detraining **33**
Skeletal muscle responses to detraining **36**
Summary **37**
EPIGENETIC **38**
Histone modifications **39**
Micro RNA **39**
DNA methylation **40**
MUSCLE MEMORY **50**
Resistance muscle memory **50**
Epi-memory to resistance training **52**
Aerobic muscle memory **53**
Epi-memory to endurance training **56**
Summary **57**

AIMS **58**

STUDY 1 ..... **60**

Near-infrared spectroscopy estimation of combined skeletal muscle oxidative capacity and O_2 diffusion capacity in humans **61**

ABSTRACT 61

INTRODUCTION 62

MATERIALS AND METHODS 64

RESULTS 71

DISCUSSION 76

CONCLUSIONS 80

STUDY 2 ..... **81**

Two repeated interventions of high-intensity interval training induce different functional and molecular adaptations of skeletal muscle in mice **82**

ABSTRACT 82

INTRODUCTION 83

MATERIALS AND METHODS 85

RESULTS 92

DISCUSSION 100

CONCLUSION 103

STUDY 3 ..... **105**

Human skeletal muscle possesses an epigenetic memory of high intensity interval training affecting mitochondrial function **106**

ABSTRACT 106

INTRODUCTION 107

MATERIALS AND METHODS 110

RESULTS 125

DISCUSSION 147

CONCLUSIONS 153

DISCUSSION **154**

CONCLUSION **158**

REFERENCES **161**

LIST OF FIGURES

Figure 1. Muscle contraction……3

Figure 2. Skeletal muscle mitochondria……...8

Figure 3. Mitochondrial energy metabolism……10

Figure 4. Wagner diagram analysis of training-induced perfusive and diffusive adaptations to endurance training…….…….23

Figure 5. The Molecular Basis of Adaptation to Exercise……25

Figure 1 (Study 1). Study design and muscle recovery rate constant (*k*) protocol by NIRS……65

Figure 2 (Study 1). Representative tissue saturation index (TSI) responses during repeated arterial occlusions of the quadriceps following moderate exercise in LOW and HIGH conditions……...….68

Figure 3 (Study 1). Individual test-retest reliability of muscle oxidative capacity by NIRS……..73

Figure 4 (Study 1). Muscle capillarization from two participants……...74

Figure 5 (Study 1). Association between *in vivo* (NIRS) and *ex vivo* (biospy) estimation of (A-B) skeletal muscle OXPHOS capacity and (C) skeletal muscle capillary density……..75

Figure 1 (Study 2). Schematic diagram of the experimental design……85

Figure 2 (Study 2). Maximal velocity from graded exercise test……..92

Figure 3 (Study 2). Mitochondrial content biomarkers……93

Figure 4 (Study 2). Mitochondrial biogenesis biomarkers……...94

Figure 5 (Study 2). Mitochondrial fusion dynamics biomarkers……95

Figure 6 (Study 2). Mitochondrial fission dynamics biomarkers……96

Figure 7 (Study 2). Mitophagy biomarkers……...97

Figure 8 (Study 2). Mitochondrial respiratory chain complexes……99

Figure 1 (Study 3). Peak values of parameters from incremental exercise before and after exposure to two identical interval training interventions separated by 3-month of detraining……...127

Figure 2 (Study 3). Oxygen uptake kinetics during constant work-rate exercise before and after exposure to two identical interval training interventions separated by 3-month of detraining……...128

Figure 3 (Study 3). Muscle oxidative capacity by NIRS before and after exposure to two identical interval training interventions separated by 3-month of detraining……..129

Figure 4 (Study 3). Mass-specific mitochondrial respiration capacity before and after exposure to two identical interval training interventions separated by 3-month of detraining……..131

Figure 5 (Study 3). Mitochondrial respiration capacity changes in training and retraining intervention……132

Figure 6 (Study 3). Mitochondrial respiration capacity changes in training and retraining intervention……133

Figure 7 (Study 3). Mitochondrial content biomarkers across repeated interval training interventions separated by 3-month of detraining……134

Figure 8 (Study 3). Mitochondrial biogenesis biomarkers across repeated interval training interventions separated by 3-month of detraining……135

Figure 9 (Study 3). Mitochondrial dynamics biomarkers across repeated interval training interventions separated by 3-month of detraining……136

Figure 10 (Study 3). Mitophagy biomarkers across repeated interval training interventions separated by 3-month of detraining……...…137

Figure 11 (Study 3). Electron transport chain complexes protein expression across repeated interval training interventions separated by 3-month of detraining……138

Figure 12 (Study 3). Myosin heavy chain isoform composition across repeated interval training interventions separated by 3-month of detraining……..139

Figure 13 (Study 3). Capillarization across repeated interval training interventions separated by 3-month of detraining……...140

Figure 14 (Study 3). Differentially methylated CpG sites frequency following training, detraining and retraining compared to baseline……...……142

Figure 15 (Study 3). MAPK signaling KEGG pathway……..143

Figure 16 (Study 3). Venn diagram overlapping DMPs in training, detraining and retraining compared to baseline……...……....144

Figure 17 (Study 3). SOM profiling depicting the temporal regulation of DMPs over the time-course of baseline, training, detraining and retraining…..……...……..145

Figure 18 (Study 3). Individual DMPs in Signature 2 identified by self-organising map (SOM)……146

LIST OF TABLES

Table 1 (Study 1). Mitochondrial O_2 flux in permeabilized muscle fibers……74
Table 1 (Study 2). List of primary and secondary antibodies used……89
Table 1 (Study 3). Participant characteristics at the initial screening test……110
Table 2 (Study 3). List of primary and secondary antibodies used……119
Table 3 (Study 3). Parameters from incremental exercise at the limit of tolerance……126
Table 4 (Study 3). Mass-specific mitochondrial respiration capacity……130

LIST OF ABBREVIATIONS

Δk	difference between k_{HIGH} and k_{LOW}
$[La]_b$	blood lactate concentration
ΔpH	electrochemical proton gradient
ΔΨm	mitochondrial membrane potential
1RM	maximal repetition
5hmC	5-hydroxymethyl cytosine
5mC	5-methylcytosine
A	amplitude
ACC	acetyl-CoA carboxylase
acetyl-CoA	acetyl coenzyme A
ACh	acetylcholine
ADP	adenosine diphosphate
AMP	adenosine monophosphate
AMPK	5′-adenosine-monophosphate-activated protein kinase
ANT	adenine nucleotide translocase
ATF2	activating transcription factor 2
ATG7	autophagy-related gene 7
ATP	adenosine triphosphate
ATP5A	ATP synthase F1 subunit alpha
BCD	bisulfite converted DNA
BSA	bovine serum albumin
C	cytosine nucleotide
C:F	capillary-to-fiber ratio
Ca^{2+}	calcium ions
CaMK	Ca^{2+}-calmodulin-dependent protein kinase
cAMP	cyclic-AMP
CaO_2	arterial O_2 concentrations
CD	capillary density
CH_3	methyl group
CI	complex I or NADH-Q reductase
CII	complex II or succinate-coenzyme Q reductase
CIII	complex III or cytochrome reductase
CIV	complex IV or cytochrome c oxidase
CV	complex V or ATP synthase
$CI+II_E$	maximal electron transport system capacity through CI+II
$CI+II_P$	maximal oxidative phosphorylation capacity through CI+II
CII_E	maximal electron transport system capacity through CII
CI_L	leak respiration through CI
CI_P	maximal oxidative phosphorylation capacity through CI
CO_2	carbon dioxide
CoA	coenzyme A
COX	cytochrome c oxidase

CpG	5’-cytosine-phospate-guanine-3’ dinucleotide pairing
CREB	cyclic AMP-responsive element binding
CS	citrate synthase
CSA	cross-sectional area
CV	coefficient of variation
CvO_2	venous O_2 concentrations
CWR	constant work-rate
DAB	diaminobenzidine
DmO_2	muscle oxygen diffusion capacity
DMP	differentially methylated position
DMR	differentially methylated region
DMSO	dimethyl sulfoxide
DNA	deoxyribonucleic acid
DNMT	DNA methyltransferase
Drp1	dynamin-related protein 1
$Drp1_{Ser616}$	phosphorylated state Drp1 at serine 616
$Drp1_{Ser637}$	phosphorylated state Drp1 at serine 637
E	maximal ETS capacity
EIF2	eukaryotic initiation factor 2
ERRs	estrogen-related receptors
ETC	electron transport chain
F0	ATP synthase proton translocation complex
$FADH_2$	flavin adenine dinucleotide
FAT	fatty acid transporter
FCCP	carbonyl cyanide-p trifluoromethoxyphenylhydrazone
Fis1	fission protein 1
FTa	type IIa fast-twitch
FTb	type IIx fast-twitch
G	guanine nucleotide
GET	gas exchange threshold
GLUT	glucose transporter
GO	gene ontology
GTP	guanosine triphosphate
GXT	graded exercise test
H^+	hydrogen ion
H_2O	water
H_2O_2	hydrogen peroxide
Hb	hemoglobin
HDAC	histone deacetylase
HIF	hypoxia-inducible factor
HIIT	high-intensity interval training
HK	hexokinase
HR	heart rate
Hsp70	heat shock protein 70

HV-HIIT	high-volume HIIT
ICC	intraclass correlation coefficient
IFM	intrafibrillar mitochondria
IL-6	interleukine 6
IMM	inner mitochondrial membrane
IMS	mitochondrial intermembrane space
IT	interval training
k	recovery rate constant
L	leak respiration
LDH	lactate dehydrogenase
LKB1	liver kinase B1
LV-HIIT	low-volume HIIT
MAPK	mitogen-activated protein kinase
Mb	myoglobin
MEF2	myocyte-specific enhancer factors 2
Mff	mitochondrial fission factor
Mfn1	mitofusin 1
Mfn2	mitofusin 2
MHC	myosin heavy chain
MICT	moderate intensity continuous training
MiD49	mitochondrial dynamics proteins of 49 kDa
MiD51	mitochondrial dynamics proteins of 51 kDa
miRNA	micro-RNA
mRNA	messenger RNA
MTCO1	cytochrome c oxidase subunit 1
mtDNA	mitochondrial DNA
mTOR	mammalian target of rapamycin
mTORC	mammalian target of rapamycin complex
$m\dot{V}O_2$	muscle oxygen uptake
Na^+	sodium ion
NAD	nicotinamide adenine dinucleotide
NADH	nicotinamide adenine dinucleotide
nDNA	nuclear DNA
NDUFB8	NADH:ubiquinone oxidoreductase subunit B8
NFAT	nuclear factor of activated T-cells
NIRS	near-infrared spectroscopy
NR4A1	nuclear receptor subfamily 4A1
NRF	nuclear respiratory factor
O/N	overnight
O_2	oxygen
OCT	optimal cutting temperature compound
OMM	outer mitochondrial membrane
OPA1	optic atrophy 1
OXPHOS	oxidative phosphorylation

p	phosphate group
P	maximal oxidative phosphorylation
pACC	phosphorylated ACC
PAM	presequence translocase-associated motor
pAMPK	phosphorylated AMPK
PCA	principle component analysis
PCr	phosphocreatine
PDK4	pyruvate dehydrogenase kinase 4
PGC-1α	peroxisome proliferator receptor-γ co-activator-1α
Pi	inorganic phosphate
$PimO_2$	O_2 partial pressure in intramyocyte
PINK1	PTEN-induced putative kinase protein 1
PKA	protein kinase A
PM	peripherally located mitochondria
$PmvO_2$	O_2 partial pressure in microvasculature
PN	physiological normalization
PPAR	peroxisome proliferator activated receptor
PVDF	polyvinylidene fluoride
$\dot{Q}$	cardiac output
r	pearson coefficient
RBC	red blood cells
RER	respiratory exchange ratio
RNA	ribonucleic acid
ROS	reactive oxygen species
RPE	rating of perceived exertion
RT	room temperature
SAM	sorting and assembly machinery
SD	standard deviation
SDHB	succinate dehydrogenase complex iron-sulfur subunit B
SIRT	sirtuin
Sirtuin	silent mating type information regulation 2 homolog protein
SIT	sprint interval training
SNP	single-nucleotide polymorphisms
SOM	self organizing map
SQSTM1	sequestosome-1
SR	sarcoplasmic reticulum
SRS	spatially-resolved spectroscopy
ST	slow-twitch oxidative fibers
SV	stroke volume
TCA	tricarboxylic acid cycle
TD	time delay
TET	ten-eleven translocation enzyme
TFAM	mitochondrial transcription factor A
TFB1M	mitochondrial transcription factor B1

TFB2M	mitochondrial transcription factor B2
TIM22	carrier translocase of the inner membrane
TIM23	presequence translocase of the inner membrane
TNF-α	tumor necrosis factor α
TOM	translocase of the outer membrane
TSI	tissue saturation index
UCP	uncoupling protein
UQCRC2	ubiquinol-cytochrome c reductase core protein 2
UTR	untranslated region
VDAC	voltage-dependent anion channel
V_E	pulmonary ventilation
VEGF	vascular endothelial growth factor
Vmax	maximal running velocity
$\dot{V}O_2$	oxygen uptake
W	power output
Δ[deoxy(Hb+Mb)]	deoxy-(hemoglobin+myoglobin)
Δ[diff(Hb+Mb)]	hemoglobin and myoglobin difference
Δ[oxy(Hb+Mb)	oxy-(hemoglobin+myoglobin)
Δ[tot(Hb+Mb)]	total hemoglobin and myoglobin
τ	time constant

CHAPTER 1

INTRODUCTION

The human body is an amazing, fascinating and impressive organism. As well explained in Lieberman's famous paper published in Nature under the title "Born to Run" and as asserted by evolutionary biology research on the basic structure of the human anatomy, physiology and genome, the human body is designed for movement. Body movements rely on the highly coordinated mechanical interaction between skeletal muscles and bones which is able to generate force and create relative movement of body segments for posture, locomotion and limb motion, under the control of the nervous system. Skeletal muscle is one of the most dynamic and plastic tissues of the human body. It constitutes about 40-50% of the total body weight and, in addition to movement, is even responsible for bioenergetic homeostasis and energy balance through a large variety of physiological processes. Apart from contractile fibers, skeletal muscle is composed of various integrated tissues, including blood vessels, nerve fibers, and connective tissue. Human skeletal muscle fibers are large, multinucleated cells highly organized in bundles called fascicles. In humans, there are three different types of fibers: type I, type IIA and type IIX. The type I fibers are slow-twitch oxidative fibers (ST) that can produce relatively low amount of force over a long period of time. Type IIA and IIX are fast-twitch (FTa and FTb respectively), more glycolytic fibers that have higher force production but low resistance to fatigue. Within each muscle fiber, myofibrils are the main contractile structures. Each myofibril is organized in repeated functional units, called sarcomeres, composed of thin actin filaments and thick myosin filaments. The process of muscular fiber shortening occurs through the insertion of thin actin filaments in between the thick ones of myosin. The whole process is regulated by troponin and tropomyosin regulatory proteins and it requires the release of calcium ions from sarcoplasmatic reticulum and adenosine triphosphate (ATP) molecules, being the latter kept approximately constant and continuously replaced from a complex bioenergetic system.

Muscle Bioenergetics. According to the first law of thermodynamics which states energy can neither be created nor destroyed, but it can only change form, skeletal muscle fibers have the capability to convert chemical energy from biological fuels into mechanical energy of muscle contraction. Indeed, sarcomeres changes in length relies on the interactions between the thin actin and the thick myosin filaments through the hydrolysis of ATP molecules, where the energy is released from the breakdown of ATP into ADP (adenosine diphosphate) and free phosphate. The availability of ATP, the main energy molecule of the human organism, is critical for the skeletal muscle contractile activity but it is also fundamental for other cellular functions. In addition to myofilament cross-bridge cycle (myosin ATPase), ATP is required for the activity of key enzymes involved in membrane excitability (Na^+/K^+ ATPase) and sarcoplasmic reticulum calcium handling (Ca^{2+} ATPase). Therefore, ATP needs to be continuously replaced. During short-lasting and intense exercise, the main source of

energy for contraction comes directly from the hydrolysis of the ATP available within the muscle cells. Simultaneously, chemical energy from creatine phosphate is transferred to form new ATP molecules. For work performed up to 90 seconds, anaerobic or glycolytic metabolism provides most of the ATP needed. Over longer periods of work, ATP is mainly produced by mitochondria through aerobic metabolism. ATP production into the mitochondria is the final step of a complex biochemical process defined oxidative phosphorylation which occurs in presence of oxygen molecules and nutrient substrates that are supplied by means of the capillary network interspersed in the fiber bundles. Therefore, mitochondrion represents an essential component for the skeletal muscle to ensure an adequate energetic supply.

Figure 1. Muscle contraction

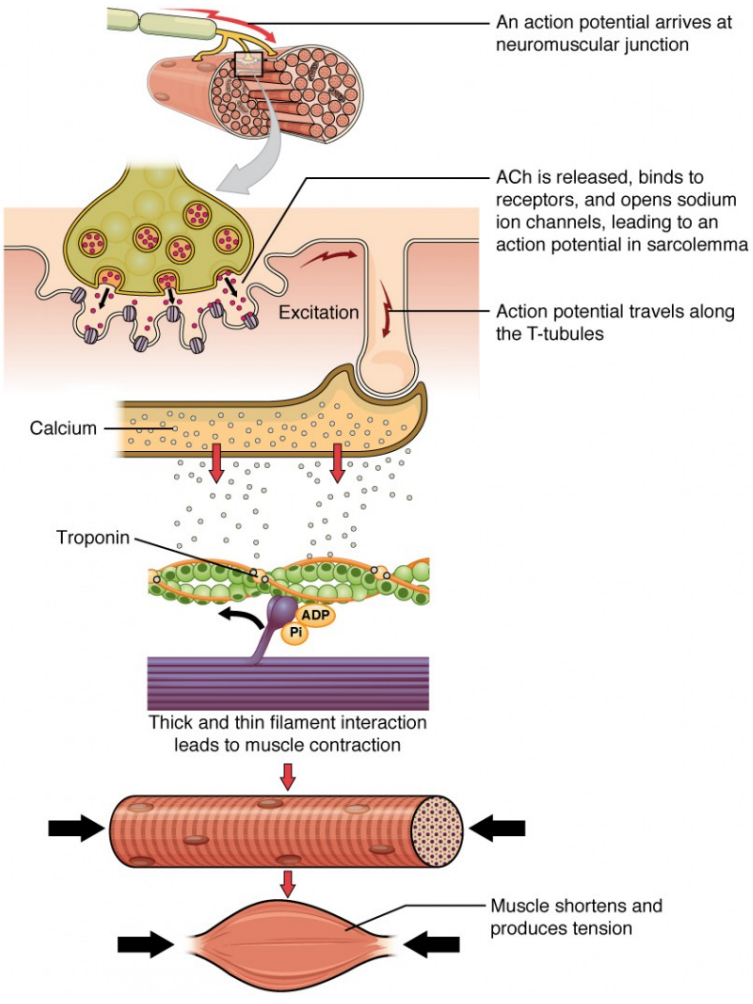

The sequence of events that result in the contraction of an individual muscle fiber begins with a signal, the neurotransmitter acetylcholine (ACh), from the motor neuron innervating that fiber. The local membrane of the fiber will depolarize as positively charged sodium ions (Na^+) enter, triggering an action potential that spreads to the rest of the membrane will depolarize, including the T-tubules. This triggers the release of calcium ions (Ca^{2+}) from storage in the sarcoplasmic reticulum (SR). The Ca^{2+} then initiates contraction, which is sustained by ATP. As long as Ca^{2+} ions remain in the sarcoplasm to bound to troponin, which keeps the actin-binding sites "unshielded," and as long as ATP is available to drive the cross-bridge cycling and the pulling of actin strands by myosin, the muscle fiber will continue to shorten to an anatomical limit. ADP, adenosine diphosphate; Pi, inorganic phosphate.

MITOCHONDRIA

Mitochondria are unique organelles that provide the energy required for almost all cellular activities, hence the moniker "powerhouse of cell". However, mitochondria play many other important functions in addition to energy production, including the generation of reactive oxygen species, redox molecules and metabolites, regulation of cell signaling and cell death, and macromolecule biosynthesis. (Vyas *et al.*, 2016). In skeletal muscles these organelles exhibit remarkable plasticity by adapting to altered metabolic demands. Biogenesis and fusion processes give rise to newly formed mitochondria which join with neighboring organelles to increase their capacity for ATP synthesis, metabolites sharing and calcium handling (Spinelli & Haigis, 2018). Conversely, where mitochondria are overabundant and/or dysfunctional, processes of mitochondrial fission and clearance (mitophagy) occur to restore metabolic homeostasis and maintain mitochondrial health within cells (Hood *et al.*, 2019; Memme *et al.*, 2021) . At all times, these opposing processes are in a state of constant change, depending on cellular metabolic demand, to regulate and promote optimal mitochondrial stability. When the cell is subjected to conditions that disrupt metabolic homeostasis, such as exercise or aging, this balance in mitochondrial regulation can shift toward either increased biogenesis and fusion, or fission and mitophagy (Mishra & Chan, 2016).

Mitochondrial Morphology

Mitochondria range generally from 0.5 to 1.0 μm in diameter (Henze & Martin, 2003) and are divided in four compartments: the outer mitochondrial membrane (OMM), the intermembrane space (IMS), the inner mitochondrial membrane (IMM) and the mitochondrial matrix. The OMM is relatively porous consisting of a phospholipid bilayer housing protein structures called porins that make it permeable to small molecules (<10 kDa), including ADP and ATP, making the intermembrane space chemically similar to the cytosol (Hood *et al.*, 2019). Conversely, the IMM is composed of a protein-rich, highly-folded complex structure permeable only to oxygen, water, and carbon dioxide. The wrinkled shape of the IMM generates several folds and pockets, called "cristae", which increase the surface area maximizing the ability to house the four electron transport chain (ETC) complexes and the ATP synthase enzyme required for oxidative phosphorylation. The matrix is the region within the IMM and hosts mitochondrial DNA (mtDNA), ribosomes, and tricarboxylic acid cycle enzymes. The latter is the final common pathway for the oxidation of fuel molecules such as carbohydrates, lipids and amino acids. Among the matrix, inner and outer membranes, and intermembrane space compartments, mitochondria consist of approximately 1200 proteins (Calvo *et al.*, 2016). Most of these proteins are transcribed from the nuclear genome, translated in the cytosol, and introduced into existing mitochondria. Only 13 mitochondrial proteins are transcribed within the organelle itself,

from the small and circular mtDNA. However, the translation of this small portion of protein complements leads to the formation of protein subunits for all ETC complexes, except for Complex II, which are vital for normal respiratory function and can lead to mitochondrial and whole organ dysfunction when absent (Cogswell *et al.*, 1993; Oliveira & Hood, 2019).

Intrafibrillar and Peripheral Mitochondria

In skeletal muscles, different populations of mitochondria have been classified based on their cellular locations. The 80-90% of the total mitochondrial population is located between the myofibrils, called intrafibrillar mitochondria (IFM), while the remaining 10-20% is found in the intracellular space between the sarcolemma and myofibrils, region that gives them the definition of peripherally located mitochondria (PM) (Vincent *et al.*, 2019). These two populations exhibit distinct characters in their structural, biochemical and functional properties. (Palmer *et al.*, 1977, 1985; Cogswell *et al.*, 1993; Takahashi & Hood, 1996; Rothstein *et al.*, 2005; Adhihetty *et al.*, 2005; Ferreira *et al.*, 2010; Picard *et al.*, 2013*b*; Glancy *et al.*, 2014, 2015, 2018; Vincent *et al.*, 2019; Willingham *et al.*, 2021). IFM are characterized by a complex and elongated shape (Hoppeler *et al.*, 1973; Picard *et al.*, 2013*b*, 2013*a*, 2015; Glancy *et al.*, 2015; Bleck *et al.*, 2018) consisting of branches extending within the intermyofibrillar spaces and wrapping around the I-band of the sarcomere (Hoppeler *et al.*, 1973; Picard *et al.*, 2013*b*, 2013*a*, 2015; Bleck *et al.*, 2018; Vincent *et al.*, 2019). These entrenched mitochondria reveal a morphology with a high surface area to volume ratio which facilitates the rapid diffusion of ATP molecules from the mitochondria to the ATPase enzyme within the myofibrillar region (Picard *et al.*, 2013*b*; Vincent *et al.*, 2019). The PM subgroup is essentially composed of "paravascular" or "paranuclear" mitochondria, which are specifically clustered together within the intracellular space surrounding embedded capillaries and nuclei (Romanul, 1964, 1965; Gauthier & Padykula, 1966; Hoppeler *et al.*, 1973; Rothstein *et al.*, 2005; Glancy *et al.*, 2014, 2015). PM are mitochondria characterized by a globular shape, which appear larger and less branched than IFM (Bakeeva *et al.*, 1978; Picard *et al.*, 2013*b*, 2013*a*; Glancy *et al.*, 2015; Bleck *et al.*, 2018; Vincent *et al.*, 2019). Most of their volume is dedicated to cristae and matrix, providing greater structure capacity for energy conversion (Willingham *et al.*, 2021). Mitochondria directly interact with other mitochondria. PM extend into the intermyofibrillar space and form direct connections with the IFM, generating a network that function to distribute energy to the whole muscle cell (Bakeeva *et al.*, 1978; Picard *et al.*, 2013*b*, 2013*a*, 2015; Glancy *et al.*, 2015, 2018; Bleck *et al.*, 2018; Vincent *et al.*, 2019). Mitochondria work together and their connection across the subcellular region function as an "effective mechanism of energy transport" (Bakeeva *et al.*, 1978). Indeed, mitochondria contact sites appear as electron-dense junctions (Picard *et al.*, 2015; Glancy *et al.*, 2015), where adjacent outer

membranes are in direct contact (<1 nm separation) (Bakeeva *et al.*, 1978; Picard *et al.*, 2013*b*, 2013*a*, 2015; Glancy *et al.*, 2015; Bleck *et al.*, 2018; Vincent *et al.*, 2019) and often exhibit trans-mitochondrial alignment of cristae (Picard *et al.*, 2015)**.** Mitochondrial connectivity and overall network configuration are fiber-type specific, such that oxidative and glycolytic muscles have grid and perpendicular orientations, respectively (Bleck *et al.*, 2018; Willingham *et al.*, 2019).

Each subfraction differs not only in structure but also in biochemical composition as well as differing capacities for mitochondrial respiration (Krieger *et al.*, 1980; Cogswell *et al.*, 1993; Adhihetty *et al.*, 2003). Intrafibrillar subgroup possesses greater oxidative enzyme activities (Palmer *et al.*, 1977, 1985; Cogswell *et al.*, 1993) and respiration rates (Joffe *et al.*, 1983; Takahashi & Hood, 1996; Ljubicic *et al.*, 2004) compared with peripherally located mitochondria. PM turn out to be less efficient in ATP production resulting in a more conspicuous proton leak (Willingham *et al.*, 2021). This lower rate of oxygen consumption directly results in a higher rate of reactive oxygen species (ROS) production. These molecules are useful when produced in moderation, acting as signaling agents which can affect the transcription of nuclear genes encoding for mitochondrial proteins (Petrosillo *et al.*, 2003; Heusch *et al.*, 2010; Barbieri & Sestili, 2012; Frank *et al.*, 2012). However, when produced in excess, an overabundance of electrons is released resulting in the oxidation of proteins, lipids and mtDNA, leading to functional defects (Lowell & Spiegelman, 2000). ROS production is highest when mitochondrial membrane potential is highest (Korshunov *et al.*, 1997; Cadenas *et al.*, 2002; Brand *et al.*, 2002), as occurs in PM under conditions of proton leak and absence of ADP. Conversely, in the presence of ADP, as in IFM characterized by a greater oxidative capacity, proton flux occurs through the ATPase enzyme, thereby reducing membrane potential and diverting electron flux to cytochrome c oxidase, and less to the formation of ROS (Cogswell *et al.*, 1993; Adhihetty *et al.*, 2003; Ljubicic *et al.*, 2004). Such difference in function between the two subgroups is well evident also in their protein composition. Indeed, the membrane potential-generating element (complex IV) and the complex responsible for ATP production (complex V) preferentially localize to PM and IFM, respectively. Specifically, the peripheral localization of Complex IV suggests that PM subgroups may support the IFM by generating proton-motive force and distributing it across the IFM network where it is used to synthesize ATP (Willingham *et al.*, 2021). Moreover, the elevated cytochrome c content in IFM is an important consequence of the enhanced oxidative phosphorylation, but also represents a larger pool of proapoptotic protein compared with PM (Adhihetty *et al.*, 2003). These findings suggest that mitochondrial subpopulations differ remarkably in their capacity to handle oxidative stress, such as IFM may be more sensitive to apoptotic stimuli while PM may be more prone to producing ROS and proton leak (Willingham *et al.*, 2021). It has been also

demonstrated that ATP production is closely related to the rate of protein import encoded by the nuclear genome within the mitochondria. The difference between the two mitochondria subgroups reveals a more pronounced translocation process in IFM subfraction (Takahashi & Hood, 1996).

In summary, in the overall network connection, peripherally located mitochondria likely serve to provide ATP for membrane transport functions and to provide energy support for nuclear processes such as transcription and nuclear molecule transport. Instead, intrafibrillar mitochondria support the energy requirements of actin-myosin interactions and contractile activity (Cogswell *et al.*, 1993; Ferreira *et al.*, 2010; Picard *et al.*, 2013*b*; Oliveira & Hood, 2019). This biochemical and functional diversity is reflected in different responses to common signaling events. In general, PM appear to adapt earlier and to a greater extent than their IFM counterparts in response to cellular perturbations. The increase in PM as a result of training for example, is about twice the response of IFM (Hoppeler, 1986). Indeed, PM are more sensitive to changes in energetic demand than IFM, by showing that the relative exercise-induced increases in mitochondrial volume are more significant in PM compared to IFM (Hoppeler *et al.*, 1973; Müller, 1976; Hoppeler, 1986; Koves *et al.*, 2005).

Figure 2. Skeletal muscle mitochondria

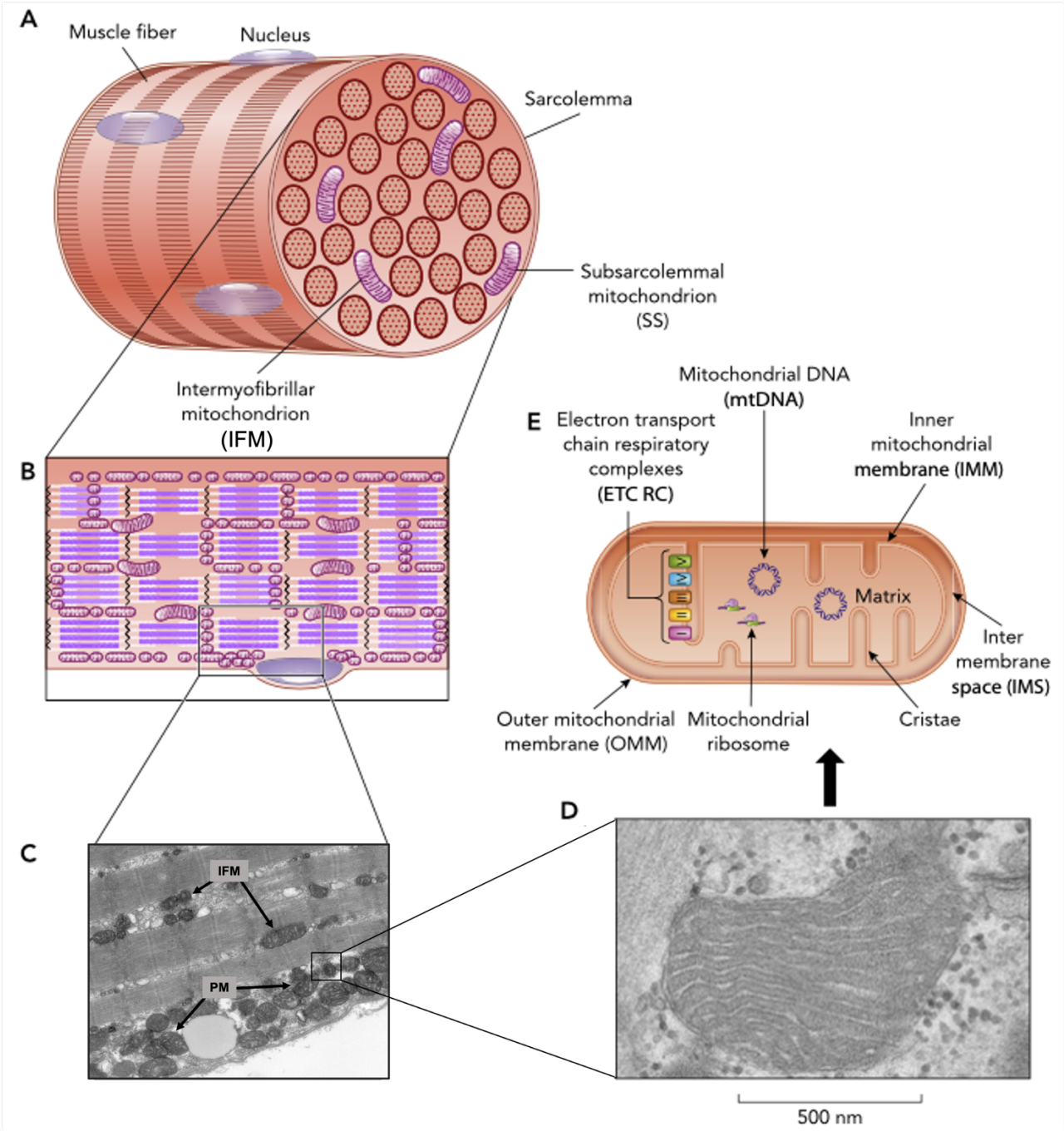

A) structure of a skeletal muscle fiber. Two sub-populations of mitochondria can be found: peripherally located mitochondria (PM) and intrafibrillar mitochondria (IFM). B) illustration of a skeletal muscle fiber. Mitochondria create a reticulum that connects PM and IFM mitochondria for optimal energy distribution. C) transmission electron microscopy longitudinal image from a human skeletal muscle biopsy showing the PM and IFM. D) image of a mitochondrion. High-resolution imaging allows visualization of the densely packed cristae within a mitochondrion. E) image of mitochondrial structure and composition. The mitochondrial DNA (mtDNA) and the mitochondrial ribosomes are found in the matrix. The electron transport chain respiratory complexes are located on the IMM and, for the most part, in the cristae. (Edited from Bishop *et al.*, 2019).

Mitochondrial Function

As previously described, mitochondria constitute the structural and functional elementary components of cell respiration whose main role is the production of ATP, the energy currency of living organisms. ATP production occurs during reactions of the tricarboxylic acid cycle, located within the matrix, and through the electron transport system (ETS), located along the inner mitochondrial membrane (IMM). The tricarboxylic acid cycle (TCA), also known as citric acid cycle or the Krebs' cycle, is the major metabolic pathway responsible for energy production in cells, providing the greater part of the reduced coenzymes that will be oxidized by the ETS to produce ATP. TCA provides a pathway for the oxidation to carbon dioxide and water of the acetate portion of acetyl coenzyme A (acetyl-CoA) arising from the oxidative decarboxylation of pyruvate (the end product of glycolysis), the β-oxidation of fatty acids, the metabolism of ethanol, ketone bodies, and a number of amino acids. Each molecule of acetyl-CoA entering the TCA cycle yields 12 ATP molecules. Acetyl-CoA undergoes oxidation to CO_2 in eight steps, and the energy produced from these reactions is stored in the reduced forms of nicotinamide adenine dinucleotide (NADH) and flavin adenine dinucleotide ($FADH_2$), that are then oxidized in the ETS terminating in ATP synthesis (Sousa *et al.*, 2018). The ETS comprises 5 multi-polypeptide complexes (complexes I to V) embedded in the inner mitochondrial membrane that receive electrons from oxidation of NADH and $FADH_2$. During the early phase, electrons are transferred along complexes I to IV of the ETS, with O_2 serving as the final acceptor to complex IV (Baar, 2014). Aerobic respiration is the reduction of molecular oxygen by electron transfer coupled with electrochemical proton translocation across the inner mitochondrial membrane. Throughout this process, protons are pumped out of the matrix into the intermembrane space, producing electrochemical proton gradient (ΔpH) and mitochondrial membrane potential ($\Delta\Psi m$) that provides the driving force enabling Complex V to generate ATP by phosphorylation of adenosine diphosphate (ADP). The combination of the latter two processes is described as oxidative phosphorylation (OXPHOS), where the catabolic reaction sequence of oxygen consumption is electrochemically coupled to the energy conversion in the phosphorylation of ADP into ATP (Mitchell, 1961, 1966; Doerrier *et al.*, 2018) (**Figure 3**).

Figure 3. Mitochondrial energy metabolism

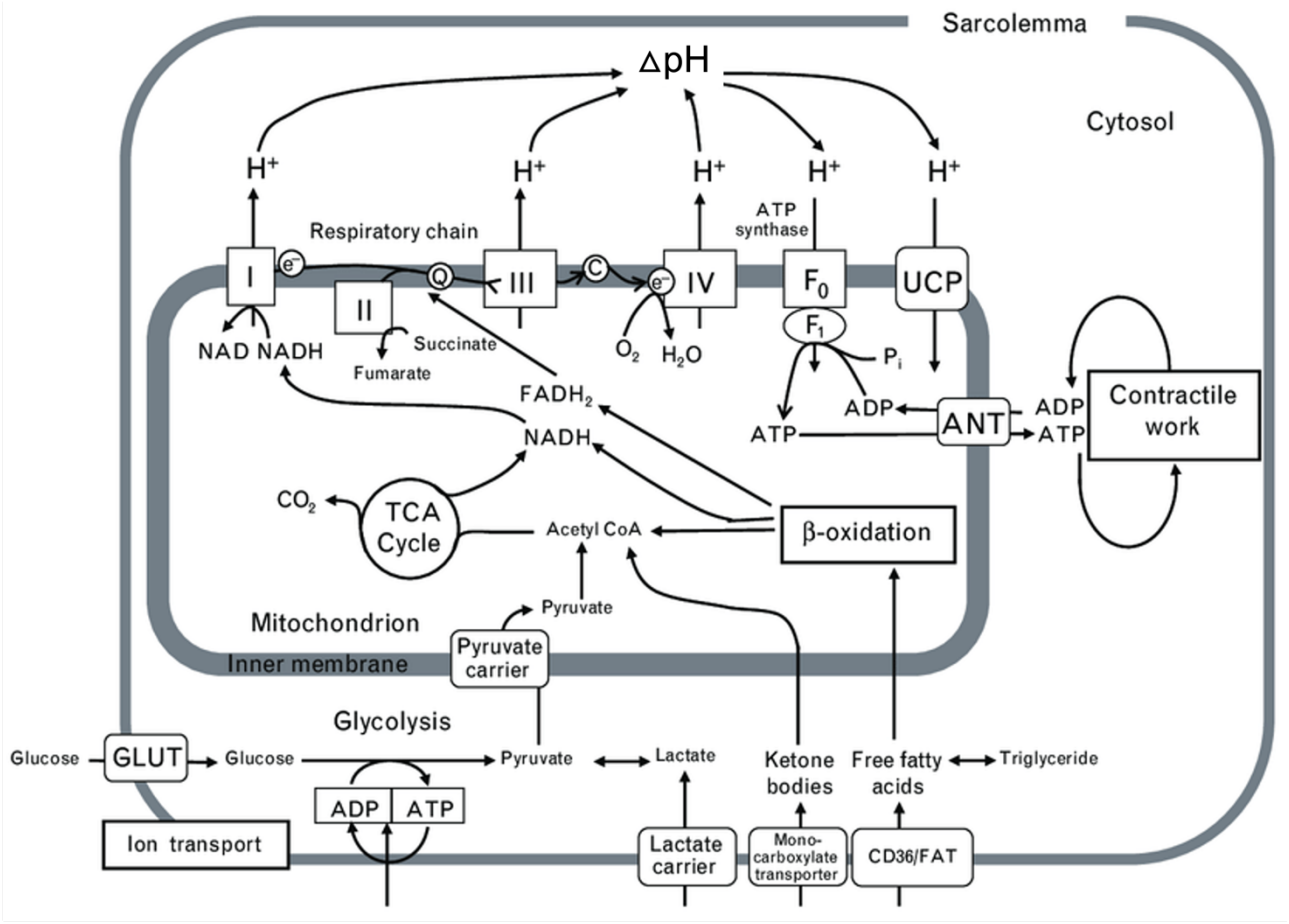

Fatty acid β-oxidation and the Krebs cycle produce nicotinamide adenine dinucleotide, reduced (NADH) and flavin adenine dinucleotide, reduced ($FADH_2$), which are oxidized by complexes I and II, respectively, of the electron transport chain, which comprises four complexes: I–IV. Electrons are transferred through the chain to the final acceptor, namely oxygen (O_2). The free energy from electron transfer is used to pump hydrogen (H^+) out of the mitochondria and generate an electrochemical gradient (ΔpH) across the inner mitochondrial membrane. This gradient is the driving force for ATP synthesis via the ATP synthase (complex V). Alternatively, H^+ can enter the mitochondria by a mechanism not coupled to ATP synthesis, via the uncoupling proteins (UCPs), which results in the dissipation of energy. F_0, ATP synthase proton translocation complex; F_1, ATP synthase catalytic complex; ANT, adenine nucleotide translocase; CoA, coenzyme A; FAT, fatty acid transporter; GLUT, glucose transporter; NAD, nicotinamide adenine dinucleotide; TCA, tricarboxylic acid. (Edited from Murray *et al.*, 2007)

Mitochondrial Biogenesis

Mitochondrial biogenesis can be defined as the growth and division of preexisting mitochondria. Indeed, although the term biogenesis is sometimes used in reference to the formation of new mitochondria, it is important to note that the mitochondrial reticulum is not made ex-novo or de-novo (Henze & Martin, 2003). Specifically, the mitochondrial reticulum recruits new proteins to the organelle resulting in continuous remodeling of the mitochondrial network (Ryan & Hoogenraad,

2007). So, more accurately, mitochondrial biogenesis refers to the generation of new mitochondrial components resulting not only in changes in the number of mitochondria, but also in the size and mass of these organelles. The process of mitochondrial biogenesis requires the co-ordination and co-expression of both nuclear and mitochondrial genomes for assembly and expansion of the reticulum. Since 95% of the genes necessary for biogenesis are encoded by the nuclear genome (Goffart & Wiesner, 2003; Chan, 2006; Baker *et al.*, 2007), there is a mechanism of identification, import, and proper assembly of proteins to ensure the appropriate remodeling of mitochondrial function and composition (Pfanner & Geissler, 2001; Wiedemann *et al.*, 2004; Jornayvaz & Shulman, 2010). The mRNAs are translated into the cytosol after activation of the nuclear genome into precursor proteins. With the assistance of molecular chaperones, mitochondrial precursor proteins are transferred to the universal entry gate of mitochondria, the TOM complex (translocase of the outer membrane), where the pathways diverge according to the protein destination in one of the mitochondrial sub-compartments. The precursors of outer membrane proteins are integrated into the outer membrane by SAM complex (sorting and assembly machinery). Preproteins destined for the matrix are transferred via TIM23 complex (presequence translocase of the inner membrane). TIM23 forms a channel across the inner membrane and cooperates with the matrix heat shock protein 70 (Hsp70) of PAM (presequence translocase-associated motor), which drives the completion of protein transport into the matrix. TIM22 complex (carrier translocase of the inner membrane) inserts precursors of carrier proteins into the inner membrane. Thus, the import machinery regulating the transport of nuclear encoded precursor proteins into the organelle are an integral part of mitochondrial biogenesis (Irrcher *et al.*, 2003). However, expression of genes promoting mitochondrial biogenesis is predominantly controlled by the global principles of gene regulation, which are the transcription initiation and interaction on DNA-binding sites at gene promoter level (Goffart & Wiesner, 2003). Therefore, transcription factors and transcriptional co-activators represent critical regulators of mitochondrial biogenesis. As noted, several transcription factors are implicated in regulating the expression of genes involved in mitochondrial biogenesis (Adhihetty *et al.*, 2003). No single transcription factor has been identified as solely responsible for coordinating mitochondrial gene expression, but a variety of candidates appear to be relevant to mitochondrial biogenesis.

PGC-1α. Peroxisome proliferator receptor-γ co-activator-1α (PGC-1α) has been identified as the master regulator of mitochondrial biogenesis in skeletal muscle due to its prominent co-activation of multiple mitochondrial transcription factors (Hood *et al.*, 2006). Indeed, PGC-1α is the core member of a transcriptional co-activator family that has been raised as a potential key regulatory factor in the mitochondrial biogenesis mechanism (Adhihetty *et al.*, 2003). This mechanism includes nuclear

respiratory factors (NRF-1, NRF-2) which are nuclear-encoded transcription factors targeted by PGC-1α (Wu *et al.*, 1999). NRF-1 and NRF-2 are implicated in the transcriptional control of several nuclear-encoded respiratory genes and are also involved in driving the expression of the mitochondrial transcription factor A (TFAM), a key component in mitochondrial DNA replication and transcription (Clayton, 2000; Scarpulla, 2002, 2006; Kanki *et al.*, 2004). Therefore, the PGC-1α–NRF-1/2–TFAM pathway is composed of PGC-1α binding and co-activation of the transcriptional function of NRF-1/2 at the level of the TFAM promoter resulting in increased TFAM expression and, thereby, enhanced ability for protein complexes assembly within mitochondria (Wu *et al.*, 1999; Scarpulla, 2006). In addition to TFAM, the PGC-1α–NRF-1/2 pathway also up-regulates the mitochondrial transcription factors B1 (TFB1M) and B2 (TFB2M), essential components of the mtDNA transcriptional machinery (Gleyzer *et al.*, 2005). There is also evidence to support a direct role played by PGC-1α in the activation of mitochondrial gene transcription. Specifically, it has been demonstrated the presence of PGC-1α within mitochondria where it interacts directly with TFAM to regulate mtDNA expression (Aquilano *et al.*, 2010; Smith *et al.*, 2013). In addition to mitochondrial replication through NRFs and TFAM, PGC-1α also interacts with and co-activates other transcription factors such as the peroxisome proliferator activated receptors (PPARs), regulators of lipid homeostasis via expression of genes involved in mitochondrial fatty acid oxidation (Vega *et al.*, 2000; Oberkofler *et al.*, 2002; Lee *et al.*, 2003), estrogen-related receptors (ERRs), which target vast gene networks involved in all aspects of energy homoeostasis, including fat and glucose metabolism, as well as mitochondrial biogenesis and function (Calvo *et al.*, 2008), and early growth response gene-1 (Egr-1) which promotes transcription of the electron transport chain protein cytochrome C oxidase (COX) (Freyssenet *et al.*, 2004). Several transcription regulators have been shown to enhance the expression of PGC-1α in skeletal muscle. In particular, activation of ubiquitous transcription factors, such as cyclic AMP-responsive element binding protein (CREB), activating transcription factor 2 (ATF2) and myocyte-specific enhancer factors 2 (MEF2), localized in the PGC-1 promoter region is involved in the upregulation of PGC-1α expression (Goffart & Wiesner, 2003; Handschin *et al.*, 2003; Akimoto *et al.*, 2005; Ljubicic *et al.*, 2010). Together, these findings provide evidence supporting the ability of PGC-1α to coordinate mitochondrial biogenesis via activation of transcription factors that increase the expression of both nuclear- and mitochondrial-encoded genes, as well as its direct implication in mtDNA transcription and replication.

Mitochondrial Dynamics

To maintain their health and function, mitochondria undergo a variety of dynamic behaviors. The main dynamic activities are: 1) fusion, (the union of two organelles into a single mitochondrion by fusing their outer and inner membranes; 2) fission, the fragmentation of the tubular mitochondria network into small organelles; 3) mitophagy, targeted destruction by means of the autophagy pathway;(Mishra & Chan, 2016; Gan *et al.*, 2018; Hood *et al.*, 2019; Memme *et al.*, 2021). On the surface, these morphological processes appear mechanistically distinct from the biochemical and metabolic processes occurring within the organelle; however, given the characteristic plasticity of these organelles, mitochondrial dynamics result to be an adaptive mechanism involved in responding to altered metabolic demands. Through process of fusion, mitochondria join neighboring organelles to increase their ability to synthesize ATP, share metabolites and Ca^{2+} handling (Spinelli & Haigis, 2018). Conversely, where mitochondria are overabundant and/or dysfunctional, mitochondrial fission and clearance (mitophagy) processes take place to restore metabolic homeostasis and preserve mitochondrial health in cells (Hood *et al.*, 2019). These opposing processes are constantly in a state of flux, depending on the metabolic necessities of the tissue, to calibrate and promote an optimal mitochondrial pool. When the cell is exposed to conditions that perturb metabolic homeostasis, such as exercise or advancing age, this balance in mitochondrial regulation may shift toward increased synthesis and fusion, or fission and mitophagy, respectively (Mishra & Chan, 2016).

Fusion. Mitochondrial fusion is a mechanism occurring to expand the organelle network that is mediated by the activity of three major GTPases of the dynamic family: Mitofusin 1 (Mfn1), Mfn2, and Optic Atrophy 1 (OPA1) (Chan, 2012; Labbé *et al.*, 2014; Gan *et al.*, 2018). Given that mitochondria possess a double membrane, mitochondrial fusion is a two-step procedure requiring fusion of the outer-membrane followed by fusion of the inner-membrane. Mfn1 and Mfn2 are proteins that facilitate outer-membrane fusion, whereas OPA1 is a multiple isoform protein which mediates inner-membrane fusion (Mishra & Chan, 2016; Memme *et al.*, 2021).

Energetic states in cells are generally associated with specific mitochondrial morphologies. Elevated OXPHOS activity correlates with mitochondrial elongation and is consistent with the notion that elongated mitochondrial networks are a more efficient source of oxidative energy production, capable of distributing energy over prolonged periods (Amchenkova *et al.*, 1988; Skulachev, 2001; Willingham *et al.*, 2021). This association between morphological and metabolic components illustrates how important the fusion process is for OXPHOS activity, including the regulation of mtDNA levels. Indeed, the absence or removal of both Mitofusins and OPA1, inducing a complete loss of mitochondrial fusion, results in a dramatic decrease in mtDNA content, membrane potential,

and reduced respiratory chain function (Chen *et al.*, 2005, 2010). Other metabolic mechanisms are also regulated by these proteins: Mfn2 is responsible for maintaining stable coenzyme Q levels (Mourier *et al.*, 2015), and OPA1 maintains the structure of mitochondrial cristae and is critical for the assembly of the respiratory chain supercomplex (Cogliati *et al.*, 2013). Vice versa, important metabolic condition sensors modulate the fusion machinery. Oxidative stress promotes binding between mitofusins of two separate mitochondria leading to organelle tethering and enhanced outer-membrane fusion (Shutt *et al.*, 2012). Increased OXPHOS activity and elevated ATP levels stimulate mitochondrial fusion to induce elongation through OPA1 activation, leading to more interconnected network (Mishra *et al.*, 2014). In contrast, metabolic stress signals that roughly uncouple mitochondria, including loss of membrane potential, result in inhibition of fusion (Mishra & Chan, 2016).

Fission. As a complement to fusion, fission of mitochondria is equally crucial for cellular physiology. Mitochondrial division is accomplished by Dynamin-related Protein 1 (Drp1), a large GTPase that is recruited to the mitochondrial outer membrane via a set of receptor proteins comprising mitochondrial fission factor (Mff), fission protein 1 (Fis1), mitochondrial dynamics proteins of 49 and 51 kDa (MiD49 and MiD51, respectively). The actions of these proteins cause restriction and cleavage of organelle fragments from the network to allow proper clearance (Chan, 2012; Losón *et al.*, 2013; Labbé *et al.*, 2014; Mishra & Chan, 2016; Toyama *et al.*, 2016; Gan *et al.*, 2018; Memme *et al.*, 2021). The main mechanism of regulation of mitochondrial fission involves phosphorylation of Drp1. Upstream of the phosphorylation process are several signaling pathways activated by metabolic events such as cAMP concentration or calcium changes which modulate PKA and Ca^{2+}-dependent phosphatases activity (Cribbs & Strack, 2007; Cereghetti *et al.*, 2008; Gomes *et al.*, 2011; Rambold *et al.*, 2011; Toyama *et al.*, 2016). The phosphorylation can either activate or inhibit Drp1, depending on the site involved. Phosphorylation at serine 637 (S637) has been demonstrated to inhibit its activity, promoting overall elongation of the mitochondrial network (Chang & Blackstone, 2007; Cribbs & Strack, 2007). Whereas phosphorylation at S616 activates Drp1 inducing mitochondrial fission and fragmentation (Mishra & Chan, 2016). Besides affecting mitochondrial morphology, fission has been implicated in multiple functions, including facilitation of mitochondrial transport, mitophagy, and apoptosis. In contrast, inhibition of Drp1 and mitochondrial fission results in increased tubulation which promotes mitochondrial ATP production and spares organelles from degradation due to their larger size (Blackstone & Chang, 2011; Mishra & Chan, 2016; Memme *et al.*, 2021). Taken together, these data provide clear evidence that the proper maintenance of

mitochondria dynamics, i.e., the balance between fission and fusion, is necessary for optimal mitochondrial health and function at the muscle level.

Mitophagy. While activation of the organelle biogenesis pathway leads to an overall increase in mitochondrial components, it is also vital to eliminate mitochondrial portions that have ended their functional utility via an autophagic process, defined mitophagy, in order to maintain or improve the quality of the mitochondrial network (Ljubicic *et al.*, 2009; Lira *et al.*, 2013*a*; Kim *et al.*, 2019). Mitophagy occurs when double-membrane vesicles, autophagosomes, phagocyte damaged organelles that are marked for degradation by specific proteins when they exhibit a decreased membrane potential and/or excessive increases in ROS production (Wei *et al.*, 2015; Kim & Hood, 2017; Chen *et al.*, 2018*b*; Triolo & Hood, 2019; Kim *et al.*, 2019). The main mitophagy pathway involves PTEN-induced putative kinase protein 1 (PINK1) and Parkin, an E3-ubiquitin ligase. Under normal conditions, PINK1 is imported into mitochondria and degraded by resident proteases. However, if the mitochondrial membrane potential dissipates, the resulting loss of function of protein import machinery leads to the accumulation of PINK1 on the outer membrane (Geisler *et al.*, 2010; Narendra *et al.*, 2010; Matsuda *et al.*, 2010; Wei *et al.*, 2015). PINK1 stabilization facilitates recruitment of Parkin, which mediates ubiquitination of various outer membrane proteins such as Mfn2 and the voltage-dependent anion channel (VDAC), targeting mitochondria to autophagy activity (Geisler *et al.*, 2010; Hood *et al.*, 2011*a*). Because Parkin selectively accumulates on dysfunctional mitochondria, intact organelles are spared from autophagic degradation (Mishra & Chan, 2016). The mitophagy process then involves the formation of the autophagic vesicle, the phagophore, from the lipidation of microtubule-associated protein 1 light chain 3 (LC3)-I into LC3-II through the activity of a cluster of autophagy-related gene products such as ATG7 (Tanida *et al.*, 2004). The adapter protein p62/SQSTM1, containing binding sites for both ubiquitin and LC3-II, functions as an anchor between the ubiquitinated mitochondrion and the double-membrane phagophore, thereby facilitating encapsulation of the organelle and formation of the mature autophagosome (Geisler *et al.*, 2010; Matsuda *et al.*, 2010; Kim & Hood, 2017; Chen *et al.*, 2018*b*, 2018*a*). The final stage of mitophagy requires the fusion of the autophagosome with lysosomes for subsequent breakdown by proteolytic enzymes within the lysosomal lumen (Vainshtein & Hood, 2016). In addition to loss of membrane potential, other metabolic stimuli have also been proposed to regulate mitophagy. Severe energy depletion leads to activation of AMPK, followed by phosphorylation and activation of protein kinases ULK1 and ULK2 (Egan *et al.*, 2011*b*). These two proteins are autophagy regulators capable of activating generalized autophagy, including mitophagy. Moreover, AMPK also inhibits the growth-promoting mTORC pathway, which typically inhibits ULKs function. These interconnected

mechanisms couple mitophagy to the energy state of the cell. Metabolic conditions that promote increased mitochondrial function and OXPHOS activity are also associated with increased mitophagy (Melser *et al.*, 2013). Under oxidative conditions, the autophagy regulator Rheb is recruited to the outer mitochondrial membrane for binding to the Nix receptor. Rheb relocalization promotes the recruitment of LC3 molecules, thereby enhancing mitophagy. The promotion of mitophagy during oxidative conditions, when mitochondrial function is increased, appears to contrast with the clearance function of dysfunctional organelles. However, increased respiratory chain activity may promote damage at the mitochondrial level through increased ROS production, which then leads to recruitment of the regulator Rheb. Alternatively, this mechanism may be in place to increase mitochondria turnover during conditions of enhanced functional demand. In either case, increased mitophagic flux promotes the overall energy efficiency of the mitochondrial population (Mishra & Chan, 2016).

PHYSIOLOGICAL RESPONSES TO EXERCISE AND TRAINING ADAPTATIONS

During exercise, skeletal muscle contraction is powered by actin-myosin crossbridge cycling according to the sliding filament theory (Podolsky & Schoenberg, 1983). Hydrolysis of ATP by myosin ATPase provides the immediate energy source for crossbridge cycling but is also largely consumed by sodium-potassium and calcium exchange dynamics required for contraction. Being skeletal muscle the major contributor to exercise-induced changes in metabolism, maximal exercise can induce a 20-fold increase in whole-body metabolic rate over resting values associated with an ATP turnover rate within the working skeletal muscle of more than 100-fold over resting values (Gaitanos *et al.*, 1993). Although resting intramuscular stores of free ATP are small, activation of metabolic pathways that drive ATP generation maintains intracellular levels of this important energy molecule. For ATP production skeletal muscle relies heavily on oxidative phosphorylation carried out at mitochondrial level. During strenuous exercise, large increases (>30-fold) in intramuscular oxygen consumption and local blood flow occur (Andersen & Saltin, 1985; Gibala *et al.*, 1998) allowing substrate supply required for electron transport system during oxidative phosphorylation. Tricarboxylic acid cycle also increases its flux by ~70- to 100-fold under maximal exercise to supply redox active coenzyme NADH and $FADH_2$ from carbohydrates and lipid substrate transformation (Gibala *et al.*, 1998).

Exercise encompasses many elements beyond simple muscle contraction that are important for a complete understanding of physiological responses to exercise and training adaptations. Muscle contraction is generated at the level of the motor cortex of the brain, which prompts the spinal cord to recruit motor units, resulting in specific movement patterns. Additionally, the recruiting fibers pattern is intensity dependent as stated by the well-recognized Henneman size principle. Slow-twitch fibers (type I), innervated by small cell bodies motor neurons, have a lower threshold of activation and will be utilized at lower exercise intensities, whereas fast-twitch fibers (type IIa and IIx), recruited by motor neurons with large cell bodies, have a higher threshold and will be increasingly activated as exercise intensity increases (Henneman, 1957). In parallel with the neural signals directed to skeletal muscle, there are also powerful neural feedforward signals to the cardiovascular, respiratory, metabolic, and hormonal systems, which, along with neural feedback from contracting skeletal muscle, generally allow metabolic demands to be met, thereby counteracting homeostasis disruptions. Numerous issues related to the speed, force, duration, and intensity of muscle contractions affect the whole organism response to the exercise stimulus. Aerobic (or endurance-based) and resistance (or strength-based) activities represent two extremes of the exercise continuum. Aerobic exercise exerts a high-frequency (repetition), low-power output (load) demand on dynamic muscle contraction,

whereas resistance exercise imposes a low-frequency, high-resistance demand sometimes using maximal force production during isometric contraction. (Egan & Zierath, 2013). Focusing specifically on endurance exercise and dynamic muscle contraction, the following sections will describe metabolic, systemic, cardiovascular and muscular adjustment occurring during aerobic stimulus.

Exercise represents a major challenge to whole-body homeostasis, and in an attempt to address this challenge, a myriad of acute and adaptive responses take place at the cellular and systemic levels that function to minimize these widespread disruptions. Voluntary, dynamic, whole-body exercise causes widespread changes in numerous cells, tissues, and organs in response to increased metabolic activity of contracting skeletal muscle through cellular mechanisms that underpin adaptation to exercise training (Bassel-Duby & Olson, 2006; Coffey & Hawley, 2007; Hoppeler *et al.*, 2011; Egan & Zierath, 2013). To address these triggers, multiple integrated and sustained responses occur to blunt the homeostasis strain provided by increased energy and O_2 demand. Systemic adaptations in the form of cardiovascular, respiratory, neural, and hormonal responses, constitute an integrated system of mechanisms necessary for supplying contracting muscles with the fuel and O_2 to sustain a large variety of activities. The underlying assumption is that adaptations at all levels of the entire system operate simultaneously to blunt the many challenges to whole-body homeostasis arising from the demands of contracting muscles (Hawley *et al.*, 2014).

Physiological bases of cardio-respiratory and metabolic responses to exercise

To describe the highest energy demand that can be met aerobically while exercising, in 1925, Nobel Laureate A.V. Hill was the first to introduce the concept of an individual's maximal oxygen uptake ($\dot{V}O_{2max}$). $\dot{V}O_{2max}$ has been demonstrated being the single best measure of cardio-respiratory performance and could be used for quantifying the adaptation at all levels of the entire systems in response to physical activity or inactivity (Bassett, 2002). $\dot{V}O_{2max}$ is determined by the combined ability of the central nervous system to recruit motor units, the pulmonary and cardiovascular systems to deliver O_2 to contracting skeletal muscles, and the ability of these muscles to consume O_2 via oxidative metabolism. At rest, whole-body O_2 consumption in healthy young adult humans averages approximately 3.5 ml/kg/min, with ~20% - 25% of this used by resting skeletal muscle. So, for a 70 kg person, O_2 consumption at rest is ~250 ml/min, of which 50 ml/min is utilized by skeletal muscle. During maximal exercise, in healthy untrained adults $\dot{V}O_{2max}$ typically reaches 10 to 15 times the resting values. In élite endurance-trained athletes, $\dot{V}O_{2max}$ values may exceed 85 ml/kg/min (Saltin & Astrand, 1967). The supply of O_2 and its utilization by skeletal muscle is a tightly interwoven process

that has been elegantly described by prof. Wagner in the so-called Wagner diagram where Fick's principle: ($\dot{V}O_2 = \dot{Q} \times (CaO_2 - CvO_2)$ where $\dot{Q}$ is cardiac output and CaO_2 and CvO_2 are arterial and venous O_2 concentrations respectively, conflates with the Fick's law: $\dot{V}O_2 = DmO_2 \times (PmvO_2 - PimO_2)$, where DmO_2 is muscle diffusion capacity for O_2 and $PmvO_2$ and $PimO_2$ are O_2 partial pressure in microvasculature and intramyocyte respectively. This interconnected mechanism allows an appreciation of the convective and diffusive conductances that summate to yield a given maximal $\dot{V}O_{2max}$.

Focusing on the convective component during maximal exercise, associated with large increases in O_2 consumption are peak values for cardiac output ($\dot{Q}$) of 40 l/min, accounting for 8-fold increases above rest. As product of heart rate (HR) and stroke volume (SV), $\dot{Q}$ increase during exercise is the results of response of both parameters. Whereas HR is modulated solely by autonomic nervous system, SV is also increased under the action of the so-called "muscle pump" that ensures the return of venous blood from the active muscle vasculature thus maintaining diastolic filling. Notably, there is only a modest (~20%) increase in mean arterial blood pressure. In addition, blood flow is redistributed away from visceral organs and inactive muscle caused by vasoconstriction in these vascular beds regulated by sympathetic activity during exercise. This allows to deliver a higher fraction of $\dot{Q}$ (80% – 90%) to active skeletal muscle and partially compensates the fall in total peripheral resistance due to skeletal muscle vasodilation. Vasodilation in active muscles is, indeed, the primary mechanism responsible for skeletal muscle hyperemia during exercise. The vasodilating response is mediated by mechanical, neural, and humoral factors, including those released from contracting skeletal muscle itself, such as nitric oxide, which are released in proportion to muscle O_2 demand and are responsible for the rise in muscle blood flow in order to counteract the muscle metabolic status (Hellsten *et al.*, 2012). Thereby, sympathetic nervous system for vasoconstriction and metabolic factors for vasodilation exert a commanding influence on total red blood cells (RBC) flux.

Regarding the diffusive component of $\dot{V}O_2$, as specified by Fick's law of diffusion, at any instant, oxygen consumption at muscle level ($m\dot{V}O_2$) must be the product of the transmembrane O_2 gradient ($PmvO_2 - PimO_2$) and the diffusing capacity for O_2 (DmO_2). As intramyocyte PO_2, or mitochondrial PO_2, falls to 1–5mmHg during muscle contractions, $PmvO_2$ approximates the PO_2 driving transmembrane O_2 flux (i.e. $m\dot{V}O_2$). Accordingly, $m\dot{V}O_2$ is the product of that $PmvO_2$ and the DmO_2 which itself is a function primarily of the number of red blood cells in flowing capillaries adjacent to the muscle fibers (Poole *et al.*, 2020). In order to facilitate fractional O_2 extraction, from rest to

exercise $PmvO_2$ remains constant as a result of increased O_2 delivery, whereas DmO_2 and blood-myocyte O_2 flux are increased as result of enhanced intramyocyte O_2 transport capacity in concert with increased capillary RBC flux and hematocrit and greater longitudinal recruitment of capillary surface area flowing capillaries (Federspiel & Popel, 1986; Groebe & Thews, 1990; Roca *et al.*, 1992; Poole, 2019; Angleys & Østergaard, 2020). In the overall mechanism, DmO2 increase is associated with increment in $\dot{V}O_2$ (Poole *et al.*, 2020).

Training modalities and Interval Training

The use of the term "training" in scientific research often encompasses several modifiable variables. These include the mode (e.g., aerobic versus resistance) and the frequency, intensity, and duration of exercise sessions, each of which are mitigating factors impacting the metabolic and molecular responses (Egan & Zierath, 2013). Focusing on aerobic exercise, various forms of training can be differentiated by their intensity and duration. Moderate Intensity Continuous Training (MICT) generally consists of long-duration aerobic exercise performed in a continuous manner at low intensity, lower than 80 % peak heart rate (American College of Sports Medicine *et al.*, 2018), while Interval Training (IT) involves intermittent bouts of high intensity exercise interspersed by recovery periods of lower-intensity exercise or complete rest within a given training session (Weston *et al.*, 2014; Gibala *et al.*, 2019). Based on exercise intensity, two basic types of interval training can be differentiated. High-intensity interval training (HIIT) is defined as "near maximal" efforts generally performed at an intensity that elicits ≥ 80% of maximal heart rate. In contrast, sprint interval training (SIT) is characterized by efforts performed at intensities that would elicit maximal stimulation of the aerobic capacity, including "all-out" or "supramaximal" efforts. In terms of volume SIT is usually characterized by intervals lasting ≤ 60s interspersed by a longer recovery period set with a work – rest ratio of 1:4 or more, whereas HIIT can be further differentiated by intervals duration. Low-volume HIIT (LV-HIIT) typically includes repeated intervals from 1 to 2 min with a rest period equal or doubled than working period and < 15 min of high-intensity efforts in total during the session. High-volume High-Intensity Interval Training (HV-HIIT) has longer intervals lasting ≥ 2 min with a shorter recovery period, typically a work – rest ratio between 2:1 to 1:1 and a total time of high-intensity efforts in the whole session ≥ 15 min (Weston *et al.*, 2014; Gibala *et al.*, 2014; MacInnis & Gibala, 2017; Williams *et al.*, 2019; Bishop *et al.*, 2019; Taylor *et al.*, 2019; Sultana *et al.*, 2019; Granata *et al.*, 2020; Sabag *et al.*, 2022). Despite a reduced total exercise volume and training time commitment, it has been widely established that interval training can induce physiological remodeling similar to or greater than traditional continuous endurance training (Milanović *et al.*, 2015; MacInnis & Gibala, 2017; Williams *et al.*, 2019). At skeletal muscle level, cellular stress and

subsequent metabolic signals for mitochondrial biogenesis are largely dependent on exercise intensity, resulting in greater adaptations in mitochondrial content and function during interval training compared with long-duration aerobic training (Jacobs & Lundby, 2013; Buchheit & Laursen, 2013; Scribbans *et al.*, 2014; MacInnis & Gibala, 2017; Bishop *et al.*, 2019; Granata *et al.*, 2020). In contrast, less evidence is available regarding the role of exercise intensity in mediating changes in skeletal muscle capillary density, maximal stroke volume, cardiac output, and blood volume (Montero *et al.*, 2015*a*; MacInnis & Gibala, 2017). In the overall combination of cardiovascular and muscular adaptations, the intensity of exercise elicited during interval training appears to be crucial in affecting physiological adaptations with a primary role in aerobic energy metabolism capacity. The following section will mainly focus on dynamic exercise and endurance training in the form of interval training.

Training Adaptations

All types of aerobic training are well known to be effective in inducing improvement in $\dot{V}O_{2max}$. In less-trained individuals, the interval training mode *per se* can improve $\dot{V}O_{2max}$ to an extent similar to or greater than MICT (Milanović *et al.*, 2015). In more trained individuals, incorporation of interval training sessions within the training programs leads to additional gains in $\dot{V}O_{2max}$ without increasing overall training volume (Gibala & Jones, 2013). Acute cardiovascular adjustments to dynamic exercise lead long-term remodeling patterns and adaptations that increase $\dot{V}O_{2max}$ and minimize disruptions in whole-body homeostasis. Whereas improvement in $\dot{V}O_{2max}$ after MICT is generally attributed to increases in maximal cardiac output ($\dot{Q}_{max}$) (Montero *et al.*, 2015*b*), largely mediated by hematological (Montero *et al.*, 2015*a*) and cardiac adaptations (Arbab-Zadeh *et al.*, 2014), it is difficult to draw strong conclusions in proving a greater effect of exercise intensity than training volume in mediating these adaptations. Despite this, interval training appears effective in eliciting cardiovascular adaptations at the same level as traditional MICT (MacInnis & Gibala, 2017; Gibala *et al.*, 2019).

In **Figure 4** the Wagner diagram facilitates analysis of training-induced perfusive and diffusive adaptations to endurance training that conflate to increase the overall $\dot{V}O_{2max}$ (Roca *et al.*, 1992; Poole *et al.*, 2018). Perfusive elements enhanced by training primarily include increased blood volume and improved heart function/structure (Baggish *et al.*, 2008; Boushel *et al.*, 2011), mirrored by increases in stroke volume (SV_{max}) and cardiac output ($\dot{Q}_{max}$) at maximal exercise. Such increase in $\dot{Q}_{max}$ is entirely the effect of enhanced SV_{max}, since maximal heart rate (HR_{max}) is unaffected by training (Saltin, 1985; Hawley, 2002; Daussin *et al.*, 2007; Murias *et al.*, 2010; Jacobs *et al.*, 2013). Indeed,

endurance training is associated with an increase in cardiac chamber size, referred volume hypertrophy, which facilitates rise of SV. This structural adaptation occurs in response to stretch of the ventricle caused by the increased venous return from the periphery during dynamic exercise and is facilitated by training-induced increases in blood volume and catecholamine concentrations. Moreover, oxygen-carrying capacity of the blood is enhanced by means of hematological adaptations (Mairbäurl, 2013; Bonne *et al.*, 2014). At peripheral level endurance training generates a decrease in systemic vascular resistances resulting from improved endothelial function and enhanced smooth muscle vasodilatation as a consequence of cellular changes in the brainstem cardiovascular center and sensory feedback that tend to be pro-vagal and sympathoinhibitory (Klausen *et al.*, 1982; Calbet *et al.*, 2006). In addition, a more efficient blood flow distribution (Kalliokoski *et al.*, 2001) to the exercising muscles occurs with this mode of training.

Diffusive improvements, especially in skeletal muscles undergoing training, include greater capillarization (i.e. increased capillary-to-fiber ratio) and capillary volume compensating for reduction in capillary RBC transit time which results from the augmented $\dot{Q}$. There is also the likelihood that there is an increased longitudinal recruitment of exchange surface area along the length of capillaries as fractional O_2 extraction increases combined with the potential for greater O_2 supply values to increase capillary hematocrit. The combination of all these adaptations at cardiovascular level may be crucial for improving O_2 supply and O_2 uptake matching within muscles.

Figure 4. Wagner diagram analysis of training-induced perfusive and diffusive adaptations to endurance training

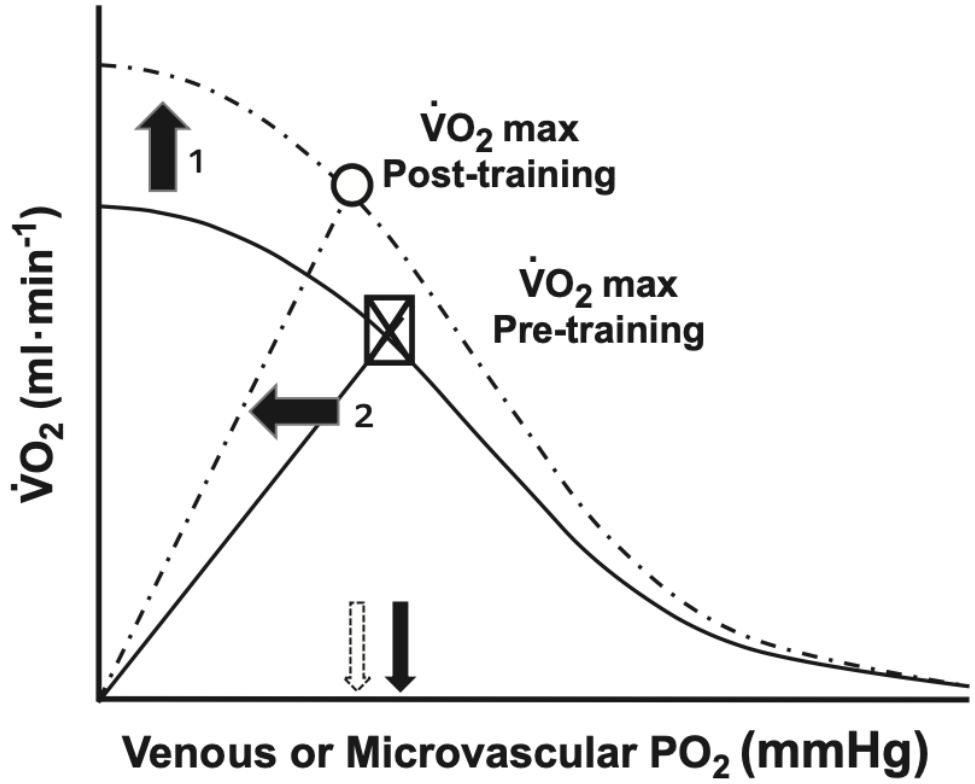

Conflation of perfusive (continuous and dashed curved lines) and diffusive (continuous and dashed straight lines from origin) O_2 conductances permits a mechanistic analysis of how these components combine to achieve a given $\dot{V}O_2$. Exercise training (dashed lines) acts to increase both perfusive ($\dot{Q}O_2$, black arrow 1) and diffusive (O_2, black arrow 2) O_2 conductances by elevating maximal cardiac output, muscle $\dot{Q}O_2$ and also DmO_2 consequent to capillary neogenesis, which increases the longitudinal recruitment of capillary surface area and also helps to constrain/prevent a reduction in mean capillary RBC transit time after training. A substantial increase in DmO_2 is required to produce even a small lowering of venous or microvascular PO_2 (i.e. increased arterial–venous O_2 difference, downward pointing arrows on x-axis; black arrow is pre- and white arrow is post-training). (From Poole & Musch, 2021).

Molecular bases of Skeletal Muscle Adaptations

Skeletal muscle is a malleable tissue capable of altering protein type and amount in response to disruptions to cellular homeostasis. Repeated, episodic bouts of muscle contraction, associated with frequent exercise training, are powerful stimuli for physiological adaptation (Flück & Hoppeler, 2003; Coffey & Hawley, 2007). Training-induced adaptations are reflected by changes in contractile protein and function (Adams *et al.*, 1993; Widrick *et al.*, 2002), mitochondrial function (Spina *et al.*, 1996), metabolic regulation (Green *et al.*, 1992), intracellular signaling (Benziane *et al.*, 2008), and transcriptional responses (Pilegaard *et al.*, 2003). The complex process of exercise- and training-induced adaptation in skeletal muscle involves specific signaling mechanisms which initiate the

replication of DNA gene sequences allowing subsequent translation of the genetic code into a series of amino acids to create new proteins (Coffey & Hawley, 2007). Contraction generates transient increases in the amount of messenger RNA (mRNA) which, for a multitude of genes, typically peaks 3–12 hours post-exercise and returns to basal levels within 24 hours (Pilegaard *et al.*, 2000; Bickel *et al.*, 2005; Yang *et al.*, 2005). Moreover, it has been demonstrated that transient DNA hypomethylation of gene-specific promoter regions, histone modifications, and micro-RNA expression (described in detail in section "Epigenetic") regulate mRNA expression in response to acute exercise (McGee & Hargreaves, 2011; Barrès *et al.*, 2012; Zacharewicz *et al.*, 2013). Consequently, the cumulative effect of exercise bouts results in increase in transcriptional activity that facilitates the synthesis of the corresponding proteins. Gradual accumulation of protein leads to a change in the steady-state level of specific protein content and enzyme function and, hence, to a new functional threshold (Perry *et al.*, 2010*a*). These training-induced adaptations intrinsic to the working skeletal muscle results in gradual structural remodeling and long-term functional adaptations leading to robust homeostasis defense during exercise challenge and improved exercise performance (Holloszy & Coyle, 1984; Booth & Thomason, 1991) (**Figure 5**).

Figure 5. The Molecular Basis of Adaptation to Exercise

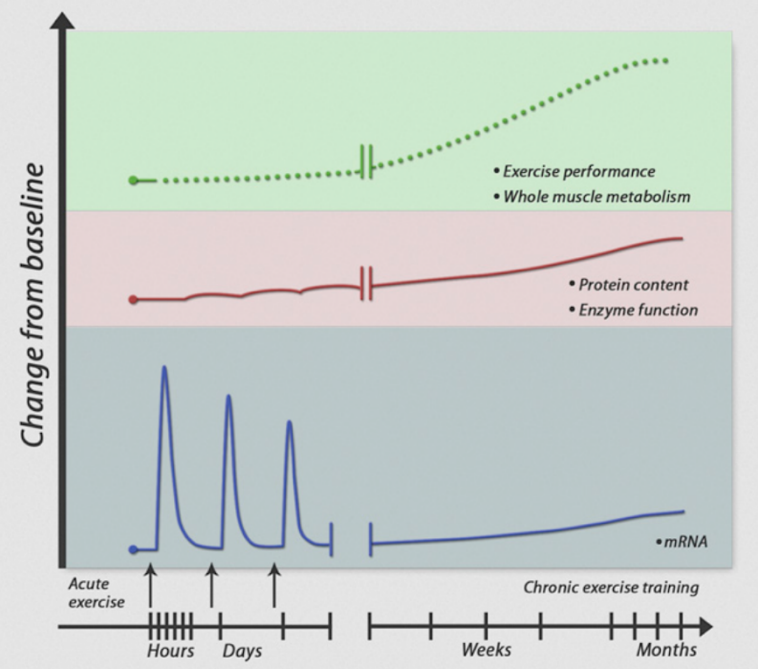

Schematic representation of changes in mRNA expression (bottom panel) and protein content (middle panel) over time as a consequence of acute exercise and chronic (repetitive) exercise training. Training-induced phenotypic adaptation is the consequence of repetition of the stimulus of individual acute exercise bouts. In order for a gene upregulated by exercise and training, an individual exercise bout elicits a rapid, but transient, increase in relative mRNA expression of a given gene during recovery. Alterations in mRNA expression several-fold from basal levels are typically greatest at 3–12 h after cessation of exercise and generally return to basal levels within 24 h. Translational processing and an elevated rate of postexercise protein synthesis result in a modest, same-directional change in protein content. Superimposition of repeated exercise bouts results in the gradual accumulation of protein in response to repeated, pulsed increases in relative mRNA expression. Thus, long-term adaptation to training is due to the cumulative effects of each acute exercise bout leading to a new functional threshold. Training-induced changes in protein content or enzyme function alter metabolic responses to exercise at the level of substrate metabolism, resulting in improved exercise performance (upper panel). (From Egan & Zierath, 2013).

The functional consequences of these adaptations are determined by training volume, intensity and frequency, and protein half-life. Moreover, many features of training adaptation are specific to the type of stimulus, such as the mode of exercise (Izquierdo *et al.*, 2004; Mahoney *et al.*, 2005). Specific exercise causes activation and/or repression of specific pathways and subsets of genes, thereby, performing multiple bouts of each training mode in isolation will eventually generate a developmental history in muscle fibers, producing a specific exercise-induced phenotype associated with long-term training (Ingalls, 2004). With aerobic exercise this well-defined network of transcription factors and coregulatory proteins exerts molecular control over contractile, metabolic, and mitochondrial adaptation, illustrated by an ability to alter the expression of key enzymes in carbohydrate and lipid metabolism, and the coordination of myogenesis and mitochondrial biogenesis in response to exercise (Hood, 2001; Flück & Hoppeler, 2003; Coffey & Hawley, 2007). Endurance training elicits a variety of metabolic and morphological adaptations, including mitochondrial biogenesis (Irrcher *et al.*, 2003), fast-to-slow fiber-type transformation (Zierath & Hawley, 2004) and substrate metabolism (Holloszy *et al.*, 1977). Specifically, these aerobic adaptations reflect increased abundance of proteins

involved in mitochondrial ATP production (Holloszy, 1967*a*), the TCA cycle (Egan *et al.*, 2011*a*), fatty acid mobilization, transport and oxidation (Talanian *et al.*, 2010), glycolytic metabolism (Tremblay *et al.*, 1994), antioxidant capacity (Powers *et al.*, 1994), glucose transport and glycogen synthesis (Perseghin *et al.*, 1996), and delivery and extraction of oxygen from skeletal muscle (Gavin *et al.*, 2007). The changes occur in all three fiber types, with the difference being somewhat greater in type IIa than in type I and type IIx fibers (Howald *et al.*, 1985).

Contraction-Induced Signal Transduction Pathways in Skeletal Muscle

The process of converting various chemical, electrical, and mechanical signals generated during muscle contraction into molecular events that promote physiological responses and subsequent adaptations in muscle cells involves signal transduction cascades resulting in activation and/or repression of specific signaling pathways regulating exercise-induced gene expression and protein synthesis/degradation. (Bassel-Duby & Olson, 2006; Hood *et al.*, 2006; Coffey & Hawley, 2007; Egan & Zierath, 2013). The nature of the exercise challenge determines the acute metabolic and molecular responses, which are then contiguous with long-term physiological adaptation of exercise training (Egan & Zierath, 2013). Specifically, interval training provides stimuli composed of short-duration dynamic muscle contractions typical of rhythmic exercise, such as cycling or running, affected by energy and metabolic perturbation combined with high intensity derived from elevated force and power production generated during each contraction (MacInnis & Gibala, 2017; Memme *et al.*, 2021). The cascade of events induced by these characteristic muscle contractions includes changes in intracellular oxygen pressure, mechanical strain, calcium flux, ATP turnover, redox balance and reactive oxygen species (ROS) production (Egan & Zierath, 2013).

Local Tissue Oxygenation and Hypoxia-Inducible Factors. Oxygen sensing is involved in the regulation of adaptive processes in cells. The major signal transduction pathway sensitive to the intracellular partial pressure of oxygen (PiO2) is regulated through hypoxia-inducible factor (HIF), composed of two subunits, HIF-1a and HIF-1b. Reduction of PiO2, occurring in contracting muscle during acute exercise (Richardson *et al.*, 1995*b*), allows for HIF-1a translocation to the nucleus to form an active complex with HIF-1b. Activation of HIF-1 induces transcription of target genes involved in erythropoiesis, angiogenesis, glycolysis, and energy metabolism (Taylor, 2008). Hence, HIF-dependent transcriptional regulation augments survival during low O_2 tension either by increasing O_2 delivery and extraction or by enhancing the ability to obtain ATP from O2-independent pathways making HIF-1 relevant to exercise-induced skeletal muscle metabolism and adaptation (Mason *et al.*, 2004; Formenti *et al.*, 2010).

Mechanical Stress and Mitogen-Activated Protein Kinase Signaling. Mechanical stimuli occurring during muscle contraction induce several adaptive processes that modulate tissue form and function (Alenghat & Ingber, 2002). The rapid and differentiated mechanochemical conversion induced by distinct patterns of mechanical stress strongly suggests the existence of mechano-transduction specificity. Among the wide variety of biochemical and biophysical processes activated by muscle contraction, exercise mediates the activation of mitogen-activated protein kinases (MAPKs). Among these, p38 MAPK is able to stimulate PGC-1α expression by phosphorylating the transcription factor ATF2 and MEF2, which in turn increase PGC-1α protein abundance by binding to and activating the CREB site on the PGC-1α promoter (Akimoto *et al.*, 2005; Wright *et al.*, 2007*b*; Egan *et al.*, 2010). Thereby, contractile activity-induced promotes mitochondrial biogenesis in skeletal muscle via activation of the p38 MAPK pathway (Akimoto *et al.*, 2005).

Calcium Flux and Calcium-Calmodulin-Dependent Protein Kinase / Calcineurin Signaling. Calcium is essential to facilitate the crossbridge interaction between myosin and actin during myofibrillar contraction. Neural activation of skeletal muscle generates an action potential that elicits Ca^{2+} release from the sarcoplasmic reticulum, whereas termination of the action potential initiates Ca^{2+} transport out of the cytosol back to the sarcoplasmic reticulum. The rate and capacity of Ca^{2+} release and uptake are altered by contractile activity, and the amplitude and duration of Ca^{2+} flux are regulated by the duration and frequency of the contractile stimulus. Specifically, high intensity exercise generates short cycles of significantly elevated intracellular [Ca^{2+}] (Baar & Esser, 1999). Calcium oscillations are translated into discrete signals that modulate the kinase activity of Ca^{2+}-calmodulin-dependent protein kinases (CaMKs), a family of multifunctional serine/threonine protein kinases implicated in muscle plasticity (Chin, 2010), whose CaMKII is the dominant isoform in human skeletal muscle, usually activated in response to endurance exercise rapidly upregulated after the onset of exercise (Rose *et al.*, 2006). Exercise increases CaMKII phosphorylation in an intensity-dependent manner (Rose *et al.*, 2006; Egan *et al.*, 2010), presumably due to the additional muscle fiber recruitment (Sale, 1987) or to higher calcium concentrations expected during increased exertion (Howlett *et al.*, 1998). Therefore, Ca^{2+} is an important regulator in the specificity of exercise-induced adaptive events, and its effects are likely altered by the mode, intensity and volume of exercise (Coffey & Hawley, 2007). CaMKs affect glucose transport (Wright *et al.*, 2004), lipid uptake and oxidation (Raney & Turcotte, 2008), and skeletal muscle plasticity (Wu *et al.*, 2000). Downstream effects of CaMKs involve transcription factors activation, such as NFAT, CREB, MEF2 or HDACs, affecting PGC-1α and GLUT4 gene expression in skeletal muscle (Pilegaard *et al.*, 2000; Chin, 2010).

CaMKII has also been shown to remain active in a Ca^{2+}-independent manner via autophosphorylation process after both acute and prolonged exercise and, therefore, is implicated as a mechanism for cellular memory of the previous level of activation (Chin, 2004). Moreover, prolonged and low-amplitude intracellular calcium transients have also been shown to increase calcineurin activity, which acts as a co-regulator in muscle hypertrophy and muscle fiber growth/regeneration (Dunn *et al.*, 1999; Musarò *et al.*, 1999; Sakuma *et al.*, 2003), but it is also involved in fast-to-slow transformation through dephosphorylation and activation of the transcriptional promoter NFAT (Naya *et al.*, 2000; Michel *et al.*, 2004; Parsons *et al.*, 2004; Talmadge *et al.*, 2004). Such paradoxical calcineurin-regulated adaptive pathways (i.e., hypertrophic vs oxidative phenotype), represents alternate adaptive responses specific to the intensity and duration of contractile activity.

Cellular Energy Status, ATP Turnover, and AMP-Activated Protein Kinase Signaling. ATP synthesis via restoration of its high energy phosphate bonds is generated by oxidative phosphorylation and/or glycolysis. Metabolites concentrations related to the maintenance of muscle phosphorylation potential ([ATP]/[ADP][Pi]), such as intracellular AMP concentration, provide feedback signals and act as regulators to balance ATP production with ATP consumption (Sakamoto & Goodyear, 2002; Hawley & Zierath, 2004). Any cellular stress that inhibits ATP synthesis or accelerates ATP consumption (e.g., exercise-induced contraction) and subsequently increases the AMP:ATP ratio initiates several downstream molecular events in skeletal muscle (Hardie & Sakamoto, 2006). As a primary messenger for adaptive signaling, phosphorylation state and energy deficit appears to exert its effect principally via a strong secondary messenger, the 5′-adenosine-monophosphate-activated protein kinase (AMPK) (Aschenbach *et al.*, 2004; Hardie & Sakamoto, 2006). AMPK acts to regulate intracellular energy metabolism by activating pathways that lead to ATP storage and generation (Kahn *et al.*, 2005). AMPK is implicated in the enhancement of ATP production and conservation by increasing uptake and oxidation of plasma glucose, stimulating fatty acids oxidation through the phosphorylation and subsequent inhibition of Acetyl-CoA carboxylase (ACC), enzyme which inhibits the beta-oxidation of fatty acids in the mitochondria (Rasmussen & Winder, 1997), and increasing expression of the glucose transporter type 4 (GLUT4) and hexokinase (HKII) (Holmes *et al.*, 1999; Aschenbach *et al.*, 2004; Hardie, 2007).

In addition, chronic activation of AMPK appears to be a crucial sensor involved in the mechanism of mitochondrial biogenesis detecting stress at the level of oxidative capacity and subsequently turning on the upregulation of PGC-1α expression and post-translational phosphorylation (Bergeron *et al.*, 2001; Hardie & Sakamoto, 2006; Leick *et al.*, 2010). These features, make AMPK a key regulator of

mitochondrial biogenesis through PGC-1α and NRFs pathways, working in response of the energy state of the muscle cell. Interestingly, acute exercise increases AMPK phosphorylation and enzymatic activity in an intensity-dependent manner (Wojtaszewski *et al.*, 2000; Egan *et al.*, 2010). In this regard, intense (~90% $\dot{V}O_{2max}$) interval training has been shown to increase AMPK activity in endurance-trained athletes (Clark *et al.*, 2004). Furthermore, AMPK phosphorylation is also significantly upregulated following short-duration (~30 seconds) supramaximal sprint cycling, probably due to the extensive and rapid reduction in cellular ATP (Chen *et al.*, 2000).

Redox Balance, NAD^+:NADH, and Sirtuins Signaling. The redox state, defined by the balance between nicotinamide adenine dinucleotide and its reduced form (NAD^+:NADH), is predominantly a result of catabolic reactions occurring with glycolytic and lipolytic metabolism in the mitochondria (Smith & Reid, 2006). The maintenance of redox potential produces volatile free oxygen molecules (e.g. reactive oxygen species (ROS)) inducing cellular oxidative stress. As a result of increase oxygen demand and enhanced metabolic pathways activity, exercise represents a stimulus capable of generating oxidative stress which may modulate exercise-induced adaptive signaling (Carrero *et al.*, 2000). Silent mating type information regulation 2 homolog proteins (Sirtuins) are NAD^+-dependent histone deacetylases (HDAC) having prominent role in metabolism regulation in response to physiological changes such as cellular NAD^+ accumulation and NAD^+/NADH ratio elevations (Tang, 2016). The deacetylase activity of two important Sirtuins members, Sirtuin-1 (SIRT1) at cytoplasmic and nuclear level, and Sirtuin-3 (SIRT3) at mitochondrial level, occurs on transcriptional regulators (Nemoto *et al.*, 2005) and mitochondrial enzymes (Hirschey *et al.*, 2010) respectively, allowing the coupling of alterations in cellular redox state to adaptive changes in gene expression and cellular metabolism (Lagouge *et al.*, 2006; Cantó *et al.*, 2009). Moreover, SIRT1 is able to deacetylate not only histones, but also proteins. Specifically, SIRT1 is known to regulate more than 40 protein targets through deacetylation activity (Nemoto *et al.*, 2005; Gerhart-Hines *et al.*, 2007; Fulco *et al.*, 2008). Among these, the post-translational deacetylation process of PGC-1α has been shown to be SIRT1-dependent, resulting in increased transcriptional activity of PGC-1α (Rodgers *et al.*, 2005; Nemoto *et al.*, 2005; Gerhart-Hines *et al.*, 2007; Amat *et al.*, 2009; Dominy *et al.*, 2010; Gurd, 2011). In addition, SIRT1 may also act upstream of AMPK by deacetylation and activation of the major AMPK activating kinase, Liver Kinase B1 (LKB1) (Lan *et al.*, 2008). Conversely, even the activity of SIRT1 depends on AMPK activation which via nicotinamide phosphoribosyl transferase (Nampt) enhances NAD^+/NADH ratio, the substrate for SIRT1 (Fulco *et al.*, 2008). Interestingly, short-term interval training has been shown to increase SIRT1 expression in skeletal muscle (Little *et al.*, 2010). Overall, enhanced SIRT1/3 activity is associated with favorable adaptations in skeletal muscle metabolism,

including improved mitochondrial function and exercise performance (Lagouge *et al.*, 2006; Gerhart-Hines *et al.*, 2007).

Mitochondrial Adaptations and Endurance Training

As noted, in response to aerobic training, numerous intracellular cascades have been implicated in regulating expression of genes and transcription factors involved in mitochondrial biogenesis (Howald *et al.*, 1985). The increase in total mitochondrial proteins in response to endurance exercise training includes those involved in β-oxidation, the tricarboxylic acid cycle, and the electron transport chain, thereby improving the capacity for energy provision to the exercising muscles (Holloszy & Booth, 1976). Prolonged endurance training typically induces an increase in mitochondrial volume up to 40–50%, and this increase in content is concomitant with improvements in respiration and oxidative capacity in each individual organelle (Baldwin *et al.*, 1972). Interval training, despite small volume of exercise performed compared to large volume moderate-intensity exercise, is able to elicit similar mitochondrial adaptations. In acute response, a single session of HIIT or SIT activates signaling pathways associated with mitochondrial biogenesis similar to MICT (Gibala *et al.*, 2009; Perry *et al.*, 2010*b*; Little *et al.*, 2011*b*; Metcalfe *et al.*, 2015). This may be explained by the crucial role played by exercise intensity that occur during interval training protocols. Indeed, cellular stress occurs in proportion to exercise intensity (Egan & Zierath, 2013), and there is strong evidence that higher intensities of exercise elicit a greater metabolic signal than moderate intensities. Firstly, ATP turnover is greater for higher intensities of exercise (Howlett et al. 1998), which also rely more on carbohydrate oxidation and utilize more glycogen than lower intensities of exercise (Gollnick *et al.*, 1974; Vollestad & Blom, 1985; Romijn *et al.*, 1993; Van Loon *et al.*, 2001). Consequently, the accumulation of intracellular lactate, creatine, AMP and ADP increases with exercise intensity (Howlett *et al.*, 1998; Van Loon *et al.*, 2001). Thereby, the subsequent activation of signaling kinases (e.g., CaMKII, p38 MAPK, AMPK) and deacetylases (e.g., SIRT1), and increases in nuclear PGC-1α protein content, which are all early events regulating mitochondrial biogenesis, appears to be regulated in an exercise intensity-dependent manner (Wojtaszewski *et al.*, 2000; Rose & Hargreaves, 2003; Rose *et al.*, 2006; Egan *et al.*, 2010). Alternatively, also the on-and-off pattern characteristic of interval training (i.e. rest–work cycles) could partially explain skeletal muscle responses to this type of exercise suggesting that the intermittent nature of interval training plays a role in the magnitude of the adaptations (Cochran *et al.*, 2014; Combes *et al.*, 2015; MacInnis & Gibala, 2017). Regular and repeated activation of exercise-induced pathway of mitochondrial biogenesis culminate in increases in mitochondrial content and/or respiratory function (Hoppeler *et al.*, 1985; Burgomaster *et al.*, 2005, 2008; Coffey & Hawley, 2007; Hood *et al.*, 2011*b*; Little *et al.*, 2011*a*; Jacobs & Lundby,

2013; Bishop *et al.*, 2014*a*, 2019; Montero *et al.*, 2015*a*; Montero & Lundby, 2017), and concomitant changes in organelle composition, such as increased cristae density (Nielsen *et al.*, 2017) or supercomplex assembly (Greggio *et al.*, 2017). Numerous studies have demonstrated that mitochondrial content increased by ~25–35% after six or seven sessions of HIIT or SIT (Burgomaster *et al.*, 2006; Gibala *et al.*, 2006; Talanian *et al.*, 2007; MacInnis & Gibala, 2017). Interval training results to be effective also in improving mitochondrial respiratory function as shown by large increase in mitochondrial respiration capacity after both SIT and HIIT training protocols (Daussin *et al.*, 2008; Granata *et al.*, 2016*a*; MacInnis & Gibala, 2017; MacInnis *et al.*, 2017).

Moreover, exercise intensity also appears to play a crucial role in these long-term adaptations. Indeed, the importance of exercise intensity is further highlighted by the greater training-induced increase in PGC-1α protein content reported following an all-out SIT period compared to MICT protocols of the same duration (Granata *et al.*, 2016*b*). Intensity also becomes relevant in regulating mitochondrial adaptations in terms of content and function. Indeed, although a parallel increase in mitochondrial content and respiratory function is sometimes assumed (Jacobs & Lundby, 2013), there is evidence that it may not always occur (Granata *et al.*, 2016*a*, 2018). Training-induced changes in mitochondrial respiratory function have been reported without concomitant changes in mitochondrial content (Jacobs & Lundby, 2013; Granata *et al.*, 2016*b*). and changes in mitochondrial content are not always paired with an increase in mitochondrial respiratory function (Yu *et al.*, 2003; Montero *et al.*, 2015*a*). Exercise at higher intensities has been reported to provide a greater stimulus to increase mitochondrial respiratory function (Granata *et al.*, 2018), suggesting a relation between mitochondrial function and training intensity. In contrast, mitochondrial content seems to be more sensitive to training volume. With training, mitochondrial adaptations may occur within any fiber types, indicating that mitochondrial adaptations are not dependent on the myosin-based fiber type per se, but are instead driven by the stimulus and the recruitment of that fiber (Lundby & Jacobs, 2016*a*).

Exercise acts as a stimulus for the induction of both organelle biogenesis and mitophagy, which act in concert to regulate mitochondrial turnover and maintain the health of the mitochondrial pool within skeletal muscle. Mitophagy is up-regulated by numerous cellular stresses, including aerobic acute exercise through activation of the AMPK signaling pathway by induced energy imbalance (Vainshtein & Hood, 2016; Erlich *et al.*, 2018; Chen *et al.*, 2018*a*; Hood *et al.*, 2019). Moreover, acute exercise promotes Parkin localization to mitochondria as well as increase in mitophagy flux, as measured by LC3II, p62 and ubiquitin immediately post-exercise (Vainshtein & Hood, 2016; Chen *et al.*, 2018*b*, 2018*a*). In response to repeated bouts of exercise in the form of endurance training,

several studies have documented increases in autophagy and mitophagy markers within muscle (Lira *et al.*, 2013*a*; Ju *et al.*, 2016; Chen *et al.*, 2018*b*). Chronic aerobic exercise induces the expression of lysosomes and autophagy-related genes to readily provide for the clearance of dysfunctional organelles, including mitochondria, when their degradation is required. Given the similar increases in mitochondrial content and function observed in HIIT and SIT compared with traditional endurance training, it is reasonable to consider that mitochondrial turnover would be induced to a similar extent in these alternative training modalities. A single bout of endurance exercise is sufficient to induce structural changes in mitochondrial morphology to promote improved function of the organelle network. Changes in the energy requirements of the cell during aerobic exercise are able to stimulate mitochondrial dynamics adaptation by adjusting their size and distribution (Picard *et al.* 2013). When exposed to chronic stimulus of endurance training, an augmented expression of fusion proteins Opa1 and Mfn2 has been revealed, along with a concomitant decrease in fission protein Drp1, effectively shifting the fusion:fission ratio in favor to organelle fusion (Hood *et al.*, 2019). Overall, the maintenance of mitochondrial morphology is critical for maintaining optimal muscle function.

Summary

Overall, endurance training elicits both central and peripheral adaptations, alters neural recruitment patterns, and causes profound changes in muscle bioenergetics and improves morphological and metabolic substrate status in skeletal muscle (Hawley, 2002). Aerobic adaptations result in increased muscle glycogen stores and reduced utilization at submaximal workloads via increased fat oxidation, enhanced lactate kinetics and morphological alterations, including a greater proportions of type I fibers per muscle area, and increased capillary density and mitochondrial biogenesis. In addition, repeated bouts of endurance exercise result in altered expression of a multiplicity of gene products, resulting in an altered muscle phenotype with improved fatigue resistance due to tighter coupling of ATP supply and demand, and, thereby, reduced disturbances to homeostasis combined with a consequent reduction in metabolic byproducts (Adhihetty *et al.*, 2003).

DETRAINING

According to the principle of training reversibility, physiological adaptations occurring at muscular and systemic levels in response to chronic exercise are partially or completely reversed during a short-term or long-term period of training cessation, impairing the acquired ability to address homeostasis perturbation. The principle of training reversibility is therefore the principle of detraining (Hawley & Burke, 1998; Mujika & Padilla, 2001). Detraining has been defined as the partial or complete loss of training-induced morphological, physiological and functional adaptations as a result of activity reduction or training interruption (Mujika & Padilla, 2000). Detraining has a marked impact on cardiovascular, respiratory, metabolic and musculoskeletal adaptations that are affected by impairment processes during cessation of training stimuli (Lacour & Denis, 1984; Sjøgaard, 1984; Wilber & Moffatt, 1994; Mujika & Padilla, 2000).

Cardiovascular and metabolic responses to detraining

In highly trained athletes cardiovascular detraining is characterized by a progressive $\dot{V}O_{2max}$ decrease between 4 and 20% to the initial values, during the first 8 weeks of training cessation (Coyle *et al.*, 1984; Pavlik *et al.*, 1986). Most studies, however, indicate that $\dot{V}O_{2max}$ ceases to decline thereafter and remains higher than untrained counterparts (Coyle *et al.*, 1984, 1985). In the longest detraining study (Coyle et al, 1984) seven endurance-trained subjects refrained from training for 84 days. $\dot{V}O_{2max}$ declined by 7% in 21 days, and by 16% in 56 days from where it stabilized at values still 17.3% higher than sedentary control subjects. A correlation of 0.93 was observed between trained $\dot{V}O_{2max}$ values and decline percentage with inactivity. A linear decrease in $\dot{V}O_{2max}$ was also observed until the 45^{th} day of training withdrawal in a group of highly trained cyclists and endurance runners during 60 days of training cessation (Pavlik *et al.*, 1986). However, it should be taken into consideration that the cardiovascular response during training cessation seems to be dependent on the duration of training performed and the training status achieved prior to undergoing the detraining period, in addition to the nature of detraining (complete cessation or reduced activity). In previously sedentary subjects, cardiovascular fitness is less affected by short-term detraining, during which $\dot{V}O_{2max}$ appears to be preserved for 2-3 weeks (Moore *et al.*, 1987; Houmard *et al.*, 1996). However, after roughly one month $\dot{V}O_{2max}$ initiates its decrement although maintaining values above pre-training conditions (Pivarnik & Senay, 1986; Wibom *et al.*, 1992)(Pivarnik & Senay, 1986; Wibom *et al.*, 1992). For longer periods of inactivity most often training-induced maximal aerobic capacity results in a complete reversal to pre-training values in recently endurance-trained individuals (Klausen *et al.*, 1981; Wang *et al.*, 1997).

A decline in blood volume appears to be largely responsible for the observed reduction in cardiovascular function during short periods of training withdrawal. In endurance athletes a 5% decrement has been observed after 10 days of detraining, rising to doubled values of decrease (9%) after 2 to 4 weeks of refraining from activity (Thompson *et al.*, 1984; Coyle *et al.*, 1986; Cullinane *et al.*, 1986). Plasma volume is also reduced during inactivity in relation to plasma protein dynamics, the loss of which appears to be accounted for 97% of the reduction in plasma volume (Pivarnik & Senay, 1986). Moreover, hemoglobin is lost in as little as 2 to 4 weeks of detraining, corresponding to 3.5% loss in total hemoglobin which may account for a portion of the reported decrease in $\dot{V}O_{2max}$ (Coyle *et al.*, 1986). As a consequence of reduced blood volume, cardiac function is impaired. In particular, the reduction in blood volume during training cessation limits ventricular filling during exercise and is largely responsible for the inactivity-induced reduction in maximal stroke volume (Coyle *et al.*, 1984, 1986). A 10% decline in stroke volume has been observed in highly-trained subjects after the initial 12 days without training, achieving values of 14-17% below trained levels between 21 and 84 days of inactivity which were not different from untrained controls, suggesting a complete reverse adaptation (Coyle *et al.*, 1984, 1986; Martin *et al.*, 1986). An association was found between changes in stroke volume and $\dot{V}O_{2max}$ during initial weeks, prompting reduction in stroke volume as factor responsible for $\dot{V}O_{2max}$ decrease during the short-term detraining period (Coyle *et al.*, 1984; Pavlik *et al.*, 1986). To counterbalance the reduced blood delivered to working muscles, heart rate is increased. Following 2 to 4 weeks of training cessation, a rise in an exercise heart rate by approximately 10% has been observed increased at submaximal intensities (Coyle *et al.*, 1986; Cullinane *et al.*, 1986; Houmard *et al.*, 1992; Madsen *et al.*, 1993). Studies of longer periods on detraining effects found that the increased heart rate during submaximal exercise stabilized after 56 days of inactivity (9). Maximal heart rate was less affected, showing a 4-5% increase after the initial 12-21 days of training interruption, but without change thereafter (Coyle *et al.*, 1984). The magnitude of the increase in exercise heart rate values that characterize cardiovascular detraining is insufficient to counterbalance the decline in stroke volume, eliciting overall a decreased cardiac output. Coyle and colleagues (Coyle *et al.*, 1984) reported that estimated maximal cardiac output stabilized at 8% below trained values after 21 days of training cessation in endurance athletes, not decline further beyond that level thereafter.

Focusing on the peripheral level of the O_2 cascade, the maximal arterial-venous oxygen difference seems to be unaffected during initial weeks of inactivity, however, after longer period without training values may be reduced by 4% to 7% (Coyle *et al.*, 1984). These observations lead to the suggestion that the initial $\dot{V}O_{2max}$ loss observed in individuals refraining from training is caused by a decreased

stroke volume, whereas the decreased arterial-venous oxygen difference would be responsible for the reduction in $\dot{V}O_{2max}$ observed between the 3rd and 12th weeks of training cessation (Coyle *et al.*, 1984). Interestingly, muscle capillarization in endurance-trained subjects appears to remain unchanged even after long-term period without training (up to 84 days) with values 50% higher than in sedentary controls (Coyle *et al.*, 1984). Also in recently trained individuals, capillarization, although slightly reduced after training, is maintained above pre-training values even after 8 weeks of training cessation (Klausen *et al.*, 1981). The retention of increased capillary density contributed to the observed partial maintenance of the ability to attain a high percentage of $\dot{V}O_{2max}$ despite long periods of detraining. Among cardiorespiratory impairment processes during detraining, mean and systolic blood pressures have been shown to increase along with peripheral resistance during 9 to 12 weeks (Martin *et al.*, 1986), and also impairment of ventilatory function as a result of training interruption has been observed in both athletes and recently trained individuals, where a decline in maximal ventilation has been reported due mostly to a reduction in maximal ventilatory volume (Drinkwater & Horvath, 1972; Houston *et al.*, 1979; Coyle *et al.*, 1985; Wang *et al.*, 1997).

From a metabolic perspective, even short-term detraining reveals increased respiratory exchange ratio (RER) at submaximal and maximal exercise intensities, suggesting a clear indication of a shift toward greater reliance on carbohydrate as energy substrate for exercising muscles, in concomitance with a decreased contribution from lipid metabolism (Drinkwater & Horvath, 1972; Coyle *et al.*, 1984, 1985; Moore *et al.*, 1987; Madsen *et al.*, 1993). In addition, whole-body glucose uptake rapidly declines during training interruption as a result of insulin sensitivity decline and reduction in muscle GLUT4 transporter (Mikines *et al.*, 1989; McCoy *et al.*, 1994; Vukovich *et al.*, 1996), and muscle glycogen concentration undergoes a rapid decline toward pre-training values within a few weeks of training cessation, in relation to a reduction in glucose-to-glycogen conversion and glycogen synthase activity (Costill *et al.*, 1985; Mikines *et al.*, 1989; Madsen *et al.*, 1993). In long-term detraining, exercise blood lactate concentration increases at submaximal intensities, and, together with a reduction in bicarbonate concentration and greater base deficit, results in a higher acidosis in response to exercise (Coyle *et al.*, 1985; Costill *et al.*, 1985; Neufer *et al.*, 1987). In addition, in endurance-trained subjects, lactate threshold has been shown to decline at lower percentage of $\dot{V}O_{2max}$, although remaining above pre-training values even 84 days after training cessation (Coyle *et al.*, 1985). In contrast, in recently trained subjects, blood lactate concentration during exercise does not appear to be affected by short-term training interruption (Wibom *et al.*, 1992), whereas long-term detraining results in reduction in submaximal and maximal exercise blood lactate concentration and in ventilatory threshold, but nevertheless maintaining above baseline values (Ready & Quinney, 1982).

Skeletal muscle responses to detraining

At skeletal muscle level several structural and enzymatic adaptation are reversed during detraining period. Muscle fiber distribution remains unchanged during the initial weeks of inactivity, but there may be a decreased proportion of ST fibers and a large shift from FTa to FTb fibers in endurance-trained individuals (Houston *et al.*, 1979; Coyle *et al.*, 1985). In addition, the cross-sectional area of ST, FTa and FTb fibers rapidly declined in previously sedentary subjects, returning to pre-training levels after one months but decreasing further thereafter without training (Klausen *et al.*, 1981), whereas, interestingly in endurance athlete fiber area may slightly increase in both slow- and fast-twitch fibers (Houston *et al.*, 1979; Houmard *et al.*, 1992). One of the main characteristics of muscular detraining is a marked decrease in skeletal muscle oxidative capacity, as shown by markedly reduced mitochondrial enzyme activities. Specifically, for highly trained subjects, enzyme activities involved in the tricarboxylic acid cycle, such as citrate synthase, succinate dehydrogenase, malate dehydrogenase, β-hydroxyacyl-CoA dehydrogenase, decline ~20% during the first 3 weeks and ~40% within 56 days of training interruption, stabilizing thereafter at such level, which is 40-50% higher than in sedentary counterparts (Chi *et al.*, 1983; Coyle *et al.*, 1984). Since CS activity is an estimation of mitochondrial content, although a rapid reduction during the initial period of detraining, a slower decrement in mitochondrial content is observed over longer period until stabilized at higher values than pre-training. Interestingly, the decrement in mitochondrial enzymes shows distinct behaviors among different fiber types, exhibiting almost complete decrease in ST fibers and a retention at 50-80% above pre-training values in FT (Chi *et al.*, 1983). As for cardiorespiratory parameters, even muscle alterations in highly trained people who have been exercising intensely on a regular basis for a long time appear to differ from individuals who have just trained for a few months. Indeed, in previously sedentary individuals, mitochondrial enzyme activities rapidly revert toward pre-training levels remaining higher than before training in the first few weeks (Moore et al., 1987; Wibom et al., 1992) but disappearing completely by the 8th week of training interruption (Klausen *et al.*, 1981). Conversely to muscle oxidative capacity, glycolytic enzyme activities undergo only minor detraining-induce changes, characterized by decrease in hexokinase and slight increment in phosphorylase, phosphofructokinase, and lactate dehydrogenase, suggesting a reliance on glycolytic energy rather than oxidative. According to the reduction in mitochondrial enzyme activity, mitochondrial ATP production rate is also markedly affected by training interruption, showing a decrease between 12 to 28% during the initial month, remaining, however, 37–70% above pretraining levels (Wibom *et al.*, 1992). These values parallel the decrease in mitochondrial respiration revealing ~15–25% after 2 weeks of training reduction (Granata *et al.*, 2016*a*), but inversely to aforementioned

ATP production data, all respiration states in permeabilized fibers return to pre-training level. These findings emphasize the rapid reversibility of gains in mitochondrial function after a period of training interruption. The protein content of mitochondrial transcription factors TFAM and Nrf1 appears to decrease during the first week of reduced activity, indicating a great sensibility of these transcription factors to short-term reductions of training (Granata *et al.*, 2016*a*). The rapid changes in the content of these transcription factors indicate that even at the cellular level, human skeletal muscle quickly responds to interruption of training stimulus and rapidly adapts to the new metabolic and energy requirements.

Summary

Overall, these findings demonstrate that cardiorespiratory and muscle adaptation acquired during an endurance training intervention are reversed following periods of detraining. Training status at the initiation of stimulus cessation is important in defining the timing and extent of impairment; however maximal aerobic capacity is rapidly reversed toward pre-training levels, primarily due to blood volume and stroke volume reduction and secondarily as a result of decline peripheral oxygen extraction. The latter impairment appears to be affected by reduction muscle oxidative capacity. Interestingly, only capillarization seems to be a component that is retained over long periods without exposure to endurance training stimulus.

EPIGENETIC

Epigenetics is an emerging area of science within molecular exercise physiology surrounding the interaction between environmental factors and our inherited DNA. The concept was first conceived by Conrad Waddington in 1940. Since then, and with the development of advanced technologies, the understanding of epigenetics has progressed significantly and the field has seen a rapid and exponential increase in attention over the past few decades (Seaborne & Sharples, 2020). The word epigenetics is of Greek origin and literally means "above" (epi) the genome. Indeed, it represents the means by which genetic components (genotype) interact with their surrounding environment to create a "phenotype", thus bridging the gap between genotype and phenotype (Sharples *et al.*, 2022). In essence, epigenetic mechanisms are modifications that affect gene function through changes in transcriptional expression without variations occurring in the DNA sequence itself (Sharples *et al.*, 2016*b*; Turner *et al.*, 2019; Seaborne & Sharples, 2020; Blocquiaux *et al.*, 2022). Following exposure to environmental stimuli, changes are produced by biological and biochemical modifications to DNA or proteins such as histones altering the chemical structure of binding sites for transcription factors and the conformational characteristic of the chromatin, helping to promote or suppress the transcription process, and thus the subsequent level of gene expression (Sharples & Seaborne, 2019). These modifications involve addition or removal of small chemical groups such as acetyl or methyl groups to specific sites on the DNA or histones (Sharples *et al.*, 2022). Epigenetic modifications allow genetically identical cells to achieve extremely different phenotypic characteristics through regulation of the transcriptional process elicited during homeostasis and after exposure to environmental stressors. The underlying mechanism by which human skeletal muscle exhibits highly variable adaptations in response to a given exercise stimulus has yet to be fully clarified; however, it is evident that epigenetic modifications play an important role in physiological adaptations to exercise (Seaborne & Sharples, 2020).

Modifications. There are several types of epigenetic modification. A large amount of highly complex biological processes is involved and the full repertoire of these epigenetic mechanisms is not yet fully understood. Currently, more than 200 modifications and associated enzymes have been identified (Minguez *et al.*, 2012; Duan & Walther, 2015). However, the most common epigenetic modifications include SUMOylation, phosphorylation, ubiquitination, acetylation, and methylation, among which **histone methylation** and **acetylation,** non-coding **miRNAs** and **DNA methylation** are the most widely studied modifications in the context of molecular exercise physiology (Sharples *et al.*, 2022).

Histone modifications

The major forms of modification involve alterations to the surrounding histones as a result of methylation, acetylation and deacetylation (Turner *et al.*, 2019). Typically, histone methylation is associated with a suppressed transcriptional state resulting in reduced gene expression. However, this mechanism does not always respect this pattern since it is highly dependent on the specific amino acid being modified and the number of methyl groups characterizing this modification (e.g., mono-, di-, or tri-methylation) (Sharples *et al.*, 2022). Generally, when a histone is acetylated, it creates a chromatin conformation that helps activate and increase gene transcription near those loci (a specific gene site or location). This is caused by the new acetyl group changing the electrical charge between the histone and DNA, repelling their tight ionic binding and rendering a more accessible chromatin structure. This condition facilitates access to the transcriptional machinery and enhancement of gene expression (Eberharter & Becker, 2002; Sharples *et al.*, 2022).

Micro RNA

Micro RNAs (miRNAs), short non-coding RNA species, are the third major epigenetic regulator. This small single-stranded RNA binds directly to the 3' UTR regions of mature mRNA molecules, thereby disrupting the mRNA strand just prior to translation into protein. Hence, this is identified as a post-transcriptional epigenetic modification as it occurs after the mRNA has been transcribed (Lujambio & Lowe, 2012). Commonly, miRNA binding to the mRNA of specific genes causes a reduction in gene expression through direct degradation of the target mRNA molecule or suppression of its translation process (Lujambio & Lowe, 2012). This occurs when the miRNA binds to the 3' UTR region of the specific mRNA, but some research has also shown that when binding occurs at the level of the coding region or at the 5' UTR region, the mechanism can result in activation and upregulation of protein translation (Ørom *et al.*, 2008). This epigenetic modification substantially affects mRNA post-transcriptional processes. Indeed, individual miRNAs have been reported to target hundreds of mature mRNAs (Selbach *et al.*, 2008), suggesting that more than 30% of human genes may be regulated by miRNAs (Orang *et al.*, 2014). Intriguingly, miRNAs have been found to interact with both histone and DNA methylation to create a miRNA-epigenetic feed-back loop. Key histone and DNA epigenetic enzymes are targeted by miRNAs consequently regulating the expression of these key enzymes (Kwa & Jackson, 2018). Viceversa, the expression of miRNAs themselves has been shown to be subjected to regulation by the local epigenetic landscape for which they are transcribed; for example, hypermethylation of the promotor region of specific miRNAs are sufficient to reduce their expression (Jin *et al.*, 2017; Shao *et al.*, 2018).

DNA methylation

DNA methylation is a crucial mechanism that regulates mRNA transcription (Eden & Cedar, 1994). The target site for this epigenetic modification is located on the "linker" genomic DNA that connects nucleosome complexes. Within the cell nucleus, 147 base pairs (bp) of double helical DNA are wrapped around the histone octamer composed of 4 pairs of histone proteins (H2A, H2B, H3 and H4) which acts as a support to allow DNA to condense into the rippled structure typical of chromatin. These protein complexes are termed nucleosomes and are often referred to as "beads on a string" due to their appearance. Each core nucleosome particle is separated by short strands of ~20-90 bp, termed "linker" DNA, which is subjected to DNA methylation. DNA methylation involves the addition or removal of a covalent methyl (CH_3) chemical group to the 5^{th} carbon position of the pyrimidine ring of a cytosine. More than 98% of methylation process occurs at 5'-cytosine-phospate-guanine-3' dinucleotide pairing site (CpG), characterized by the presence of a cytosine nucleotide (C) followed by a guanine nucleotide (G) that are linked by a phosphate (p) group within the same strand of DNA. The majority of annotated gene regulatory regions contain CpG dinucleotide rich locations, known as CpG islands (Bird, 1986; Sharples & Seaborne, 2019). Located upstream and downstream of CpG islands are CpG shores and CpG shelves, which are less dense and exhibit greater tissue-specific methylation profiles (Irizarry *et al.*, 2009). The human genome contains ~28 million CpG sites (~ less than 1% of the whole genome), with the majority of these sites (70–80%) being methylated (Lister *et al.*, 2009; Gifford *et al.*, 2013).

However, the methylation status of a CpG site may be modified, or differentially methylated, by biochemical processes arising from surrounding environmental stimuli. The addition of a methyl group to CpG sites yields increased in methylation, or more commonly referred to as hypermethylation. In contrast, the removal of a methyl group from cytosine results in a reduction in methylation, also known as hypomethylation or demethylation.

The process of change in DNA methylation is regulated by several key enzymes that determine whether the CpG sites are either methylated or unmethylated. Specific enzymes are required to either promote, maintain, or remove methyl groups and are referred to as "writers", "readers" and "erasers", respectively. DNA methyltransferases (DNMTs) are the main family of enzymes that promote methylation. DNMT3a and DNMT3b control de novo or "new" methylation by promoting the addition of a methyl group to the cytosine resulting in 5-methylcytosine (5mC) and thereby establishing DNA hypermethylation (Trasler *et al.*, 2003; Sharples & Seaborne, 2019; Seaborne & Sharples, 2020). DNMT1 enzyme is most responsible for maintaining methylation once modification

has occurred. It acts largely on CpG sites during cellular division, installing previous modifications and enabling daughter cells to preserve methylation profiles that would otherwise be lost without DNMT1 enzyme activity (9,10 book). Indeed, a lack of DNMT1 enzyme activity results in the passive loss of DNA methylation during DNA replication. Additionally, there is also an active mechanism responsible for reducing DNA methylation. Active hypomethylation occurs through another set of important enzymes known as the ten-eleven translocation enzymes (TETs), including TET1, 2, and 3, which convert 5mC to 5-hydroxymethyl cytosine (5hmC) by directly catalyzing the removal of methyl groups through a base excision repair process (Tahiliani *et al.*, 2009; Ito *et al.*, 2010).

As described previously, CpG islands are often located within specific DNA regulatory regions, such as gene promoter, enhancer, and silencing regions (Bird, 1986). Given that these specific DNA sequences are responsible for initiation, upregulation, and suppression of mRNA expression, respectively, it is possible that alterations in the methylation status of these gene regions may modulate the level of gene expression. In case of methylation changes occurring in gene promoter or enhancer regions, a general rule is that hypermethylated DNA typically results in reduced gene expression, whereas demethylated or hypomethylated DNA in these regions typically results in increased gene expression (Bogdanović & Veenstra, 2009; Turner *et al.*, 2020). One mechanism responsible for this phenomenon during the methylated state condition or after increased methylation of CpG sites (or multiple sites in a CpG island) is the binding inhibition of the transcriptional "machinery" (i.e., RNA polymerase and transcription factors) driven by the recruitment of CpG methyl-binding proteins, which, consequently, blocks the initiation of gene transcription (Bogdanović & Veenstra, 2009), resulting in reduced gene expression (Bogdanović & Veenstra, 2009; Turner *et al.*, 2020). In addition, DNA methylation induces the recruitment of chromatin modifying protein complexes that remodel or tighten the adjacent chromatin (termed heterochromatin), also inhibiting the gene transcriptional process (Jones *et al.*, 1998). Conversely, where there is unmethylated or hypomethylated DNA, binding of the transcriptional apparatus and loosening of the chromatin (termed euchromatin) are facilitated, enabling and increasing gene transcription. As noted above, this inverse relation between methylation status and gene expression level occurs when the modification affects promoter or enhancer regions. The opposite occurs if the DNA methylation modification affects gene silencer regions, where a positive correlation is more likely. For example, within these regions, increased methylation may lead to an enhancement in gene expression, whereas reduced methylation may lead to a reduction in gene expression. However, it is important to be aware that regulation of gene expression related to methylation changes is not limited only to promoter, enhancer, or silencer regions, as for some specific genes there is also evidence of reduced

transcription associated with gene body methylation (Ball *et al.*, 2009; Brenet *et al.*, 2011; Anastasiadi *et al.*, 2018).
As we focus on DNA methylation in the context of exercise in the following sections, it is worth noting that when assessing DNA methylation across the genome (or the 'epigenome'), it is more appropriate to refer to this as the methylome.

DNA methylation and exercise. Exercise is an external stressor that generates an extensive coordinated response in several organs and tissues. The cellular and molecular response to exercise stimuli leading to skeletal muscle and systemic adaptations is underpinned by a series of sequential mechanisms. Exercise, depending on the modality and intensity, leads to the secretion by various glands, tissues and organs of a multitude of extracellular molecules such as, but not limited to, calcium, hormones (testosterone, cortisol, growth hormone), growth factors (insulin, insulin-like growth factors), catecholamines (epinephrine, norepinephrine), cytokines (TNF-α, IL-6), and nitric oxide.

These extracellular molecules bind to specific cell surface receptors or are transported via carrier proteins across cell membranes whether protein-based on non-protein-based molecules, respectively. Once bound to the membrane or translocated into the cell, these extracellular molecules lead to a cascade of intracellular signaling responses. These responses change the activity of specific proteins resulting in activation or deactivation of transcription factors and translocation of key molecules. Transcription factors bind to DNA to promote or silence gene expression (mRNA transcription), as well as key post-translational modifications also occur.
After resistance and aerobic exercise, changes in gene expression occur in a transient pattern, increasing markedly approximately 2-4 h after stimulus before returning to basal levels approximately 20-24 h later (Seaborne & Sharples, 2020). Such transient changes in mRNA expression are the key hallmark of the following adaptation that leads to a consecutive increase/decrease in the abundance of translated proteins that are synthesized by the ribosome (Seaborne & Sharples, 2020). Proteins are then able to perform their function in maintaining cellular homeostasis, and upon chronic and repetitive exposure to certain exercise stimuli, increases in protein abundance over time may result in significant adaptations at both the cellular and tissue levels to counteract and maintain homeostasis during prolonged or repeated encounters with a similar stressor (Perry *et al.*, 2010*b*). All of these sequential processes create a coordinated and time-dependent response to specific exercise stresses (Egan & Zierath, 2013).

The mRNA transcriptional processes rely on the accessibility of the fundamental transcriptional machinery to the gene loci of interest. Therefore, during the post-exercise "window", in order to enable adaptations to occur, it is important that chromatin structure and regulatory gene binding regions are functionally permissive so that transcription factors and polymerase apparatus are able to recognize, bind, and transcribe the target DNA sequence. Epigenetic modifications converge on regulatory sites to alter chromatin chemical structure and accessibility, generating activation/promotion or inactivation/suppression of transcription for specific genes involved in exercise adaptations. This essential biological mechanism may be critical in facilitating post-exercise adaptation and enabling skeletal muscle tissue remodeling. Skeletal muscle is, indeed, the specific site where endurance exercise adaptations occur that elicit an increase in the size, strength, and contractile properties of myofibers. Skeletal muscle is also the fundamental site involved in aerobic adaptations at the peripheral level where the improvement of oxidative capacity and energy production activity occurs involving those cellular components responsible for muscle bioenergetics, such as mitochondria.

As skeletal muscle is the tissue primarily used for experimentation to investigate mechanisms of exercise adaptation, including epigenetic modifications, the following section will therefore provide an overview of studies focused on DNA methylation in response to acute and chronic aerobic and resistance exercise, specifically in skeletal muscle.

Resistance exercise and DNA methylation. Resistance exercise is defined as any exercise that allows muscles to contract under a relatively high load for a short period of time. Resistance training, or strength training, is designed to improve muscular fitness with the expectation of increases in strength, power, and hypertrophy. Research examining the interplay between resistance exercise, modifications to the epigenome and the consequential effect on physiological adaptations is currently being investigated. Only in the most recent years the scientific community has become interested in epigenetic modifications following acute and chronic resistance exercise. Nevertheless, the research that has been produced to date has revealed some interesting findings regarding the role played by these modifications on the regulation of physiological adaptations in muscle.

To date, the majority of epigenetic analysis after resistance exercise has focused on DNA methylation, with the first of these studies published in 2014. Rowlands and colleagues found that, following 16 weeks of resistance training (6-8 reps until failure of 8 exercises targeting all major muscle groups 3 times per week), skeletal muscle genome in obese type-II diabetic participants exhibited a considerable reduction in the methylation profile (Rowlands *et al.*, 2014). This work was the first to suggest that after chronic resistance exercise, muscle methylome in humans is preferentially

hypomethylated, and these changes may be associated with key tissue adaptation processes, such as tissue morphology, cellular development, and cellular assembly/organization. The finding that resistance exercise creates a hypomethylated change in the human methylome was initially supported by leukocyte studies (Denham *et al.*, 2016; Dimauro *et al.*, 2016). Subsequently, with the development of sequencing technology, researchers were able to examine the human muscle methylome following resistance exercise more extensively. Seaborne and colleagues in 2018, used a genome-wide analysis to investigate human muscle methylome following both acute and chronic resistance exercise (Seaborne *et al.*, 2018*a*, 2018*b*). Both at the acute level (30 minutes after exercise cessation) and after 7-week training, the authors reported a significant reduction in the methylation profile compared with pre-exercise levels, again suggesting a preferentially hypomethylated human methylome after resistance exercise.

In the attempt to understand the consequence of changes in the DNA methylation level, Turner and colleagues (2019) undertook large-scale bioinformatic analyses of pooled transcriptome data after acute and chronic resistance exercise in the majority of studies conducted (using publicly available transcriptome data sets) (Turner *et al.*, 2019), and overlapped these data with the methylome changes derived from Seaborne and colleagues (Seaborne *et al.*, 2018*a*, 2018*b*) after similar time frame. This study was the first to investigate and identify a relationship between fluctuations in DNA methylation profile and gene expression following both acute and chronic resistance exercise. The authors reported a partial association between gene expression and DNA methylation levels immediately after acute resistance exercise and also following resistance training, demonstrating a preferential hypomethylated profile, particularly after chronic resistance exercise. The enriched hypomethylated and gene turned on signatures identified were associated to pathways involved in growth, remodelling of extracellular matrix, actin structure and mechano-transduction, and are already known to be altered at the gene expression level after resistance exercise due to their role in muscle mass remodeling and regulation. In a recent work (Ruple *et al.*, 2021) it has been examined the mtDNA methylome in elderly untrained human subjects following six weeks of whole-body resistance training, giving for the first time information on the effects of resistance training in areas outside of the traditional nuclear genome. Epigenetic analyses reported a significant reduction in global DNA methylation of the mtDNA genome, particularly in the D-loop/control region, confirming previous findings of a preferentially hypomethylated remodeling following resistance training in human subjects. Given that these changes occurred with resistance exercise, whereas greater changes to mitochondria might be expected with aerobic exercise, it could be interesting to examine changes in mtDNA methylation after endurance exercise or training.

In conclusion, changes in DNA methylation after both acute chronic resistance exercise have been shown to be associated with muscle mass regulation, revealing a clear and potentially important regulation of integral modifications at the CpG methylation level in the molecular response to resistance exercise.

Aerobic exercise and DNA methylation. Given the well-established role of PGC-1α in metabolic and mitochondrial adaptations to endurance exercise, it should not surprise that some of the first studies investigating promoter DNA methylation and changes in gene expression after exercise in skeletal muscle, focused on PGC-1α pathway. The inverse relation between DNA methylation profile of the PGC-1α promoter and its gene expression was firstly identified in a non-exercise context comparing type-II diabetes (glucose-intolerant) and healthy (glucose-tolerant) individuals (Barrès *et al.*, 2009). The authors identified a higher PGC-1α methylation in type-II diabetes subjects muscle with a corresponding reduced gene expression compared with healthy individuals, which presented lower methylation level and larger gene expression. A similar inverse relation pattern was confirmed after a 9-days bed rest that revealed an increase in PGC-1a DNA methylation and reduction in the corresponding gene expression (Alibegovic *et al.*, 2010). Individuals were later exposed to 4 weeks of endurance training (30 mins cycling at 70% $\dot{V}O_{2max}$ for 6 days/week). Although aerobic exercise was supposed to be able to counteract deconditioning, only a trend toward reduced DNA methylation in PGC-1α and increased gene expression was found, but pre-bed rest levels were not recovered (Alibegovic *et al.*, 2010). In 2012, Barres and colleagues (Barrès *et al.*, 2012) provided the first evidence to suggest alterations in DNA methylation of PGC-1α in skeletal muscle in response to endurance exercise itself. This study demonstrated that, in healthy individuals undertaking a single high-intensity aerobic exercise session (cycling at 80% $\dot{V}O_{2peak}$ until 1674 kJ/400 kcal was expended), PGC-1α, alongside other mitochondrial-related genes (TFAM, PDK4 and PPAR-δ), were significantly hypomethylated within hours of acute bout and also gene expression displayed significant increases (Barrès *et al.*, 2012). Interestingly, this study revealed that these modifications only occurred when performing high-intensity (80% $\dot{V}O_{2peak}$) compared with lower-intensity (40% $\dot{V}O_{2peak}$) matched for the same energy expenditure amount. This fascinating finding suggested that exercise intensity could be an important regulator of DNA methylation modification in skeletal muscle. Despite some clear epigenetic changes in key metabolic genes of PGC-1α pathway, very little is known about most of the genes involved in other important pathways associated with the aerobic exercise response, such as AMPK and MAPKs, important sensor of energy and oxidative stress respectively. This lack of information is due to few or no studies using genome-wide array or sequencing technology to profile DNA methylation across healthy human muscle "methylome" after

acute endurance exercise. An exception is a recent study that used DNA microarray technology to profile around 850,000 CpG sites to compare straight line running with change of direction running exercise (Maasar *et al.*, 2021). Although distance and speed were the same in both groups, change of direction running induced greater physiological (heart rate), metabolic (lactate), and mechanical stress than straight line. Change of direction exercise also evoked higher levels of hypomethylation especially in genes within the AMPK, MAPK and insulin pathways. Moreover, hypomethylation also affected promoter regions of angiogenic genes and metabolic transcription factors, particularly Vascular Endothelial Growth Factor A (VEGFA) and Nuclear Receptor Subfamily 4A1 (NR4A1), known to be associated with PGC-1α pathway (Rundqvist *et al.*, 2019; Pillon *et al.*, 2020). Indeed, even though no change in PGC-1α methylation was found, gene expression of PGC-1α, alongside VEGFA and NR4A1 were increased. Overall, this study extends previous work demonstrating that acute exercise induces a global reduction in DNA methylation. In addition, the use of genome-wide analysis allowed the implication of the AMPK, MAPK, and insulin signaling pathways in response to exercise. Another important finding was that identified hypomethylation signatures in skeletal muscle were more prominent in these pathways after 30 minutes from the cessation of exercise than after 24 hours, suggesting that methylation changes are extremely rapid and dynamic after exercise and likely precede changes in gene expression that can typically peak between 3-6 hours after exercise. Moreover, this study confirms the previous finding of Barres et al, (2012) suggesting that exercise intensity and the involvement of anaerobic stimuli in endurance exercise (e.g. sprint interval exercise) could significantly affect the DNA methylation modification in skeletal muscle (Barrès *et al.*, 2012). More studies are certainly needed to investigate in depth methylome changes after acute endurance exercise and especially if these lead to concomitant alterations at the level of gene expression and protein expression, as would also be interesting to understand the temporal sequence of coding, transcription and translation processes.

Compared to acute exercise, a greater number of studies have investigated genome-wide DNA methylation after chronic endurance training. This approach allows for the simultaneous analysis of a large number of CpG sites across the entire genome thereby allowing for the identification or 'discovery' of genes that are most consistently altered across the investigated population. The detection of differentially methylated genes can be further validated in future experiments by looking at whether such alterations in DNA methylation are also associated with changes in gene expression or even alterations in protein levels. In addition, a genome-wide analysis provides the opportunity to target specific pathways implicated in training adaptations. However, it must be kept in consideration that most epigenetic aerobic training studies have not been conducted in healthy populations.

The first aerobic training study profiled methylome DNA around 29,000 CpG sites in skeletal muscle in individuals with a family history of type II diabetes (Nitert *et al.*, 2012). The training protocol included 6 months of supervised aerobic training (3 days/week), although intensity was not defined $\dot{V}O_{2max}$ increased after training suggesting improved aerobic fitness. As with previously described acute exercise, chronic endurance exercise was able to evoke a predominantly hypomethylated signature by involving genes associated with insulin and calcium signaling pathways and carbohydrate and retinol metabolism (Nitert *et al.*, 2012). Genome-wide analysis using higher coverage microarray technology (450,000 CpG sites) was also conducted in obese type II diabetics to study DNA methylation after 4-month progressive endurance training (3 days/week of 40-60 min cycling at 65%-85% of reserve heart rate) (Rowlands *et al.*, 2014). As in the previously described study, aerobic training elicited more hypomethylated than hypermethylated CpG sites, and pathway analysis suggested that the affected genes were involved in lipid and carbohydrate metabolism, metabolic disease, cell death and survival, cardiovascular system development/function, and hematological system development/function. Furthermore, this study was the first to compare endurance training with resistance training, identifying a similar hypomethylated profile after both exercise modalities, suggesting that both exercises could lead to a more permissive and transcriptionally functional state. Moreover, crucially, this comparison revealed that the biological processes involved were different between the exercise programs, suggesting that DNA methylation in human muscle is differently responsive to the specific exercise it is exposed to (Rowlands *et al.*, 2014). In the same year Lindholm and colleagues (Lindholm *et al.*, 2014) further confirmed that altered methylation profiles occurred after long-term endurance training in gene pathways associated with metabolism and oxidative phosphorylation furthermore, strengthening the findings with transcriptome-wide gene expression analysis. In this study, healthy untrained subjects performed 3 months of progressive unilateral endurance training (45 mins of unilateral knee-extension exercise, 4 days/week) (Lindholm *et al.*, 2014). In slight contrast to previous studies, the authors reported similar numbers of hypomethylated and hypermethylated CpG sites after training (Lindholm *et al.*, 2014). However, complementary transcriptome-wide gene expression analysis in tandem with genome-wide methylation analysis showed that most of the significant correlation of changes in DNA methylation to changes in gene expression was found in the groups representing either decrease in methylation with a concomitant increase in expression or vice versa. This could reflect the classical view on reciprocal inverse relationship between methylation and gene expression. Another interesting finding of this study is that most of the training-induced alterations in methylation occurred in so-called enhancer regions and less frequently in promoter regions (Lindholm *et al.*, 2014). However, although alterations in promoter methylation were less frequent in response to endurance training, those CpG

sites that were differentially methylated in promoter regions were the most capable of affecting corresponding gene expression levels. The gene pathways most involved in promoter hypomethylation were those associated with muscle structure, actin-myosin interaction, oxidative metabolism and calcium release (Lindholm *et al.*, 2014). Other studies have further investigated DNA methylation using the most recent and comprehensive microarray technology (over 850,000 CpG sites profiled) in type-II diabetics in response to chronic aerobic exercise (4 days/ week, 10 weeks of progressive intensity) (Stephens *et al.*, 2018). Importantly, the authors categorized their patients into either non-responders or responders to exercise according to their phosphocreatine (PCr) recovery rates. Responders and non-responders revealed differential methylation after training. In these differentially methylated CpG sites, non-responders showed reduced promoter methylation for genes involved in glutathione metabolism, insulin signaling, and mitochondrial metabolism pathways (Stephens *et al.*, 2018). Given the previously described studies suggesting that exercise promoted a hypomethylated profile across the genome, it may be assumed that responders would have predominantly possessed a hypomethylated profile with increased gene expression compared to non-responders. However, since in this study hypomethylation was associated with non-responder individuals, it may be hypothesized that exercise responders began training with greater hypomethylation across the genome at baseline, contributing to these findings and requiring further confirmatory investigation. Although these studies present largely agreeable results, it is worth noting that another study found little change in DNA methylation after endurance training in healthy individuals. 450,000 CpG sites were investigated in both young and elderly adults following 12 weeks of chronic aerobic exercise, that consisted of a combination of 2 days/week high-intensity interval exercise (>90% $\dot{V}O_{2peak}$ 4×4 min intervals, 3 min rest between intervals) and 2 other days/week 45-min continuous aerobic exercise (70% $\dot{V}O_{2peak}$) (Robinson *et al.*, 2017). Authors reported that training resulted in less than a 10% change in CpG methylation compared with pre-training (Robinson *et al.*, 2017), which contrasts with the studies described above demonstrating altered methylation after both acute and chronic endurance exercise. One possible explanation for the absence of a significant change in methylation in this study is that rigorous statistical "cut offs" were used to identify methylation changes with relatively small numbers of participants (Sharples & Seaborne, 2019).

In summary, long-term endurance training appears to elicit reduction of DNA methylation in promoter region associated with specific genes involved in metabolic and oxidative pathways, but also in calcium signaling and contractile function signaling. Further studies are required to deepen whether and how aerobic training-induced DNA hypomethylation might directly affect mitochondrial adaptation toward improved function. In addition, the modification of DNA methylation induced by

endurance training result to be dependent on the intensity and duration of the stimulus, as well as on aerobic fitness status and the ability to respond to the training stimulus.

MUSCLE MEMORY

Skeletal muscle memory has been defined as: *"The capacity of skeletal muscle to respond differently to environmental stimuli in an adaptive or maladaptive manner if the stimuli have been previously encountered"* (Sharples et al., 2016b). The concept refers to the retention of modifications at both cellular and tissue levels generated by previous environmental stimuli or stressors such as those resulting from acute or chronic exercise, muscle damage, disease or changes in nutrients which lead to an altered response if the stimulus is encountered again. This mechanism is important for skeletal muscle because if the environment encountered is affecting adaptations positively, the muscle may respond to these stimuli in later life with additional muscle improvement or healthy maintenance across the lifespan; conversely, if the environment is detrimental, the muscle may become more susceptible to impairments later in life. This has important consequences in quality of life, as adequate quantity and quality of skeletal muscle is not only essential for performance in elite sports, but also for improving daily life activities and promoting health in older age (Sharples *et al.*, 2015).

Resistance muscle memory

Concerning exercise and training, muscle encounters this memory mechanism in an adaptively advantageous manner. Indeed, it is becoming evident that molecular and phenotypic responses to chronic exercise are enhanced during subsequent training when a previous similar training has been performed. It has been demonstrated that hypertrophy generated in the muscle as a result of resistance training can be accentuated with a faster and larger muscle growing in response to a second period of similar training which is performed after a prolonged period of detraining or reduced activity in which hypertrophic stimuli are ceased and muscle resumes its phenotypic state to its pre-exercise condition (Egner *et al.*, 2013; Gundersen, 2016; Lee *et al.*, 2018).

Kristian Gundersen's lab was the first to demonstrate the evidence of a muscle capacity to retain and "remember" previous anabolic stimuli and adaptations at cellular level. In 2010, they suggested that the increase in myonuclei in EDL mouse muscle fibers acquired through a mechanical overload stimulus is retained during a subsequent period of denervation-induced muscle atrophy (Bruusgaard *et al.*, 2010). This study was expanded by the same group in 2013 using testosterone administration to mice for 14 days (Egner *et al.*, 2013). The treatment led to robust muscle hypertrophy accompanied by an increase in the number of myonuclei acquired from satellite cells fusion. Following a 3-week testosterone "wash-out" period, although muscle size was reduced to pre-testosterone levels, acquired myonuclei were maintained. Most importantly, when mechanical overload was undertaken after prolonged absence of hypertrophic stimuli, previously testosterone-treated mice exhibited a 31% increase in muscle cross-sectional area compared to the untreated control group that showed a non-

significant 6% increase in muscle size with the same stimulus (Egner *et al.*, 2013). This study alludes to a mechanism whereby muscles which had previously received a hypertrophic stimulus (testosterone) are able to grow their size faster and larger when encountering exercise later, consistent with the muscle memory definition (Egner *et al.*, 2013; Gundersen, 2016). Another study employed a more physiological approach, consisting of an actual resistance training protocol on rats, to assess whether a second retraining may elicit larger muscle size adaptations when the muscle has been previously exposed to a similar training, and whether this mechanism may be facilitated by the acquisition and retention of myonulcei during the first training stimulus and subsequent cessation of activity (Lee *et al.*, 2018). In this study, animals underwent 8 weeks of resistance training (3 sets × 5 reps of loaded ladder climbing from 50% body weight and progressively increased to 300% body weight, twice per day, every third day). The 8-weeks training period was later repeated after 20 weeks of detraining. As previously demonstrated, also in this study, myonuclei increased during training and were retained throughout the duration of detraining. Although cross-sectional area and absolute muscle mass were not characterized by larger increase after retraining, relative muscle mass was further enhanced following the repeated training compare with the previous exercise (Lee *et al.*, 2018). Collectively, these studies have led to the "muscle memory by myonuclear permanence" hypothesis, in which anabolic stimuli such as testosterone, mechanical loading or resistance exercise are able to promote the acquisition of new myonuclei that can be retained throughout stimulus cessation allowing muscle to "remember" its previous encounters during subsequent exposure.

It is worth mentioning that all the studies mentioned so far have been performed in rodent muscle. An important question, therefore, is whether human skeletal muscle possesses a memory by myonuclear permanence as seen in rodent muscle. Currently there is only one study that attempted to directly test this hypothesis. In the study by Psilander and collegues (Psilander *et al.*, 2019), healthy young men performed 10 weeks of unilateral resistance exercise training (3 times per week of leg extension and leg press exercise at 70-85% 1RM), followed by 20 weeks of detraining and a 5 subsequent weeks of bilateral retraining. Skeletal muscle thickness and strength increased significantly in response to the initial exercise training period, which were mostly lost during subsequent detraining. During retraining, however, muscle thickness and strength did not differ between the previously trained leg and the untrained leg. Muscle fiber cross-sectional area showed an increment after the first training, however, remained unchanged during detraining as well as during retraining. In addition, no changes in myonuclear content were detected in response to initial training, detraining, or retraining period. Thereby, since no increase in myonuclei number was found during the initial training and no clear detraining effect was observed for muscle fiber size during the detraining period, this study does not refute the existence of human muscle memory (Psilander *et al.*,

2019). These intriguing findings along with the accessibility of the raw data released by the authors enabled other scientists to perform a secondary analysis on the dataset and publish their own interpretations of this study as a viewpoint in the *Journal of Applied Physiology*. Murach and colleagues (Murach *et al.*, 2019) , given the heterogeneity of human response to exercise training, retrospectively clustered the participants into two groups based on single muscle fiber analyses and immunohistochemical myonuclear data, yielding 11 participants with myonuclear density values higher than baseline after the initial training and the remaining 8 subjects showing no change. Since nine out of the eleven subjects who demonstrated an exercise-induced increase in myonuclear content, subsequently showed a decline during detraining, the authors suggested that the "newly acquired myonuclei" during exercise training were not maintained during detraining. However, in a small subset of participants, myonuclei number was retained and, as the authors of the original article appropriately pointed out in response to this "secondary analysis" (Eftestøl *et al.*, 2020), the new interpretation might also be due to the regression towards the mean pattern, consequently highlighting the absence of myonuclei loss throughout detraining. Based on this it seems there is currently no consensus within the scientific community on the existence of muscle memory via myonuclear retention in human skeletal muscle.

Epi-memory to resistance training

Interestingly, in parallel to memory by myonuclear retention, the role of epigenetics has also emerged as another important mechanism involved in muscle memory enabling muscle to "remember" previous exercise in humans.

Adam Sharples' group demonstrated that DNA methylation signatures in response to resistance training, may be essential in the exercise-induced muscle memory process. In this study (Seaborne *et al.*, 2018*b*) genome-wide and targeted gene expression analyses were performed on human muscle tissue from quadriceps that had undergone a repeated resistance training intervention. The protocol consisted of initial 7 weeks of resistance exercise 3 days per week (training), a rest period lasting 7 weeks (detraining) in which participants returned to normal habitual activity, and a second 7-week period of chronic resistance training (retraining). After the first training period, that was associated with increases in lean leg mass, there were also slightly larger number of hypomethylated compared to hypermethylated CpG sites. Interestingly the number of both hypomethylated and hypermethylated CpG sites remained stable during detraining even as lean muscle mass returned to baseline values. Moreover, following retraining, where the greatest increase in lean mass was observed in participants, the number of hypomethylated CpG sites substantially increased by more than double compared with training and detraining whereas the total number of hypermethylated sites remained constant. When

interrogating the specific genes that were epigenetically modified, the authors identified two key signatures of DNA methylation and associated inverse changes in gene expression across the time course of training, detraining and retraining. The first temporal pattern included genes displaying hypomethylation with corresponding increase in gene expression after the initial training period and induced hypertrophy. Interestingly, hypomethylation of these genes was maintained during detraining, and, fascinatingly, gene expression also remained elevated, despite participants undertaking no exercise and lean leg mass returning to pre-exercise levels. Additionally, these CpG gene sites also demonstrated continued hypomethylation throughout retraining, with a subset of genes showing even greater hypomethylation and enhanced gene expression. Therefore, this gene profile suggests, at DNA methylation level, the presence of an epigenetic memory of previous training-induced hypertrophic stimulus that led to the retention of methylation during detraining and subsequent larger hypomethylation and enhanced gene expression after later retraining. The second temporal pattern included genes that also demonstrated hypomethylation and enhanced gene expression following the first training, but where methylation and gene expression returned to baseline (pre-exercise) levels during detraining. Interestingly however, these genes displayed an even larger increase in hypomethylation and further enhanced gene expression after retraining again suggestive of an epigenetic memory of earlier muscle growth (Seaborne *et al.*, 2018*b*). Together this would suggest that resistance exercise training leads to an enhanced hypomethylated state of genes, which may also be retained during prolonged rest period, and enables greater transcription of these genes during retraining and, thereby, allowing for an enhanced muscle fiber growth response. It remains to be determined whether training-induced DNA hypomethylation persists over a longer period, independent of changes in myonuclear content, and promotes greater muscle fiber hypertrophy during retraining after a more prolonged period of detraining (even up to decades).

Aerobic muscle memory

Even though further insights are still required to clarify the underlying mechanisms of muscle memory, as shown so far, it has been well investigated in relation to resistance exercise with two possible interpretations attributable to myonuclear permanence at the cellular level or through DNA methylation retention at the epigenetic level, respectively. Conversely, little is the knowledge status concerning endurance exercise where the potential presence of an aerobic training-induced skeletal muscle memory is still in the early stage of investigation.

Very few studies utilized a repeated intervention design involving aerobic training. In 1987, Simoneau and colleagues investigated in six sedentary people the effects of two repeated 15-weeks high-intensity training on cycle ergometer interspersed by 7 weeks of detraining on human skeletal

muscles and performance (Simoneau *et al.*, 1987). High-intensity interval training induced improvement in both aerobic ($\dot{V}O_{2max}$) and anaerobic (10 s and 90 s maximal work output) performance parameters and also enzyme involved in both metabolic pathways were increased. Interestingly, in response to the second training program changes were less marked than those observed after the first 15 weeks of training, about 50% less for 10 s maximal output and for $\dot{V}O_{2max}$ and 25% less for 90 s maximal output. However, it worth to note that during detraining all these values did not return to pre-training level and most important 10 s maximal output remained similar to post-training values. The presence of a not completed wash-out could explain the reduction in adaptation during second training period, supported by the notion that response to training become less when maximum trainability is reached (Bouchard *et al.*, 1986). On the opposite, absolute values from anaerobic performance test revealed higher values after second training compared to the initial 15 weeks. Interestingly, according to performance data patterns, the glycolytic markers remained high after 7 weeks of detraining while the oxidative indices dropped almost to the pre-training level. Collectively, all these results suggest that repetitive exercise of high intensity implicates largely oxidative metabolism but also heavily solicited the energy sources rapidly available, modifying the levels of enzymes involved in both the glycolysis and the citric acid cycle. Thereby, after high-intensity interval training anaerobic enzymes and performance are preserved also during 7 weeks of inactivity revealing a greater extent in adaptations after the second training, whereas oxidative parameters showed no maintenance and no different response between the two training periods, excluding any indication of muscle memory pattern. A similar experimental design was recently utilized by Brendon Gurd's group to investigate the reproducibility of training-induced adaptations in response to repeated intervention of high-intensity interval training. The aim was to clarify whether individuals demonstrate similar observed responses when they are repeatedly exposed to the same exercise training intervention. In two different studies, conversely to their hypothesis, authors found that both cardiorespiratory and skeletal muscle adaptations differ when individuals are re-exposed to the same training stimulus after a wash-out period (Del Giudice *et al.*, 2020; Islam *et al.*, 2021). In the first study conducted by Del Giudice and colleagues (Del Giudice *et al.*, 2020) a group of recreationally active participants was exposed to two identical 4-weeks periods of standardized high-intensity interval training separated by a three-month wash-out period. Despite mean changes in maximal oxygen uptake were not different, individual responses in $\dot{V}O_{2max}$ were not reproducible suggesting a potential carryover effects from the first training period to the second one. From this study, a subset of participants had available muscle tissue at each time-point, before and after both training periods, and were included in a second study to assess reproducibility also of indices of skeletal muscle adaptations across the two independents, albeit identical, training periods. In this

second study (Islam *et al.*, 2021) authors not only observed weak or poor non-significant associations between training-induced changes in indices of CS maximal activity, OXPHOS, PGC-1α and LDH-A protein content, and capillary density, but, unexpectedly, they also observed divergent group-level responses for some of the OXPHOS complex subunits, as indicated by the significant interaction effects for CII, CIII and CIV protein expression, demonstrating that an individual (or group of individuals) can exhibit dissimilar adaptive responses in skeletal muscle when re-exposed to the same training stimulus. Collectively, this two works highlight the intra-individual variability in the observed response to endurance exercise and the authors themselves discussed that differences in responsiveness to repeat training periods may be attributable to the influence of a prior training on aerobic adaptation that can affect the subsequent training periods through the muscle memory mechanism. It is important to mention an animal study, which, despite having the purpose of deepening the topic of muscle memory related to hypertrophy, pointed out an interesting finding concerning the possible existence of a memory mechanism for specific aerobic physiological markers. Lee and colleagues (Lee *et al.*, 2018), investigating the myonuclear retention on rats with a repeated resistance training intervention, showed that, although exercise was composed by ladder climbing, also mitochondrial adaptations were affected by training and, more importantly, the authors demonstrated that mitochondria may retain the ability to respond more consistently to repeated noncontinuous stimuli. Indeed, the results of this study revealed a higher concentration of proteins regulating mitochondrial biogenesis processes (PGC-1α, Mfn2, Fis1, Drp1) during the second training period. Similarly, mitochondrial DNA copy number and mitochondrial content (measured by quantifying VDAC protein, a major component of the outer mitochondrial membrane) were also higher at the end of the second training period, also suggesting a greater amount of mitochondria (Lee *et al.*, 2018). A possible explanation for this mechanism may derive from the existence of mechanisms that during the period of interruption of a training stimulus may "protect" specific markers involved in mitochondrial biogenesis processes, allowing them to remain over-expressed for several months after a training stimulus affecting adaptations in response to a subsequent stimulus. A study on mouse model (Kang *et al.*, 2015) genetically modified and able to express a higher amount of PGC-1α (a condition attributable to the effects of aerobic training), seems to confirm this hypothesis. Indeed, unmodified animals, after undergoing 2 weeks of immobilization and subsequent 5 days of return to normal activity, showed significantly lower levels of mitochondrial markers (cytoplasmic COX IV, mtDNA/nDNA ratio, mitochondrial density, mitochondrial citrate synthase activity, and mitochondrial function) compared to control unimmobilized animals, indicating a permanence of deconditioning state over the period of 5 days of normal life-style activity. In contrast to these deconditioned mice, in animals with PGC-1α overexpression, these markers showed values

significantly higher or even equal to those of control unimmobilized animals after 5 days from the cessation of immobilization/of return to normal activity. This result suggests that PGC-1α overexpression may have a significant therapeutic potential in counteracting deleterious consequence of muscle immobilization and facilitating its recovery. Thereby, could be also hypothesize that training-induced enhancement of transcription factors such as PGC-1α may promote better mitochondrial adaptations in skeletal muscle upon administration of a repeated noncontinuous training stimulus. This evidence could suggest the presence of a training-induced mitochondrial memory at skeletal muscle level.

Epi-memory to endurance training

As for muscle memory related to resistance training the epigenetic modifications may be involved also in memory mechanisms concerning aerobic exercise field. Unfortunately, overall, it remains to be established if any of DNA modifications are retained after chronic endurance exercise, even if exercise training ceases. Currently, there is a considerable lack of research looking at the notion of epigenetic memory in response to endurance training, detraining and retraining. However, one study investigated the potential presence of a skeletal muscle transcriptional memory in response to endurance training (Lindholm *et al.*, 2016). Authors investigated the retention of transcriptional memory from earlier training using gene expression profiles analyses via RNA sequencing, in subjects who performed two 12-week one-legged aerobic training periods (45 min, 4 times/week) with a 9-month break in between. In the first training period individuals trained one randomized leg and the other leg remained untrained, whereas in the second period both lower limbs were trained with the same identical protocol as the trained leg in the previous training. Results suggested that there was not a retention of gene expression profiles during detraining period. Furthermore, despite authors found differences in few training-responsive genes between untrained and trained leg following retraining (EIF2 and mTOR signaling were downregulated in untrained leg), these differences were not significant enough to introduce global differences. Also, mitochondrial adaptations, such as citrate synthases activity for mitochondrial content estimation, were not different between the two training interventions. The current evidence does not support the presence of a differential response due to a skeletal muscle memory effect. In this study DNA methylation was not reported, and it remains to be determined if a prior exposition to endurance stimuli evokes an epigenetic memory. Moreover, in this context the exercise paradigm involved was a moderate-intensity endurance training (45min knee-extension at submaximal intensity), but as exposed in the work by Barrès and colleagues (2012) (Barrès *et al.*, 2012) methylation and gene expression involved in mitochondrial biogenesis are more affected with high-intensity exercise. Thereby the lack of

evidence of muscle memory may be explained by the absence of specific stimulus to induce epigenetic modifications on mitochondrial transcription factors. Furthermore, the use of the contralateral leg as a control is recognized to be controversial, as training in only one leg could induce effects on the rest of the body through vascular or systemic components. Skeletal muscle tissue, indeed, releases myokines into the circulation (Pedersen & Febbraio, 2012) that could potentially induce effects even in the untrained leg. All these elements shows that although the response was very consistent, differences in responsiveness to repeat training periods might exist. Unfortunately, it was not possible with this experimental setup to determine whether these slight differences are due to natural biological variability, or some type of memory mechanism.

Summary

Overall, given the studies described above, future work is required to investigate whether cellular adaptations or DNA methylation changes in the muscle tissue are retained in humans after aerobic exercise training and in addition how long they are maintained before being lost after cessation of stimulus. Repeated intervention studies might be the appropriate method to test whether maintenance of adaptations results in an increased metabolic or oxidative response to subsequent exposure to the same aerobic stimulus. Additionally, specific investigations at the cellular and molecular level could deepen our understanding of the mechanism underpinning a potential aerobic muscle memory phenomenon. If the scientific community could identify what type, intensity, and frequency of exercise is required to maintain a memory of aerobic exercise over long periods of time, then this information could be used to optimize training programs for athletes and recovery from injury in previously active individuals (i.e., individuals who are detrained/unconditioned), as well as improve activities of daily living and promote health in elderly or metabolic disease conditions.

CHAPTER 2

AIMS

The overarching aim of the present thesis was to investigate the potential presence of skeletal muscle memory in response to repeated high-intensity endurance training interventions. In addition, a methodological project was carried out to assess a novel *in vivo* approach to estimate muscle oxygen diffusion capacity.
Therefore, a series of studies were conducted to achieve the following aims:

Study 1 aimed to assess a novel *in vivo* approach to estimate muscle oxygen diffusion capacity based on non-invasive near-infrared spectroscopy measurement via an innovative protocol of arterial occlusions performed in both oxygen limiting and not limiting conditions.

Study 2 aimed to investigate functional and molecular adaptations of skeletal muscle in response to two repeated interventions of high-intensity interval training in mice to deepen our understanding of the potential presence of skeletal muscle memory induced by aerobic training.

Study 3 aimed to investigate whether repeated endurance training interventions may rely on muscle memory mechanism in humans exploring aerobic adaptations at all levels of the entire human organism, from the epigenetic level to the whole-body response to exercise, across repeated exposure to two identical interval training interventions separated by long-term period of detraining.

CHAPTER 3

STUDY 1

Near-infrared spectroscopy estimation of combined skeletal muscle oxidative capacity and O_2 diffusion capacity in humans

Pilotto AM[1,2], Adami A[3], Mazzolari R[2,4], Brocca L[2], Crea E[2], Zuccarelli L[1], Pellegrino MA[2,5], Bottinelli R[2,5], Grassi B[1], Rossiter HB[6] and Porcelli S[2,7]

[1] Department of Medicine, University of Udine, Udine, Italy

[2] Department of Molecular Medicine, University of Pavia, Pavia, Italy

[3] Department of Kinesiology, University of Rhode Island, Kingston, RI, USA

[4] Department of Physical Education and Sport, University of the Basque Country (UPV/EHU), Vitoria-Gasteiz, Spain

[5] Interdipartimental Centre for Biology and Sport Medicine, University of Pavia, Pavia, Italy

[6] Division of Respiratory and Critical Care Physiology and Medicine, The Lundquist Institute for Biomedical Innovation at Harbor–UCLA Medical Center, Torrance, CA, USA

[7] Institute of Biomedical Technologies, National Research Council, Milan, Italy

ABSTRACT

PURPOSE: The final steps of the O_2 cascade during exercise depend on the product of the microvascular-to-intramyocyte PO_2 difference and muscle O_2 diffusing capacity (DmO_2). Non-invasive methods to determine DmO_2 in humans are currently unavailable. Muscle oxygen uptake ($m\dot{V}O_2$) recovery rate constant (k), measured by near-infrared spectroscopy (NIRS) using intermittent arterial occlusions, is associated with muscle oxidative capacity *in vivo*. We reasoned that k would be limited by DmO_2 when muscle oxygenation is low (k_{LOW}), and hypothesized that: i) k in well-oxygenated muscle (k_{HIGH}) is associated with maximal O_2 flux in fiber bundles; and ii) Δk (k_{HIGH}-k_{LOW}) is associated with capillary density (CD). METHODS: Vastus lateralis k was measured in 12 participants using NIRS after moderate exercise. The timing and duration of arterial occlusions were manipulated to maintain tissue saturation index (TSI) within a 10% range either below (LOW) or above (HIGH) half-maximal desaturation, assessed during sustained arterial occlusion. RESULTS: Maximal O_2 flux in phosphorylating state was 37.7±10.6 $pmol \cdot s^{-1} \cdot mg^{-1}$ (~5.8 $ml \cdot min^{-1} \cdot 100g^{-1}$). CD ranged 348 to 586 mm^{-2}. k_{HIGH} was greater than k_{LOW} (3.15±0.45 vs 1.56±0.79 min^{-1}, $p<0.001$). Maximal O_2 flux was correlated with k_{HIGH} ($r=0.80$, $p=0.002$) but not k_{LOW} ($r=-0.10$, $p=0.755$). Δk ranged -0.26 to -2.55 min^{-1}, and correlated with CD ($r=-0.68$, $p=0.015$). CONCLUSIONS: $m\dot{V}O_2$ k reflects muscle oxidative capacity only in well-oxygenated muscle. Δk, the difference in k between well- and poorly-oxygenated muscle, was associated with CD, a mediator of DmO_2. Assessment of muscle k and Δk using NIRS provides a non-invasive window on muscle oxidative and O_2 diffusing capacity.

INTRODUCTION

The primary source of ATP supply in skeletal muscle during endurance exercise is ADP phosphorylation coupled to the reduction of O_2 (Picard *et al.*, 2016). Two primary resistances, limiting the maximal conductance of O_2 from the atmosphere to the muscle mitochondrion, reside within the cardiovascular system (i.e., convective O_2 transport) and at the muscle capillary-myocyte interface (i.e., diffusive O_2 transport) (Wagner, 1992, 1995, 2000; Richardson *et al.*, 1995*a*).

The interaction of the maximum rate of convective O_2 transport and muscle O_2 diffusing capacity (DmO_2) determines the maximal muscle O_2 uptake ($m\dot{V}O_2$) (Roca *et al.*, 1992), the final steps of the O_2 cascade determining $m\dot{V}O_2$ depend on the product of the transmembrane PO_2 gradient (microvascular (mv) to intramyocyte (im) PO_2) and the muscle diffusing capacity for O_2 (DmO_2) (Fick's law of diffusion):

$$m\dot{V}O_2 = DmO_2 \times (PmvO_2 - PimO_2) \qquad \text{Eq. 1 (Study 1)}$$

where ($PmvO_2 - PimO_2$) is strongly dependent on convective O_2 delivery and muscle O_2 demand (as a function of power output). This results in $PimO_2$ becoming essentially constant at ~1-5 mmHg during exercise above ~50% maximum O_2 uptake ($\dot{V}O_{2max}$) (Richardson *et al.*, 1995*b*; Clanton *et al.*, 2013). DmO_2, on the other hand, is a complex function of muscle capillarity, the surface area of apposition of red blood cells to capillary endothelium, red blood cell capillary transit time, haemoglobin volume, and the O_2 solubility properties within the diffusion pathway (Honig *et al.*, 1984; Groebe & Thews, 1986; Bebout *et al.*, 1993; Wagner, 1995; Poole *et al.*, 2020). Notwithstanding these confounding variables, DmO_2 is related to capillary density (CD; the number of capillaries per summed muscle fiber cross-sectional area) (Saltin & Gollnick, 1983; Hepple *et al.*, 2000; Poole *et al.*, 2020, 2021, 2022). The observed linear relationship between estimated $PmvO_2$ and $\dot{V}O_{2max}$ supports the concept that DmO_2 is a major limiting variable for $m\dot{V}O_{2max}$ in humans (Roca *et al.*, 1992; Richardson *et al.*, 1999). Methods to estimate DmO_2 in humans *in vivo* are complex and previous attempts on quadriceps muscle required invasive procedures with repeated exercise tests using breathing of gas mixtures containing high and low fractions of inspired O_2. Another approach, using non-invasive venous occlusion plethysmography to assess capillarity filtration (Brown *et al.*, 2001) provides an indirect estimation of limb capillarity, but is sensitive to changes in oncotic pressure, endothelial tight junctions and influenced by all tissues within the limb, not only muscle (Hunt *et al.*, 2013).

We sought to simplify assessment of DmO_2 in human quadriceps using a more muscle specific approach. We reasoned that, if we could make non-invasive measurements of $m\dot{V}O_2$ under two different ($PmvO_2 – PimO_2$) conditions (i.e. HIGH and LOW), we would be able to solve for DmO_2 by simultaneous subtraction of the two unknowns ($m\dot{V}O_2$ and $PmvO_2$, respectively) in Eq. 1, assuming, as in Roca et al. (1992), that $PimO_2$ is negligible. Near-infrared spectroscopy (NIRS) provides a relatively simple and non-invasive means to estimate muscle oxidative capacity (Grassi & Quaresima, 2016; Hamaoka & McCully, 2019). The recovery rate constant of $m\dot{V}O_2$ (k) established from the rate of decline in muscle tissue saturation index (TSI) under serial, intermittent, arterial occlusions (Hamaoka *et al.*, 1996; Motobe *et al.*, 2004; Ryan *et al.*, 2012; Adami *et al.*, 2017; Adami & Rossiter, 2018) shows good agreement with estimates of muscle oxidative capacity by other techniques e.g., phosphocreatine recovery time constant (r = 0.88 – 0.95) (Ryan *et al.*, 2013*b*) or respiratory rates in fiber bundles (r = 0.61 – 0.74) (Ryan *et al.*, 2014).

We modified the NIRS-based assessment of $m\dot{V}O_2$ by manipulating the timing and duration of the intermittent arterial occlusions, thereby controlling the mean ($PmvO_2 – PimO_2$) at, separately, both HIGH (non-O_2 limiting) and LOW (O_2 limiting) values following moderate exercise. More specifically, we used k as proxy for $m\dot{V}O_2$ and TSI as a proxy of PmvO2. Although not without limitations, this approach led us to solve the Fick's law of diffusion as follows:

$$k = DmO_2 \times TSI$$

where PimO2 is considered negligible.

Then, we calculated k for both HIGH (k_{HIGH}) and low (k_{LOW}) TSI values and we compared the k values with variables obtained from biopsy taken from the same muscle location and individuals. We hypothesized that the recovery rate constant of $m\dot{V}O_2$ in high TSI conditions (k_{HIGH}) is associated with muscle oxidative capacity assessed using high resolution respirometry of permeabilized muscle fiber bundles.

Finally, we estimated DmO_2 from the difference in k values obtained in HIGH and LOW conditions ($\Delta k = k_{HIGH} - k_{LOW}$) and by calculating ΔTSI, according to the following equation:

$$\Delta k / \Delta TSI = DmO_2 \sim CD$$

We then tested the hypothesis that the difference in the recovery rate constant of $m\dot{V}O_2$ between HIGH and LOW TSI conditions (Δk) is associated with capillary density (CD) from biopsy histology.

MATERIALS AND METHODS

Subjects

Twelve moderately trained male (n = 7) and female (n = 5) adult participants (age 28 ± 5 yrs; weight 64.3 ± 10.2 kg; height 173 ± 7 cm) were recruited from the local community. All participants completed a health history questionnaire to ensure there was no presence of chronic disease. None of the participants took any medications known to alter metabolism. Participants were fully informed about the aims, methods, and risks, and gave their written informed consent prior to enrollment. All procedures were in accordance with the Declaration of Helsinki and the study was approved by the local ethics committee (Besta 64-19/07/2019).

Study Design

Participants visited the laboratory on four non-consecutive days over a 2-wk period (**Fig. 1**). They were instructed to abstain from strenuous physical activity for at least 24 h prior to each testing session (48 h for the biopsy trial). At visit 1, anthropometric measurements were taken, and an incremental cardiopulmonary exercise test to the limit of tolerance was administered on an electronically braked cycle ergometer (LC-6, Monark, Sweden) to determine $\dot{V}O_{2peak}$ and gas exchange threshold (GET). At visits 2 and 3, participants performed repeated muscle oxidative capacity tests within HIGH or LOW muscle oxygenation conditions (2 repeats at each visit), immediately after 5 min constant work-rate cycling at 80% GET (Zuccarelli *et al.*, 2020). At visit 4, approximately 100 mg of skeletal muscle was obtained from the *vastus lateralis* muscle by percutaneous conchotome muscle biopsy under local anesthesia (1% lidocaine) for muscle respirometry and morphology.

Figure 1 (Study 1). Study design and muscle recovery rate constant (*k*) protocol by NIRS

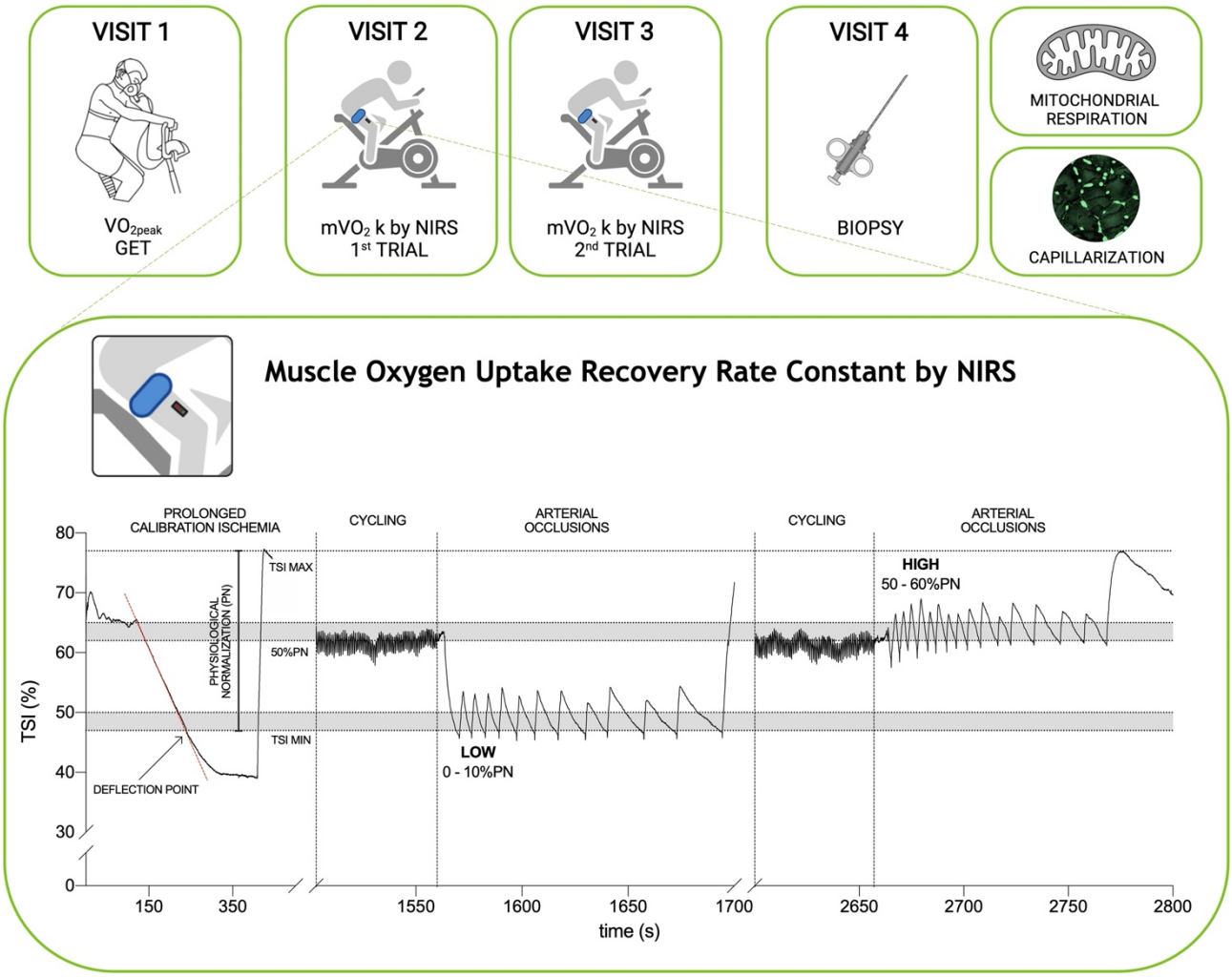

Participants visited the laboratory on 4 occasions. Visit 1 was used to determine peak oxygen uptake ($\dot{V}O_{2peak}$) and gas exchange threshold (GET). Visits 2 and 3 were used to determine the physiological normalization (PN) of quadriceps TSI following sustained arterial occlusion, and the muscle $\dot{V}O_2$ recovery rate constant (*k*) in well-oxygenated (HIGH) and poorly-oxygenated (LOW) conditions. Two *k* measurements were performed at each visit. To measure *k*, participants initially cycled for 5 min at 80% GET, followed immediately by 10-20 intermittent arterial occlusions (300 mmHg). The duration and timing of repeated occlusions were modulated in order to maintain TSI in two different ranges: from 0 to 10% of PN (LOW) and from 50 to 60% of PN (HIGH). A muscle biopsy was obtained in visit 4.

Incremental exercise

Power during step-incremental cycling was increased 10-15 W every minute, depending on the individual's fitness. Participants were instructed to maintain constant cadence at their preferred value (between 70 and 85 rpm). Intolerance was defined when participants could no longer maintain their chosen pedaling frequency despite verbal encouragement. Pulmonary gas exchange and ventilatory variables were determined breath-by-breath using a metabolic cart (Vyntus CPX, Vyaire Medical GmbH, Germany), which was calibrated following the manufacturer's instructions before each test.

HR was recorded by using a chest band (HRM-Dual, Garmin, Kansas, USA), and rating of perceived exertion (RPE) was determined using Borg® 6–20 scale (Borg, 1982). At rest, and at 1, 3, and 5 min of recovery, 20 μL of capillary blood was obtained from a preheated earlobe for blood lactate concentration (Biosen C-line, EKF, Germany). Peak cardiopulmonary variables were measured from the highest 20 s mean values prior to intolerance. GET was determined by two independent investigators by using the modified "V-slope" method (Beaver *et al.*, 1986). The power at GET was estimated after accounting for the individual's $\dot{V}O_2$ mean response time (Whipp *et al.*, 1981).

Muscle Oxygen Uptake Recovery Rate Constant by NIRS

The m$\dot{V}O_2$ recovery *k* was measured using an approach modified from Zuccarelli et al. (Zuccarelli *et al.*, 2020). Oxygenation changes of the *vastus lateralis* were sampled at 10 Hz by a wireless, portable, continuous-wave, spatially-resolved, NIRS device (PortaLite, Artinis, The Netherlands). Briefly, this device is equipped with three fiber optic bundles: NIR light is emitted from three optodes at two wavelengths (760 nm and 850 nm) and received from a fourth optode for transmission back to the data acquisition unit to determine the relative concentrations of deoxy- and oxy-genated heme groups contained in hemoglobin (Hb) and myoglobin (Mb). This method does not distinguish between the contributions of Hb and Mb to the NIRS signal, but Mb signal was assumed to be of minor impact compared to the contribution of Hb (Grassi & Quaresima, 2016; Hamaoka & McCully, 2019). Relative concentrations of deoxy-(hemoglobin+myoglobin) (Δ[deoxy(Hb+Mb)]) and oxy-(hemoglobin+myoglobin) (Δ[oxy(Hb+Mb)] were measured in the tissues approximately 1.5 – 2 cm beneath the probe, with respect to an initial value obtained at rest before any procedure arbitrarily set equal to zero. From these measurements, relative changes in total hemoglobin and myoglobin (Δ[tot(Hb+Mb)] = Δ[oxy(Hb+Mb)] + Δ[deoxy(Hb+Mb)]) and the Hb difference (Δ[diff(Hb+Mb)] = Δ[oxy(Hb+Mb)] – Δ[deoxy(Hb+Mb)]) were calculated. In addition, the tissue saturation index (TSI, %) was measured using the spatially-resolved spectroscopy (SRS) approach (Ferrari *et al.*, 2004).

The skin at the NIRS probe site was shaved before the probe was placed longitudinally on the lower third of *vastus lateralis* muscle (~10 cm above the knee joint), and secured with a black patch and elastic bandage. The location of the probe was marked using a skin marker to ensure the placement location was similar across all visits. The mean thickness of the skin and subcutaneous tissue at the NIRS probe site (7.8 ± 3.1 mm) was measured by skinfold caliper (Holtain Ltd, Crymych, UK). A 13 × 85 cm rapid-inflation pressure-cuff (SC12D, Hokanson, USA) was placed proximally on the same thigh and attached to an electronically-controlled rapid cuff-inflator (E20, Hokanson, USA).

While participants were seated on a cycle ergometer, baseline TSI and Δ[tot(Hb+Mb)] were measured over 2 min of rest. Subsequently, a prolonged arterial occlusion (300 mmHg) was performed until TSI plateaued (typically ~120 s). The cuff was instantly deflated and muscle reoxygenation was recorded until a steady-state was reached (typically ~3 min). This procedure identified the physiological normalization (PN) of TSI which was standardized to 0% at the deflection point (TSI min) and 100% at the maximum value reached during reperfusion (TSI max) (Adami *et al.*, 2017) (**Fig. 1**). Participants then cycled for 5 min at a target of 80% GET, followed by an immediate stop and 10-20 intermittent arterial occlusions at 300 mmHg. Duration and timing of the repeated occlusions were controlled by the investigator to maintain TSI in two different ranges: from 0 to 10% of PN (LOW) and from 50 to 60% of PN (HIGH), where the total amplitude of PN was used as 0-100% reference range (**Fig. 1**). The HIGH range was selected to ensure that occlusions were performed under well oxygenated conditions, and to avoid the reduction in PO_2 could limit $m\dot{V}O_2$ (i.e. maintaining TSI above 50% of the physiological normalization) (Haseler *et al.*, 2004)(Adami & Rossiter, 2018). The LOW range was selected as the lowest boundary to evaluate $m\dot{V}O_2$ recovery *k* in poorly-oxygenated conditions, without overstepping the deflection point (i.e., where TSI during occlusions loses linearity). On the same day two repetitions of repeated occlusions protocol, separated by a resting period (typically ~5 min), were performed in a randomized order for both the LOW and HIGH experimental conditions.

The rate of muscle desaturation during each intermittent arterial occlusion (TSI, $\%\cdot s^{-1}$) was fitted to estimate the exponential $m\dot{V}O_2$ recovery or *k*, as previously described (Adami *et al.*, 2017) (**Fig. 2**). Data were quality-checked before curve fitting to remove invalid values or outliers i.e., low initial TSI values, or incomplete occlusions (Beever *et al.*, 2020). The test-retest variability of *k* was first assessed. Subsequently *k* within each condition (k_{HIGH} and k_{LOW}) was calculated from the mean of the two repeated measurements, and the difference between these conditions was calculated ($\Delta k = k_{HIGH.} - k_{LOW}$). Δ[tot(Hb+Mb)] above rest was measured during the arterial occlusions of both HIGH and LOW conditions.

Figure 2 (Study 1). Representative tissue saturation index (TSI) responses during repeated arterial occlusions of the quadriceps following moderate exercise in LOW and HIGH conditions

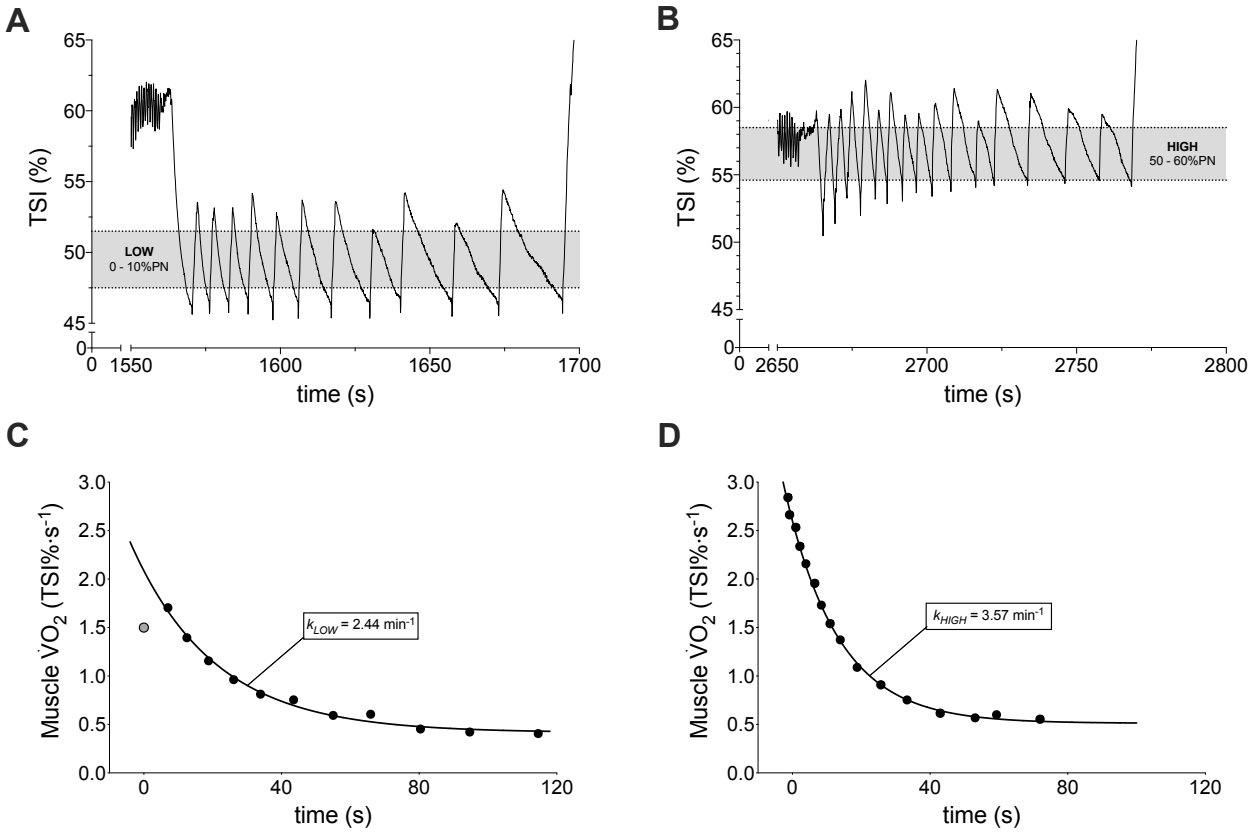

Representative muscle TSI profiles and m$\dot{V}O_2$ recovery kinetics during intermittent arterial occlusions following 5 min moderate intensity cycling. **A)** TSI profile in poorly-oxygenated (LOW; TSI = 0-10% of physiological normalization) condition. **B)** TSI profile in well-oxygenated (TSI = 50-60% of physiological normalization) condition. **C)** m$\dot{V}O_2$ recovery and exponential fit (black line) for calculation of k_{LOW}. **D)** m$\dot{V}O_2$ recovery and exponential fit (black line) for calculation of k_{HIGH}. Grey point represents outlier, excluded from the analysis (see methods). *k* is the recovery rate constant. n=1.

Muscle Biopsy

Resting muscle biopsies were taken from the *vastus lateralis* muscle using a 130 mm (6") Weil-Blakesley rongeur (NDB-2, Fehling Instruments, GmbH&Co, Germany) under local anesthesia (1% lidocaine). After collection, muscle samples were cleaned of excess blood, fat, and connective tissue in ice-cold BioPS, a biopsy-preserving solution containing (in mM) 2.77 CaK_2EGTA, 7.23 K_2EGTA, 5.77 Na_2ATP, 6.56 $MgCl_2$, 20 taurine, 50 MES (2-(N-morpholino)ethanesulfonic acid), 15 Na_2phosphocreatine, 20 imidazole, and 0.5 dithiothreitol adjusted to pH 7.1 (Doerrier *et al.*, 2018). A portion of each muscle sample (~10-20 mg) was immediately placed in BioPS plus 10% (w/v) fatty acid free bovine serum albumin (BSA) and 30% (v/v) dimethyl sulfoxide (DMSO) and quickly frozen in liquid nitrogen; subsequently this portion was stored at -80°C for measurements of mitochondrial

respiration within one month (Kuznetsov *et al.*, 2003). The remaining portion were fixed in OCT (Tissue-Tek, Sakura Finetek Europe, Zoeterwoude, The Netherlands) embedding medium, frozen in N_2-cooled isopentane and stored at -80°C for subsequent histology.

Preparation of Permeabilized Fibers

Fiber bundles were quickly thawed at room temperature by immersion in BioPS containing 2 mg·ml^{-1} BSA to remove any residual DMSO from the tissue (Kuznetsov *et al.*, 2003; Wüst *et al.*, 2012). Fibers were mechanically separated with pointed forceps in ice-cold BioPS under magnification (70×) (Stereomicroscope CRYSTAL-PRO, Konus-optical & sports systems, Italy). The plasma membrane was permeabilized by gentle agitation for 30 min at 4°C in 2 ml of BioPS containing 50 µg·ml^{-1} saponin, washed for 10 min in 2 ml of MiR06 (MiR05 + catalase 280 IU·ml^{-1}) (in mM, unless specified) 0.5 EGTA, 3 $MgCl_2$, 60 potassium lactobionate, 20 taurine, 10 KH_2PO_4, 20 HEPES (4-(2-hydroxyethyl)piperazine-1-ethanesulfonic acid), 110 sucrose, and 1 g·L^{-1} BSA, essentially fatty acid–free (pH 7.1) (Doerrier *et al.*, 2018) and blotted prior to being weighed.

Mitochondrial Respiration

Mitochondrial respiration was measured in duplicate or triplicate, using 3-6 mg wet weight of muscle fibers, in 2ml of MiR06 at 37°C containing myosin II-ATPase inhibitor (25µM blebbistatin dissolved in DMSO 5mM stock) to inhibit contraction (Perry *et al.*, 2011) (Oxygraph-2k, Oroboros, Innsbruck, Austria). Chamber O_2 concentration was maintained between 250 and 450 nmol·ml^{-1} (average O_2 partial pressure 250 mmHg) to avoid O_2 limitation of respiration. Intermittent reoxygenation steps were performed during the experiments by injections of 1-3 µl of 0.3 mM H_2O_2, which was instantaneously dismutated by catalase, already present in the medium, to O_2 and H_2O. Instruments were calibrated according to the manufacturer's instructions (Pesta & Gnaiger, 2012).

A substrate-uncoupler-inhibitor titration protocol was used (Salvadego *et al.*, 2016, 2018; Doerrier *et al.*, 2018) in the following order: glutamate (10 mM) and malate (4 mM) was added to assess LEAK respiration through complex I (CI_L). ADP (10 mM) was added to assess maximal oxidative phosphorylation (OXPHOS) capacity through CI (CI_P). Succinate (10 mM) was added to assess OXPHOS capacity through CI + complex II ($CI+II_P$). Cytochrome c (10 µM) added to test for outer mitochondrial membrane integrity. Stepwise additions of carbonyl cyanide-p trifluoromethoxyphenylhydrazone (FCCP) (0.5 – 1.5 µM) were used to measure electron transport system capacity through CI+II ($CI+II_E$). Inhibition of CI by rotenone (1 µM) determined electron transport system capacity through CII (CII_E), while addition of antimycin A (2.5 µM) was used to

measure residual oxygen consumption, which was subtracted from all measurements. Results were expressed in pmol·s^{-1}·mg^{-1} wet weight calculating mean values of duplicate analyses. At the conclusion of each experiment, muscle samples were removed from the chamber, immediately frozen in liquid nitrogen and then stored at -80°C until measurement of CS activity.

Citrate Synthase Activity

Muscle samples were thawed and underwent a motor-driven homogenization in a pre-cooled 1 mL glass-glass potter (Wheaton, USA). The muscle specimen was suspended 1:50 w/v in a homogenization buffer containing sucrose (250 mM), Tris (20 mM), KCl (40 mM) and EGTA (2 mM) with 1:50 v/v protease (P8340-Sigma) inhibitors. The specimen was homogenized in an ice-bath with 20 strokes at 500 rpm; before the last hit Triton X-100 (0.1% v/v) was added to the solution. After this, the sample was left in ice for 30 min. The homogenate was centrifuged at 14,000 g for 10 min. The supernatant was used to evaluate protein concentration according to the method of Lowry et al. (1951) (Lowry *et al.*, 1951). Protein extracts (5–10–15 µg) were added to each well of a 96-well-microplate along with 100 µl of 200 mM Tris, 20 µl of 1 mM 5, 5'-dithiobis-2-nitrobenzoate (DTNB), freshly prepared, 6 µl of 10mM acetyl-coenzyme A (Acetyl-Co-A) and mQ water to a final volume of 190 µl. A background ΔAbs, to detect any endogenous activity by acetylase enzymes, was recorded for 90 s with 10 s intervals at 412 nm at 25°C by an EnSpire 2300 Multilabel Reader (PerkinElmer). The ΔAbs was subtracted from the one given after the addition of 10 µl of 10 mM oxalacetic acid that started the reaction. All assays were performed at 25°C in triplicate on homogenates. Activity was expressed as nmol·min^{-1} (mU) per mg of protein. This protocol was modified from (Srere, 1969; Spinazzi *et al.*, 2012).

Cross-Sectional Area (CSA) Analysis

Muscle fiber CSA was determined from several transverse sections (10 µm thick) obtained from muscle samples and probed with anti-Dystrophin antibody. Fluorescence images were visualized with Olympus microscope (U-CMAD3). Fiber CSA was measured with Image J analysis software (NIH, Bethesda, MD, USA) and expressed in square micrometers. 125 to 150 fibers per sample were measured.

Capillarization

Several transverse 10 µm sections were obtained from muscle samples mounted in OCT. Sections were collected at – 20-22°C on the surface of a polarized glass slide. Cryosections were fixed with methanol in ice for 15 min, washed 3 times (5 min each) in PBS (NaCl 136mM, KCl 2mM, Na_2HPO_4

6mM, KH_2PO_4 1mM) at room temperature (RT) and incubated in 1%Triton-100x in PBS for 30 min (RT). Cryosections were then incubated with blocking reagents (4% BSA in 1% Triton X-100 in PBS + 5% Goat Serum) for 30 min (RT), raised with PBS (3 times of 5 min each) and probed with anti-CD31 (1:100 dilution, Abcam) overnight at 4°C. After 3 washes (5 min each) in PBS, cryosections were incubated with Alexa-Fluor 488 anti-mouse (1:200 dilution; Abcam) for 60 min at room temperature. Finally, the samples were probed with anti-Dystrophin (1:500 dilution, Abcam) for 60 min at room temperature and then with Alexa-Fluor 488 anti-rabbit (1:200 dilution; Abcam) for 60 min at room temperature. Fluorescence intensity was visualized with Olympus microscope (U-CMAD3). 125 to 150 fibers were measured in each sample. Capillary density was defined as total number of capillaries per cross-sectional area of the associated muscle fibers (Hoppeler *et al.*, 1981; Mathieu-Costello *et al.*, 1988, 1991, 1992; Hepple *et al.*, 2000).

Statistical Analysis

Results are mean ± SD. Normal distribution was verified with Shapiro–Wilk test, and paired Student's t-test was used to compare differences between two means. $p < 0.05$ was considered significant. To assess within-subject test–retest reliability, Pearson coefficient (r), coefficient of variation (CV) and intraclass correlation coefficient (ICC) were calculated for *k* measurements performed on different days. Correlation between respirometry variables and *k* was performed to compare *ex vivo* and *in vivo* estimates of muscle oxidative capacity. Correlation between CD and Δk was performed to examine the validity of NIRS to estimate DmO_2. Correlation analyses were expressed as Pearson coefficient (r). Prism 8.0 (GraphPad) was used for data analysis.

RESULTS

Incremental Exercise

$\dot{V}O_{2peak}$ was 37.1 ± 8.0 $ml \cdot min^{-1} \cdot kg^{-1}$ (range, 22.0 – 50.2 $ml \cdot min^{-1} \cdot kg^{-1}$) at 214 ± 52 W. Peak heart rate was 192 ± 9 $beats \cdot min^{-1}$, approximately 102% of the age-predicted maximum value. RER was 1.28 ± 0.08; $[La]_b$ was 11.27 ± 2.24 $mmol \cdot l^{-1}$, and RPE was 19 ± 1. GET was 1.73 ± 0.41 $l \cdot min^{-1}$ (69% of $\dot{V}O_{2peak}$), corresponding to 129 ± 34 W.

Muscle Oxygen Uptake Recovery Rate Constant by NIRS

A total of 48 $m\dot{V}O_2$ recovery kinetics assessments were performed (24 in each of HIGH and LOW conditions) after 5-min moderate intensity exercises (87 ± 26 W). Average $\dot{V}O_2$ from last 60 s of exercise was 1.43 ± 0.38 $l \cdot min^{-1}$ and RER was 0.95 ± 0.03. At the end of exercise RPE was 10 ± 2

and $[La]_b$ was 1.47 ± 0.39 mmol·l^{-1}. During last 20 s of cycling quadriceps TSI averaged 62.7 ± 3.9% (corresponding to 50.4 ± 6.4% of PN).

k_{HIGH} was 3.15 ± 0.45 min^{-1} and 2.79 ± 0.55 min^{-1} for the first and second repeat respectively (range 1.88 - 4.01 min^{-1}). k_{HIGH} was not different between repeats (p = 0.1057). k_{LOW} was 1.56 ± 0.79 min^{-1} and 1.53 ± 0.57 min^{-1} for first and second repeat, respectively (range 0.38 - 2.65 min^{-1}). k_{LOW} was not different between repeats (p = 0.9299). Coefficient of variation for repeated measurements was 26% and 12% for LOW and HIGH, respectively. In all participants and each repeat, k_{HIGH} was greater than k_{LOW} (both p < 0.001). The individual test-retest reliability of k_{HIGH} and k_{LOW}, assessed on different days, was good (r = 0.67, p < 0.001; ICC = 0.68, CV = 19%) (**Fig. 3**). Having established reproducibility, the mean *k* for each condition was calculated for comparison with biopsy variables. Mean k_{HIGH} was 2.97 ± 0.36 min^{-1} and mean k_{LOW} was 1.54 ± 0.55 min^{-1}. Δ*k* ranged from 0.26 to 2.55 min^{-1} with a mean value of 1.42 ± 0.69 min^{-1}. Immediately before the first cycling exercise, Δ[tot(Hb+Mb)] was 3.14 ± 0.77 µM and increased to 9.57 ± 4.52 µM and 11.20 ± 4.05 µM during arterial occlusions in HIGH and LOW respectively. During arterial occlusions, Δ[tot(Hb+Mb)] was significantly greater than rest (p = 0.007 and p = 0.002 for HIGH and LOW, respectively).

Figure 3 (Study 1). Individual test-retest reliability of muscle oxidative capacity by NIRS

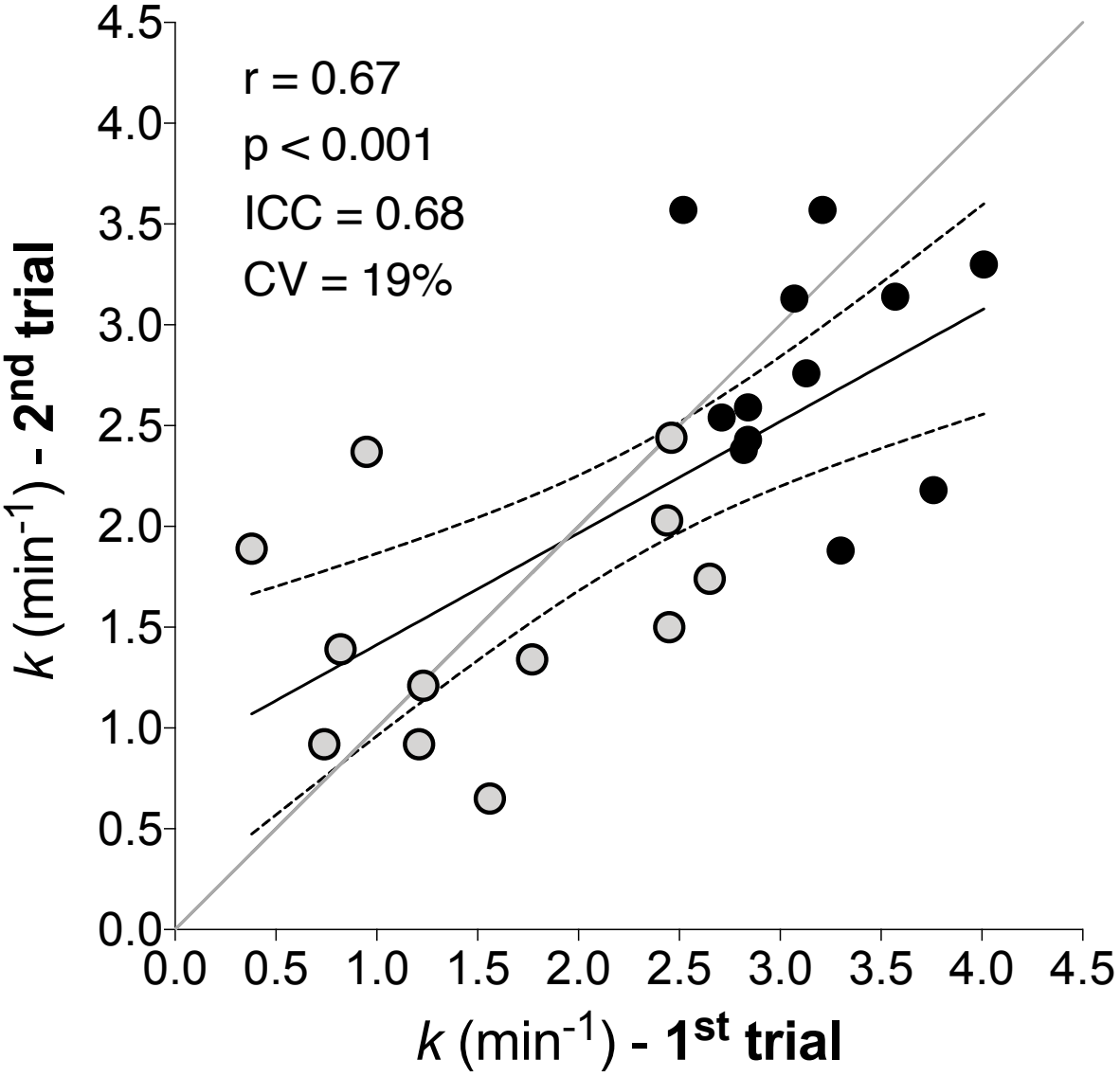

The individual test-retest reliability of recovery rate constant (*k)* assessed by NIRS in different days during both HIGH (black circles) and LOW (grey circles) on 12 participants. Straight line represents linear regression curve and dashed line represent 95% confidence intervals. Grey line represents identity. Circles represent *k* values obtained during first and second trial.

Muscle Mitochondrial Respiration and Capillarization

Measurements of mitochondrial O_2 flux in permeabilized muscle fibers are shown in **Table 1**. Maximal O_2 flux in phosphorylating state (CI+II$_P$) was 37.7 ± 10.6 pmol·s^{-1}·mg^{-1} (corresponding to 5.8 ml·min^{-1}·100g^{-1}) and maximal uncoupled O_2 flux (CI+II$_E$) was 56.8 ± 19.8 pmol·s^{-1}·mg^{-1} (corresponding to 8.8 ml·min^{-1}·100g^{-1}). CS activity was 74.3 ± 50.9 mU·mg^{-1} protein.

Two typical images of CD capillary density measurement are shown in **Figure 4**. Mean fiber CSA, fiber number and capillary number in each sample were 5083 ± 73 μm^{-2}, 134 ± 47 and 311 ± 108, respectively. CD was 469 ± 73 mm^{-2}, ranging from 348 to 586 mm^{-2} among individuals.

Table 1 (Study 1). Mitochondrial O_2 flux in permeabilized muscle fibers

Mass specific ($pmol \cdot s^{-1} \cdot mg^{-1}$)	CI_L	CI_P	$CI+II_P$	$CI+II_E$	CII_E
Mean ± SD	6.0 ± 3.2	14.6 ± 5.8	37.7 ± 10.6	56.8 ± 19.8	45.3 ± 14.8
Min	0.0	4.5	23.0	33.6	29.1
Max	11.3	23.9	54.3	99.9	76.6

CI_L, leak respiration through CI; CI_P, maximum coupled mitochondrial respiration through CI; $CI+II_P$, maximum coupled mitochondrial respiration through CI+II; $CI+II_E$, maximum noncoupled mitochondrial respiration through CI+II; CII_E, maximum noncoupled mitochondrial respiration through CII. Mitochondrial respiration was measured in duplicate or triplicate, n=12.

Figure 4 (Study 1). Muscle capillarization from two participants

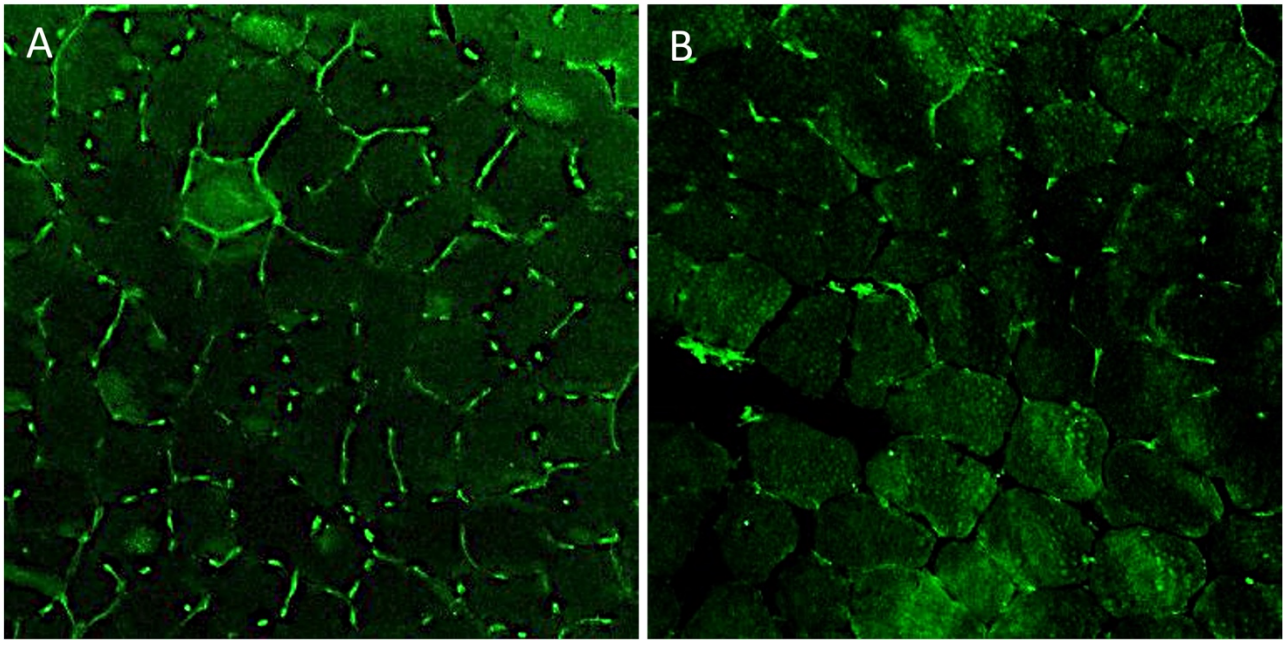

Immunofluorescent identification of capillaries in cross sections of *vastus lateralis* from two participants. **A)** Participant with the highest capillary density. **B)** Participant with the lowest capillary density. After immunostaining using anti-CD31, capillaries appear green. (n=2).

Correlations

k_{HIGH} was correlated with CI+II$_P$ (r = 0.80, p < 0.01) and CI+II$_E$ (r = 0.81, p < 0.01). k_{LOW} was not correlated with either CI+II$_P$ or CI+II$_E$ (r = -0.10 and r = -0.11, respectively) (**Fig 5A-B**). Δ*k* was significantly correlated with capillary density (r = -0.68, p = 0.015) (**Fig. 5C**).

Figure 5 (Study 1). Association between *in vivo* (NIRS) and *ex vivo* (biospy) estimation of (A-B) skeletal muscle OXPHOS capacity and (C) skeletal muscle capillary density

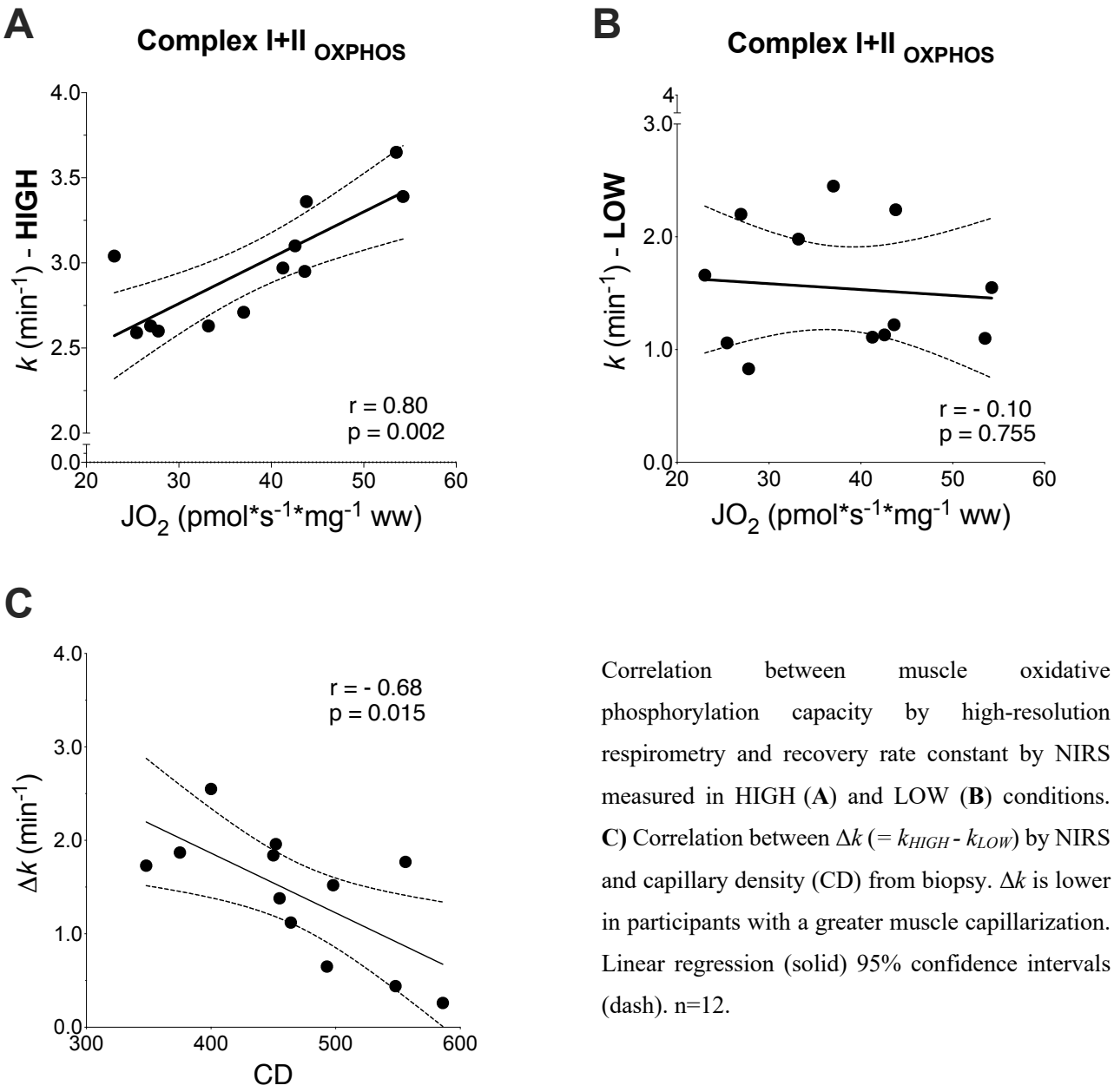

Correlation between muscle oxidative phosphorylation capacity by high-resolution respirometry and recovery rate constant by NIRS measured in HIGH (**A**) and LOW (**B**) conditions. **C)** Correlation between Δ*k* (= k_{HIGH} - k_{LOW}) by NIRS and capillary density (CD) from biopsy. Δ*k* is lower in participants with a greater muscle capillarization. Linear regression (solid) 95% confidence intervals (dash). n=12.

DISCUSSION

This study tested the hypotheses that $m\dot{V}O_2$ *k* is associated with muscle oxidative capacity only in high TSI conditions and that the difference in $m\dot{V}O_2$ *k* between well-oxygenated and poorly-oxygenated muscle provides insight into DmO_2. Our data confirmed previous findings (Ryan *et al.*, 2014) that, in well-oxygenated tissue, $m\dot{V}O_2$ recovery rate constant measured by NIRS, k_{HIGH}, is correlated with maximal muscle O_2 flux in fiber bundles. Additionally, we showed for the first time that this relationship did not hold when tissue oxygenation was reduced below 50% of the physiological normalization; and, k_{LOW} was not associated with any variable describing muscle O_2 flux in fiber bundles. This finding is consistent with Fick's law in that $m\dot{V}O_2$ becomes increasingly dependent on DmO_2 as microvascular-to-myocyte PO_2 difference is reduced (see Eq. 1). From this, we demonstrated that Δk, the difference between k_{HIGH} and k_{LOW}, was associated with capillary density ~~C:F~~ in biopsy samples of the same tissue, a primary structural determinant of DmO_2. Thus, the NIRS-derived response measured under conditions of both well-oxygenated and poorly-oxygenated skeletal muscle provided a non-invasive means of assessing both muscle oxidative capacity and muscle diffusing capacity *in vivo*. The application of this NIRS protocol may be of great interest for the study of skeletal muscle oxidative and diffusing capacities in response to exercise training or in disease states (e.g., heart failure, chronic obstructive pulmonary disease, myopathies).

NIRS and muscle oxidative capacity

In health, skeletal muscle oxidative capacity is strongly correlated with whole-body aerobic capacity and exercise performance (Holloszy, 1967*b*; Hoppeler *et al.*, 1985; Hood *et al.*, 2011*a*). Moreover, muscle oxidative capacity and mitochondrial function are impaired in conditions of physical inactivity (Buso *et al.*, 2019; Zuccarelli *et al.*, 2021), aging (Layec *et al.*, 2013) and chronic disease, such as obesity (Menshikova *et al.*, 2005; Lazzer *et al.*, 2013), diabetes (Joseph *et al.*, 2012) myopathy (Grassi *et al.*, 2019, 2020), pulmonary obstructive disease (Adami *et al.*, 2017, 2020), and neuromuscular disease (Breuer *et al.*, 2013). Traditionally, muscle oxidative capacity has been studied using *ex vivo* approaches involving muscle biopsy samples and measurement of enzyme activity, or mitochondrial respiratory capacity in isolated mitochondrial preparations and permeabilized muscle fibers (Chance & Williams, 1955; Holloszy, 1967*b*; Gnaiger, 2009; Brand & Nicholls, 2011; Perry *et al.*, 2013). For a long time, *in vivo* approaches were limited to ^{31}P nuclear magnetic resonance spectroscopy (^{31}P-MRS) to measure the recovery rate of phosphocreatine (PCr) after exercise, which is associated with maximal O_2 flux in muscle (Kemp *et al.*, 1993; Blei *et al.*, 1993; Kent & Fitzgerald, 2016). Over the past decade, however, NIRS coupled with intermittent arterial occlusions, has proven a valuable tool to assess the $m\dot{V}O_2$ recovery rate constant, *k*, which is

directly associated with muscle oxidative capacity (Hamaoka *et al.*, 1996; Motobe *et al.*, 2004; Ryan *et al.*, 2012; Grassi & Quaresima, 2016; Adami *et al.*, 2017; Adami & Rossiter, 2018; Hamaoka & McCully, 2019). The estimation of muscle oxidative capacity using NIRS has been already examined in upper and lower limb muscles and in both healthy subjects and patients affected by chronic diseases (Meyer, 1988; Erickson *et al.*, 2013, 2015; Ryan *et al.*, 2013*b*, 2014; Harp *et al.*, 2016; Adami *et al.*, 2017; Willingham & McCully, 2017). However, muscle oxidative capacity estimation by NIRS relies on two main assumptions (Adami & Rossiter, 2018; Chung *et al.*, 2018): i) muscle contractions are sufficient to maximally activate mitochondrial oxidative enzymes, and ii) O_2 concentration at skeletal muscle level is not a limiting factor to oxidative phosphorylation. Regarding the first point, it has been demonstrated that the first-order relationship between PCr dynamics and ATP production by oxidative phosphorylation is valid only when mitochondrial oxidative enzymes are maximal activated. Additionally, experiments on isolated single frog muscle fibers show that maximal activation of mitochondrial enzymes may not be achieved when muscle stimulation (or contraction frequency) is too low (Wüst *et al.*, 2013). For this reason, we used 5 min of moderate intensity cycling to stimulate OXPHOS and activate a wide range of regulated enzymes within the mitochondrial matrix, with the goal to reach a high, ideally, maximal mitochondrial activation. Our data for k_{HIGH} show a good correlation with maximal O_2 flux in biopsy samples (either phosphorylating or uncoupled), consistent with the findings of others. These data confirm that NIRS provides a reasonable non-invasive estimate of muscle oxidative capacity when the tissue is well-oxygenated.

The second assumption, that O_2 concentration is not limiting in the NIRS test, has received relatively less attention. Because $m\dot{V}O_2$ depends in part on the O_2 pressure difference between the microvasculature and the inner mitochondrial membrane in the myocyte to facilitate O_2 diffusion, it stands to reason that reducing $PmvO_2$ could reduce O_2 flux and limit $m\dot{V}O_2$ *k*. This suggestion was confirmed previously by the reduction in $m\dot{V}O_{2max}$ and PCr recovery rate constant under conditions of reduced $PmvO_2$ imposed by breathing hypoxic gas mixtures (Haseler *et al.*, 1999, 2004; Richardson *et al.*, 1999). By reducing ($PmvO_2$ – $PimO_2$) in hypoxia, $m\dot{V}O_2$ becomes increasingly dependent on DmO_2 (Eq. 1). Despite this, no study to date investigated whether NIRS-derived $m\dot{V}O_2$ *k* estimation is affected by changes in O_2 availability. We investigated the reliability and validity of NIRS-derived $m\dot{V}O_2$ *k* to reflect muscle oxidative capacity under conditions of well- and poorly-oxygenated muscle. As expected, k_{HIGH} was associated with maximal O_2 flux in fiber bundles performed in a hyperoxic environment (i.e. in non-limiting O_2 availability), when TSI was maintained above 50% of PN (r = 0.80 to 0.81; **Fig 5A**) and showed good reproducibility (test-retest r = 0.67, ICC = 0.68, **Fig. 3**). The regression coefficient between methods was very similar to that observed

by Ryan et al. (2014) (Ryan *et al.*, 2014). However, our data also show that this association was lost (r = -0.11 to -0.10) when the arterial occlusion protocol was experimentally manipulated to hold TSI between 0-10% PN. In the k_{LOW} condition, good test-retest reproducibility was maintained, but the association with maximal O_2 flux by tissue respirometry was absent (**Fig. 5B**).

The two NIRS tests assessed the same muscle region in tests applied a few minutes apart, therefore differences between k_{HIGH} and k_{LOW} could not reasonably reflect structural or functional properties in the skeletal muscle mitochondria. Rather, the difference reflects the increasing importance of DmO_2 in k_{LOW}, when ($PmvO_2$ - $PimO_2$) was reduced by experimental manipulation of the occlusion protocol. Thus, $m\dot{V}O_2$ *k* is only valid method to estimate muscle oxidative capacity when assessed as k_{HIGH} i.e., above 50% PN (Adami & Rossiter, 2018).

NIRS and muscle O_2 diffusion

As previously described, $m\dot{V}O_2$ is dependent on the interplay between both convective and diffusive transport (Roca *et al.*, 1992). In our protocol, we estimated muscle oxidative capacity from the TSI slope during repeated arterial occlusions, which minimizes the effects of O_2 delivery on the estimation of muscle oxidative capacity. Moreover, we effectively manipulated arterial occlusions such that the sum of ($PmvO_2$ - $PimO_2$) was either large or small, in the HIGH and LOW conditions respectively. In these conditions, convective O_2 transport may have an influence on our surrogate measure of DmO_2 by modifying capillary Hb volume, RBC transit time, or RBCs immediately adjacent to active muscle fibers during the reperfusion phase between two occlusions. However, the absence of differences in Δ[tot(Hb+Mb)] between HIGH and LOW supports the notion that, under these strictly controlled experimental conditions, convective O_2 transport did not influence $m\dot{V}O_2$ *k*.

By measuring $m\dot{V}O_2$ under these two conditions we could simultaneously solve by elimination for DmO_2 (Eq. 1). Using NIRS the absolute value of ($PmvO_2$ - $PimO_2$) is unknown; rather the ranges of TSI used reflected two relative oxygenation values (i.e., HIGH and LOW). Also, absolute values of $m\dot{V}O_2$ are not precisely known using NIRS, although they may be estimated assuming values for tissue [Hb+Mb] (among other assumptions). Nevertheless, the NIRS-based protocol we used allows for relative measurement of $m\dot{V}O_2$ and ($PmvO_2$ - $PimO_2$), such that solving Eq. 1 for a relative estimate of DmO_2 is possible. We used the *k* value for $m\dot{V}O_2$, rather than $m\dot{V}O_2$ itself, because as demonstrated k_{HIGH} reflects muscle oxidative capacity and because the kinetics $m\dot{V}O_2$ are ~~agnostic~~ unrelated to absolute measurements (thereby reducing potential variability introduced by comparing absolute $m\dot{V}O_2$ values from NIRS). Assessment of DmO_2 was performed by capillary density and the

finding that Δ*k* was correlated with CD (**Fig. 5C**) supports the validity of NIRS-based protocol to estimate DmO_2.

Although CD ~~C:F~~ does not assess length and diameter of vessels, the measurement of capillary density in a muscle cross section may provide information to understand the O_2 diffusing capacity of skeletal muscle (Saltin & Gollnick, 1983; Hepple *et al.*, 2000; Poole *et al.*, 2020, 2021, 2022). Our CD values ranged from 348 to 586 mm^{-2}, in line with published data (Poole *et al.*, 2020). On the other hand, Δ*k* ranged more widely from 0.26 to 2.55 min^{-1}. This is presumably because Δ*k* is also influenced by muscle oxidative capacity, therefore changes in Δ*k* under fixed TSI conditions may vary more widely than capillary structure alone. Nevertheless, the finding of a significant association between Δ*k* and CD may allow a valid non-invasive estimation of CD *in vivo*.

The ability to measure O_2 dynamics in microvessels in human skeletal muscles is currently beyond reach (Koga *et al.*, 2014; Lundby & Montero, 2015). Previous studies have attempted this by measuring structural components related to the path through plasma and capillary wall to the cytoplasm (e.g. capillary density) or calculating the ratio of $m\dot{V}O_2$ and O_2 pressure gradient between microvessels and mitochondria using the method developed by Wagner-and colleagues (Roca *et al.*, 1989, 1992; Richardson *et al.*, 1999; Hepple *et al.*, 2000). Although these elegant experiments were fundamental to move forward knowledge in the field, they do not fully account for the physiological mechanisms of *in vivo* regulation and reduce a complex diffusion process to a few key variables (Hepple *et al.*, 2000).

A step towards a more physiological approach was used by Brown et al. (Brown *et al.*, 2001). In endurance and resistance trained athletes, Brown et al. estimated capillary filtration capacity with plethysmography during small incremental steps in venous occlusion pressure. They found an association between filtration capacity and muscle capillarity, consistent with a relationship between capillary filtration and capillary surface area (Brown *et al.*, 2001; Hunt *et al.*, 2013). In our study we used NIRS to follow the flux of O_2 rather than fluid within the capillary-to-myofiber. In addition, NIRS is able to estimate changes in Δ[tot(Hb+Mb)] within the microvasculature, such that our NIRS-based method likely more closely reflects apposition of red-blood cells with capillary endothelium and therefore the O_2 diffusion pathway. The action of repeated occlusions has the effect of increasing Δ[tot(Hb+Mb)] in the microvasculature (~10 μM in Δ[tot(Hb+Mb)] from rest which should account for an increase in hematocrit of ~18%, leading to a total hematocrit of 33%), thereby generating a diffusional surface area that may be closer to *in vivo* condition when DmO_2 is maximized i.e., high

longitudinal capillary recruitment at approach exercise at maximal aerobic capacity. That NIRS measures the oxygenation of all [Hb+Mb] within the field of view, may therefore, be a more valid reflection the final steps in O_2 cascade than structural properties of the capillaries alone. However, as yet undeveloped, more advanced techniques are needed to test this hypothesis.

The correlation coefficients of *k* with muscle oxidative capacity and Δ*k* with CD were relatively small when compared with correlations for clinical techniques (Hanneman, 2008). However, the Pearson correlation coefficient resulting in our study (r = 0.80 and r = -0.68, respectively) was similar with other validation studies comparing *in vivo* methods with *ex vivo* approaches using NIRS (r = 0.61 – 0.74) (Ryan *et al.*, 2014). While NIRS and biopsy were taken from the same muscle region, the volumes assayed by each of these techniques are different (~2-3 cm^3 and ~1 mm^3, respectively). In addition, the structural and functional assessments differ between NIRS and biopsy. Unlike NIRS, maximal O_2 flux in fiber bundles in respirometry is assessed using supraphysiologic concentrations of substrates, including O_2, and reflects all fibers in the sample. Maximal O_2 flux based on NIRS signals derive from only those fibers that were active during the exercise, and therefore may be biased towards low order fibers (slow, oxidative). As discussed, CD is a structural contributor to DmO_2, but may not reflect to the true capacity for O_2 diffusion in tissue with variable capillary content of red blood cells. Therefore, variability between methods is expected, with the NIRS potentially having the advantage that it assays a larger muscle volume than the biopsy, and assays under physiologic conditions *in vivo*.

CONCLUSIONS

In summary, we report reliability and accuracy of NIRS measurements of $m\dot{V}O_2$ during intermittent arterial occlusions protocols to estimate muscle oxidative capacity and muscle DmO_2 *in vivo*. The $m\dot{V}O_2$ recovery rate constant, *k*, was a reasonable and reliable method to assess muscle oxidative capacity only when assessed in well-oxygenated quadriceps muscle (>50% of TSI physiological normalization). Experimental manipulation of TSI through timing and duration of intermittent arterial occlusions provided a new variable, Δ*k*, which was the difference in *k* between well-oxygenated and poorly-oxygenated experimental conditions. As hypothesized, we found that Δ*k* was associated with CD, a structural determinant of DmO_2. Therefore, the NIRS-based protocol we describe represents a cost-effective and non-invasive means of assessing both muscle oxidative capacity and muscle O_2 diffusive capacity *in vivo*.

CHAPTER 4

STUDY 2

STUDY 2

Repeated interventions of high-intensity interval training in mice differentially affect mitochondrial adaptations at skeletal muscle level

Pilotto AM[1,2], Brocca L[2], Crea E[2], Bottinelli R[2,3], Porcelli S[2] and Pellegrino MA[2]

[1] Department of Medicine, University of Udine, Udine, Italy

[2] Department of Molecular Medicine, University of Pavia, Pavia, Italy

[3] Interdipartimental Centre for Biology and Sport Medicine, University of Pavia, Pavia, Italy

ABSTRACT

PURPOSE: In murine model a first exposure to hypertrophic stimuli, such as testosterone, mechanical loading or resistance exercise, has been shown to lead to faster and larger growth of skeletal muscle when subsequently repeated. This mechanism, called muscle memory, has been related to the retention of acquired myonuclei or epigenetic modifications. Interestingly, greater changes in mitochondrial content and biogenesis were also observed after repeated resistance training interventions. Thereby, even mitochondrial adaptations might be influenced by muscle memory, and it remains to be explored whether repeated endurance training interventions can rely on the same mechanism. The aim of the study was to investigate functional and molecular adaptations of skeletal muscle to two repeated interventions of high-intensity interval training (HIIT) in mice. METHODS: Forty-eight C57BL/6 adult mice were assigned to six groups (n = 8 each group). Three interventions group: TR, subjected to one period of training, DETR, undergoing detraining period after training; RETR, exposed to repeated training period after detraining; and three corresponding control group in order to match the duration of the intervention (CTRL TR, CTRL DETR and CTRL RETR). Each HIIT (10 bouts of 2 min separated by 2 min of recovery) intervention lasted 8 wks. Physiological adaptations were compared across training, detraining and retraining conditions by calculating the difference between interventions and relevant control group. Maximal running velocity (Vmax) was assessed 48 h prior to sacrifice by graded exercise test (GXT). Markers of mitochondrial biogenesis and content, fusion-fission mitochondrial key factors and mitophagic biomarkers were analyzed on gastrocnemius muscle by western Blot. RESULTS: Vmax increased more after retraining than initial training (+10.4 ± 3.2 vs +6.5 ± 1.9 $m \cdot min^{-1}$, respectively, $p<0.001$). Mitochondrial content measured on CS protein resulted higher in retraining than training ($p<0.05$). Mitochondrial biogenesis changes were larger after repeated interventions than single-training in PGC-1α, pAMPK and pACC (all $p<0.01$). Comparison of mitochondrial dynamics between single-training period and repeated interventions revealed increase in fusion through Mfn2 ($p<0.001$) and a reduction in fission dynamics through Fis1 and $Drp1_{Ser637}$ after retraining (both $p<0.05$). Mithopagic protein Parkin, along with

autophagy protein p62 were more increased after retraining than training (both $p < 0.05$). Subunits of complex I, III and IV of respiratory chain followed a smaller increase after retraining (all $p < 0.05$). CONCLUSIONS: Repeated interventions of HIIT induced a greater improvement in aerobic performance after the second exposure to the aerobic training stimulus. This enhanced response appears to be determined by larger expression of mitochondrial biogenesis factors that induced an increase in mitochondrial content, as well as changes mitochondrial dynamics that likely promoted healthier and more functional mitochondria. In conclusion, mitochondria adaptations to a HIIT are different if the stimulus has been previously encountered, thereby supporting the hypothesis of a mitochondrial memory.

INTRODUCTION

Skeletal muscle memory has been defined as: "The capacity of skeletal muscle to respond differently to environmental stimuli in an adaptive or maladaptive manner if the stimuli have been previously encountered" (Sharples et al., 2016b). The concept refers to the retention of cellular and tissue-level changes generated by previous environmental stimuli or stressors such as those resulting from exercise, muscle damage, disease or changes in nutrients which lead to an altered response if the stimulus is encountered again. This mechanism is important for skeletal muscle because if the environment encountered is positively influencing adaptations, the muscle may respond to these stimuli later in life with further muscle improvement or healthy maintenance across the lifespan. This has important consequences on quality of life, as adequate quantity and quality of skeletal muscle is not only essential for performance in elite sports, but also for improving daily life activities and promoting health in older age (Sharples et al., 2015, 2016a). Concerning exercise and training, muscle encounters this memory mechanism in an adaptively advantageous manner. Indeed, it is becoming evident that molecular and phenotypic responses to chronic exercise are enhanced during subsequent training when similar previous training has been performed.

In rodent model this mechanism has been proven in response to anabolic stimuli, such as testosterone, mechanical loading, or resistance exercise, demonstrating how muscles previously exposed to a hypertrophic stimulus are able to grow their size faster and larger when encountering a similar stimulus later, after a prolonged period of hypertrophic stimuli cessation in which muscle resumes its phenotypic state to pre-exercise condition (Egner *et al.*, 2013; Gundersen, 2016; Lee *et al.*, 2018; Murach *et al.*, 2020). Acquired myonuclei permanence and epigenetic modification retention are parallel processes that appear to be involved in the hypertrophy memory mechanism (Gundersen, 2016; Snijders *et al.*, 2020; Wen *et al.*, 2021). It is important to focus the attention on an animal study

that observed after repeated resistance training interventions not only greater muscle mass but also greater changes in mitochondrial adaptations in response to retraining compared to the previous intervention (Lee *et al.*, 2018). Authors demonstrated that mitochondria may retain the ability to respond more consistently to repeated noncontinuous stimuli resulting in higher increase in proteins regulating mitochondrial biogenesis and markers of mitochondrial content during the second training period (Lee *et al.*, 2018). This interesting finding pointed out the possible existence of a memory mechanism for specific aerobic physiological markers. A possible explanation for mitochondrial memory observed in the aforementioned study may derive from the existence of mechanisms that during the interruption period from a training stimulus may "protect" specific markers involved in mitochondrial adaptation processes, allowing them to remain elevated for a long-term period after a training stimulus, hence, affecting larger response extent to a subsequent stimulus. Genetically modified mice study with animals able to express a higher amount of PGC-1α (a condition attributable to the effects of aerobic training), seems to corroborate this hypothesis (Kang *et al.*, 2015). Authors showed that PGC-1α overexpressed animals were able to counteract deleterious consequences of muscle immobilization and facilitate mitochondrial content and function recovery during the period of return to normal activity (Kang *et al.*, 2015). This result suggests that previous enhancement in mitochondrial transcription factors may promote better mitochondrial adaptations in skeletal muscle upon administration of a repeated noncontinuous stimulus.

Overall, this evidence suggests that even mitochondrial adaptations might be influenced by muscle memory, and it remains to be explored whether repeated endurance training interventions can rely on the same mechanism. In order to deepen our understanding of the potential presence of skeletal muscle memory induced by aerobic training, the aim of this study was to investigate functional and molecular adaptations of skeletal muscle in response to two repeated interventions of endurance training in mice. High-intensity interval training has been used here to serve as endurance training paradigm because, as demonstrated by Barrès and colleagues (2012), high-intensity exercise is more effective in inducing DNA hypomethylation and subsequent increase in gene expression in the mitochondrial biomarker than low-intensity training (Barrès *et al.*, 2012). The underlying mechanism could be related to the elevated load and intermittent nature of high-intensity interval training, which could mediate the muscle memory effect through epigenetic modifications.

MATERIALS AND METHODS

Animals and Experimental design

Forty-eight C57BL/6 adult male mice from the breeding facility of Charles River Laboratories (Calco, Italy) were used. Animals were housed single and kept under a standard 12:12 h light/dark cycle and room temperature of 21°C. Rodents were allowed access to water and food *ad libitum*. All animal care and experimental procedures were approved by the local Committee on Animals in Research. All animals were randomly assigned into six groups (n = 8 each group). Three groups were subjected to different interventions: TR, subjected to one period of training, DETR, undergoing detraining period after training; RETR, exposed to repeated training period after detraining. Each intervention group was paired with a corresponding control group in order to match the duration of the intervention (CTRL TR, CTRL DETR and CTRL RETR relevant to TR, DETR and RETR, respectively). A schematic diagram of each condition is provided in **Figure 1**. At the termination of each respective intervention at which mice underwent, animals were sacrificed to collect gastrocnemius muscle tissue. A graded exercise test (GXT) was performed before every training period in TR, DETR and RETR to set training intensity. In addition, for each group GXT was performed 48h prior to tissue collection; for TR and RETR group the latter GXT test has been arranged to be accomplished 48h after the last training session. Before the first GXT, each mouse participated in rodent treadmill acclimation.

Figure 1 (Study 2). Schematic diagram of the experimental design

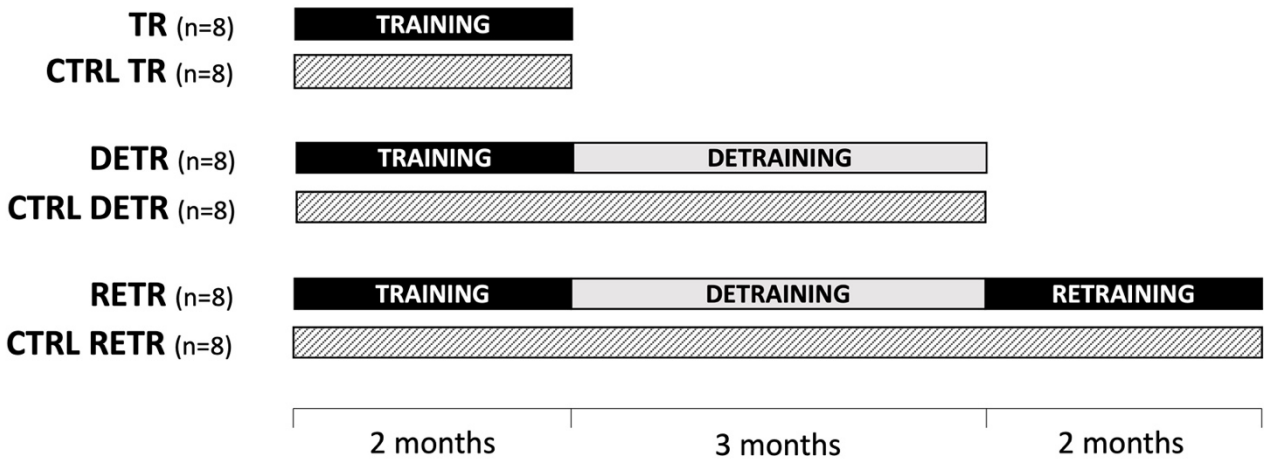

All animals were randomly assigned into six groups (n = 8 each group). Three groups were subjected to different interventions: TR, subjected to one period of training lasting two months, DETR, undergoing 3 months of detraining period after training; RETR, exposed to repeated training period after detraining. Each intervention group was paired with a corresponding control group in order to match the duration of the intervention (CTRL TR, CTRL DETR and CTRL RETR relevant to TR, DETR and RETR, respectively).

Acclimation

Rodent treadmill (Exer-6M, Columbus, Ohio, USA) was composed by 6 lanes. For running space each lane was 5.5 cm in width, 42 cm in length and with side walls of 12.5 cm height. Treadmill was set at 5° incline for acclimation, GXT and training sessions. Treadmill was equipped with a shock grid at the back of the treadmill belt to discourage mice from stopping.

Acclimation sessions were conducted on three separate days allowing mice to become familiar with equipment, space features and running exercise as suggested by animal care and use guidelines (Baertschi & Gyger, 2011). During the first day mice were placed on treadmill in near stationary condition (2 $m \cdot min^{-1}$) for 15 min to explore and acclimate with smells, spaces, and noises of room and instrument. In the second day mice familiarized with running condition for 5 min at 6.5 $m \cdot min^{-1}$, afterwards familiarization with speed variations was performed by switching treadmill speed between 5 $m \cdot min^{-1}$ and 9 $m \cdot min^{-1}$ every 2 min for a total of 10 min. In the same acclimation session, mice became familiar with the shock grid that was progressively increased in shock frequency and magnitude (from 1 Hz and 0.3 mA to 3 Hz and 3 mA). Day three was used to familiarize with high intensities by means of sprints of 10/20 s duration performed every minute interspersed with recovery at 5 $m \cdot min^{-1}$. Sprint velocity was progressively increased from 9 $m \cdot min^{-1}$ to 20 $m \cdot min^{-1}$ and shock grid was set at 3 Hz and 3 mA.

Graded Exercise Test

Graded exercise test to exhaustion was carried out to assess maximal running velocity (V_{max}). A maximum of 3 mice were tested at the same time. Mice were run to exhaustion using a protocol consisting of a 5-min warm-up at initial speed of 9 $m \cdot min^{-1}$, after which the speed was increased by 1 $m \cdot min^{-1}$ every minute (McMullan *et al.*, 2018). Maximal running velocity was defined as the last speed the mouse was able to maintain for at least 10s before exhaustion, if the step duration was less than 10s, the previous completed speed was considered as maximal velocity. Exhaustion was defined as the inability or refusal to run on the treadmill for 10 s continuously despite stimulus via shock grid or manual prodding (Malek & Olfert, 2009; Malek *et al.*, 2010; Hüttemann *et al.*, 2012; McMullan *et al.*, 2018). GXT was performed twice on each mouse on two separate days and the higher value of V_{max} ($m \cdot min^{-1}$) was recorded (McMullan *et al.*, 2018).

Endurance training and detraining intervention

Each training period consisted of high-intensity interval exercises performed on rodent treadmill 3 times/week for 8 weeks. Based on V_{max} resulting from GXT, training mice were divided into training groups with similar aerobic fitness level where the average V_{max} were used to set training intensity.

Each training sessions was composed of 8 min of warm up at 40% of V_{max} followed by 10 bouts of 2-min intervals at 90% - 120% of V_{max} interspersed by 2-min of active recovery running at 30% of V_{max}. After the session a cool down of 8 min was performed at 40% of V_{max} (Henríquez-Olguín *et al.*, 2019). To avoid stagnation, the training stimulus of high-intensity intervals was progressively incremented in subsequent training sessions by increasing the relative exercise intensity from 90% to 120% of V_{max}. An identical training protocol was applied for both training and retraining sessions. During detraining, animals were kept in cage for 12 consecutive weeks without training sessions with access to water and food *ad libitum*.

Tissue collection

At 48 hours after the last GXT, mice were sacrificed by cervical dislocation. An incision was made through the skin around ankle area and the skin was reflected to expose the muscles of the lower leg. The Achilles tendon was cut, and gastrocnemius was carefully dissected and used for molecular analyses. The muscle samples were rapidly frozen by immersion in liquid nitrogen and used for proteomic and genomic analysis. All frozen muscle samples were stored in ultrafreezer at −80° C until analyzed.

Proteomic Analysis

Sample Preparation: muscle lysis and protein extraction. Frozen muscles were pulverized in a steel mortar using a ceramic pestle, with the constant addition of liquid nitrogen in order to maintain muscle components' properties. The powder thus obtained was homogenized with a lysis buffer containing TRIS-HCl 20mM, Triton 100x 1%, Glycerol 10%, NaCl 150mM, EDTA 5mM, NaF 100mM and NaPPi 2mM supplemented with protease inhibitor 5X, phosphatase inhibitors 1X (Protease Inhibitor Cocktail, Sigma-Aldrich, St. Louis MO) and PMSF 1mM. The lysis of tissue was performed on ice for 40 minutes. The homogenate obtained was centrifuged at 13500 rpm for 20 minutes at 4° C and the supernatant was transferred to clean eppendorf tubes and stored at -80° C until use. The protein concentration of the lysates was determined using the RC-DC™ (reducing agent and detergent compatible) protein assay (Bio-Rad) that is a colorimetric assay for protein determination in the presence of reducing agents and detergents.

Western Blot. Equal amounts of muscle samples were loaded on gradient precast gels purchase from BioRad (AnyKd) and subjected to electrophoresis. Electrophoretic run was carried out at constant current (100V) for about 2 hours in a running buffer at pH 8.8 (Tris 25 mM, Glycine 192 mM, SDS 1%). To monitor protein separation, a protein molecular weight marker constituted by a mixture of

proteins with known molecular weight (Preistained Protein Ladder Marker, BIORAD) was loaded on the gel. Proteins were electro-transferred to polyvinylidene fluoride (PVDF) membranes at constant voltage at 100V for 2 hours at 4° C or at 35 mA overnight (O/N) in a transfer buffer containing Tris 25 mM, Glycine 192mM, and methanol 20%. The effective protein transfer to the membrane was verified by staining with Ponceau Red (Sigma) in acetic acid (Ponceau Red 0.2% in acetic acid 3%) for 15 minutes under stirring at room temperature. Nonspecific binding sites present on the PVDF membrane were saturated with a blocking solution consisting of 5% fat-free milk in TBS-T (Tris 0.02 M, NaCl 0.05 M and Tween-20 0.1%) for 2 hours at room temperature with constant shaking. At the end of incubation, the membrane was washed with TBS-T for three times 10 minutes each. After that the membranes were probed with specific primary antibodies (**Table 1**) overnight at 4° C. Thereafter, the membranes were incubated in HRP-conjugated secondary antibody. Proteins detection was made using ECL advance detection system (GE Healthcare Life Sciences) which highlights the HPRT substrate by a chemiluminescent reaction. The membrane was gained through an analysis software ImageQuant LAS 4000 (GE Healthcare Life Sciences). The content of each protein investigated was assessed by determining the brightness–area product of the protein band as previously described (Cannavino *et al.*, 2014). Tubulin was used as housekeeping protein for internal loading control to normalize protein expression.

Following the previously well described procedure for general western Blot protocol, the detection of the subunits from the five mitochondrial complexes (NDUFB8, SDHB, UQCRC2, MTCO1, ATP5A for complex I, II, III, IV, and V, respectively) that make up the respiratory chain can be performed in the same PVDF membrane by using a cocktail of the five antibodies targeting the five proteins. 5 µg of quantified proteins were prepared with adjusted amounts of Laemmli Buffer 4X and PBS 1X and denatured at 37° C for 5 min. Following 5 min of acclimation at room temperature, a protein molecular weight marker and samples were loaded on gradient Precast acrylamide/bisacrylamide gels (Bio-Rad) and electrophoresis was carried out at constant current (100V) for about 2 h in running buffer. At the end of the gel run, gels undergo transfer of proteins to a PVDF membrane prior to methanol activation. The transfer was carried out at constant voltage at 100V for 2 h at 4° C or at constant 35 mA overnight (O/N) in cold transfer buffer. Then, nonspecific binding sites present on the PVDF membrane were saturated with a blocking solution consisting of 5% fat-free milk in TTBS 1X for 2 h at room temperature with constant shaking. After that, membranes were washed three times, 10 min each, with TTBS 1X and incubated O/N at 4° C with the specific primary antibody against the mitochondrial complexes of the respiratory chain (OXPHOS 1:1000, Abcam) in 5% fat-free milk in TTBS 1X. Subsequently, membranes were washed three times

in TTBS 1X and then incubated 1 h at room temperature in constant agitation, with the HRP-conjugated donkey anti-mouse secondary antibody (1:10000, Dako) in 5% fat-free milk. After final three washes of 10 min each in TTBS 1X, the last one was made in TBS 1X. Proteins detection was made by using Amersham ECL Select™ detection system (Cytiva Life Sciences, ex GE Healthcare) and membranes gained through the ImageQuant™ LAS 4000 software (GE Healthcare Life Sciences), with the exposure time adjusted in an automatic manner or editable depending on the intensity of the emitted signal. After, to visualize the total protein amount present on the membrane, these were subjected to a Coomassie PVDF-specific staining (0.1% Coomassie Blue R-250, 50% Methanol, 10% Acetic Acid) for 20 min and destained with a destain composed by 40% Methanol and 10% Acetic Acid. Air dried membranes were then digitalized with a scanner and analysed. Data were expressed as the ratio between the BAP of samples from each of the five complexes and of total protein amount stained with Coomassie (arbitrary units).

Table 1 (Study 2). List of primary and secondary antibodies used

TARGET PROTEIN	PROTEIN LYSATE (µg)	SATURATION	Ab I	COMPANY	Ab II	COMPANY
PGC-1α	40	milk 5%	1:1000 milk 5%	Abcam	anti-Rabbit (1:10000) milk 5%	Cell Signaling
p-AMPK	40	milk 5%	1:1000 BSA 5%	Cell Signaling	anti-Rabbit (1:10000) milk 5%	Cell Signaling
AMPK	40	milk 5%	1:1000 BSA 5%	Cell Signaling	anti-Rabbit (1:10000) milk 5%	Cell Signaling
Sirt1	40	milk 5%	1:1000 BSA 5%	Cell Signaling	anti-Mouse (1:5000) milk 5%	DAKO
pACC	40	milk 5%	1:1000 BSA 5%	Cell Signaling	anti-Rabbit (1:10000) milk 5%	Cell Signaling
ACC	40	milk 5%	1:1000 BSA 5%	Cell Signaling	anti-Rabbit (1:10000) milk 5%	Cell Signaling

TOM20	15	milk 5%	1:1000 milk 5%	Santa Cruz	anti-Rabbit (1:10000) milk 5%	Cell Signaling
CS	15	milk 5%	1:2000 milk 5%	Abcam	anti-Rabbit (1:10000) milk 5%	Cell Signaling
OPA1	40	milk 8%	1:3000 milk 5%	Abcam	anti-Mouse (1:5000) milk 5%	DAKO
p-Drp1$_{(Ser616)}$	40	milk 5%	1:1000 BSA 5%	Cell Signaling	anti-Rabbit (1:10000) milk 5%	Cell Signaling
p-Drp1$_{(Ser637)}$	40	milk 5%	1:1000 BSA 5%	Cell Signaling	anti-Rabbit (1:10000) milk 5%	Cell Signaling
Drp1	40	milk 5%	1:1000 BSA 5%	Cell Signaling	anti-Rabbit (1:10000) milk 5%	Cell Signaling
Mfn1	40	milk 5%	1:1000 milk 5%	Abcam	anti-Mouse (1:5000) milk 5%	DAKO
Mfn2	40	milk 5%	1:1000 milk 5%	Abcam	anti-Rabbit (1:10000) milk 5%	Cell Signaling
Fis1	40	milk 8%	1:1000 milk 5%	Abcam	anti-Rabbit (1:10000) milk 5%	Cell Signaling
Tub	40	milk 5%	1:2000 milk 5%	SIGMA aldrich	anti-Mouse (1:5000) milk 5%	DAKO
OXPHOS	5	milk 5%	1:1000 milk 5%	Abcam	anti-Mouse (1:10000) milk 5%	DAKO

Statistical Analyses

Analysis was performed using statistical software package Prism 8.0 (GraphPad Software Inc, California, USA). All data are reported as the mean ± standard deviation (SD).

To identify effect of single period of high-intensity interval training on outcome measures, comparison between TR and CTRL TR was analyzed using unpaired Student's t-test. $p < 0.05$ was considered statistically significant.

To identify effect of each intervention on outcome measures, single-training, detraining and repeated interventions were normalized to relevant controls by calculation of differences in means and pooled SD between TR, DETR, RETR and CTRL TR, CTRL DETR, CTRL RETR respectively. Outcome measures were then assessed using one-way ANOVA to determine significant overall main effects of TRAINING, DETRAINING and RETRAINING interventions. Once an overall effect was confirmed, statistical significance of the measured difference between groups was assessed further by Bonferroni's post hoc analysis, and adjusted P values with the corresponding 95% confidence interval are reported.

RESULTS

Graded Exercise Test

Functional data from GXT revealed V_{max} significantly higher in the TR compared to CTRL TR (29.5 ± 2.3 vs 23.1 ± 1.4 m·min^{-1}, respectively, $p < 0.001$).

Normalized data showed a larger V_{max} increment after retraining compared to the single-training (10.4 ± 3.2 vs 6.5 ± 1.9, $p < 0.001$), whereas in detraining condition lower values (2.3 ± 2.5 m·min^{-1}) were found compared to both training and retraining (both $p < 0.001$) (**Fig. 2**).

Figure 2 (Study 2). Maximal velocity from graded exercise test

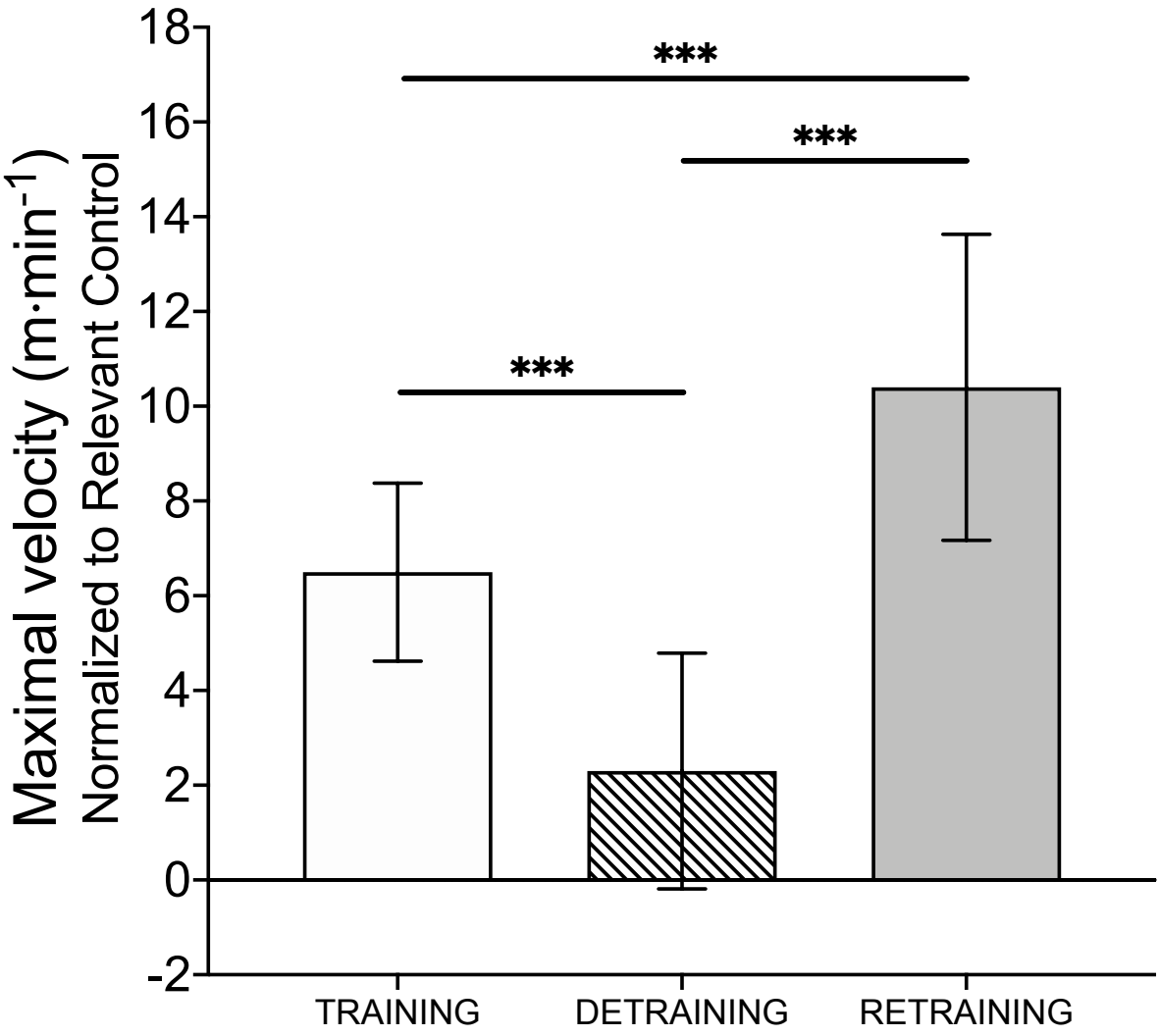

Maximal velocity attained during graded exercise test to exhaustion on rodent treadmill. Protocol consisting of a 5-min warm-up at initial speed of 9 m·min^{-1}, after which the speed was increased by 1 m·min^{-1} every minute. Exhaustion was defined as the inability or refusal to run on the treadmill for 10 s continuously despite stimulus via shock grid or manual prodding. TRAINING, DETRAINING, RETRAINING represent the effect of single-training, detraining and repeated intervention normalized on relevant controls. All values are means ± SD. ***$p < 0.001$.

Mitochondrial Content Biomarkers

Mitochondrial content was assessed using both TOM20 and CS protein expression measurements. TOM20 was greater in TR compared to CTRL TR ($p < 0.01$) whereas CS was not statistically different after the initial training intervention ($p = 0.38$).

Across the conditions CS was larger in RETRAINING compared to TRAINING and DETRAINING (both $p < 0.05$) (**Fig. 3A**). TOM20 protein showed a reduction after detraining, lower than training and retraining conditions (both $p < 0.01$), and comparison between delta changes in training and retraining showed a lower increase in TOM20 in RETRAINING compared to TRAINING (+5% vs +45%, respectively, $p < 0.01$) (**Fig. 3B**).

Figure 3 (Study 2). Mitochondrial content biomarkers

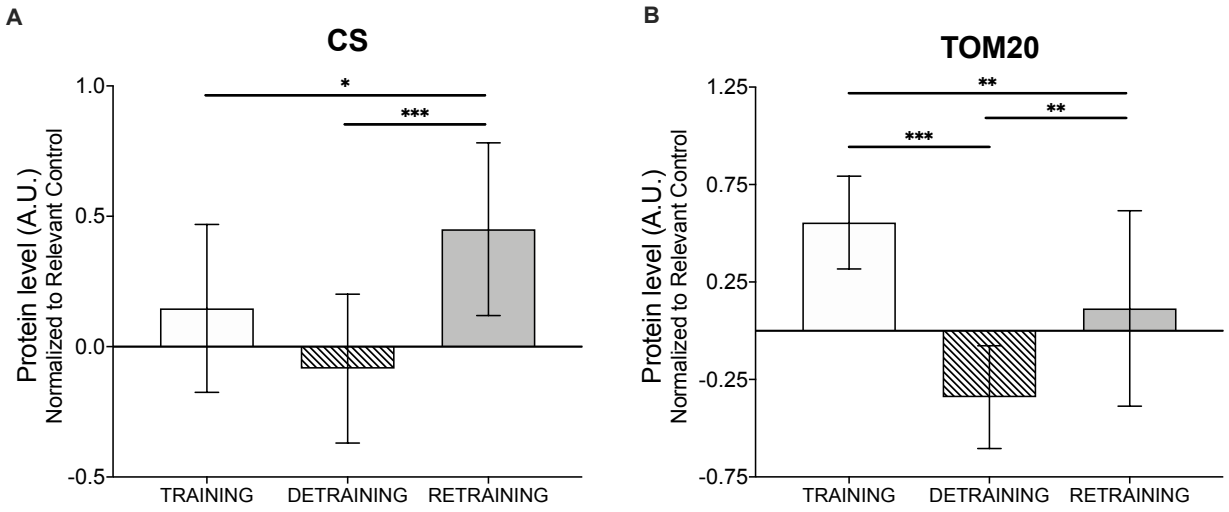

Fold change in single-training, detraining and repeated interventions compared to relevant controls of the protein expression of CS (A) and TOM20 (B) measured in *gastrocnemius* muscle tissue by western Blot. Muscles were collected after training (TR), detraining (DETR) and retraining (RETR) interventions and in corresponding control conditions (CTRL TR, CTRL DETR and CTRL RETR, respectively). All values are means ± SD. **$p < 0.01$; ***$p < 0.001$.

Mitochondrial Biogenesis Biomarkers

Mitochondrial biogenesis was assessed investigating the main transcriptional factors of this pathway (PGC-1α, AMPK, Sirt1 and ACC). After the single-training intervention, AMPK and ACC activated in phosphorylated state and SIRT1 protein expression were not different between TR and CTRL TR conditions (all variables $p \geq 0.24$), whereas PGC-1α protein showed a tendency to increase after the initial training ($p = 0.052$).

Across the conditions delta changes revealed a larger increase in protein expression after retraining compared to training for PGC-1α (+32% vs +19%, respectively), pAMPK (+30% vs -12%) and pACC

(+15% vs -55%, all variables $p < 0.05$). Compared to training condition (+19%), PGC-1α was reduced in detraining conditions (-6%, $p < 0.01$), and more enhanced after retraining (+32%, $p < 0.05$). Moreover, after retraining PGC-1α protein was higher than detraining ($p < 0.001$) (**Fig. 4A**). Across the conditions delta changes revealed also a larger increase in protein expression after retraining compared to training for pAMPK (+30% vs -12%, respectively) and pACC (+15% vs -55%, both $p < 0.01$), and lower values in detraining compared to retraining (both $p < 0.05$) (**Fig. 4B and Fig. 4D**). Sirt1 protein expression was not different between conditions ($p \geq 0.60$) (**Fig. 4C**).

Figure 4 (Study 2). Mitochondrial biogenesis biomarkers

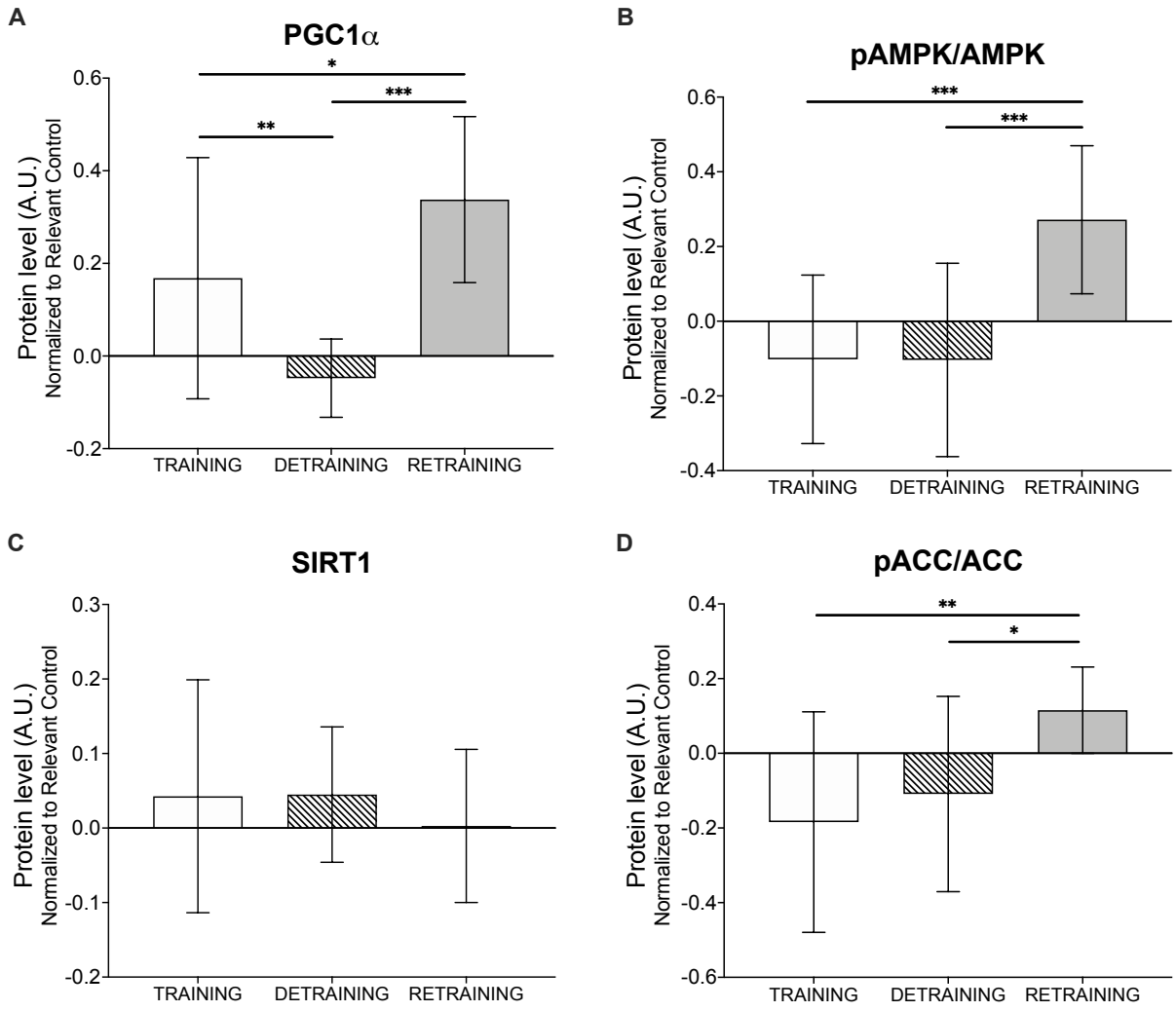

Fold change in single-training, detraining and repeated interventions compared to relevant controls of the protein expression of PGC-1α (A), phosphorylated state of AMPK (B), Sirt1 (C) and phosphorylated state of ACC (D) measured in *gastrocnemius* muscle tissue by western Blot. Muscles were collected after training (TR), detraining (DETR) and retraining (RETR) interventions and in corresponding control conditions (CTRL TR, CTRL DETR and CTRL RETR, respectively). All values are means ± SD. *$p < 0.05$; **$p < 0.01$; ***$p < 0.001$.

Mitochondrial Dynamics

Fusion. OPA1, Mitofusin1 (Mfn1) and Mitofusin2 (Mfn2) protein expression were analyzed to assess mitochondrial fusion dynamics at both the inner and outer membrane level. Compared to CTRL TR, after TR, OPA1 was greater ($p < 0.01$) whereas Mfn2 was lower ($p < 0.05$). Mfn1 was not affected by the first training intervention ($p = 0.55$).

Fold change of OPA1 showed a decreased in DETRAINING which was different from both TRAINING and RETRAINING (both $p < 0.05$) (**Fig. 5A**). Comparison between delta changes in training and retraining for Mfn2 revealed a significant increase in RETRAING compared to the reduction occurred in TRAINING (+11% vs -20%, $p < 0.001$) (**Fig. 5C**). Mfn1 was not affected by significant modification across conditions ($p \geq 0.15$) (**Fig. 5B**).

Figure 5 (Study 2). Mitochondrial fusion dynamics biomarkers

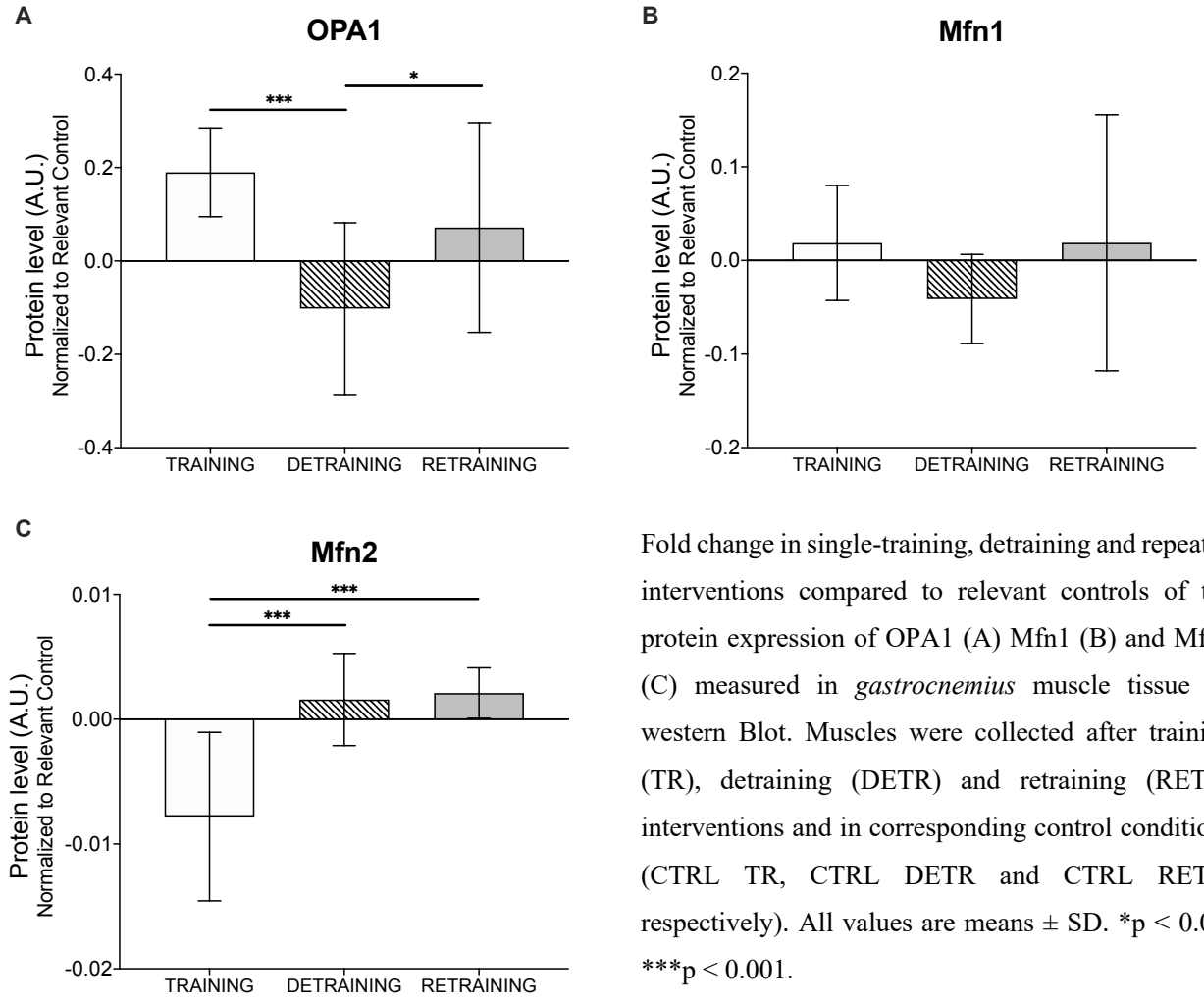

Fold change in single-training, detraining and repeated interventions compared to relevant controls of the protein expression of OPA1 (A) Mfn1 (B) and Mfn2 (C) measured in *gastrocnemius* muscle tissue by western Blot. Muscles were collected after training (TR), detraining (DETR) and retraining (RETR) interventions and in corresponding control conditions (CTRL TR, CTRL DETR and CTRL RETR, respectively). All values are means ± SD. *$p < 0.05$; ***$p < 0.001$.

Fission. Fis1 and Drp1 (phosphorylated at both serine 616 at 637) protein expression were measured to assess mitochondrial fission dynamics. After the first training period Fis1 was significantly increased ($p < 0.001$) and $Drp1_{Ser637}$ showed a tendency to reduction ($p = 0.052$), whereas no significant change was found in $Drp1_{Ser616}$ ($p = 0.45$).

Fis1 fold change was significantly higher in the training and retraining compared to detraining conditions (both $p < 0.01$). Moreover, Fis1 increase after retraining was significantly lower compared to training (+14% vs +52%, respectively, $p < 0.001$) (**Fig. 6A**). Decrease in Drp1 phosphorylates at serine 637, activation of which inhibits fission and fragmentation, was reduced after retraining compared to training (-15% vs -27%, respectively, $p < 0.05$) (**Fig. 6C**). $Drp1_{Ser616}$ did not show any significant difference across conditions ($p \geq 0.28$) (**Fig. 6B**).

Figure 6 (Study 2). Mitochondrial fission dynamics biomarkers

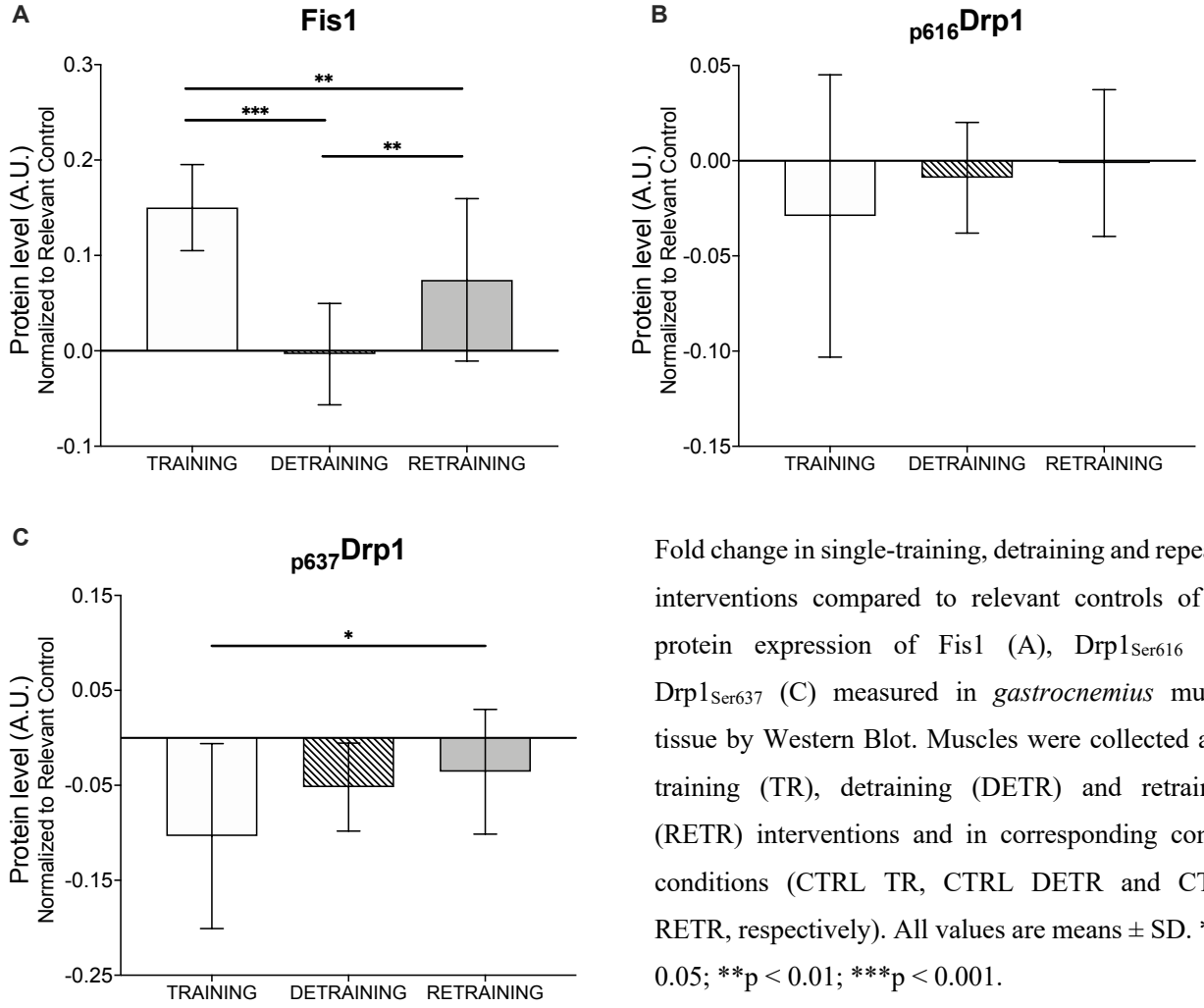

Fold change in single-training, detraining and repeated interventions compared to relevant controls of the protein expression of Fis1 (A), $Drp1_{Ser616}$ (B), $Drp1_{Ser637}$ (C) measured in *gastrocnemius* muscle tissue by Western Blot. Muscles were collected after training (TR), detraining (DETR) and retraining (RETR) interventions and in corresponding control conditions (CTRL TR, CTRL DETR and CTRL RETR, respectively). All values are means ± SD. *$p < 0.05$; **$p < 0.01$; ***$p < 0.001$.

Mitophagy

To investigate mitochondrial autophagic flux LC3B and p62 protein expression were measured, and Parkin and PINK1 protein were analyzed to assessed mitophagy dynamics. After the first training period no changes were observed for all the proteins ($p \geq 0.26$).

Protein p62 showed a larger increase after retraining compared to training (+9% vs -2%, respectively, $p < 0.05$) (**Fig. 7B**). Similarly, was observed an increase in Parkin protein after retraining significantly different from the reduction occurred during training conditions (+18% vs -12%, respectively, $p < 0.05$) (**Fig. 7C**). PINK1 showed a reduction during detraining significantly different from both training and retraining (both $p < 0.05$) (**Fig. 7D**). LC3B was not affected by significant changes across conditions ($p \geq 0.86$) (**Fig. 7A**).

Figure 7 (Study 2). Mitophagy biomarkers

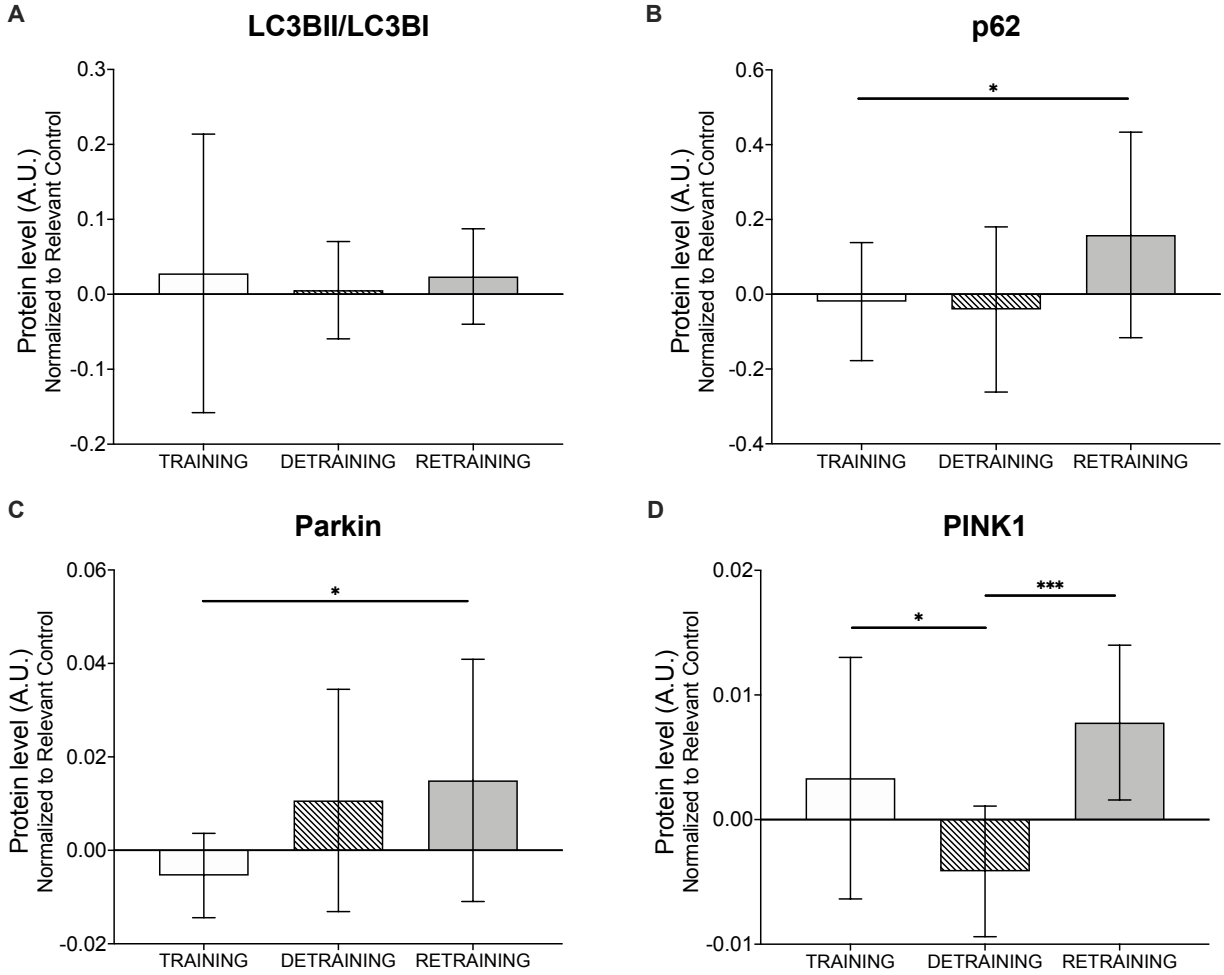

Fold change in single-training, detraining and repeated interventions compared to relevant controls of the protein expression of LC3B (A), p62 (B), Parkin (C) and PINK1 (D) measured in *gastrocnemius* muscle tissue by western Blot. Muscles were collected after training (TR), detraining (DETR) and retraining (RETR) interventions and in corresponding control conditions (CTRL TR, CTRL DETR and CTRL RETR, respectively). All values are means ± SD. *$p < 0.05$; ***$p < 0.001$.

Mitochondrial respiratory chain

Complex I, III and IV protein expressions resulted increased after the first training period (all variables $p < 0.05$), whereas complex II and V were not significantly affected by the initial intervention ($p \geq 0.67$).

Compared to training, fold change values revealed a lower increase after retraining in complex I (+172% vs +14%), complex III (+78% vs +12%) and complex IV (+98% vs +10%, all variables $p < 0.05$) (**Fig. 8A**, **Fig. 8C** and **Fig. 8D**). Protein expression of complex I and complex III were reduced during detrain condition compared to both training and retraining (all variables $p < 0.05$) (**Fig. 8A** and **Fig. 8C**), whereas for complex IV reduction after detraining was significantly different only compared to training condition ($p < 0.001$) (**Fig. 8D**). Complex II and complex V were not affected by modification across conditions ($p \geq 0.32$) (**Fig. 8B and Fig. 8E**).

Figure 8 (Study 2). Mitochondrial respiratory chain complexes

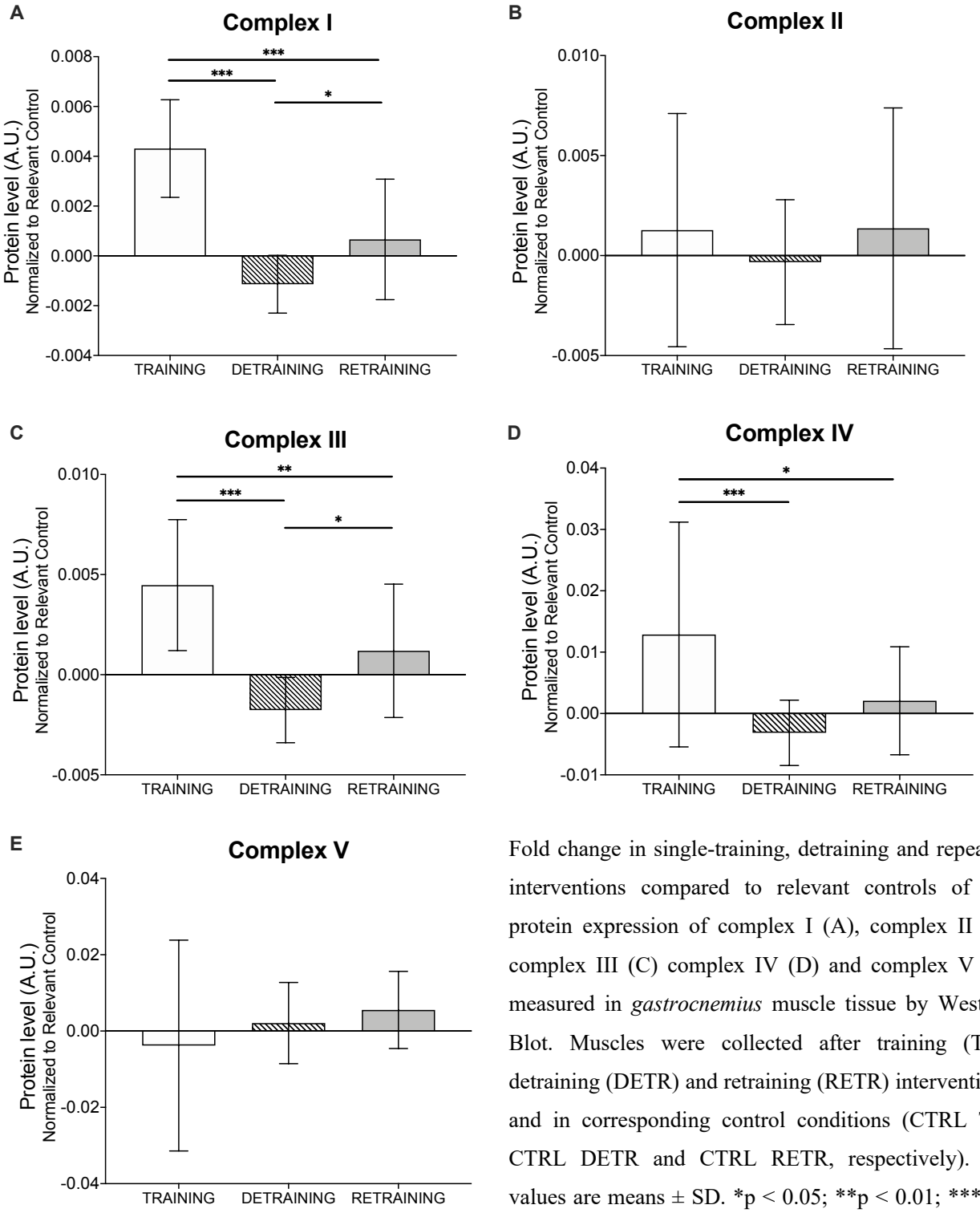

Fold change in single-training, detraining and repeated interventions compared to relevant controls of the protein expression of complex I (A), complex II (B) complex III (C) complex IV (D) and complex V (E) measured in *gastrocnemius* muscle tissue by Western Blot. Muscles were collected after training (TR), detraining (DETR) and retraining (RETR) interventions and in corresponding control conditions (CTRL TR, CTRL DETR and CTRL RETR, respectively). All values are means ± SD. *$p < 0.05$; **$p < 0.01$; ***$p < 0.001$.

DISCUSSION

The present study aimed to investigate the functional response and molecular adaptations of skeletal muscle in response to two repeated interventions of high-intensity interval training in mice. Functional aerobic parameters, biomarkers of mitochondrial biogenesis, mitochondrial content and dynamics, and proteins of electron transport chain complexes were assessed under three different conditions of single training, prolonged period or interruption of training and repeated interventions, in order to investigate changes in aerobic adaptations related to the mitochondrial response to training when stimulus has been previously encountered. To the author's knowledge this study is the first to investigate mitochondrial adaptations in response to repeated endurance interventions allowing us to observe the change in muscle aerobic phenotype affected by memory using a specific aerobic training stimulus. High-intensity interval training has been used here to serve as endurance training paradigm due to the elevated load and intermittent nature, which could mediate the muscle memory effect through epigenetic modifications (Barrès *et al.*, 2012).

From functional results of maximum running velocity, it is interesting to appreciate a larger endurance performance elicited after retraining when similar training stimulus was previously encountered interspersed with a long-term period of detraining which restored functional adaptations to pre-training conditions. This finding leads to suggest the potential existence of a memory mechanism generated by high-intensity interval training at the level of oxidative metabolism in mice, which also shows up at the phenotypic level. Previous studies have investigated the mechanism of muscle memory in the rodent model in response to the resistance training stimulus to explore the effects of repeated interventions on hypertrophic adaptations (Lee *et al.*, 2018). Although authors confirmed muscle memory through myonuclear retention, functional parameters were not assessed, leading the present study to be the first to investigate the memory profile even from a phenotypic perspective.

The observed improved endurance performance during retraining might be determined by larger mitochondrial biogenesis that induced an increased mitochondrial content, as well as changes in mitochondrial dynamics that likely promoted healthier and more functional mitochondria. Increased in mitochondrial number, along with larger mitochondrial size, influence the overall increment in mitochondrial volume density which has been correlated with improve in aerobic performance (Lundby & Jacobs, 2016*b*). High-intensity interval training has been shown to be effective in producing an increase in mitochondrial content, highlighting mitochondrial adaptations as a major factor affecting aerobic performance (Talanian *et al.*, 2006; Burgomaster *et al.*, 2006; Gibala *et al.*,

2006; Granata *et al.*, 2016*a*, 2018; MacInnis & Gibala, 2017). In the present study, following the initial training period, TOM20 protein expression increased, suggesting not only an increase in mitochondrial content, but also an enhancement of the mitochondrial import machinery from the cytosol in response to high-intensity interval training. TOM20 is part of the outer membrane translocase complex responsible for the import of proteins and transcription factors from the cytosol to the mitochondrion (Irrcher *et al.*, 2003). Comparing protein changes between training and retraining conditions we observed a greater increase in citrate synthase along with a simultaneous reduction in TOM20. In addition to providing evidence of a higher mitochondrial content in response to repeated intervention, these conflicting data might be explained by a change in mitochondrial morphology suggesting an adaptation involving differently the outer membrane (represented by TOM20) and the content of the mitochondrial matrix in which the Krebs cycle takes place.

Greater augmentation in mitochondrial content after retraining is supported by larger enhancement in mitochondrial biogenesis when muscle is exposed to a retraining stimulus after a long period of detraining. In the present study we investigated the main proteins involved in PGC-1α pathways, the master regulator of mitochondrial biogenesis in skeletal muscle due to its prominent co-activation of multiple mitochondrial transcription factors, such as nuclear respiratory factors (NRF-1, NRF-2) and mitochondrial transcription factor A (TFAM) implicated in the transcriptional control of respiratory genes and mitochondrial DNA replication and transcription (Wu *et al.*, 1999; Clayton, 2000; Scarpulla, 2002, 2006; Kanki *et al.*, 2004; Hood *et al.*, 2006). Chronic activation of AMPK appears to be a crucial sensor involved in the upregulation of PGC-1α expression in response to energy stress affecting muscle cells during training (Bergeron *et al.*, 2001; Hardie & Sakamoto, 2006; Leick *et al.*, 2010). Acetyl-CoA carboxylase (ACC) is downstream of the AMPK pathway in response to energy stress, in which phosphorylation and subsequent inhibition of ACC occurs to increase ATP production and storage by stimulating fatty acid oxidation in the mitochondria. (Rasmussen & Winder, 1997). Another pathways related to PGC-1α activity is represented by Sirtuins, proteins involved in metabolic regulation in response to physiological changes such as cellular NAD^+ accumulation and NAD^+/NADH ratio elevations that occur during exercise (Tang, 2016). Specifically, SIRT1 is known to affect the post-translational deacetylation process of PGC-1α resulting in an increase in PGC-1α transcriptional activity (Rodgers *et al.*, 2005; Nemoto *et al.*, 2005; Gerhart-Hines *et al.*, 2007; Amat *et al.*, 2009; Dominy *et al.*, 2010; Gurd, 2011). In the present study, it would appear that the response to mitochondrial biogenesis during the single-training intervention was little affected, showing only a tendency towards improved PGC-1α expression. However, a greater increase in PGC-1α and the phosphorylated proteins AMPK and ACC was observed after

retraining, suggesting a significant improvement in the mitochondrial biogenesis process during repeated intervention driven mainly by the AMPK pathway but not by Sirtuins. It is well-known that interval training and endurance stimulus induce increased PGC-1α protein expression ((Granata *et al.*, 2016*b*)), the novel findings in the present study is the enhanced response after repeated aerobic training stimulus confirming data resulting from resistance training in rats that exhibited greater PGC-1α protein expression after second period of ladder climbing training (Lee *et al.*, 2018).

During initial training, results from analyses of fusion dynamics showed an increase in the OPA1 protein together with a reduction in Mitofusin 2. These results may suggest a mitochondrial fusion process that was mainly activated at the inner membrane, the site where OPA1 operates. Similarly, the significant increase in Fis1 protein revealed the facilitation of mitochondrial fission dynamics after training. A concomitant increase in fusion and fission dynamics might suggest an improvement in the mitochondrial turnover process in response to a period of high-intensity interval training that could generate a more efficient mitochondrial network. Looking at changes occurring after retraining mitochondrial fusion was improved as demonstrated by the increase in Mitofusin 2 that was significantly different from the reduction occurred after the first training. Conversely, for fission dynamics, Fis1 protein revealed a lower increase after retraining. This observation occurred in concomitance with a lower reduction in $Drp1_{Ser637}$ which is related to inhibition of fission mechanisms (Chang & Blackstone, 2007; Cribbs & Strack, 2007). Thereby, results from Fis1 and $Drp1_{Ser637}$ are consistent in describing a reduction in mitochondrial fission dynamic after retraining compared to the initial training. Overall, from fusion and fission biomarker adaptations, mitochondrial dynamics appear to be strongly affected by repeated exposure to high-intensity aerobic stimulus where it is interesting to appreciate a shift towards fusion rather than fission, indicating larger and more elongated mitochondria and likely a more interconnected network. This response in mitochondrial dynamics is in agreement with previous literature data demonstrating that exercise training remodels skeletal muscle mitochondrial fission and fusion machinery towards a pro-elongation phenotype (Axelrod *et al.*, 2019). This phenomenon has been explained by the stimulation of mitochondrial fusion in inducing elongation and more interconnected network in response to increased OXPHOS activity and elevated ATP levels (Mishra *et al.*, 2014).

Mitophagy and autophagic flux processes were not affected after exposure to a single-training stimulus. However, interestingly, the response of both mechanisms was evident when the stimulus was encountered a second time. Parkin protein increased significantly after retraining and, correspondingly, an increase in p62 protein was observed after the repeated intervention.

Although it is still unclear as to the precise role of mitophagy in coordinating mitochondrial adaptations to chronic exercise training, our results are in agreement with some studies suggesting that chronic exercise training results in an increase in basal mitophagy in trained skeletal muscle reflecting an increase in mitochondrial turnover observed in this tissue (Ju *et al.*, 2010; Lira *et al.*, 2013*b*). The novelty of the present study lies in the observation that this mechanism occurred in the muscle only after repeated interventions, suggesting a larger improvement in mitochondrial turnover after subsequent exposure to aerobic training stimulus.

Results from protein expression analyses of electron transport chain complexes revealed adaptation in response to the first training period solely for complexes I, III and IV. This interesting finding might be linked with the concept of supercomplexes formation in response to endurance training (Cogliati *et al.*, 2013; Greggio *et al.*, 2017), complex I aggregates in quaternary functional respiratory chain supercomplexes with complexes III and IV (I + III or I + III + IV) (Acín-Pérez *et al.*, 2008; Lapuente-Brun *et al.*, 2013). When observing the changes across the conditions, differently from the first training period, retraining induced a significantly lower increase in the amount of the three complexes affected by improvement during the previous training. This result is not necessarily associated with a reduction in mitochondrial function. Regulation of mitochondrial complexes by the Parkin protein has been demonstrated, showing that higher Parkin values, such as those found in our results after retraining, correlate with lower mitochondrial complex content (Gouspillou *et al.*, 2018). The mechanism is well explained in study from Gouspillou and colleagues (2018), where Parkin overexpressed mice exhibit significantly lower values of COXI subunit content than Parkin knockout mice, but simultaneously greater mitochondrial respiration was observed. This association reflects a mechanism in which mitophagy is activated to remove damaged respiratory chain complexes in order to ensure healthy mitochondria and efficient energy production.

CONCLUSION

In summary, repeated interventions of high-intensity interval training induced a greater improvement in aerobic performance after the second exposure to the aerobic training stimulus. This enhanced response appears to be determined by larger expression of mitochondrial biogenesis factors that induced an increase in mitochondrial content, as well as changes mitochondrial dynamics that likely promoted healthier and more functional mitochondria. Indeed, compared to the first intervention, a second exposure to the training stimulus induced larger increment in mitochondrial biogenesis, mainly driven by AMPK pathway, resulting in a greater increase in mitochondrial content. Mitochondrial dynamics were shifted mainly towards fusion, suggesting larger and more elongated

mitochondria and likely a more interconnected network. Finally, the retraining period elicited increased mitophagic flux, which, associated with a smaller increment in the amount of respiratory chain complexes, suggests an improvement in clearance of damaged mitochondria or complex subunits in order to ensure healthier mitochondria and more efficient respiratory function. In conclusion, mitochondria adaptations to a high-intensity interval training intervention are different if the stimulus has been previously encountered, thereby supporting the hypothesis of a mitochondrial memory.

The present study paved the way for the presence of memory mechanism affecting muscle aerobic phenotype, suggesting insight into potential aerobic muscle memory to high-intensity interval training. This mechanism has important consequences on the quality of life, since if the stimulus encountered affects positively aerobic adaptations at skeletal muscle level, the organism as a whole may further benefit. This may be beneficial both in terms of sports performance, but also to improve the activities of daily living by promoting health in the elder age with lifelong healthy maintenance.

CHAPTER 5

STUDY 3

Human skeletal muscle possesses an epigenetic memory of high intensity interval training affecting mitochondrial function

Pilotto AM[1,2], Mazzolari R[3], Zuccarelli L[1], Crea E[2], Brocca L[2], Pellegrino MA[2], Bottinelli R[2,4], Grassi B[1], Porcelli S[2].

[1] Department of Medicine, University of Udine, Udine, Italy

[2] Department of Molecular Medicine, University of Pavia, Pavia, Italy

[3] Department of Physical Education and Sport, University of the Basque Country (UPV/EHU), Vitoria-Gasteiz, Spain

[4] Interdipartimental Centre for Biology and Sport Medicine, University of Pavia, Pavia, Italy

ABSTRACT

PURPOSE: A first exposure to hypertrophic stimuli, such as testosterone, mechanical loading or resistance exercise, has been shown to lead to faster and larger growth of skeletal muscle when subsequently repeated. Acquired myonuclei permanence and epigenetic modification retention are parallel processes that appear to be involved in the hypertrophy memory mechanism. Interestingly, greater changes in mitochondrial content and biogenesis were also observed after repeated resistance training interventions. Thereby, even mitochondrial adaptations might be influenced by muscle memory, and it remains to be explored whether repeated endurance training interventions can rely on the same mechanism. The aim of this study was to investigate aerobic adaptations and epigenetic modifications in human muscle across repeated exposure to subsequent interval training interventions separated by long-term detraining. METHODS: Sixteen subjects low aerobically fit and never involved in structured program underwent to repeated aerobic training periods (training and retraining) separated by 12 wks of detraining. Each training (combination of cycling high-intensity interval training and sprint interval training) lasted 8 wks. At baseline, training, detraining and retraining time points peak oxygen consumption ($\dot{V}O_{2peak}$) and peak power output (W_{peak}) were measured, and muscle sample was collected from 11 subjects' *vastus lateralis* for mitochondrial respiration (O_2 flux) and epigenetics analysis. RESULTS: $\dot{V}O_{2peak}$ and W_{peak} improved during both training and retraining (all $p<0.001$), but increment changes were not different between the two interventions ($p=0.58$ and $p=0.45$, respectively for $\dot{V}O_{2peak}$ and W_{peak}). O_2 flux improved at maximal phosphorylating and maximal uncoupled states during training (both $p<0.05$). During retraining O_2 flux improved in all mitochondrial respiration states (all $p<0.05$). O_2 flux changes occurred during retraining were greater than changes observed in training. Interval training induced hypomethylation in larger number of DMPs (14,516) than hypermethylated (7,089). Number of hypomethylated DMPs

was maintained elevated during detraining and retraining, whereas hypermethylation returned to baseline level in both conditions. Self-organising map profiling highlighted two memory profile including DMR related to genes such as *FOXK2*, *INPP5a, MTHFD1L*, *SLC16A3*. CONCLUSIONS: Two repeated interventions of interval training interspersed by prolonged training interruption induced different response at epigenetic and mitochondrial level providing evidence of epigenetic memory mechanism in humans. Greater improvement in mitochondrial function during retraining might be associated with DNA hypomethylation induced by interval training. Across repeated intervention two memory profiles were highlighted at epigenetic level characterized by retention of hypomethylation during long-term detraining period. These profiles were related to genes involved in skeletal muscle metabolic pathways.

INTRODUCTION

Skeletal muscle memory has been defined as "the capacity of skeletal muscle to respond differently to environmental stimuli in an adaptive or maladaptive manner if the stimuli have been previously encountered" (Sharples et al., 2016b). The concept refers to the retention of cellular and tissue-level changes generated by previous environmental stimuli or stressors such as those resulting from exercise, muscle damage, disease or changes in nutrients which lead to an altered response if the stimulus is encountered again. This mechanism is important for skeletal muscle because if the environment encountered is positively influencing adaptations, the muscle may respond to these stimuli later in life with further muscle improvement or healthy maintenance across the lifespan. This has important consequences on quality of life, as adequate quantity and quality of skeletal muscle is not only essential for performance in elite sports, but also for improving daily life activities and promoting health in older age (Sharples et al., 2015, 2016a). Concerning exercise and training, muscle encounters this memory mechanism in an adaptively advantageous manner. Indeed, it is becoming evident that molecular and phenotypic responses to chronic exercise are enhanced during subsequent training when similar previous training has been performed.

It has been proven that muscle hypertrophy response induced by anabolic stimuli, such as testosterone, mechanical loading, or resistance exercise, can be accentuated with a faster and larger muscle growing when encountering a similar stimulus later, after a prolonged period of hypertrophic stimuli cessation in which muscle resumes its phenotypic state to pre-exercise condition (Egner *et al.*, 2013; Gundersen, 2016; Lee *et al.*, 2018; Murach *et al.*, 2020). Collectively, these studies have led to the "muscle memory by myonuclear permanence" hypothesis, in which acquisition of new myonuclei can be retained throughout stimulus cessation allowing muscle to "remember" its previous encounters

during subsequent exposure. Currently there is only one study that attempted to directly test this hypothesis in humans (Psilander *et al.*, 2019). The authors found that after 10 weeks of unilateral resistance training followed by a 20-week detraining period skeletal muscle thickness and strength increased significantly in response to the initial exercise training period, which were mostly lost during subsequent interruption. However, during subsequent 5 weeks of bilateral retraining, muscle thickness and strength did not differ between the previously trained leg and the untrained leg. Moreover, muscle fiber cross-sectional area showed an increment after the first training and remained unchanged during detraining as well as during retraining. In addition, no changes in myonuclear content were detected in response to initial training, detraining, or retraining period (Psilander *et al.*, 2019). Although the results seem to suggest evidence to confute the presence of hypertrophy muscle memory in humans, since no increase in myonuclei number was found during the initial training and no clear detraining effect was observed for muscle fiber size during the detraining period, this study may not provide conclusive evidence on the existence of human muscle memory by myonuclear permanence, currently leading to no consensus within the scientific community as shown by debates in the *Journal of Applied Physiology* viewpoint (Murach *et al.*, 2019; Eftestøl *et al.*, 2020). Interestingly, in parallel to memory by myonuclear retention, the role of epigenetics has also emerged as another important mechanism involved in muscle memory enabling muscle to "remember" previous exercise in humans. Seaborne and colleagues (2018) (Seaborne *et al.*, 2018*a*) found after repeated resistance training intervention a larger increase in lower limb lean mass compared to the increment occurred during the previous training stimulus and after being reported to baseline values during detraining period. This pattern was accompanied with DNA methylation modification which revealed memory temporal profiles characterized by retention of hypomethylation acquired during initial training even during detraining period or followed by larger hypomethylation after later detraining (Seaborne *et al.*, 2018*a*). These signatures associated with enhanced expression of targeted genes may be essential in the exercise-induced muscle memory process allowing for an enhanced muscle fiber growth response to repeated resistance training.

It is important to focus the attention on an animal study that observed after repeated resistance training interventions not only greater muscle mass but also greater changes in mitochondrial adaptations in response to retraining compared to the previous intervention (Lee *et al.*, 2018). Authors demonstrated that mitochondria may retain the ability to respond more consistently to repeated noncontinuous stimuli resulting in higher increase in proteins regulating mitochondrial biogenesis and markers of mitochondrial content during the second training period (Lee *et al.*, 2018). This interesting finding pointed out the possible existence of a memory mechanism for specific aerobic physiological

markers. Furthermore, the results of study 2 revealed a more enhanced improvement in aerobic performance in mice in response to the repeated intervention of high-intensity interval training, mainly driven by a greater increase in mitochondrial biogenesis, which resulted in larger mitochondrial content and changes in mitochondrial dynamics, potentially leading to the promotion of a healthier and more functional mitochondrial network. Thereby, the previous study in the present thesis has paved the way for the existence of a memory mechanism affecting muscle aerobic phenotype, suggesting an insight into potential aerobic muscle memory to high-intensity interval training.

Currently, little research has been conducted on the potential presence of skeletal muscle memory induced by aerobic training in humans, but some key information could be obtained from repeated endurance intervention studies. Physiological response to aerobic repeated intervention separated by long-term detraining period were firstly examined in a study in 1987 (Simoneau *et al.*, 1987). Authors showed that subsequent high-intensity interval training periods did not induce retention in oxidative adaptations and no different response between the two training periods was found, excluding hence any indication of aerobic muscle memory pattern. However anaerobic performance revealed higher values after retraining compared to the previous training stimulus in association with a retention of anaerobic enzymes during 7 weeks of inactivity, suggesting that memory could potentially involve anaerobic mechanisms. More recently studies from Gurd's research group demonstrated that individuals respond differently to repeated high-intensity interval training in both cardiorespiratory and skeletal muscle adaptations when a re-exposed to the same training stimulus after a long-term wash-out period (Del Giudice *et al.*, 2020; Islam *et al.*, 2021). Although mean changes in maximal oxygen uptake were not different, individual responses in maximal aerobic capacity were not reproducible suggesting a potential carryover effects from the first training period to the second one (Del Giudice *et al.*, 2020). Moreover individuals also reported dissimilar adaptive responses in skeletal muscle when re-exposed to the same training stimulus, in particular at mitochondrial oxidative capacity, suggesting that differences in responsiveness to repeat training periods may be attributable to the influence muscle memory mechanism that can affect the subsequent training periods (Islam *et al.*, 2021). To deeply investigate the potential presence of a skeletal muscle in response to endurance training Lindholm and colleagues (2016) (Lindholm *et al.*, 2016) examined transcriptional response to subsequent 12-week one-legged aerobic training periods (45 min, 4 times/week) with a 9-month break in between. Results showed no retention of gene expression profiles during detraining period and even mitochondrial adaptations, such as citrate synthases activity for mitochondrial content estimation, were not different between the two training interventions refuting, thus, the presence of a differential response in endurance training due to a

skeletal muscle memory effect (Lindholm *et al.*, 2016). Collectively, the topic of aerobic training-induced skeletal muscle memory is still debated and in the early stage of investigation.

In order to deepen our understanding of the potential presence of skeletal muscle memory induced by endurance training, the aim of the present study was to investigate aerobic adaptations at all levels of the entire human organism, from the molecular to the functional level, across repeated exposure to two identical interval training interventions separated by long-term period of detraining. Investigation of the exercise response from the epigenetic level up to the whole-body scale has therefore provided a broad overview of the mechanism underpinning this phenomenon.

MATERIALS AND METHODS

Subjects

Sixteen male (n = 8) and female (n = 8) adult participants (age 25 ± 5 years; weight 64.0 ± 11.2 kg; height 171 ± 6 cm) were recruited from the local community. Inclusion criteria required that subjects had never been involved in structured training programs, moreover, through the initial screening test, aerobically fit individuals ($\dot{V}O_{2peak}$ > 45 ml·min^{-1}·kg^{-1}) were excluded. All participants completed a health history questionnaire to ensure there was no presence of chronic disease. None of the the aims, methods, and risks, and gave their written informed consent prior to enrollment. All procedures were in accordance with the Declaration of Helsinki and the study was approved by the local ethics committee (Besta 64-19/07/2019).

Table 1 (Study 3). Participant characteristics at the initial screening test

	Age (years)	Weight (kg)	Height (cm)	$\dot{V}O_{2peak}$ (ml·min^{-1}·kg^{-1})	$\dot{V}O_{2peak}$ (l·min^{-1})
Males (n = 8)	28 ± 6	69.7 ± 11.6	176 ± 4	38.2 ± 9.4	2.603 ± 0.506
Females (n = 8)	23 ± 3	58.2 ± 7.6	167 ± 4	34.4 ± 5.6	1.985 ± 0.330

Participants anthropometrics and physiological characteristics measured during the initial screening test grouped according to sex. $\dot{V}O_{2peak}$, peak oxygen uptake. All values are means ± SD.

Study design

The current study exposed the same individuals to two identical 8-week interval training periods (termed training and retraining, respectively) separated by a three-month washout period of detraining during which participants were instructed to return to their pre-study levels of physical activity. Measurements were examined at four different time points: at baseline (BAS), after the first training period (TR), following detraining (DETR) and after retraining (RETR). For each time point

participants visited the laboratory on three separate occasions separated by 24–48 h. During the first visit of testing, anthropometric measurements were taken and a cycle incremental cardiopulmonary exercise test to the limit of tolerance was performed to determine $\dot{V}O_{2peak}$ and gas exchange threshold (GET). Forty-eight hours after incremental exercise the second visit was arranged wherein 100 mg of skeletal muscle was obtained from the *vastus lateralis* muscle by percutaneous conchotome muscle biopsy under local anesthesia (1% lidocaine) for muscle respirometry, morphology and epigenetics analyses. At visit 3, participants performed three 5-min constant work-rate (CWR) cycling at 80% GET to evaluate $\dot{V}O_2$ kinetics; the first two out of three exercises were immediately followed by repeated muscle oxidative capacity tests (Zuccarelli *et al.*, 2020) to assess muscle oxidative capacity. Both incremental exercise test and CWR were administered on an electronically braked cycle ergometer (LC-6, Monark, Sweden). Following training, the order of the three visits was identical to pre-training and the first post-training visit occurred 48h after the final training session. Participants were instructed to abstain from strenuous physical activity for at least 24 h prior to each testing session (48 h for the biopsy trial).

Training

Training consisted of two identical 8-week periods separated by a three-month wash-out period. During both training and retraining, participants trained independently three times per week with interval training sessions on electronically braked cycle ergometer (Nowa, Diadora, Italia) for a total of 12 training sessions for each period. Interval training involved high-intensity interval training (HIIT), in both low-volume (interval duration ≤ 2 min) and high-volume (interval duration > 2 min) paradigm/types, and sprint interval training (SIT). To avoid stagnation, the training stimulus of high-intensity intervals was progressively incremented in subsequent training sessions by increasing the relative exercise intensity and repetitions (Granata *et al.*, 2016*a*).

Overall, each training period consisted of the following different training exercise modalities. 1) Four training sessions were composed of 4-min cycling intervals interspersed with 2-min recovery at 30-50% W_{GET}. Training intensities were defined as $W_{GET} + x\,(W_{peak} - W_{GET})$, where x = 0.35, 0.50, 0.65, and 0.75 for sessions 1–4, respectively. Number of repetitions was 4, 5, 6 and 6 for sessions 1–4, respectively. 2) Two training sessions comprised 10 bouts of 2-min cycling intervals interspersed with 1-min recovery at 30-50% W_{GET}. Training intensities in the two sessions were defined as $W_{GET} + x\,(W_{peak} - W_{GET})$, where x = 0.80 and 0.90, respectively. 3) Three training sessions were structured with 1-min cycling intervals interspersed with 2-min recovery at 30-50% W_{GET}. Training intensities were defined as 100, 110, 120% of W_{peak} for sessions 1–3, respectively. Number of repetitions was 6, 8 and 10 for sessions 1–3, respectively. 4) Three training sessions consisted of “all-out” 30-s cycle

sprints interspersed with 4-min self-managed recovery. Repetitions were 6, 7 and 8 for sessions 1–3, respectively. During this training mode cycle ergometer was set in hyperbolic mode with a resistance that allowed to elicit power of 170% W_{peak} with 80 rpm and participants were instructed to pedal as faster as possible. Exercises were alternated during the training period to facilitate participant motivation and compliance, as detailed previously (Robach *et al.*, 2014). An identical training protocol was applied for both training and retraining period.

Incremental exercise

Power during step-incremental cycling was increased 10-15 W every minute, depending on the individual's fitness. Participants were instructed to maintain constant cadence at their preferred value (between 70 and 85 rpm). Intolerance was defined when participants could no longer maintain their chosen pedaling frequency despite verbal encouragement.

Pulmonary ventilation ($\dot{V}_E$, in BTPS [body temperature (37°C), ambient pressure and gas saturated with water vapor]), oxygen consumption ($\dot{V}O_2$), and CO_2 output ($\dot{V}CO_2$), both in STPD (standard temperature [0°C or 273 K] and pressure [760 mmHg] and dry [no water vapor]), were determined breath-by-breath by a metabolic cart (Vyntus CPX, Vyaire Medical GmbH, Germany). Before each test, gas analyzers were calibrated with ambient air and a gas mixture of known concentration (O_2: 16%, CO_2: 4%) and the turbine flowmeter was calibrated with a 3-L syringe at three different flow rates. RER was calculated as $\dot{V}CO_2/\dot{V}O_2$. HR was recorded by using a HR chest band (HRM-Dual, Garmin, Kansas, USA). Rating of perceived exertion (RPE) was determined using Borg® 6–20 scale every 2 min through the test (Borg, 1982). At rest, and at 1, 3, and 5 min of recovery, 20 μL of capillary blood was obtained from a preheated earlobe for blood lactate concentration (Biosen C-line, EKF, Germany); the analyzer was frequently calibrated with a standard solution containing 12 $mmol \cdot L^{-1}$ of lactate. Peak cardiopulmonary variables were measured from the highest 20 s mean values prior to intolerance when at least two of the following criteria were found: 1) maximal levels (>15) of RPE; 2) HR values higher than 85% of the age-predicted maximum; 3) RER values equal or above 1.1; and 4) $[La]_b$ during recovery higher than 8 $mmol \cdot L^{-1}$. Peak values were further verified after 30 min of recovery by means of a supramaximal verification trial performed at 90% of peak power output (W_{peak}). GET was determined by two independent investigators by using the modified "V-slope" method (Beaver *et al.*, 1986) and "secondary criteria". The power at GET was estimated after accounting for the individual's $\dot{V}O_2$ mean response time (Whipp *et al.*, 1981).

For cardiac response, stroke volume (SV) was estimated beat-by-beat by means of transthoracic impedance cardiography (PhysioFlow, Manatec Biomedical, France) and averaged every 10 beats during all exercise tests. The accuracy of this device has been previously evaluated during incremental exercise in healthy subjects against the direct Fick method (Richard *et al.*, 2001). A detailed description of the method has been provided elsewhere (Charloux *et al.*, 2000). Briefly, the Physio Flow emits a 75-kHz, 1.8-mA alternating electrical current via two sets of electrodes (two "transmitting" and two "sensing" electrodes) applied above the supraclavicular fossa at the left base of the neck and next to the spine corresponding to the xiphoid process of the subject, respectively. Another set of two electrodes is used to monitor a single ECG lead. Verification of the correct signal quality is accomplished by visualization of the ECG signal, the impedance waveform, and their first derivatives. Then, the subject stands or sits still and relaxed for at least 5 min, during which the auto-calibration procedure is performed to obtain reference curves and data necessary to measure SV variations. HR was obtained from the R-R interval determined on the ECG first lead. Cardiac output ($\dot{Q}$) was then calculated by multiplying SV and HR.

Constant work-rate exercise

Participants completed three CWR exercises of 5-min duration at moderate intensity (corresponding to 80% of GET power output). Each transition was preceded by 2 min of baseline cycling at unload pedaling before an abrupt transition to the target work rate. A passive recovery of 10 min separated the transitions. Subjects were free to choose the cadence they cycled during their first transition which was then maintained (± 5 rpm) throughout the remaining transitions.

Pulmonary gas exchange and ventilatory variables were determined breath-by-breath using a metabolic cart (Vyntus CPX, Vyaire Medical GmbH, Germany). HR was recorded by using a chest band (HRM-Dual, Garmin, Kansas, USA), and rating of perceived exertion (RPE) was determined using Borg® 6–20 scale every 2 min through the test (Borg, 1982). Rating of perceived exertion (RPE) was determined using Borg® 6–20 scale after each repeat (Borg, 1982). At rest and after completion of exercise 20 µL of capillary blood was obtained from a preheated earlobe for blood lactate concentration (Biosen C-line, EKF, Germany).

For the determination of $\dot{V}O_2$ kinetics, errant breaths, defined as any value lying more than 4 SDs away from the local mean (e.g., caused by swallowing, coughing, sighing, etc.), were removed. The $\dot{V}O_2$ responses from the three transitions were averaged before any analysis to enhance the signal-to-noise ratio and improve the 95% confidence interval surrounding the calculation of the parameters derived from the model fits (Lamarra *et al.*, 1987; Whipp & Rossiter, 2005).

Subsequently, the $\dot{V}O_2$ responses for the three transitions were linearly interpolated to give 1-s values and then averaged. The breath-by-breath data obtained during the three identical repetitions were time aligned to the start of exercise for each individual and were subsequently linearly interpolated to provide values every 10 s (Lamarra *et al.*, 1987; Whipp & Rossiter, 2005). The first 20 s of data after the onset of exercise (i.e., the phase I response or "cardiodynamic" phase (Whipp *et al.*, 2005)) were deleted (Whipp & Rossiter, 2005), thus, $\dot{V}O_2$ kinetics analysis focused mainly on the phase II (or "fundamental" component) of the response. A nonlinear least squares algorithm was used to fit the data thereafter. A mono-exponential model was used to characterize the $\dot{V}O_2$ responses to moderate exercise as described in the following equation:

$$\dot{V}O_2(t) = \dot{V}O_{2\,baseline} + A\,[1 - e^{-(t-TD)/\tau}] \qquad \text{Eq. 1 (Study 3)}$$

where $\dot{V}O_2(t)$ represents the absolute $\dot{V}O_2$ at a given time t; $\dot{V}O_{2baseline}$ represents the mean $\dot{V}O_2$ in the baseline period; *A*, *TD*, and τ represent the amplitude, time delay and time constant, respectively, describing the phase II increase in $\dot{V}O_2$ above baseline. An iterative process was used to minimize the sum of the squared errors between the fitted function and the observed values. $\dot{V}O_{2baseline}$ was defined as the mean $\dot{V}O_2$ measured over the final 60 s of unload pedaling. The end-exercise $\dot{V}O_2$ was defined as the mean $\dot{V}O_2$ measured over the final 30 s of exercise. The absolute fundamental component amplitude (absolute A) was defined as the sum of $\dot{V}O_{2baseline}$ and A.

Muscle Oxidative Capacity by NIRS

For this measurement one female subject was excluded from analysis cause of impossibility to analyze signal at DETR, thus for muscle oxidative capacity sample size is n = 15.

The protocol proposed and validated in study 1 was applied to assess the muscle oxidative capacity (Pilotto *et al.*, 2022). The recovery rate constant (*k*) of muscle oxygen uptake ($m\dot{V}O_2$) was measured using an approach modified from Zuccarelli et al. (Zuccarelli *et al.*, 2020). Oxygenation changes of the *vastus lateralis* were sampled at 10 Hz by a wireless, portable, continuous-wave, spatially-resolved, NIRS device (PortaLite, Artinis, The Netherlands). Relative concentrations of deoxy-(hemoglobin+myoglobin) (HHb for simplicity) and oxy-(hemoglobin+myoglobin) (HbO_2) were measured in the tissues approximately 1.5 – 2 cm beneath the probe, with respect to an initial value arbitrarily set equal to zero. From these measurements, relative changes in total hemoglobin and myoglobin (tHb = HHb+HbO_2) and the Hb difference (Hbdiff = HbO_2−HHb) were calculated. In addition, the tissue saturation index (TSI, %) was measured using the SRS approach (Ferrari *et al.*, 2004).

The skin at the NIRS probe site was shaved before the probe was placed longitudinally on the lower third of *vastus lateralis* muscle (~10 cm above the knee joint) and secured with a black patch and elastic bandage. The location of the probe was marked using a skin marker to ensure the placement location was similar across all measurements. The mean thickness of the skin and subcutaneous tissue at the NIRS probe site (8.1 ± 2.7 mm) was measured by skinfold caliper (Holtain Ltd, Crymych, UK). A 13 × 85 cm rapid-inflation pressure-cuff (SC12D, Hokanson, USA) was placed proximally on the same thigh and attached to an electronically-controlled rapid cuff-inflator (E20, Hokanson, USA).

While participants were seated on a cycle ergometer, baseline TSI was measured over 2 min of rest. Subsequently, a prolonged arterial occlusion (300 mmHg) was performed until TSI plateaued (typically ~120 s). The cuff was instantly deflated and muscle reoxygenation was recorded until a steady-state was reached (typically ~3 min). This procedure identified the physiological normalization (PN) of TSI under resting conditions between the TSI deflection point and the TSI peak (Adami *et al.*, 2017). Participants then cycled for 5 min at a power output corresponding to 80% GET to desaturate the muscle to a target of 50% of the physiological normalization amplitude, the cycling exercise was followed by an immediate stop and 10-15 intermittent arterial occlusions at 300 mmHg. Duration and timing of the repeated occlusions were controlled by the investigator to maintain TSI in the range from 50 to 60% of PN in order to assess muscle oxidative capacity as demonstrated in study 1 (Pilotto *et al.*, 2022). On the same day two repetitions were performed separated by a resting period (typically ~10 min).

The rate of muscle desaturation during each intermittent arterial occlusion (TSI, $\%\cdot s^{-1}$) was fitted to estimate the exponential $m\dot{V}O_2$ recovery or *k*, as previously described (Adami *et al.*, 2017). During the repeated oxidative capacity tests, for each intermittent arterial occlusion the negative slope of TSI ($\%\cdot s^{-1}$) was fitted by a linear function to estimate relative $m\dot{V}O_2$. Note that during occlusion the rate of deoxygenation (the negative slope of TSI) is inversely proportional to $m\dot{V}O_2$ and is therefore reported as a positive value ($\%\cdot s^{-1}$). Post-exercise $m\dot{V}O_2$ measurements were fit to a mono-exponential function (OriginPro v8.6, OriginLab Co., Northampton, USA) (Wüst et al., 2013) as follows:

$$y = (end - delta) \times e^{-kt} \qquad \text{Eq. 2 (Study 3)}$$

where *y* is the relative $m\dot{V}O_2$ during the arterial occlusion, *end* is the $m\dot{V}O_2$ immediately following exercise, *delta* is the amplitude change in $m\dot{V}O_2$ from end-exercise to rest, *k* is the recovery rate constant and *t* is time in minutes. According to this first-order metabolic model, the recovery kinetics follow a mono-exponential function which is independent of exercise intensity (Crow & Kushmerick,

1982; Mahler, 1985; Meyer, 1988; Paganini *et al.*, 1997; Walter *et al.*, 1997; Ryan *et al.*, 2013*a*). Data were quality-checked before curve fitting to remove invalid values or outliers i.e., low initial TSI values, or incomplete occlusions (Beever *et al.*, 2020). The recovery rate constant *k* was used as an index of mitochondrial oxidative capacity, as previously described (Ryan *et al.*, 2013*b*).

Muscle Biopsy

Eleven participants out of 16 (male (n = 8) and female (n = 3) (age 25 ± 5 years; weight 66.7 ± 13.1 kg; height 174 ± 5 cm)] agreed to undergo muscle biopsy for all the time points required by the experimental protocol. Resting muscle biopsies were taken from the *vastus lateralis* muscle using a 130 mm (6") Weil-Blakesley rongeur (NDB-2, Fehling Instruments, GmbH&Co, Germany) under local anesthesia (1% lidocaine). After collection, a specimen of ~20 mg of muscle tissues was immediately submerged in Allprotect Tissue Reagent (Qiagen, Netherlands) following the manufacturer's instructions to stabilize and protect cellular DNA and RNA and was stored at -20°C for subsequent DNA methylome analysis. Remaining muscle samples were cleaned of excess blood, fat, and connective tissue in ice-cold BioPS, a biopsy-preserving solution containing (in mM) 2.77 CaK_2EGTA, 7.23 K_2EGTA, 5.77 Na_2ATP, 6.56 $MgCl_2$, 20 taurine, 50 MES (2-(N-morpholino)ethanesulfonic acid), 15 Na_2phosphocreatine, 20 imidazole, and 0.5 dithiothreitol adjusted to pH 7.1 (Doerrier *et al.*, 2018). A portion of each muscle sample (~10-20 mg) was placed in a plate containing clean ice-cold BioPS for preparation of permeabilized fiber bundles as previously described (Perry *et al.*, 2011). A portion of ~20-30 mg from each muscle sample was rapidly frozen by immersion in liquid nitrogen and stored at -80°C for proteomic analysis. The remaining portion were fixed in OCT (Tissue-Tek, Sakura Finetek Europe, Zoeterwoude, The Netherlands) embedding medium, frozen in N_2-cooled isopentane and stored at -80°C for subsequent histology. Only muscle samples from five (out of 11) participants were analyzed (age 29 ± 6 yrs; weight 66.5 ± 9.7 kg; height 175 ± 6 cm) for DNA methylome, proteomic, and histological analysis.

Preparation of Permeabilized Fibers

Fibers bundles were mechanically separated with pointed forceps in ice-cold BioPS. The plasma membrane was permeabilized by gentle agitation for 30 min at 4°C in 2ml of BioPS containing 20 $\mu g \cdot ml^{-1}$ saponin, washed for 10-min MiR05 (in mM, unless specified) 0.5 EGTA, 3 $MgCl_2$, 60 potassium lactobionate, 20 taurine, 10 KH_2PO_4, 20 HEPES (4-(2-hydroxyethyl)piperazine-1-ethanesulfonic acid), 110 sucrose, and 1 $g \cdot L^{-1}$ bovine serum albumin (BSA), essentially fatty acid–free (pH 7.1) (Doerrier *et al.*, 2018) and blotted prior to being weighed.

Mitochondrial Respiration

Mitochondrial respiration was measured in duplicate, using 3-6 mg wet weight of muscle fibers, in 2 ml of MiR05 at 37°C containing myosin II-ATPase inhibitor (25 µM blebbistatin dissolved in DMSO 5mM stock) to inhibit contraction (Perry *et al.*, 2011) (Oxygraph-2k, Oroboros, Innsbruck, Austria). Chamber O_2 concentration was maintained between 250 and 450 nmol·ml^{-1} by periodic O_2 injection. Instruments were calibrated according to the manufacturer's instructions (Pesta & Gnaiger, 2012).

A substrate-uncoupler-inhibitor titration protocol was used (Salvadego *et al.*, 2016, 2018; Doerrier *et al.*, 2018) in the following order: glutamate (10 mM) and malate (4 mM) was added to assess LEAK respiration through complex I (CI_L). ADP (10 mM) was added to assess maximal oxidative phosphorylation (OXPHOS) capacity through CI (CI_P). Succinate (10 mM) was added to assess OXPHOS capacity through CI + complex II ($CI+II_P$). Cytochrome c (10 µM) added to test for outer mitochondrial membrane integrity. Stepwise additions of carbonyl cyanide-p trifluoromethoxyphenylhydrazone (FCCP) (0.5 µM) were used to measure electron transport system capacity through CI+II ($CI+II_E$). Inhibition of CI by rotenone (1 µM) determined electron transport system capacity through CII (CII_E), while addition of antimycin A (2.5 µM) was used to measure residual oxygen consumption, which was subtracted from all measurements. Results were expressed in pmol·s^{-1}·mg^{-1} wet weight calculating mean values of duplicate analyses.

Proteomic Analysis

Sample Preparation: muscle lysis and protein extraction. Frozen muscles were pulverized in a steel mortar using a ceramic pestle, with the constant addition of liquid nitrogen in order to maintain muscle components' properties. The powder thus obtained was homogenized with a lysis buffer containing TRIS-HCl 20 mM, Triton 100x 1%, Glycerol 10%, NaCl 15 0mM, EDTA 5 mM, NaF 100 mM and NaPPi 2 mM supplemented with protease inhibitor 5X, phosphatase inhibitors 1X (Protease Inhibitor Cocktail, Sigma-Aldrich, St. Louis MO) and PMSF 1 mM. The lysis of tissue was performed on ice for 40 minutes. The homogenate obtained was centrifuged at 13500 rpm for 20 minutes at 4° C and the supernatant was transferred to clean eppendorf tubes and stored at -80° C until use.

The protein concentration of the lysates was determined using the RC-DC™ (reducing agent and detergent compatible) protein assay (Bio-Rad) that is a colorimetric assay for protein determination in the presence of reducing agents and detergents.

Western Blot. Equal amounts of muscle samples were loaded on gradient precast gels purchase from BioRad (AnyKd) and subjected to electrophoresis. Electrophoretic run was carried out at constant

current (100V) for about 2 hours in a running buffer at pH 8.8 (Tris 25 mM, Glycine 192 mM, SDS 1%). To monitor protein separation, a protein molecular weight marker constituted by a mixture of proteins with known molecular weight (Preistained Protein Ladder Marker, BIORAD) was loaded on the gel. Proteins were electro-transferred to polyvinylidene fluoride (PVDF) membranes at constant voltage at 100V for 2 hours at 4° C or at 35 mA overnight (O/N) in a transfer buffer containing Tris 25 mM, Glycine 192 mM, and methanol 20%. The effective protein transfer to the membrane was verified by staining with Ponceau Red (Sigma) in acetic acid (Ponceau Red 0.2% in acetic acid 3%) for 15 minutes under stirring at room temperature. Nonspecific binding sites present on the PVDF membrane were saturated with a blocking solution consisting of 5% fat-free milk in TBS-T (Tris 0.02 M, NaCl 0.05 M and Tween-20 0.1%) for 2 hours at room temperature with constant shaking. At the end of incubation, the membrane was washed with TBS-T for three times 10 minutes each. After that the membranes were probed with specific primary antibodies (**Table 1**) overnight at 4° C. Thereafter, the membranes were incubated in HRP-conjugated secondary antibody. Proteins detection was made using ECL advance detection system (GE Healthcare Life Sciences) which highlights the HPRT substrate by a chemiluminescent reaction. The membrane was gained through an analysis software ImageQuant LAS 4000 (GE Healthcare Life Sciences). The content of each protein investigated was assessed by determining the brightness–area product of the protein band as previously described (Cannavino *et al.*, 2014). Tubulin was used as housekeeping protein for internal loading control to normalize protein expression.

Following the previously well described procedure for general western Blot protocol, the detection of the subunits from the five mitochondrial complexes (NDUFB8, SDHB, UQCRC2, MTCO1, ATP5A for complex I, II, III, IV, and V, respectively) that make up the respiratory chain can be performed in the same PVDF membrane by using a cocktail of the five antibodies targeting the five proteins. 5 µg of quantified proteins were prepared with adjusted amounts of Laemmli Buffer 4X and PBS 1X and denatured at 37° C for 5 min. Following 5 min of acclimation at room temperature, a protein molecular weight marker and samples were loaded on gradient Precast acrylamide/bisacrylamide gels (Bio-Rad) and electrophoresis was carried out at constant current (100V) for about 2 h in running buffer. At the end of the gel run, gels undergo transfer of proteins to a PVDF membrane prior to methanol activation. The transfer was carried out at constant voltage at 100V for 2 h at 4° C or at constant 35 mA overnight (O/N) in cold transfer buffer.

Then, nonspecific binding sites present on the PVDF membrane were saturated with a blocking solution consisting of 5% fat-free milk in TTBS 1X for 2 h at room temperature with constant shaking.

After that, membranes were washed three times, 10 min each, with TTBS 1X and incubated O/N at 4° C with the specific primary antibody against the mitochondrial complexes of the respiratory chain (OXPHOS 1:1000, Abcam) in 5% fat-free milk in TTBS 1X. Subsequently, membranes were washed three times in TTBS 1X and then incubated 1 h at room temperature in constant agitation, with the HRP-conjugated donkey anti-mouse secondary antibody (1:10000, Dako) in 5% fat-free milk. After final three washes of 10 min each in TTBS 1X, the last one was made in TBS 1X. Proteins detection was made by using Amersham ECL Select™ detection system (Cytiva Life Sciences, ex GE Healthcare) and membranes gained through the ImageQuant™ LAS 4000 software (GE Healthcare Life Sciences), with the exposure time adjusted in an automatic manner or editable depending on the intensity of the emitted signal. After, to visualize the total protein amount present on the membrane, these were subjected to a Coomassie PVDF-specific staining (0.1% Coomassie Blue R-250, 50% Methanol, 10% Acetic Acid) for 20 min and destained with a destain composed by 40% Methanol and 10% Acetic Acid. Air dried membranes were then digitalized with a scanner and analysed. Data were expressed as the ratio between the BAP of samples from each of the five complexes and of total protein amount stained with Coomassie (arbitrary units).

Table 2 (Study 3). List of primary and secondary antibodies used

TARGET PROTEIN	PROTEIN LYSATE (µg)	SATURATION	Ab I	COMPANY	Ab II	COMPANY
PGC-1α	40	milk 5%	1:1000 milk 5%	Abcam	anti-Rabbit (1:10000) milk 5%	Cell Signaling
p-AMPK	40	milk 5%	1:1000 BSA 5%	Cell Signaling	anti-Rabbit (1:10000) milk 5%	Cell Signaling
AMPK	40	milk 5%	1:1000 BSA 5%	Cell Signaling	anti-Rabbit (1:10000) milk 5%	Cell Signaling
TOM20	15	milk 5%	1:1000 milk 5%	Santa Cruz	anti-Rabbit (1:10000) milk 5%	Cell Signaling
CS	15	milk 5%	1:2000 milk 5%	Abcam	anti-Rabbit (1:10000) milk 5%	Cell Signaling

OPA1	40	milk 8%	1:3000 milk 5%	Abcam	anti-Mouse (1:5000) milk 5%	DAKO
p-Drp1$_{(Ser616)}$	40	milk 5%	1:1000 BSA 5%	Cell Signaling	anti-Rabbit (1:10000) milk 5%	Cell Signaling
p-Drp1$_{(Ser637)}$	40	milk 5%	1:1000 BSA 5%	Cell Signaling	anti-Rabbit (1:10000) milk 5%	Cell Signaling
Drp1	40	milk 5%	1:1000 BSA 5%	Cell Signaling	anti-Rabbit (1:10000) milk 5%	Cell Signaling
Mfn1	40	milk 5%	1:1000 milk 5%	Abcam	anti-Mouse (1:5000) milk 5%	DAKO
Mfn2	40	milk 5%	1:1000 milk 5%	Abcam	anti-Rabbit (1:10000) milk 5%	Cell Signaling
Fis1	40	milk 8%	1:1000 milk 5%	Abcam	anti-Rabbit (1:10000) milk 5%	Cell Signaling
PINK1	40	milk 5%	1:1000 milk 5%	Invitrogen	anti-Rabbit (1:10000) milk 5%	Cell Signaling
Parkin	40	milk 5%	1:1000 milk 5%	Invitrogen	anti-Mouse (1:5000) milk 5%	DAKO
Tub	40	milk 5%	1:2000 milk 5%	SIGMA aldrich	anti-Mouse (1:5000) milk 5%	DAKO
OXPHOS	5	milk 5%	1:1000 milk 5%	Abcam	anti-Mouse (1:10000) milk 5%	DAKO

Morphological and Histological Investigation

Several transverse sections with a thickness of 10 μm each were obtained from muscle samples mounted in OCT (Tissue-Tek, Sakura Finetek Europe, Zoeterwoude, Netherlands) embedding medium for both myosin heavy chain isoform content and capillarization analysis. The working temperature, to ensure the consistency suitable for cutting of the muscles, was set at -20-22° C. Sections were collected on the surface of a glass slide polarized, which guarantees the permanent adhesion. Images of the stained sections were captured from a light microscope (Leica DMLS) and transferred to a personal computer using a video camera (LeicaDFC280). Fiber CSAs were measured with Image J analysis software (NIH, Bethesda, MD, USA) and expressed in μm^2.

Myosin heavy chain isoform. Several cross-cryosections obtained from the muscles analyzed were immunostained using antibodies specific for MHC-I, MHC-IIa and MHC-IIx isoform. A secondary rabbit antimouse immunoglobulin G (IgG) antibody conjugated with peroxidase (P-0260, DAKO, Glostrup, Denmark) was used to reveal the binding of primary antibodies. The primary antibodies were diluted (dilution 1:7 for BA-F8, 1:5 for SC-71) in a solution of PBS + BSA 1% (w / v) (PBS = aqueous solution containing NaCl 13 6 mM, KCl 2 mM, Na_2HPO_4 6 mM, KH_2PO_4 1 mM; BSA = bovine serum albumin). The secondary antibody conjugated with peroxidase has been diluted 1:50 in PBS + 1% BSA (w / v). The solution with primary antibodies was distributed on the surface of the slides so as to completely cover each section and were allowed to react for 40 minutes at 37° C. After the incubation with primary antibodies, slides were washed 3 times, 5 minutes each in PBS at room temperature. Then, secondary antibody solution was distributed on the slides at 37° C for 40 minutes, and finally, after 3 washes of 5 minutes each in PBS at room temperature, we proceeded to visualization of positive immunostained cells where the reaction antigen-antibody occurred. The visualization of positive cells was performed by incubating muscle sections with a solution containing Diaminobenzidine (DAB) and hydrogen peroxide, which produced brown coloration on positive immunostained cells; the color reaction was carried out at room temperature in about 1 minute and was, then, blocked by dipping the slides in cold distilled water. The slides were then dehydrated in alcoholic solutions as described for Hematoxylin-eosin Staining and finally closed by using a cover slip fixed with Eukitt ® Mountant (Bio-Optica). The sections of muscles so colored were examined using a computerized image analyzer, consisting of a camera (Digital Vision) placed on a light microscope (Leitz, Laborlux D) and connected via a digital interface to a computer equipped with specific software (Twain, 32). With this system, it was possible to view images of preparations on the screen, to evaluate the distribution of the two different isoforms MHCs and by using Scion Image program (NIH, Bethesda, MD, USA), calculate the area of each section.

MHC isoform composition was assessed in the whole biopsy. Frozen portion of biopsy was pulverized in a steel mortar with liquid nitrogen to obtain a powder that was immediately resuspended in a Laemmli solution (Soriano *et al.*, 2006). The samples were incubated on ice for 20 min and finally spun at 18 000 *g* for 30 min. Protein concentration in the dissolved samples was determined with a protein assay kit (RC DC, Bio-Rad, Hercules, CA, USA). About 10 μg of proteins for each sample was loaded on 6% SDS-polyacrylamide gels and electrophoresis was run overnight at 100V; following Coomassie staining, three bands corresponding to MHC isoforms were separated and their densitometric analysis was performed to assess the relative proportion of isoforms MHC-I, MHC-IIa and MHC-IIx in the samples (Brocca *et al.*, 2017). Image gels were acquired using a scanner (Epson Expression 1680 Pro) and densitometry was performed with a provided software (2202 Ultroscan Laser Densitometric Lkb). During analysis, protein bands were visualized as peaks and areas below peaks were measured and compared. In this way, it was possible to determine the percentage ratio between every isoform. Analysis of each sample was repeated three times and an average of the three repeated measurements was calculated. The single value of MHC distribution obtained from each sample was averaged with the other values of subjects of the same group to assess the mean MHC isoform distribution.

Capillarization. Remaining cryosections were fixed with methanol in ice for 15 min, washed 3 times (5 min each) in PBS (NaCl 136 mM, KCl 2 mM, Na_2HPO_4 6 mM, KH_2PO_4 1 mM) at room temperature (RT) and incubated in 1%Triton-100x in PBS for 30 min (RT). Cryosections were then incubated with blocking reagents (4% BSA in 1% Triton X-100 in PBS + 5% Goat Serum) for 30 min (RT), raised with PBS (3 times of 5 min each) and probed with anti-CD31 (1:100 dilution, Abcam) overnight at 4º C. After 3 washes (5 min each) in PBS, cryosections were incubated with Alexa-Fluor 488 anti-mouse (1:200 dilution; Abcam) for 60 min at room temperature. Finally, the samples were probed with anti-Dystrophin (1:500 dilution, Abcam) for 60 min at room temperature and then with Alexa-Fluor 488 anti-rabbit (1:200 dilution; Abcam) for 60 min at room temperature. Fluorescence intensity was visualized with Olympus microscope (U-CMAD3). 125 to 150 fibers were measured in each sample. Capillary-to-fiber ratio was defined as total number of capillaries divided by number of fibers counted within the sample.

Epigenetics Analysis

Tissue Homogenization, DNA Isolation, and Bisulfite Conversion. Power analysis was conducted to detect a greater than 1.05 (5%) fold change in methylation based on our previous studies (Seaborne *et al.*, 2018*a*), $n = 3$ in a within-subject design was determined as sufficient to detect statistically significant changes in methylation over the baseline, training, detraining and retraining time points. Thereby, five subjects analyzed in the present study were sufficient to infer conclusion on changes in methylation. Tissue samples were homogenized for 45 s at 6,000 rpm × 3 (5 min on ice in between intervals) in lysis buffer (180 µl buffer ATL with 20 µl proteinase K) provided in the DNeasy spin column kit (Qiagen, United Kingdom) using a Roche Magnalyser instrument and homogenization tubes containing ceramic beads (Roche, United Kingdom). The DNA was then bisulfite converted using the EZ DNA Methylation Kit (Zymo Research, CA, United States) as per manufacturer's instructions.

Infinium Methylation EPIC Beadchip array. All DNA methylation experiments were performed in accordance with Illumina manufacturer instructions for the Infinium Methylation EPIC 850K BeadChip Array (Illumina, USA). Methods for the amplification, fragmentation, precipitation and resuspension of amplified DNA, hybridization to EPIC BeadChip, extension and staining of the bisulfite converted DNA (BCD) can be found in detail in paper from Seaborne and colleagues (Seaborne *et al.*, 2018*b*). EPIC BeadChips were imaged using the Illumina iScan System (Illumina, United States).

DNA methylation analysis, CpG enrichment analysis (GO and KEGG pathways), differentially methylated region (DMR) analysis and Self Organizing Map (SOM) profiling. Following DNA methylation quantification via Methylation EPIC BeadChip array, raw.IDAT files were processed using Partek Genomics Suite V.7 (Partek Inc. Missouri, USA) and annotated using the MethylationEPIC_v-1-0_B4 manifest file. We first checked the average detection p-values for each sample across all probes. The mean detection p-value for all sample across all probes was 0.000295, and the highest for any given sample was only 0.000597, which is well below the recommended 0.01 in the Oshlack workflow (Maksimovic *et al.*, 2017). We also produced density plots of the raw intensities/signals of the probes per sample. These demonstrated that all methylated and unmethylated signals were over 11.5 (mean median signal for methylated probes was 11.56 and unmethylated probes 11.69), and the mean difference between the median methylation and median unmethylated signal was 0.13, well below the recommended difference of less than 0.5 (Maksimovic *et al.*, 2017). Upon import of the data into Partek Genomics Suite we removed probes that spanned X and Y

chromosomes from the analysis due to having both males and females in the study design, and although the average detection p-value for each sample was on average very low (no higher than 0.000597) we also excluded any individual probes with a detection p-value that was above 0.01 as recommended (Maksimovic *et al.*, 2017). Out of a total of 865,859 probes removing those on the X & Y chromosome (19,627 probes) and with a detection p-value above 0.01 (4,264 probes) reduced the total probe number to 843,355 (note some X&Y probes also had detection p-values of above 0.01). We also filtered out probes located in known single-nucleotide polymorphisms (SNPs) and any known cross-reactive probes using previously defined SNP and cross-reactive probe lists identified in earlier EPIC BeadChip 850K validation studies (Pidsley *et al.*, 2016). This resulted in a final list of 791,084 probes to be analysed. Following this, background normalization was performed via functional normalization (with noob background correction), as previously described (Maksimovic *et al.*, 2012). Following functional normalization, we also undertook quality control procedures via Principle Component Analysis (PCA), density plots by lines as well as box and whisker plots of the normalized data for all samples.

Any outlier samples were detected using Principle Component Analysis (PCA) plot and the normal distribution of β-values. Outliers were detected if they fell outside 2 standard deviations (SDs) of the ellipsoids and/or if they demonstrated different distribution patterns to the samples of the same condition. We confirmed that no samples demonstrated large variation [variation defined as any sample above 2 standard deviations (SDs) – depicted by ellipsoids in the PCA plots and/or demonstrating any differential distribution to other samples, depicted in the signal frequency by lines plots]. Therefore, no outliers were detected in this sample set.

Following normalization and quality control procedures, we undertook differentially methylated position (DMP) analysis by converting β-values to M-values [M-value = log2(β/(1 − ββ)], as *M*-values show distributions that are more statistically valid for the differential analysis of methylation levels (Du *et al.*, 2010). We undertook a one-way ANOVA for comparisons of baseline, training, detraining and retraining muscle tissue. Any differentially methylated CpG position (DMP) with an unadjusted p-value of ≤ 0.01 was used as the statistical cut off for the discovery of DMPs.

We then undertook CpG enrichment analysis on these differentially methylated CpG lists within gene ontology (GO) and KEGG pathways (Kanehisa & Goto, 2000; Kanehisa *et al.*, 2016, 2017) using Partek Genomics Suite and Partek Pathway. Differentially methylated region (DMR) analysis, that identifies where several CpGs are consistently differentially methylated within a short chromosomal location/region, was undertaken using the Bioconductor package DMRcate (DOI: 10.18129/B9.bioc.DMRcate). Finally, in order to plot and visualize temporal changes in methylation

across the timepoints we implemented Self Organizing Map (SOM) profiling of the change in mean methylation within each condition using Partek Genomics Suite.

Statistical Analysis

Results are reported as the mean ± SD. Outcome measures were assessed using one-way ANOVA to determine significant overall main effects across baseline, training, detraining and retraining time points. Once an overall effect was confirmed, statistical significance of the measured difference between groups was assessed further by Bonferroni's post hoc analysis, and adjusted p values with the corresponding 95% confidence interval are reported.

To identify effect of initial training and retraining on outcome measures from high-resolution respirometry, difference between TR and BAS and between RETR and DETR time points for each subject was calculated to determine training and retraining respectively. Mean and SD of differences were calculated for each intervention period. Comparison between training and retraining was then analyzed using paired Student's t-test. $p < 0.05$ was considered statistically significant. Statistical software package Prism 8.0 (GraphPad Software Inc, California, USA) was used for data analysis.

Proteomic, morphological and histological analysis has been completed only on 5 participants out of 11. Thereby, due to the small statistical power, descriptive statistics has been performed on these data, but inferential statistics has not been processed.

For epigenetics analysis methylome wide array data sets for baseline, training and retraining were analysed for significant DMPs in Partek Genomics Suite (version 6.6). All gene ontology and KEGG signaling pathway analysis was performed in Partek Genomics Suite and Partek Pathway, on generated CpG lists of statistical significance ($p < 0.01$) across conditions (ANOVA) or contrasts between paired conditions. For follow up M-value difference in CpG DNA methylation analysis was performed via ANOVA in MiniTab Statistical Software (MiniTab Version 17.2.1). Statistical values were considered significant at the level of $p \leq 0.01$. All data represented as mean unless otherwise stated.

RESULTS

Incremental exercise

Pulmonary gas exchange, ventilatory, cardiac and metabolic variables attained at the limit of tolerance at baseline, training, detraining and retraining are reported in **Table 2**.

Initial training period improved significantly $\dot{V}O_{2peak}$ in both relative and absolute values (+4.8 ± 2.5 $ml \cdot min^{-1} \cdot kg^{-1}$ and +0.297 ± 0.162 $l \cdot min^{-1}$, respectively) corresponding to +13% and +13%, respectively (both $p < 0.001$, **Fig. 1B-C**). W_{peak} was also significantly increased of 31 ± 12 W after

training (+16% compared to baseline, $p < 0.001$, **Fig. 1A**). SV_{peak} revealed a significant increase of 15 ± 14 ml after training (+15%, $p < 0.01$, **Fig. 1E**), whereas HR_{peak} did not show any statistically significant change (-1 ± 6 beats·min^{-1}, $p > 0.99$, **Fig. 1D**). Consistently with the latter, $\dot{Q}_{peak}$ was not different from baseline showing a not-significant increment of 1.5 ± 3.0 l·min^{-1} (+7% from baseline, $p = 0.20$, **Fig 1F**).

Retraining was effective in inducing physiological adaptations, but for all the variables changes were similar to the initial training highlighting not-significant difference between two training periods. During retraining increment in $\dot{V}O_{2peak}$ (+4.8 ± 1.8 ml·min^{-1}·kg^{-1}) and W_{peak} (28 ± 10 W) were not different compared to the first training ($p = 0.97$ and $p = 0.45$, respectively). Similarly, concerning the cardiac response, the increase of 13 ± 19 ml in SV_{peak} was not different from the effect of the first training ($p = 0.55$), whereas no difference was found in HR_{peak} and $\dot{Q}_{peak}$ compared to the previous training stimulus (0 ± 4 beats·min^{-1}, +13 ± 19 ml, 1.8 ± 3.1 l·min^{-1}, all variables $p \geq 0.67$).

Table 3 (Study 3). Parameters from incremental exercise at the limit of tolerance

Time point	W	$\dot{V}O_2$ (ml·min^{-1}·kg^{-1})	$\dot{V}O_2$ (l·min^{-1})	$\dot{V}CO_2$ (l·min^{-1})	$\dot{V}_E$ (l·min^{-1})	RER
Baseline	200 ± 46	36.2 ± 7.8	2.288 ± 0.528	2.992 ± 0.652	116.2 ± 27.0	1.26 ± 0.08
Training	231 ± 48 *#	40.9 ± 7.3 *#	2.580 ± 0.542 *#	3.304 ± 0.761 *#	124.0 ± 26.0 #	1.23 ± 0.09
Detraining	198 ± 46	35.7 ± 7.5	2.244 ± 0.579	2.975 ± 0.824	109.7 ± 29.4	1.26 ± 0.06
Retraining	227 ± 48 *#	40.7 ± 7.2 *#	2.538 ± 0.563 *#	3.208 ± 0.742 *#	123.7 ± 31.6 #	1.22 ± 0.06

(continued)

Table 3 (Study 3). Continued

Time point	HR (beats·min^{-1})	SV (ml)	$\dot{Q}$ (l·min^{-1})	RPE
Baseline	189 ± 8	101 ± 16	19.5 ± 3.1	18 ± 1
Training	188 ± 8	116 ± 21 *#	21.0 ± 3.6	18 ± 2
Detraining	187 ± 11	102 ± 19	19.3 ± 3.0	18 ± 2
Retraining	187 ± 8	115 ± 24 *#	21.2 ± 4.0	19 ± 1

Peak values of pulmonary gas exchange, ventilatory, cardiac and metabolic variables attained at the limit of tolerance at baseline, training, detraining and retraining time points. W, peak power output; $\dot{V}O_2$, oxygen uptake; $\dot{V}CO_2$, carbon dioxide production; $\dot{V}_E$, pulmonary ventilation; RER, respiratory exchange ratio; HR, heart rate; SV, stroke volume; $\dot{Q}$, cardiac output; RPE, rating of perceived exertion. * $p < 0.05$ *vs.* baseline; # $p < 0.05$ *vs.* detraining. All values are means ± SD. (n = 16).

Figure 1 (Study 3). Peak values of parameters from incremental exercise before and after exposure to two identical interval training interventions separated by 3-month of detraining

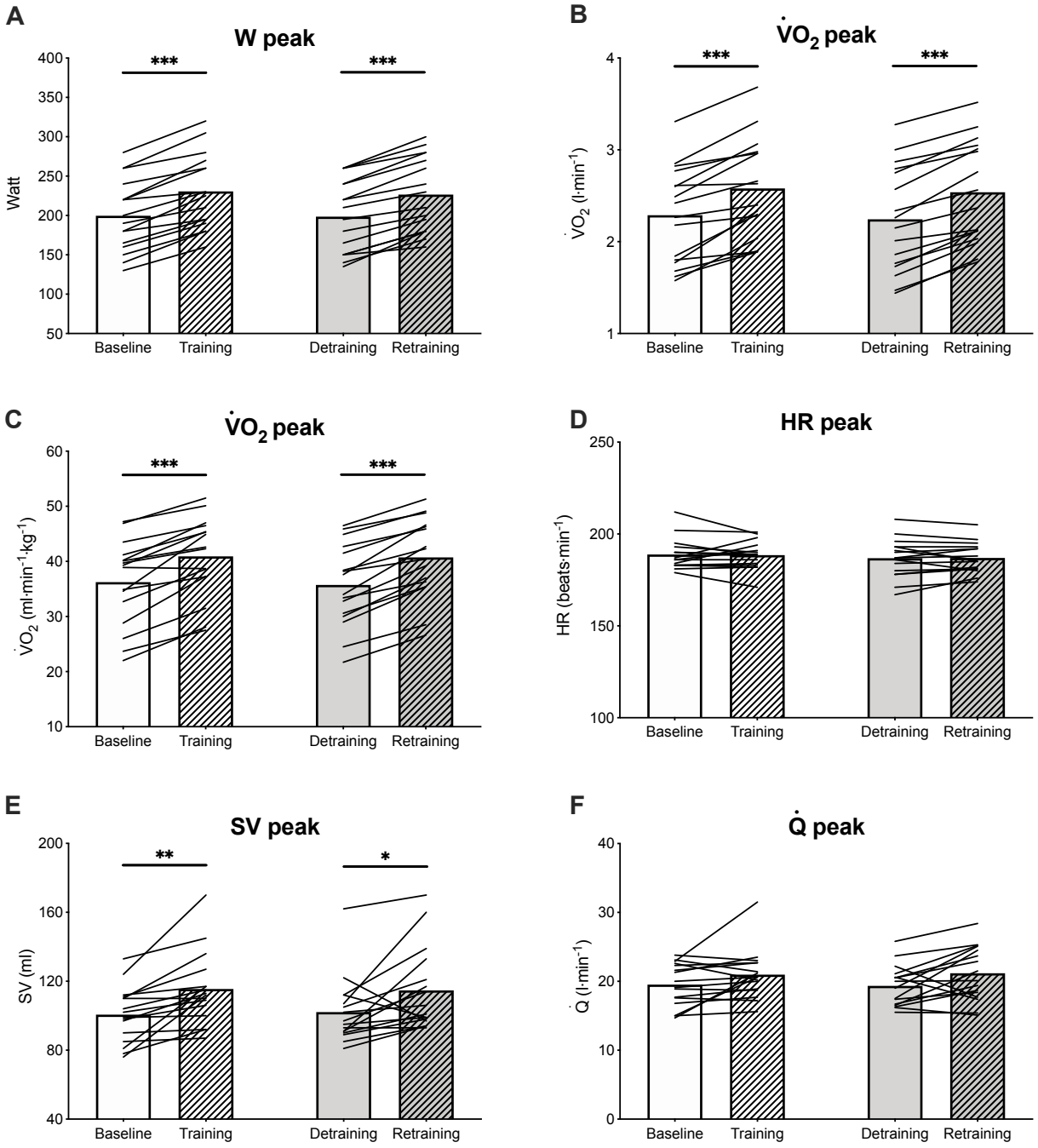

Peak values of peak power output (A), absolute (B) and relative (C) peak oxygen uptake, heart rate (D), stroke volume (E) and cardiac output (F) attained at the limit of tolerance of incremental exercise at baseline, training, detraining and retraining time points. All values are means ± SD. * $p < 0.05$; *** $p < 0.001$. (n = 16).

Constant work-rate exercise

The first training period induce reduction in $\dot{V}O_2$ kinetics decreasing τ from 36.0 ± 14.1 s at baseline to 28.5 ± 9.3 s after training. During detraining τ increased to 31.1 ± 9.5 s, and was subsequently decreased after retraining (23.2 ± 7.6 s). Post-hoc analysis revealed significant reduction in $\dot{V}O_2$ kinetics between BAS and TR and between DETR and TR (both $p < 0.05$). Although detraining remained lower compared to baseline (-14%), no difference resulted between the two time-points ($p = 0.30$). $\dot{V}O_2$ kinetics were significantly affected by initial training with a decrement of 7.5 ± 9.2 s (21%), similarly retraining generated a 25% reduction in τ (-7.8 ± 6.0 s). Changes in training and retraining were not statistically different ($p = 0.90$) (**Fig. 2**).

Figure 2 (Study 3). Oxygen uptake kinetics during constant work-rate exercise before and after exposure to two identical interval training interventions separated by 3-month of detraining

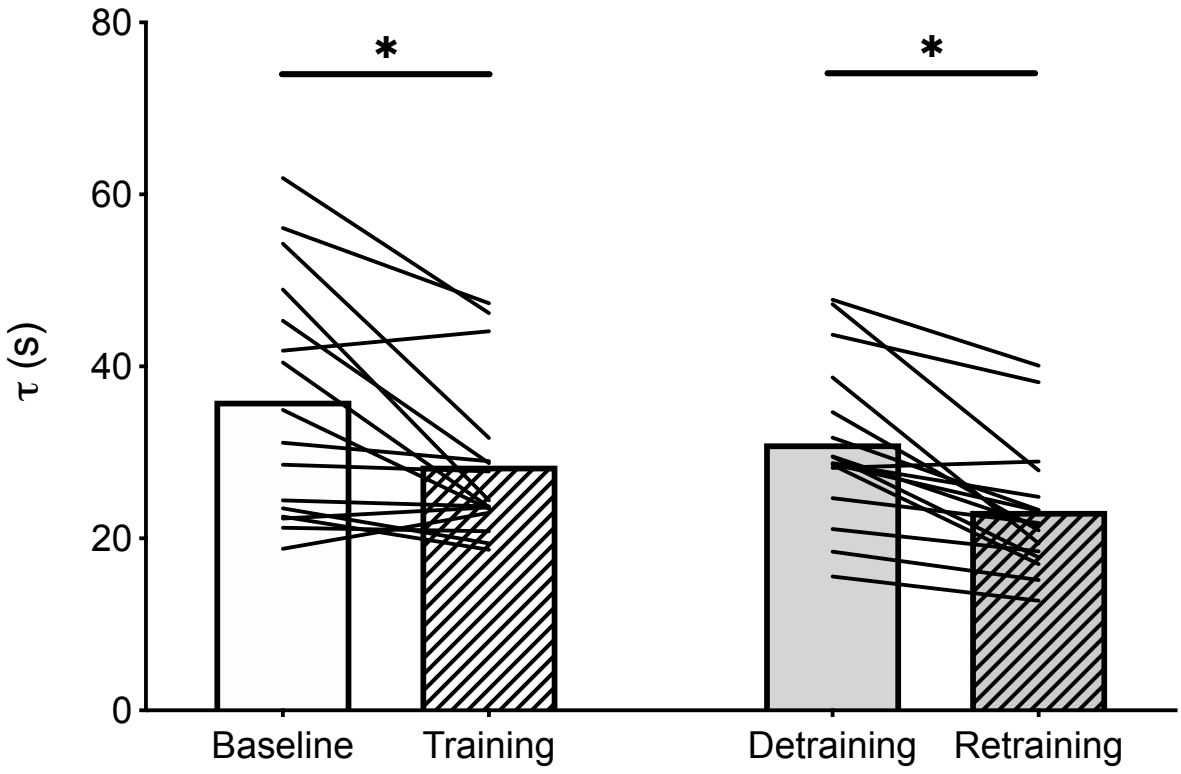

Oxygen uptake kinetics measured during constant work-rate cycling exercise at 80% of GET power output at baseline, training, detraining and retraining time points. τ, time constant. All values are means ± SD. * $p < 0.05$. ($n = 16$).

Muscle Oxidative Capacity by NIRS

Both trainings induce improvement in muscle oxidative capacity showing increase in *k* from BASE to TR (2.31 ± 0.67 min^{-1} and 3.05 ± 0.75 min^{-1}, respectively) and from DETR to RETR (2.13 ± 0.56 min^{-1} and 2.94 ± 0.67 min^{-1}, respectively), with both increments statistically significant ($p < 0.001$). Comparison between training and retraining effect on *k* did not reveal any significant difference ($p = 0.76$) (**Fig. 3**).

Figure 3 (Study 3). Muscle oxidative capacity by NIRS before and after exposure to two identical interval training interventions separated by 3-month of detraining

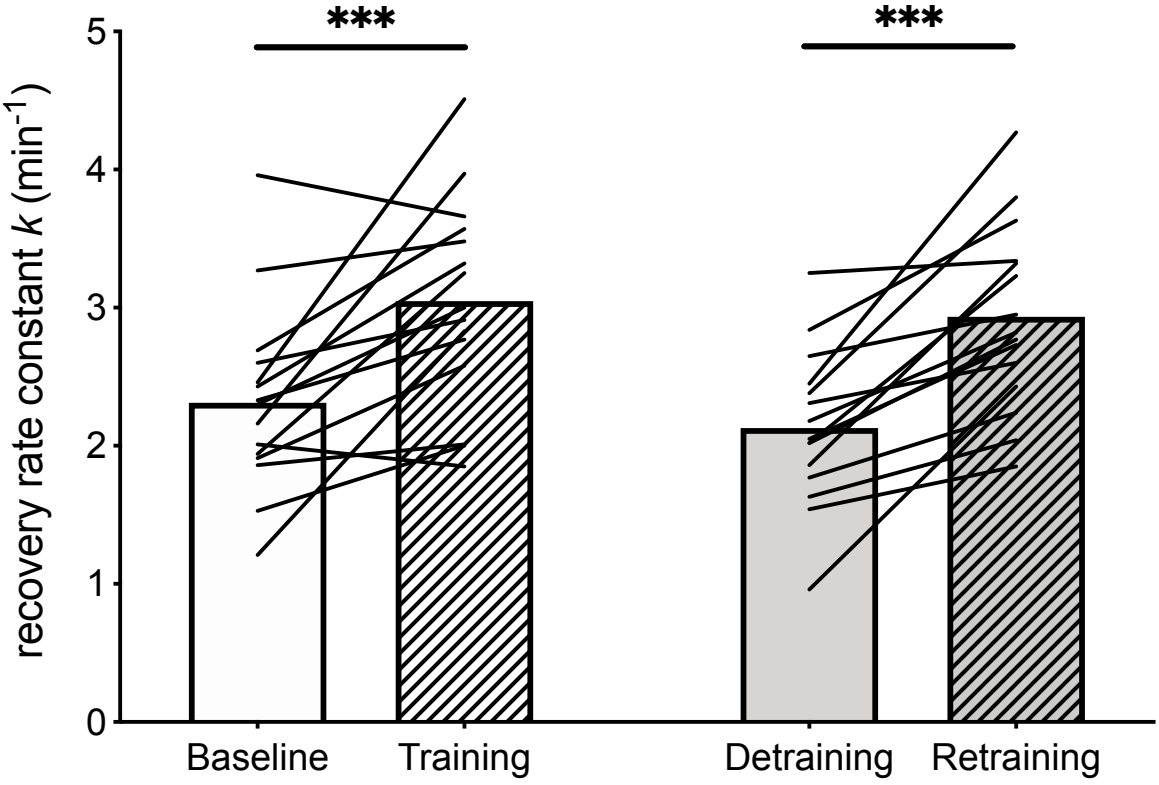

Muscle oxidative capacity measured by near-infrared spectroscopy using intermittent arterial occlusion protocol immediately after constant work-rate cycling exercise at 80% of GET power output at baseline, training, detraining and retraining time points. *k*, muscle oxygen uptake recovery rate constant.

All values are means ± SD. *** $p < 0.001$. (n = 15).

Mitochondrial Respiration

Measurements of mass-specific mitochondrial O_2 flux in permeabilized muscle fibers from 11 subjects undergone to biopsy are shown in **Table 2**. Mitochondrial respiration was significantly improved during initial training in maximal O_2 flux in oxidative phosphorylation ($CI+II_P$) (+8.6 ± 12.0 $pmol \cdot s^{-1} \cdot mg^{-1}$ from BAS to TR) (**Fig. 4C**) and maximal uncoupled O_2 flux ($CI+II_E$) (+13.1 ± 17.8 $pmol \cdot s^{-1} \cdot mg^{-1}$ from BAS to TR) (**Fig. 4D**), both $p < 0.05$. CI_L was not different from baseline

after first training ($p = 0.42$) (**Fig. 4A**). CI_P and CII_E showed a tendency to increase but was not found any statistical difference (both $p \geq 0.07$) (**Fig. 4B** and **Fig. 4E**).

Retraining was effective in inducing improvement in all mitochondrial respiration state investigated. Increment from DETR to RETR was +2.7 ± 3.1 pmol·s^{-1}·mg^{-1} for CI in LEAK state (**Fig. 4A**); in oxidative phosphorylation state, CI_P and $CI+II_P$ increased of 8.6 ± 3.7 pmol·s^{-1}·mg^{-1} and 17.4 ± 14.1 pmol·s^{-1}·mg^{-1}, respectively (**Fig. 4B-C**); O_2 flux in CI+II and CII during uncoupled respiration increased of 24.1 ± 16.0 pmol·s^{-1}·mg^{-1} and 15.5 ± 14.7 pmol·s^{-1}·mg^{-1}, respectively (**Fig. 4D-E**) (all $p < 0.05$).

Comparison between training effects revealed a greater mass-specific mitochondrial respiration for CI_L, CI_P, $CI+II_E$ and CII_E in retraining than initial training (all $p < 0.05$). Changes in $CI+II_P$ showed a trend in being greater during retraining but did not result significantly different between the two training periods ($p = 0.11$) (**Fig. 5** and **Fig. 6**).

The data presented in this study showed no effect of the addition of cytochrome c as a control for outer mitochondrial membrane integrity.

Table 4 (Study 3). Mass-specific mitochondrial respiration capacity

Time point	CI_L (pmol·s^{-1}·mg^{-1})	CI_P (pmol·s^{-1}·mg^{-1})	$CI+II_P$ (pmol·s^{-1}·mg^{-1})	$CI+II_E$ (pmol·s^{-1}·mg^{-1})	CII_E (pmol·s^{-1}·mg^{-1})
Baseline	6.3 ± 1.9	24.7 ± 7.5	51.1 ± 18.6	64.3 ± 15.3	39.0 ± 7.4
Training	5.5 ± 2.6	26.1 ± 11.0 $^{\#}$	59.7 ± 20.0 $^{*\#}$	77.4 ± 21.3 $^{*\#}$	44.9 ± 12.7 $^{\#}$
Detraining	3.5 ± 2.7	18.2 ± 10.4	43.7 ± 16.6	55.9 ± 20.7	34.3 ± 8.4
Retraining	6.2 ± 2.4 $^{\#}$	26.8 ± 11.1 $^{\#}$	61.1 ± 23.3 $^{\#}$	80.0 ± 23.0 $^{\#}$	49.8 ± 12.7 $^{*\#}$

Mass-specific mitochondrial O_2 flux values (in picomoles O_2 per second per milligram of wet weight) measured with high-resolution respirometry in permeabilized fibers obtained from biopsy on *vastus lateralis* muscle at baseline, training, detraining and retraining time points. CI_L, leak respiration through CI; CI_P, maximum coupled mitochondrial respiration through CI; $CI+II_P$, maximum coupled mitochondrial respiration through CI+II; $CI+II_E$, maximum noncoupled mitochondrial respiration through CI+II; CII_E, maximum noncoupled mitochondrial respiration through CII. All values are means ± SD. * $p < 0.05$ *vs.* baseline; $^{\#}$ $p < 0.05$ *vs.* detraining. ($n = 11$).

Figure 4 (Study 3). Mass-specific mitochondrial respiration capacity before and after exposure to two identical interval training interventions separated by 3-month of detraining

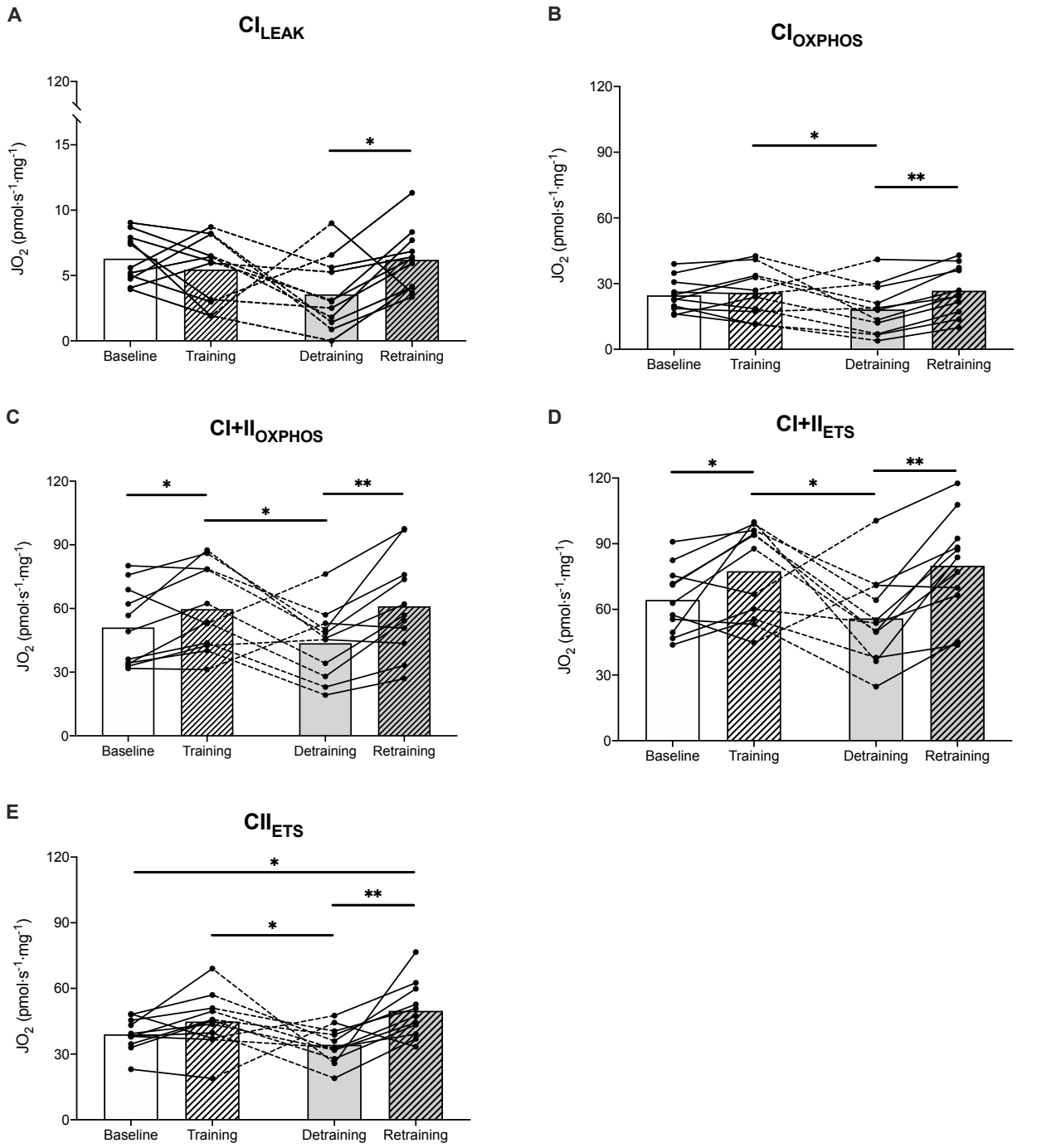

Mass-specific mitochondrial O_2 flux values of leak respiration through CI (A), maximum coupled mitochondrial respiration through CI (B), maximum coupled mitochondrial respiration through CI+II (C), maximum noncoupled mitochondrial respiration through CI+II (D) and maximum noncoupled mitochondrial respiration through CII (E) measured with high-resolution respirometry in permeabilized fibers obtained from biopsy on *vastus lateralis* muscle at baseline, training, detraining and retraining time points. All values are means ± SD. * $p < 0.05$, ** $p < 0.01$. (n = 11).

Figure 5 (Study 3). Mitochondrial respiration capacity changes in training and retraining intervention

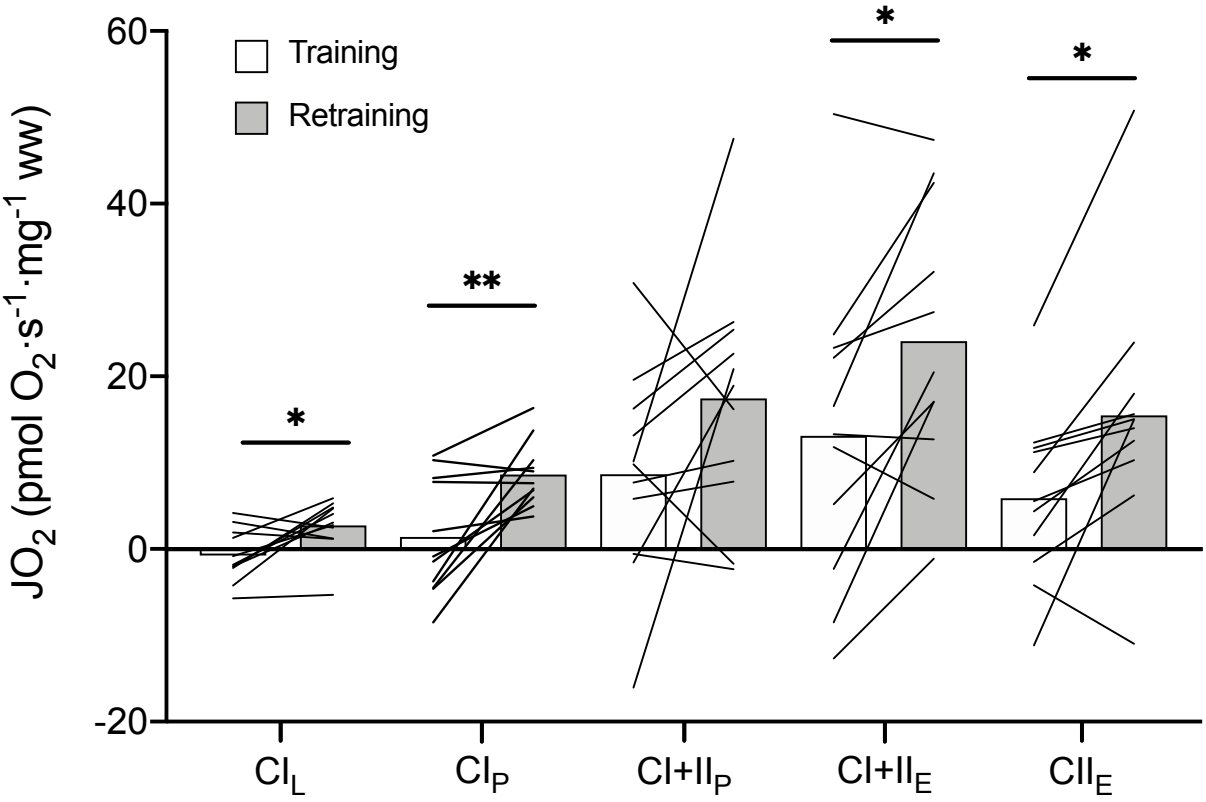

Mitochondrial respiration changes in training (white bars) and retraining (grey bars) intervention measured with high-resolution respirometry in permeabilized fibers obtained from biopsy on *vastus lateralis* muscle in the following respiration state: CI_L, leak respiration through CI; CI_P, maximum coupled mitochondrial respiration through CI; $CI+II_P$, maximum coupled mitochondrial respiration through CI+II; $CI+II_E$, maximum noncoupled mitochondrial respiration through CI+II; CII_E, maximum noncoupled mitochondrial respiration through CII. All values are means ± SD. * $p < 0.05$, ** $p < 0.01$. ($n = 11$).

Figure 6 (Study 3). Mitochondrial respiration capacity changes in training and retraining intervention

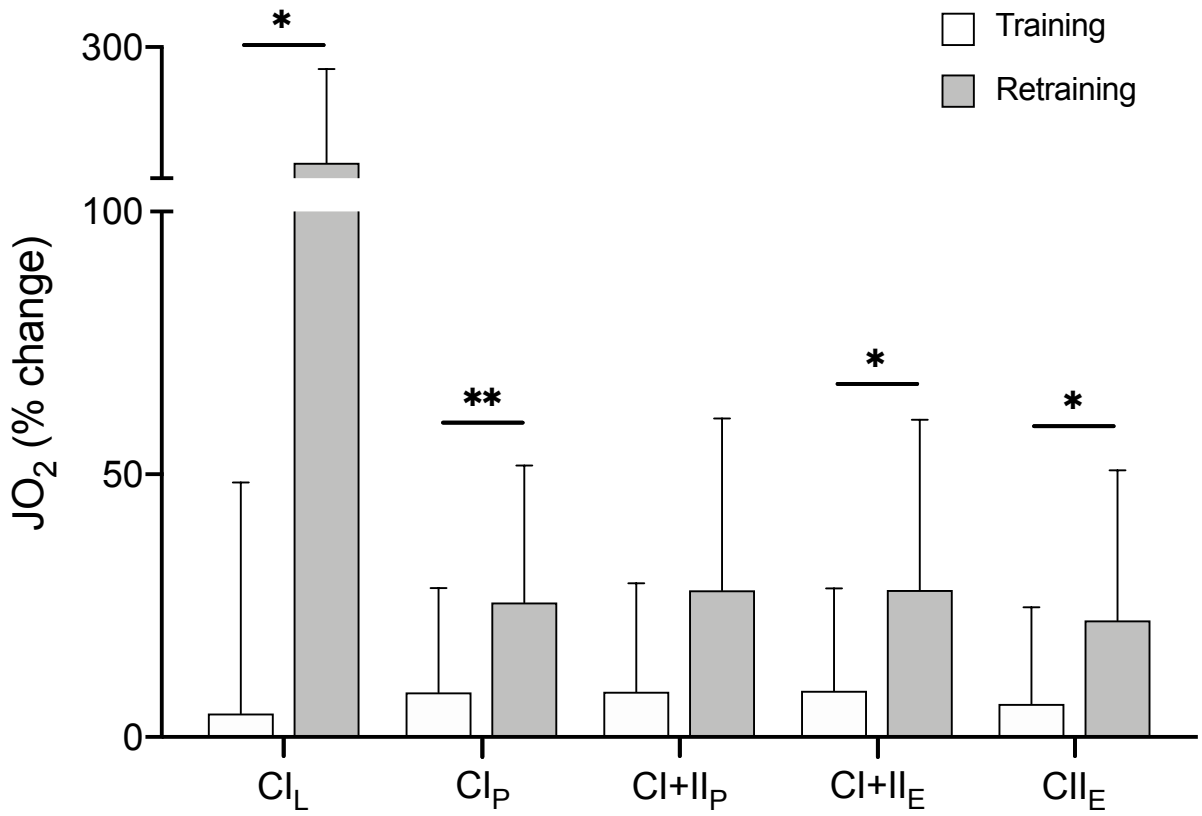

Mitochondrial respiration percentage changes in training (white bars) and retraining (grey bars) intervention measured with high-resolution respirometry in permeabilized fibers obtained from biopsy on *vastus lateralis* muscle in the following respiration state: CI_L, leak respiration through CI; CI_P, maximum coupled mitochondrial respiration through CI; $CI+II_P$, maximum coupled mitochondrial respiration through CI+II; $CI+II_E$, maximum noncoupled mitochondrial respiration through CI+II; CII_E, maximum noncoupled mitochondrial respiration through CII. All values are means ± SD. * $p < 0.05$, ** $p < 0.01$. (n = 11).

Proteomic Analysis

In **Figure 7** changes in mitochondrial content biomarkers (CS and TOM20 protein expression) are reported. No clear changes are evident in the patterns across repeated training interventions in the five subjects' muscles analyzed.

Figure 7 (Study 3). Mitochondrial content biomarkers across repeated interval training interventions separated by 3-month of detraining

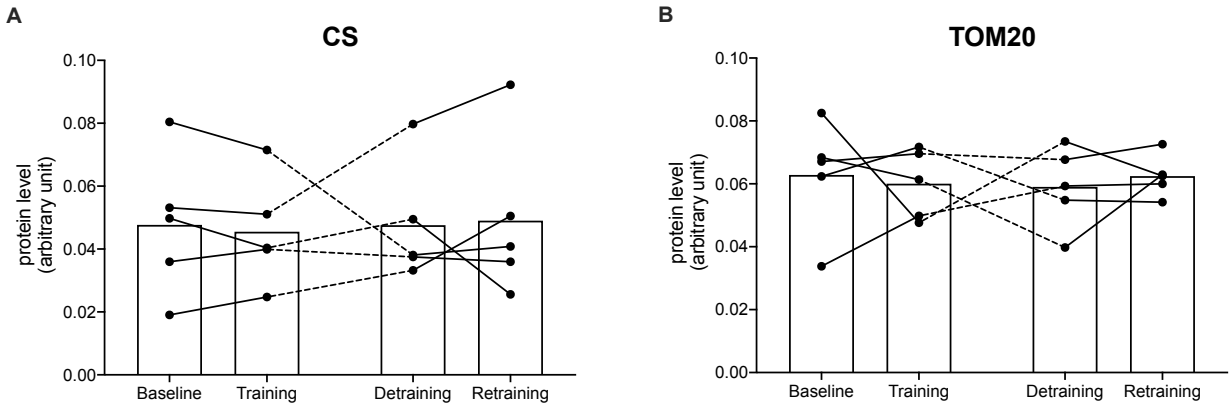

Time course of single values of cytrate synthase (A) and translocase of the outer membrane 20 (B) protein expression measured in muscle tissue by western Blot in only five subjects across baseline, training, detraining and retraining time points. (n = 5).

Mitochondrial biogenesis adaptations during the two training interventions are described by changes in PGC-1α protein expression and phosphorylation level of AMPK (**Fig. 8**). One subject showed an increment in AMPK during the first training period and, following a reduction after detraining, a larger increase during retraining (**Fig. 8B**).

Figure 8 (Study 3). Mitochondrial biogenesis biomarkers across repeated interval training interventions separated by 3-month of detraining

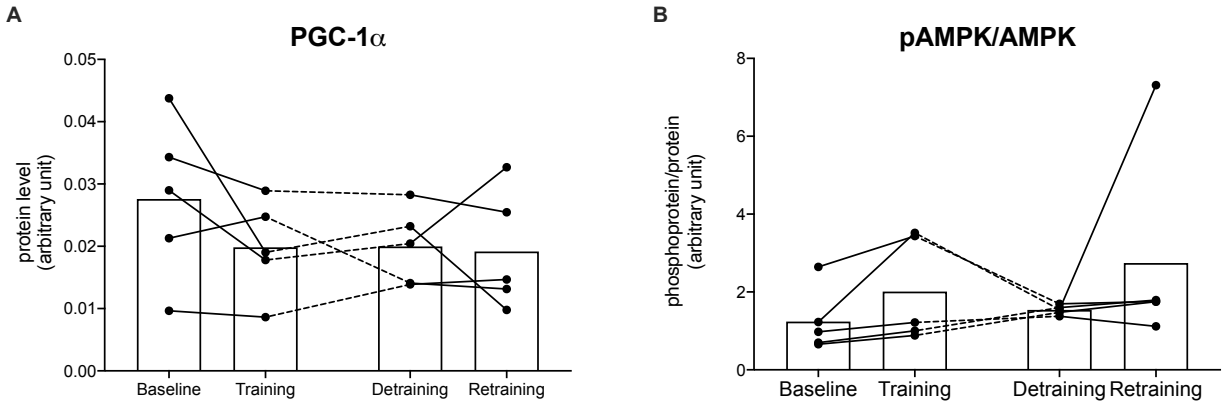

Time course of single values of PGC-1α (A) and phosphorylated state of AMPK (B) protein expression measured in muscle tissue by western Blot in only five subjects across baseline, training, detraining and retraining time points. (n = 5).

Mitochondrial fusion dynamics are represented by Mfn1, Mfn2 and OPA1 trend, whereas Fis1 and phosphorylated state of Drp1 at serine 637 and serine 616 describe fission dynamics (**Fig. 9**). $Drp1_{Ser637}$, related to mitochondrial fusion inhibition, showed a decreasing trend during initial training (**Fig. 9D**). All 5 subjects revealed an increment in OPA1 and Mfn2 during retraining period (**Fig. 9B-C**).

Figure 9 (Study 3). Mitochondrial dynamics biomarkers across repeated interval training interventions separated by 3-month of detraining

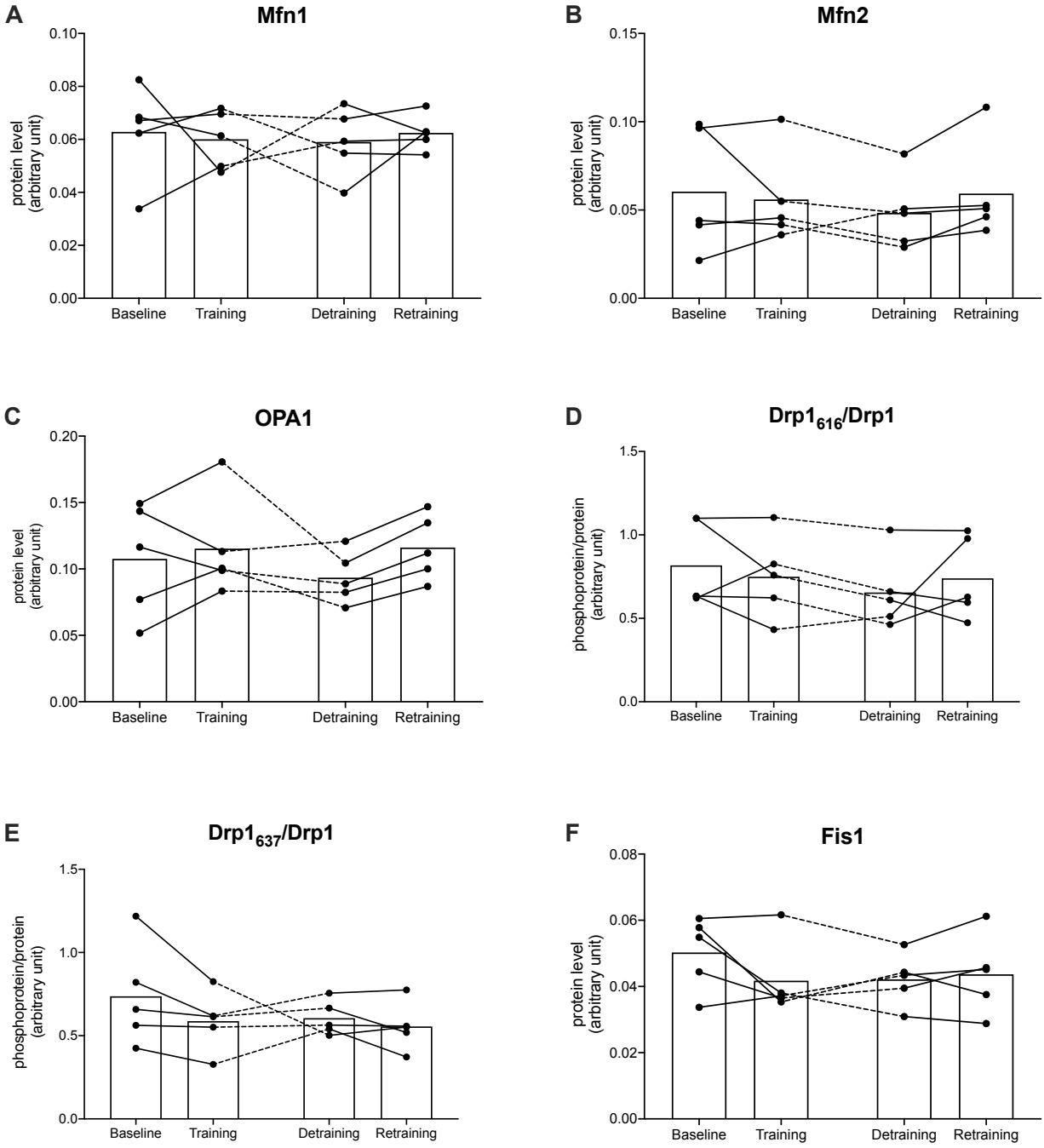

Time course of single values of Mfn1 (A), Mfn2 (B), OPA1 (C), phosphorylated state Drp1 at serine 616 (D), phosphorylated state Drp1 at serine 637 (E), Fis1 (F) protein expression measured in muscle tissue by Western Blot in only five subjects across baseline, training, detraining and retraining time points. (n = 5).

Regarding mitophagy PINK1 and Parkin enzyme expression was evaluated. Parkin showed a negative trend during the first training and a retention of lower level during retraining in four subjects out of 5 (**Fig. 10**).

Figure 10 (Study 3). Mitophagy biomarkers across repeated interval training interventions separated by 3-month of detraining

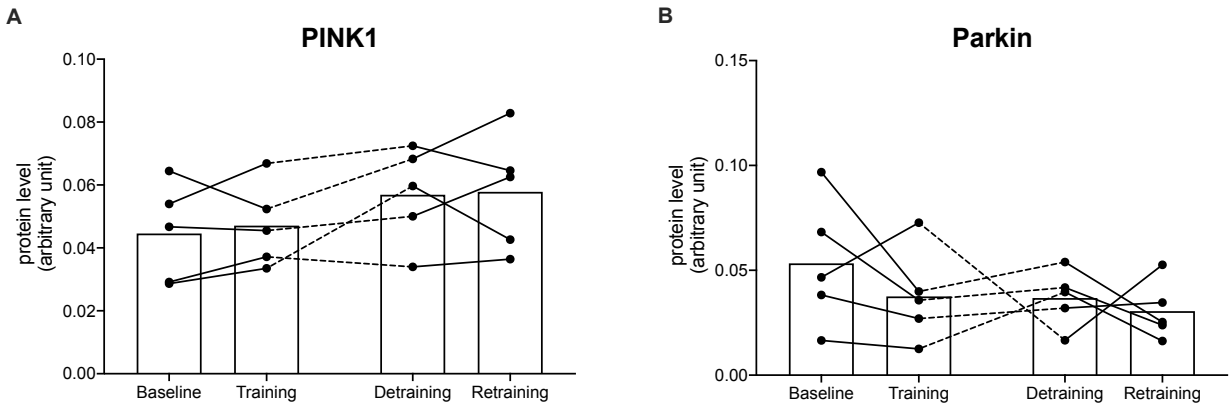

Time course of single values of PINK1 (A) and Parkin (B) protein expression measured in muscle tissue by western Blot in only five subjects across baseline, training, detraining and retraining time points. (n = 5).

First training appears to be effective in inducing increment in protein expression for all five electron transport chain complexes (**Fig. 11**). For three subjects this trend also occurred during retraining for CI, CII, CIII, CIV, CV. For the other two subjects protein level showed a decrement or no visible change after retraining that is usually related to an high protein expression maintained during detraining.

Figure 11 (Study 3). Electron transport chain complexes protein expression across repeated interval training interventions separated by 3-month of detraining

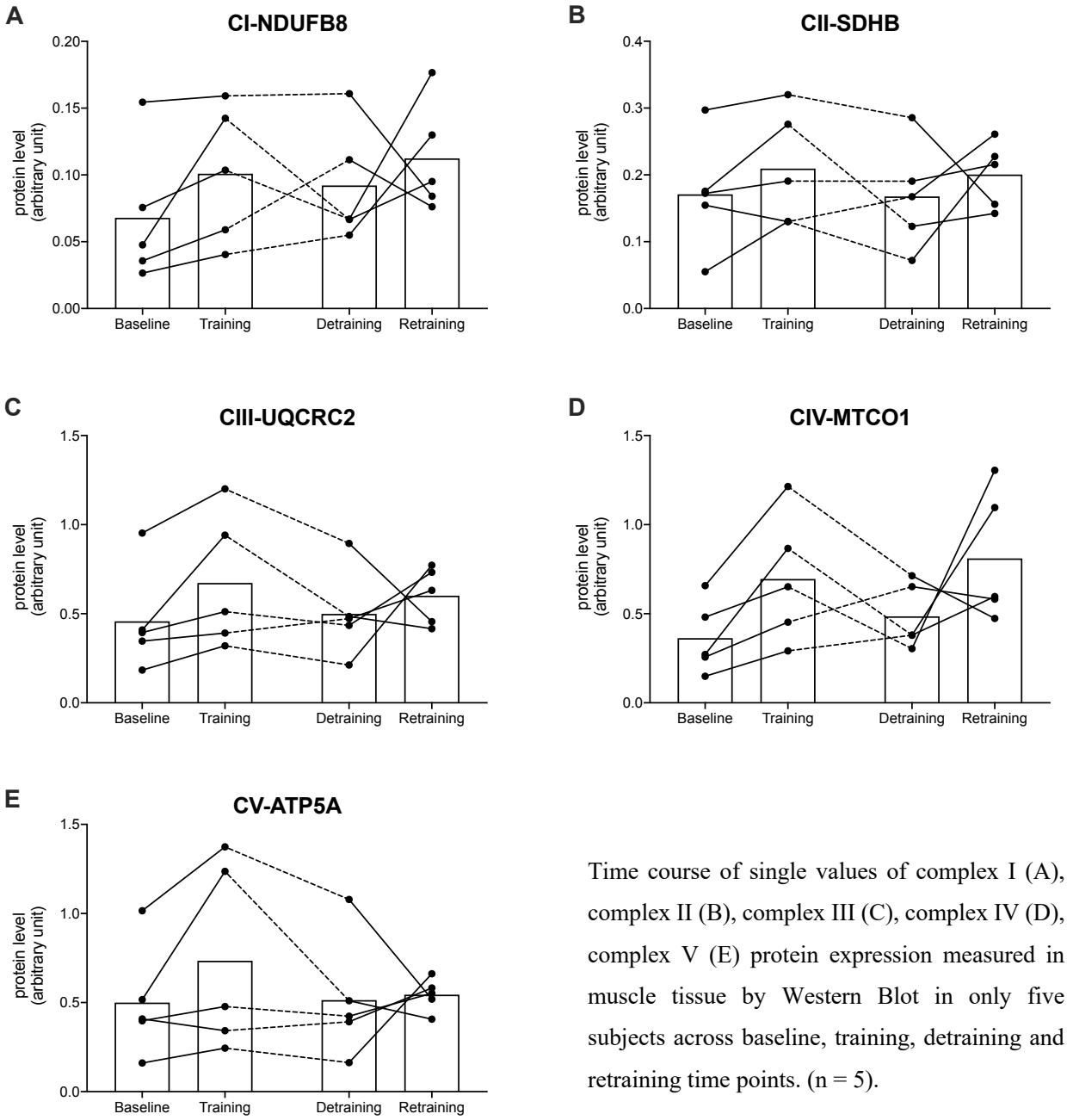

Time course of single values of complex I (A), complex II (B), complex III (C), complex IV (D), complex V (E) protein expression measured in muscle tissue by Western Blot in only five subjects across baseline, training, detraining and retraining time points. (n = 5).

Morphological and histological Analysis

Analysis of myosin heavy chain isoform composition revealed a common pattern in all of the subjects to a slight reduction in MHC-I during first training, whereas MHC-IIa resulted increased and MHC-IIx did not show changes. During detraining MHC-I remained stable, MHC-IIa showed a slight decrease associated with an increasing trend in MHC-IIx in all the subjects excepted one. Retraining period induced increase in both MHC-I and MHC-IIa, conversely, MHC-IIx resulted in a decrement (**Fig. 12**).

Capillarization was affected by initial training resulting in increment in C:F uniformly in all five participants. After detraining C:F showed a tendency to decrease however maintaining values above baseline. During retraining an increase was again observed in C:F (**Fig. 13**).

Figure 12 (Study 3). Myosin heavy chain isoform composition across repeated interval training interventions separated by 3-month of detraining

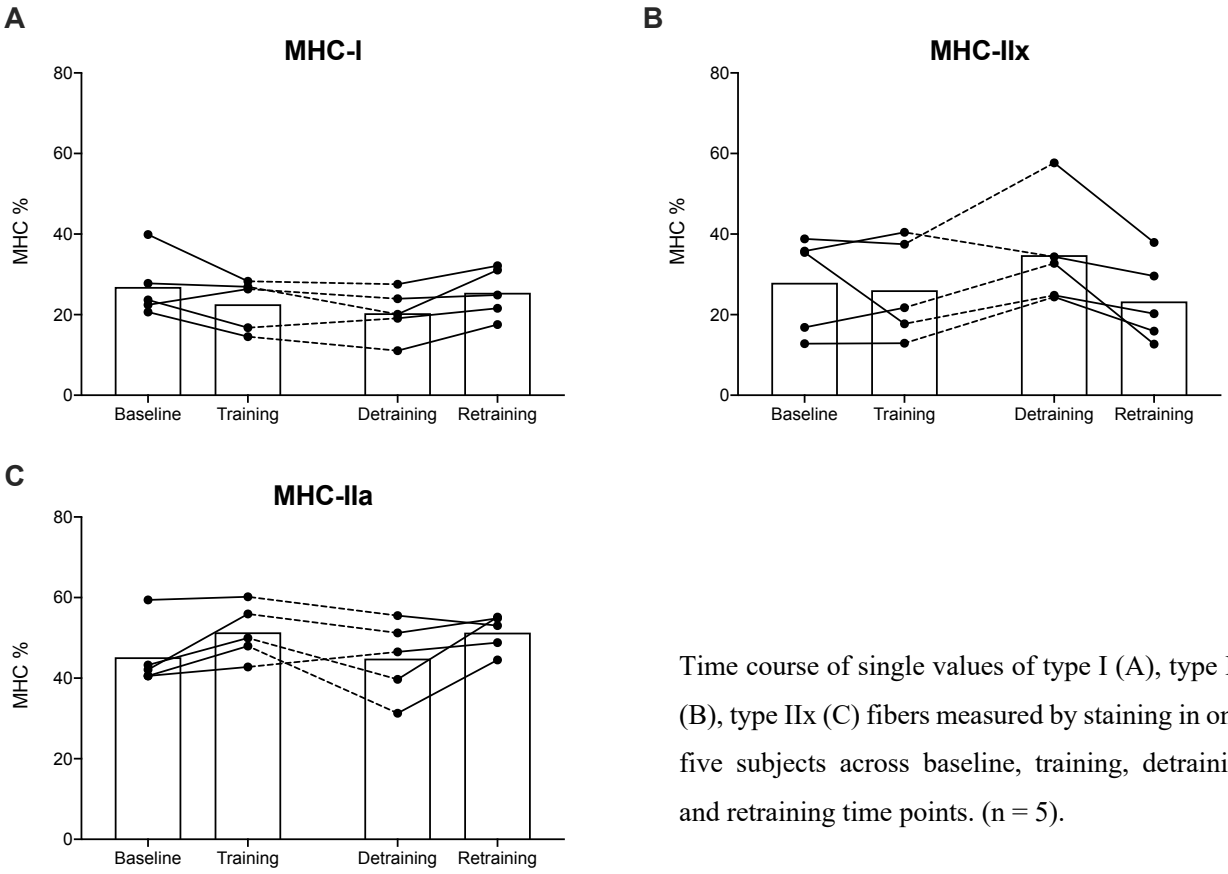

Time course of single values of type I (A), type IIa (B), type IIx (C) fibers measured by staining in only five subjects across baseline, training, detraining and retraining time points. (n = 5).

Figure 13 (Study 3). Capillarization across repeated interval training interventions separated by 3-month of detraining

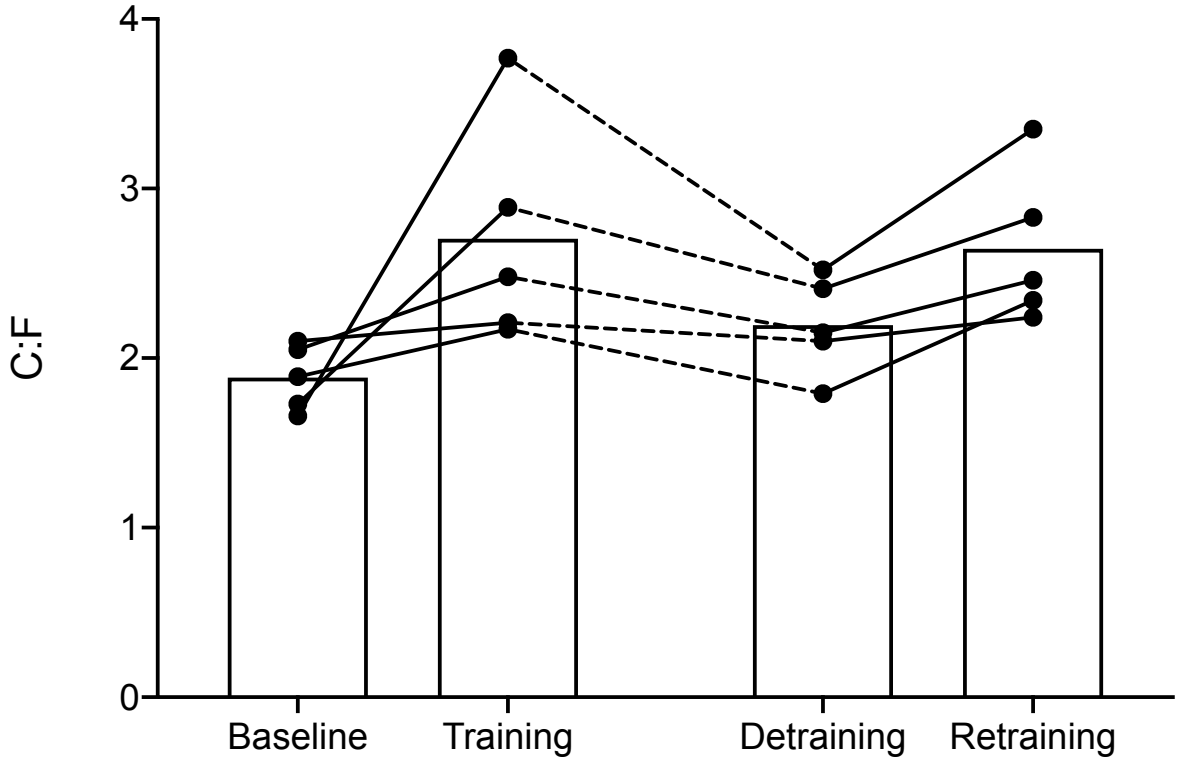

Capillary-to-fiber ratio measured by immunofluorescence in cross sections of *vastus lateralis* in only five subjects across baseline, training, detraining and retraining time points. (n = 5).

Genome-wide DNA methylation analysis

The frequency of statistically ($p < 0.01$) differentially methylated CpG positions (DMPs) in each condition was analysed (**Fig. 14**) and a list of 35,855 DMPs was identified. Following initial interval training 21,605 CpG sites were significantly differentially methylated compared to baseline, with a larger number being hypomethylated (14,516) compared to hypermethylated (7,089). After detraining, the total number of DMPs (3,854), most of which were hypomethylated (3,349), whereas hypermethylated DNA sites nearly reverted to baseline (505). Following retraining we observed another increase in the number of DMPs (10,396), with most CpGs hypomethylated (9,644) compared to hypermethylated DNA sites that remained similar to detraining (752). Although increment in hypomethylated CpGs during retraining was smaller compared to initial training period, when expressed as percentage of total differentially methylated sites, we observed a shift towards a hypomethylated profile across training (67%), detraining (87%) and retraining (93%) (**Fig. 14B**). Fascinatingly, this was due to both another large increase in hypomethylation after retraining, but also a much smaller number of DMPs that were hypermethylated (752) during retraining compared to the earlier training period (7,089).

Figure 14 (Study 3). Differentially methylated CpG sites frequency following training, detraining and retraining compared to baseline

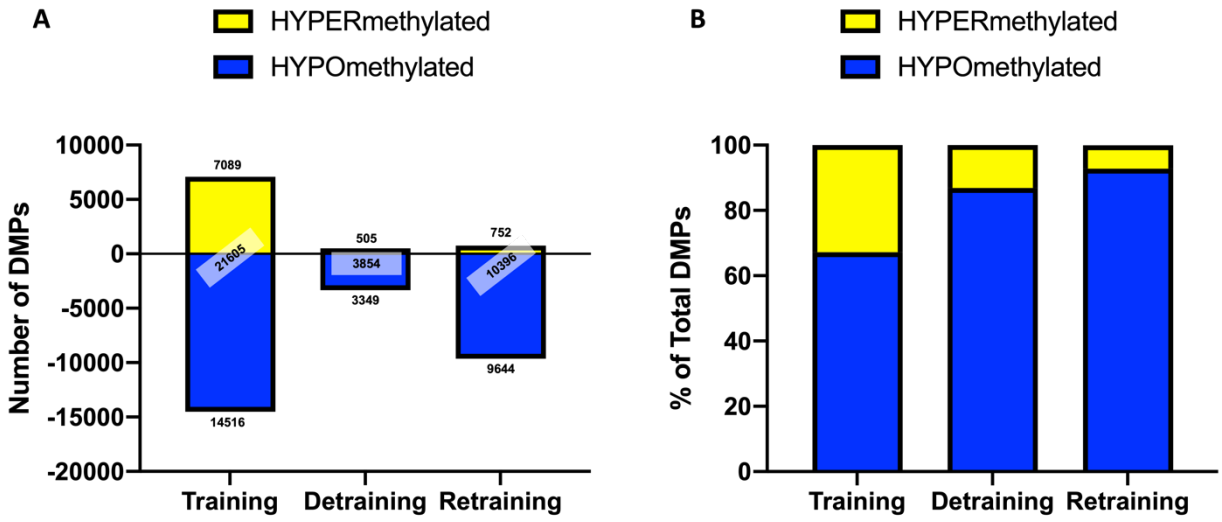

Number of differentially methylated CpG sites following training, detraining and retraining compared to baseline identified by Infinium Methylation EPIC BeadChip arrays (850K CpG sites). Number of hypomethylated (blue bars) and hypermethylated (yellow bars) CpG sites expresses in absolute number (A) or percentage values (B). (n = 5).

Analysis of Gene Ontology (GO) terms significantly enriched over the time-course of baseline, training, detraining and retraining upon all pairwise comparisons identified DMPs in nine GO terms: (1) anatomical structure development, (2) cell junction, (3) developmental process, (4) movement of cell or subcellular component, (5) positive regulation of cellular process, (6) protein binding, (7) regulation of cell communication, (8) regulation of developmental process, (9) regulation of signaling. Enriched KEGG pathways common to baseline, training, detraining and retraining included: (1) axon guidance, (2) calcium signaling pathway, (3) cholinergic synapse, (4) circadian entrainment, (5) focal adhesion, (6) MAPK signaling pathway, (7) pathways in cancer, (8) Rap1 signaling pathway.

We focused our attention on calcium and MAPK signaling pathway, critical pathways stimulated by biochemical alterations and mechanical stress occurring during muscle contractile activity that are involved in several cellular signals including muscle plasticity and mitochondrial biogenesis. We attempted to elucidate how these pathways were differentially regulated across experimental conditions. Intuitively, we report that calcium and MAPK pathways were significantly enriched upon all pairwise comparisons of baseline versus training, detraining and retraining, respectively, suggesting that pathways were epigenetically modified following periods of skeletal muscle perturbation. Moreover, KEGG pathway reported that genes involved in MAPK signaling were predominantly hypomethylated (blue) in retraining compared to baseline condition (**Fig. 15**).

Figure 15 (Study 3). MAPK signaling KEGG pathway

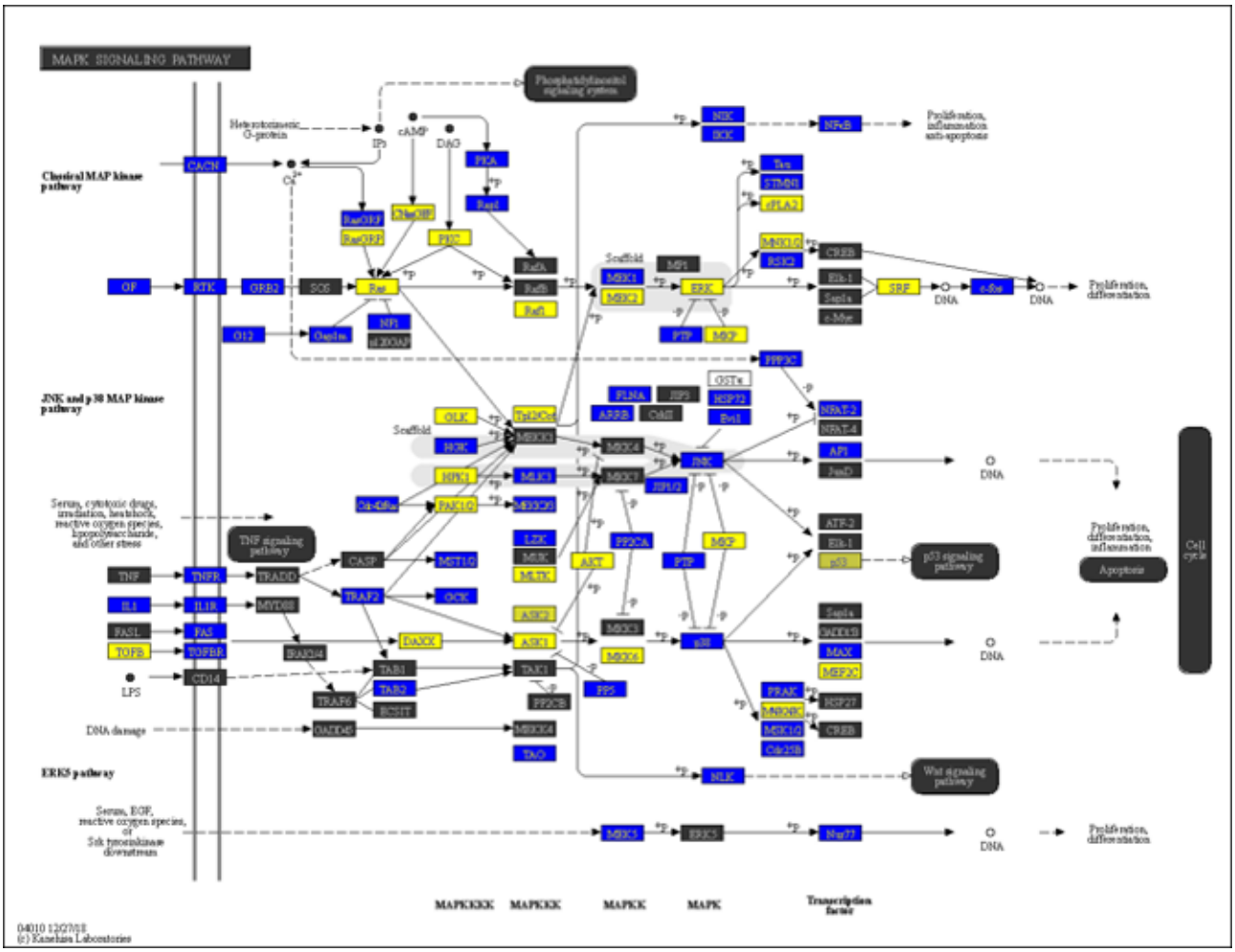

Illustration of the KEGG pathway "MAPK signaling" demonstrating predominantly hypomethylation (blue) in retraining vs. baseline. Note, the most significant (lowest p-value) DMP for each gene is used to color this pathway image. Therefore, this is not always accurate where multiple DMPs occur for a single gene and the image is therefore only a visual representation of the overarching methylation profile in this pathway.

In order to investigate whether there were any similarly altered DMPs between training, detraining and retraining, we overlapped DMP lists from analysis described above to detect CpG sites differentially methylated in the three conditions versus baseline. 5334 DMPs were identified overlapping across training, detraining and retraining. Among these, 806 were common to all conditions (**Fig. 16**).

Figure 16 (Study 3). Venn diagram overlapping DMPs in training, detraining and retraining compared to baseline

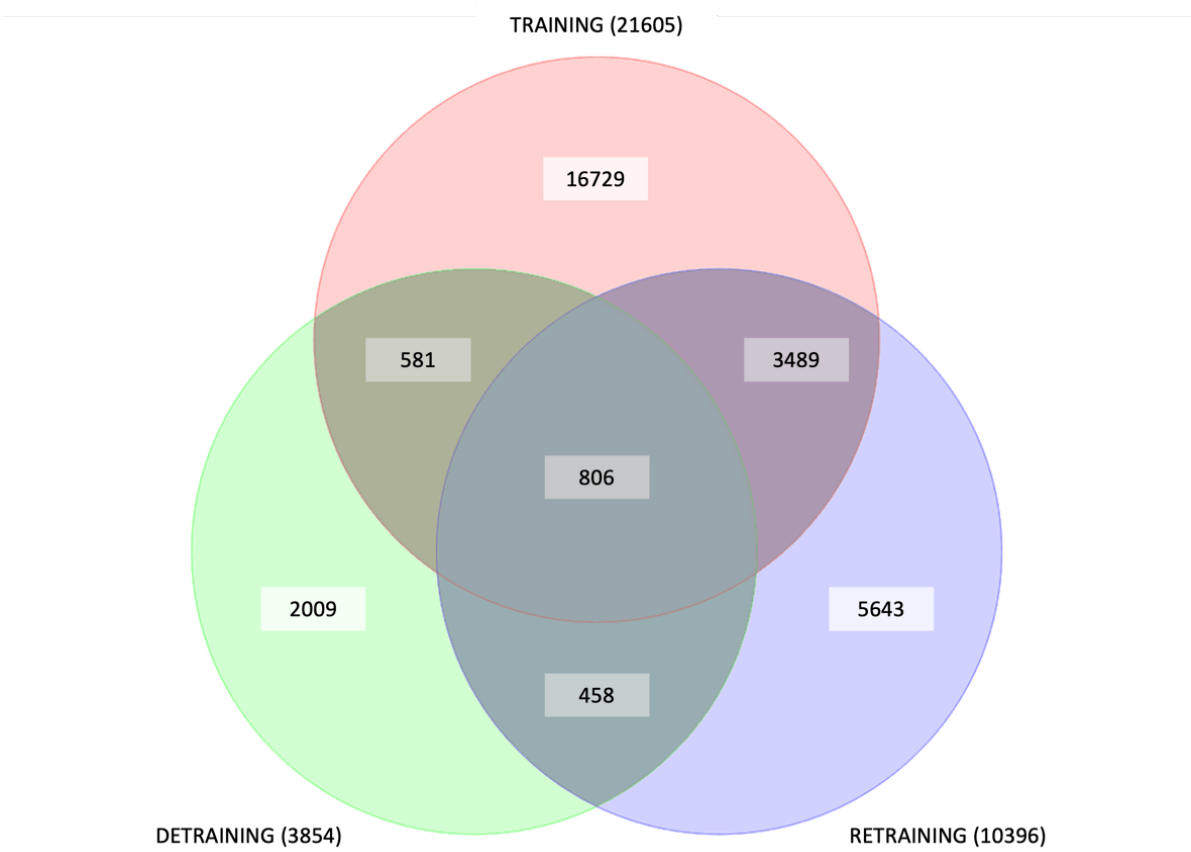

Venn diagram analysis of the statistically differentially regulated CpG sites following training, detraining and retraining compared to baseline. Ellipsis reports number of common overlapping significant DMPs across each condition. (n = 5).

Changes in genome-wide DNA methylation related to the 5334 DMPs commonly identified across experimental conditions were further analysed, and self-organising map (SOM) profiling highlighted four temporal trend profiles of the DMPs (**Fig. 17**). The first profile (named Signature 1) included 1190 DMPs and displayed enhanced hypomethylation as a result of first training period. Signature 1 genes were hypermethylated at baseline and became hypomethylated after initial training. Importantly, hypomethylation was then retained/"remembered" even during complete cessation of exercise/detraining, when $\dot{V}O_{2peak}$ and mitochondrial O_2 flux returned to baseline levels, and this hypomethylation was then maintained into the later retraining period (**Fig. 17A**). The second temporal trend (Signature 2) included 2000 DMPs and also displayed an enhanced hypomethylated state after initial training. Signature 2 genes showed a reduction in hypomethylation as a result of detraining,

although maintaining slightly hypomethylated status. As with Signature 1, retraining led to further hypomethylation during retraining at similar or greater level than original training (**Fig. 17B**). Indeed, in **Figure 18** the individual DMPs identified in Signature 2 are clearly shown highlighting in a few a greater hypomethylation in retraining than in training. The third profile (Signature 3) included 1675 DMPs and, as previous two, displayed hypomethylation with first bout of training. Differently, this cluster became hypermethylated with detraining, but reverted back to hypomethylation state after retraining (**Fig. 17C**). The final profile (Signature 4) included 469 DMPs and was hypomethylated at baseline, became hypermethylated after initial training. Then, genes showed a reduction in hypermethylation with detraining reverted to a hypermethylated state after retraining (**Fig. 17D**).

Figure 17 (Study 3). SOM profiling depicting the temporal regulation of DMPs over the time-course of baseline, training, detraining and retraining

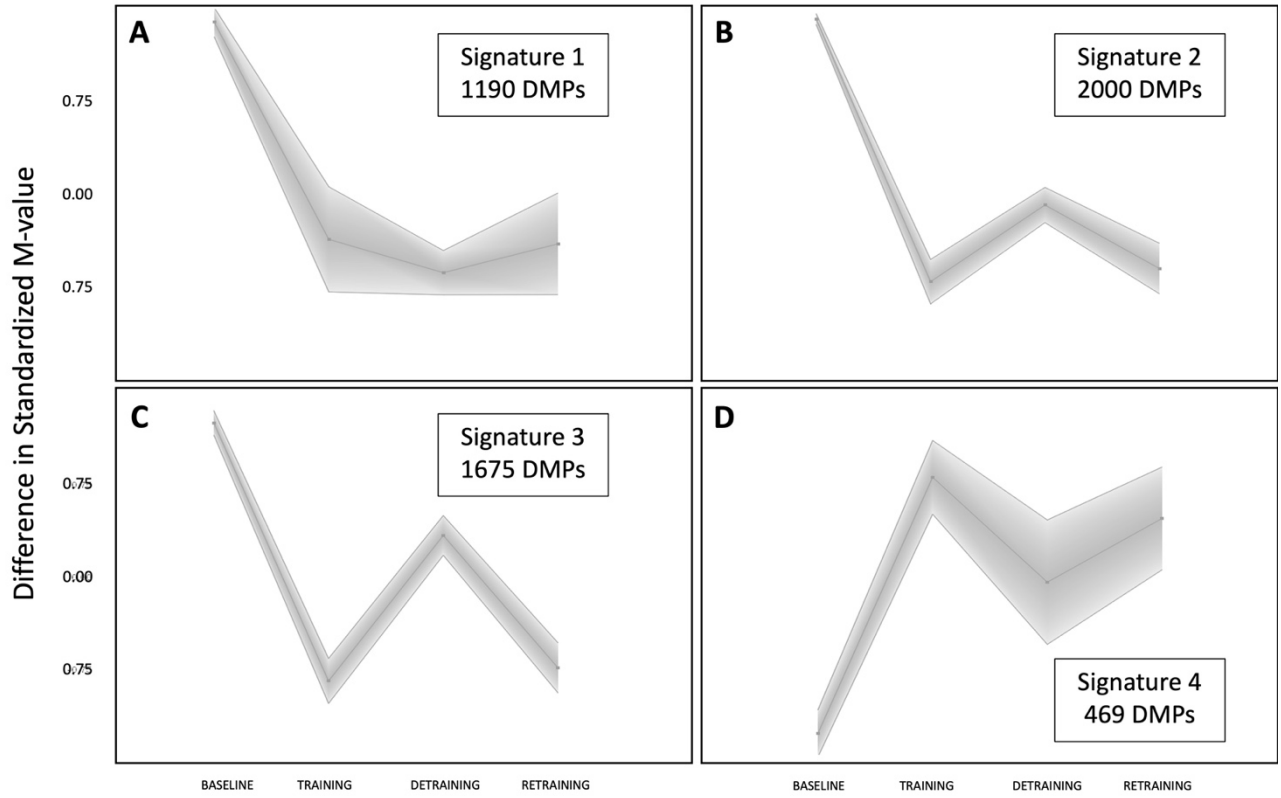

SOM profiling depicting the temporal regulation of DMPs over the time-course of baseline, training, detraining and retraining. A) Signature 1 displayed methylated state at baseline becoming hypomethylated in training and maintaining hypomethylation across detraining and retraining. B) Signature 2 displayed methylated state at baseline becoming hypomethylated in training; hypomethylation is reduced during detraining and reverted to similar or greater hypomethylated state after retraining. C) Signature 3 displayed methylated state at baseline becoming hypomethylated in training, hypermethylated in detraining and reverted to hypomethylation after retraining. D) Signature 1 displayed hypomethylated state at baseline becoming hypermethylated; hypermethylation is reduced during detraining and reverted to greater hypermethylated state after retraining.

Figure 18 (Study 3). Individual DMPs in Signature 2 identified by self-organising map (SOM)

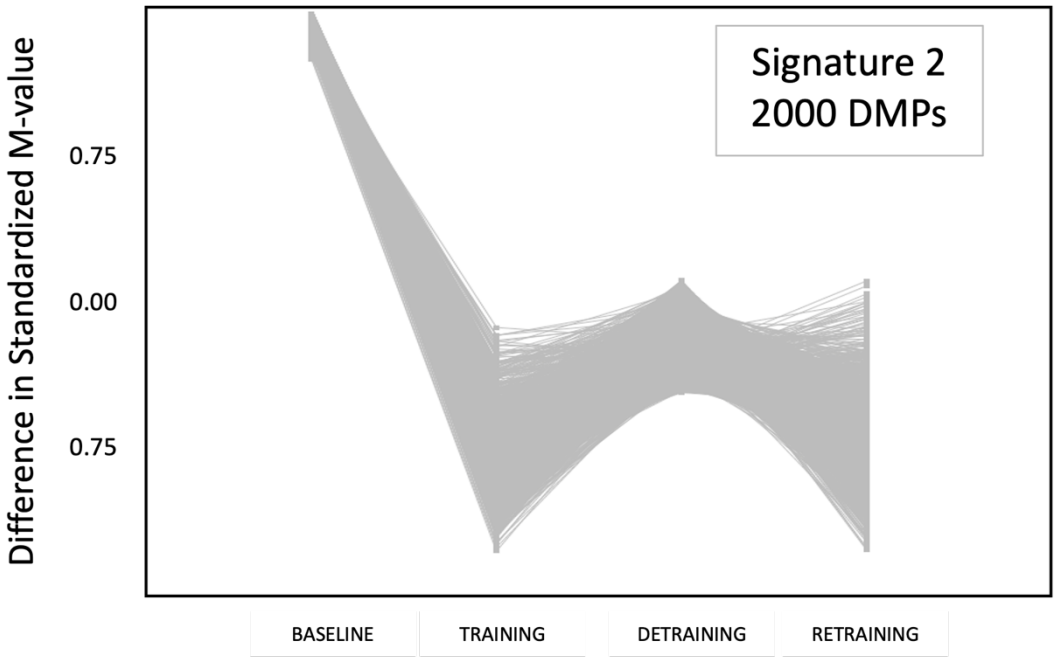

SOM profiling depicting the temporal regulation of individual DMPs over the time-course of baseline, training, detraining and retraining identified in Signature 2. It is possible to appreciate a number of DMPs that showed a greater hypomethylation in retraining than in training.

To assess whether the changes in DNA methylation across all conditions affected specific genes, modified CpG sites involved in the four Signatures were deeply investigated. DMRs analysis identified several regions located in or close to annotated genes with enriched (multiple CpGs in short chromosomal regions) differential methylation were identified. Cross reference with the most frequently occurring CpG modifications in pairwise comparisons of all conditions resulted in identification of six genes following temporal trend outlined by Signature 1 (*ADAM19, FOXK2, GNGT2, INPP5a, MTHFD1L, TMEM40*). Signature 2 characterized only one gene (TPM2). Five genes were characterized by Signature 3 profile (*CAPN2, PDGFB, MB21D2, SLC16A3, SPPL2C*). No genes with DMRs from cross reference were detected for Signature 4.

DISCUSSION

The present study aimed to investigate oxidative metabolism adaptations in humans in response to repeated endurance interval training interventions interspersed with a prolonged period of detraining. Investigation was focused specifically on mitochondrial adapting response at skeletal muscle level in order to deepen our understanding of the potential presence of skeletal muscle memory induced by aerobic training. The study was structured to investigate the training response at each of the organism's levels, ranging from functional to genetic aspects. The most outward analysis involved metabolic and cardiovascular adaptations at the whole-body level, focusing then on muscle oxidative capacity at the peripheral level using both *in vivo* and *ex vivo* measurements. Morphological and histological aspects of muscle offered a perspective on cellular modification, whereas mitochondrial biomarkers provided insight into molecular adaptations. In addition, epigenetic analysis was performed on the muscle sample to explore the endurance training-induced modification on the methylome and whether the epigenomic changes affected by repeated intervention could lead to upstream oxidative adaptations at the level of skeletal muscle and whole-body function.

Interval training composed by a combination of high-intensity interval training and sprint interval training was used in the present study to serve as training program because as previously demonstrated interval training was found to be more efficient in inducing improvement in mitochondrial function compared to moderate intensity training (Bishop *et al.*, 2014*b*, 2019; Granata *et al.*, 2016*b*). Moreover, high-intensity exercise is a more effective modality of leading to DNA hypomethylation and subsequent increase in gene expression in the mitochondrial biomarker compared to low-intensity training (Barrès *et al.*, 2012), which leads to the suggestion that the same pattern may occur in response to chronic interventions.. The underlying mechanism could be related to the elevated load and intermittent nature of interval training, that we hypothesized might likely mediate a muscle memory effect through epigenetic modifications.

Both interval training periods were effective in inducing metabolic adaptations at whole-body level showing an increment in $\dot{V}O_{2peak}$ and subsequently reflected on endurance performance with increased W_{peak} attained (**Fig. 1A-C**). However, both endurance performance and maximal aerobic capacity were not different between training and detraining. This result is accordance with two previous study on repeated interventions where no difference was found in $\dot{V}O_{2peak}$ or functional aerobic performance comparing two repeated interventions of high-intensity interval training interspersed by long-term period of training cessation (Simoneau *et al.*, 1987; Del Giudice *et al.*, 2020). Physiological and functional response were associated with enhanced adaptations at peripheral

level as shown by results from m$\dot{V}O_2$ *k* measured by NIRS and τ measured during constant work-rate exercise (**Fig. 2** and **Fig. 3**). Indeed, NIRS protocols provide *in vivo* estimation of muscle oxidative capacity (Ryan *et al.*, 2012, 2014; Adami *et al.*, 2017; Adami & Rossiter, 2018) and $\dot{V}O_2$ kinetic analyzed during constant work-rate exercise provides a close reflection of $\dot{V}O_2$ response in the exercising muscle determined by both muscle O_2 supply and muscle O_2 demand (Krustrup *et al.*, 2009; Hughson, 2009; Rossiter, 2011). However, enhancement of oxidative metabolism did not show evidence of difference between training and retraining. Accordingly, interval training also affects cardiovascular adaptations showing increased in maximal stroke volume after both training periods but with no difference between the first and the second exposure to the aerobic training stimulus (**Fig. 1E**). Conversely to stroke volume, maximal cardiac output was not affected by significant changes during training interventions (**Fig. 1F**). Overall, as discussed extensively in several reviews the present results demonstrated the impact of interval training in inducing an improvement in oxidative metabolism due to the combined cardiovascular and peripheral response (MacInnis & Gibala, 2017; Gibala *et al.*, 2019). In accordance to previous data on detraining (Coyle *et al.*, 1984, 1985; Pavlik *et al.*, 1986), three months of training interruption in the present study resulted adequate in reporting all whole-body aerobic physiological parameters similar to the baseline level. These *in vivo* results seem to suggest that physiological and functional adaptations at the whole-body level do not appear to benefit from repeated interventions, thus counteracting the hypothesis of an aerobic memory profile on the phenotype.

Although no significant insights into muscle memory have been found at the whole-body level, it is not excluded that a more in-depth investigation at the skeletal muscle level may detect a cellular or molecular response characterized by a memory pattern. Hence, further exploring the adaptive responses to repeated interval training interventions of oxidative metabolism within skeletal muscle, we investigated specific modification of mitochondrial function directly on muscle fibers. Both eight-week interval training periods elicited improvement in mitochondrial respiration capacity (**Fig 4**). These data confirmed previous findings demonstrating that chronic high intensity exercise is effective in producing improvement in mitochondrial function (Daussin *et al.*, 2008; Granata *et al.*, 2016*a*; MacInnis & Gibala, 2017; MacInnis *et al.*, 2017). The novel finding in the present study is the different response between repeated interventions. First training period induced improvement in mitochondrial respiration only at maximal substrate stimulations (maximal phosphorylating state and maximal respiration rate, **Fig. 4C-D**), whereas during retraining mitochondrial function was enhanced in each of the measured respiration states (**Fig. 4**). More importantly, comparison between mitochondrial respiration changes during training and retraining revealed a larger improvement after

the second intervention for all of the respiration states except one, which nevertheless showed a non-significant trend towards higher increment (**Fig. 5** and **Fig. 6**). These important results suggest that previous interval training intervention could affect response in mitochondrial function when muscle is subsequently exposed to a similar training stimulus, providing, hence, evidence for a muscle memory induced by endurance interval training occurring in the adaptive response of mitochondria. Thereby, although physiological adaptions at whole-body level seems not to benefit from repeated interventions, positive effects are evident at cellular level where mitochondrial function is more enhanced after retraining.

Skeletal muscle response to repeated interventions of high-intensity interval training has been previously investigated. As in the present study, Islam and colleagues (2021) (Islam *et al.*, 2021) found that an individuals exhibited dissimilar adaptive responses in skeletal muscle when re-exposed to the same training stimulus, specifically for some of the OXPHOS complex subunits. On the contrary, our results are in contrast to result from Lindholm and colleagues (2016) which showed no difference in mitochondrial adaptations in terms of citrate synthase activity between two training interventions composed by moderate-intensity exercise (45 min knee-extension at submaximal intensity) (Lindholm *et al.*, 2016). However, as previously described gene expression involved in mitochondrial biogenesis are more affected with high-intensity exercise (Barrès *et al.*, 2012). Thereby the lack of evidence of enhanced mitochondrial response during retraining may be explained by the absence of specific stimulus to induce modifications on mitochondrial transcription factors. Collectively, it might be concluded that differences in responsiveness in mitochondrial function to repeated training periods may be attributable to the influence of a prior high-intensity training on aerobic adaptation at skeletal muscle level that can affect, through a muscle memory mechanism, the subsequent mitochondrial response when exposed to same training stimulus later.

From preliminary data on only five subjects, however, it is difficult to infer a clear conclusion about protein changes during repeated interval training intervention that can explain the greater improvement in mitochondrial respiratory capacity occurring in retraining.
Nonetheless, these preliminary data could suggest some important information related to morphological and histological modifications. Interval training performed in the present study induced increase in type IIa fibers during first intervention for the five subjects analyzed. This adaptation was accompanied by a slight decrement in type I (**Fig. 12A-B**). These observation are in accordance to the skeletal muscle recruitment pattern that occurs in proportion to exercise intensity, implying that higher intensities of exercise could elicit greater responses in type II fibers relative to

lower intensities of exercise (Henneman, 1957; Vollestad & Blom, 1985; Sale, 1987). Indeed, although aerobic training, exercise performed during interval training, such as in the present study is characterized by elevated force and power production during muscle contraction favoring recruitment of fast twitch type fibers and subsequent modification in such fibers (MacInnis & Gibala, 2017). Interestingly, during retraining, in addition to an increase in type IIa fibers similarly to the previous intervention, type I fibers followed a slight tendency to increase. both changes occurred in shifts of reduced type IIx fiber content. Overall, this observation suggests that in the repeated aerobic high-intensity stimulus, the muscle perturbation might act in a fiber type-specific manner differently than in the previous intervention.

From histological adaptations the five subjects showed a training-induced increase in capillarization during both training and retraining (**Fig. 13**). According to data previously reported by Coyle and colleagues (1984) (Coyle *et al.*, 1984) where capillarization is maintained for a long-term period after activity interruption, in two out of five subjects in the present study capillarization shows no return to the baseline values after three months of detraining.

Epigenetics analysis on skeletal muscle tissue revealed interesting findings showing a large modification in the state of DNA methylation across training, detraining and retraining. Total number of differentially methylated CpG sites increased during both training period, with a less exaggerated response after retraining, and reduced after detraining (**Fig. 14A**). Simultaneously, the change also affects the state of methylation modification, which appears to gradually shift towards a more hypomethylated profile throughout conditions (**Fig. 14B**). As previously described (Nitert *et al.*, 2012; Rowlands *et al.*, 2014; Stephens *et al.*, 2018) endurance training induced greater hypomethylation at CpG sites compared to number of hypermethylated positions suggesting (greater ability to switch on expression on some specific gene). Consistently, a cessation of training reduced the total number of differentially methylated positions, however, although reduced, number of hypomethylated DMPs remained higher showing absence of reversion to the baseline level of the epigenome condition. In contrast, hypermethylated CpG sites were nearly reversed toward baseline values, indicating a deactivation of gene expression inhibition. Interestingly during retraining, although in smaller extent compared to the initial training, hypomethylation increased again, but surprisingly number of hypermethylated DMPs was maintained similar to the previous condition after detraining, indicating that subsequent interval training stimulus elicited a different remodeling on the epigenome and more specifically did not generate any hypermethylated modification along with inhibition DNA expression. This increase in hypomethylation and reduced hypermethylation coincided with the largest increase in mitochondrial respiration in retraining.

Among DMPs enriched over the time-course of baseline, training, detraining and retraining were identified two important gene ontology terms related to muscle contractile activity and affecting mitochondrial biogenesis: calcium and MAPK signaling pathway. Both pathways are crucial elements involved in the contraction-induced signal transduction pathways able to promote physiological responses and subsequent adaptations in muscle cells resulting in activation and/or repression of specific signaling regulating exercise-induced gene expression and protein synthesis/degradation (Bassel-Duby & Olson, 2006; Hood *et al.*, 2006; Coffey & Hawley, 2007; Egan & Zierath, 2013). Specifically, calcium and MAPK pathways are respectively modulated by mechanical and biochemical stress (Baar & Esser, 1999; Alenghat & Ingber, 2002) generated with muscle contraction occurring especially during exercise stimulus of high intensity nature. Interestingly downstream signals of calcium and MAPK pathways involve transcription factors activation, such as ATF2, NFAT, CREB, MEF2 or HDACs, affecting PGC-1α gene expression in skeletal muscle (Pilegaard *et al.*, 2000; Akimoto *et al.*, 2005; Wright *et al.*, 2007*a*; Chin, 2010; Egan *et al.*, 2010). Thereby, epigenetically modification of these pathway across training, detraining and retraining periods could be connecting factor that relates muscle perturbations induced by repeated endurance training stimuli with enhancement in mitochondrial adaptations providing a hint to recognize underlying aerobic muscle memory mechanisms.

More specific DNA methylation analysis identified signatures of temporal DNA methylation patterns that provide initial evidence of an epigenetic memory (**Fig. 17**). All the four Signatures reported similar DNA methylation status between training and retraining profile (hypomethylated for Signatures 1, 2 and 3, and hypermethylated for Signature 4), suggesting recurrence of epigenetic modifications from the first training period to the later retraining phase. During detraining, cluster from Signatures 3 and 4 revealed a decrement of their previous DNA methylation state consistently to the reduction observed in total frequency DMPs. This evidence may therefore suggest that the small number of CpG sites differentially methylated observed during detraining could be mostly part of Signature 1 and 2 temporal trends characterized by retention of hypomethylation profile during long-term interruption phase from training stimulus. Therefore, Signature 1, and even Signature 2 in a slightly reduced form, were highlighted as memory profile at epigenetic level. A similar pattern was previously found by Seaborne and colleagues (2018) (Seaborne *et al.*, 2018*a*) in response to resistance training, demonstrating the presence of an epigenetic memory at DNA methylation level of previous training-induced hypertrophic stimulus that led to the retention of methylation during detraining and subsequent larger hypomethylation after later retraining. In the present study, deeply investigation of Signature 1 and 2 identified several regions located in or close to annotated genes with enriched differential methylation that could likely be affected by more pronounced gene expression. Among

these were found genes related to glucose metabolism and aerobic glycolysis (*FOXK2*), membrane protein that mobilizes intracellular calcium (*INPP5a)*, synthesis of tetrahydrofolate in the mitochondrion (*MTHFD1L*) and lactic acid and pyruvate transport across plasma membranes (*SLC16A3*). After identifying the genes affected by memory profiles during the repeated endurance training intervention, further analysis should be conducted to provide the temporal profile of gene expression in order to understand whether the DNA methylation pattern is matched with the transcription of target genes.

Our results are in contrast with a previous transcriptomic study where authors, investigating gene expression via RNA sequencing in response to repeated unilateral endurance training, did not find evidence in support to the presence of a transcriptomic memory (Lindholm *et al.*, 2016). However, in the above study DNA methylation was not investigated and more importantly the exercise paradigm involved was a moderate-intensity endurance training, but as previously described methylation and gene expression involved in mitochondrial biogenesis are more affected with high-intensity exercise (Barrès *et al.*, 2012). Thereby the lack of evidence of muscle memory may be explained in the study of Lindholm et al. (2016) by the absence of specific stimulus to induce epigenetic modifications.

Limitations

Although most mitochondrial proteins are nuclear encoded, 13 important proteins are transcribed from mitochondrial DNA and are vital for normal respiratory function by leading to the formation of the subunits of four ETC complexes (Cogswell *et al.*, 1993; Oliveira & Hood, 2019). Unfortunately, in the present study mtDNA methylome was not investigated lacking therefore to investigate an important element regarding epigenetic responses and consequent implications at mitochondrial level and oxidative metabolism. Indeed, has been demonstrated that aerobic training affect DNA methylation on mitochondrial DNA level leading therefore to important consequence in gene and protein expression that could be involved in aerobic muscle memory mechanism (Ruple *et al.*, 2021).

Another limitation in the present study is the lacking in a connecting link between epigenetic memory to mitochondrial function due to lacking complete genomic and proteomic analysis necessary to explore transcription and translation response to interval training repeated interventions. To date preliminary data on five subjects are insufficient to infer conclusions, thus leaving an important puzzle component of the aerobic memory mechanism unresolved.

CONCLUSIONS

In summary, two repeated interventions of interval training interspersed by prolonged training interruption induced different response at epigenetic and mitochondrial level providing evidence of epigenetic memory mechanism affecting muscle aerobic phenotype, suggesting insight into potential aerobic muscle memory to interval training. Although response in functional and oxidative metabolism parameter measured in physiological conditions were similar between training and retraining, previously high intensity aerobic stimulus was effective in elicit greater improvement in mitochondrial function when subsequently exposed to an identical stimulus after long-term detraining period. A possible explanation for this mechanism could reside in epigenetic modifications induced by interval training which led to DNA hypomethylation. Moreover, two memory profiles were highlighted at epigenetic level characterized by retention of hypomethylation even during the prolonged detraining period. These profiles revealed differentially methylated regions related with genes involved in skeletal muscle metabolic pathways. Overall, the present study provides evidence for a mechanism of memory elicited by high-intensity endurance training that initiates at the epigenetic level and extends upstream to affect mitochondrial function. Further genomic and proteomic analyses could elucidate the transcription and translation processes involved in the aerobic muscle memory mechanism connecting epigenetic modification to mitochondrial adaptations.

CHAPTER 6

DISCUSSION

The work conducted in the present thesis aimed to investigate the potential presence of skeletal muscle memory in response to repeated high-intensity endurance training interventions. In addition, a methodological project was carried out to assess a novel *in vivo* approach to estimate muscle oxygen diffusion capacity.

Study 1 aimed to assess a novel *in vivo* approach to estimate muscle oxygen diffusion capacity based on non-invasive near-infrared spectroscopy measurement via a novel protocol of arterial occlusions performed in both oxygen limiting and not limiting conditions. We tested the hypotheses that $m\dot{V}O_2$ recovery rate constant, *k*, is associated with muscle oxidative capacity only in not-limiting oxygen conditions and that the difference in $m\dot{V}O_2$ recovery rate constant between well-oxygenated and poorly-oxygenated muscle provides insight into DmO_2. Our data confirmed previous findings (Ryan *et al.*, 2014) demonstrating a correlation between $m\dot{V}O_2$ recovery rate constant measured by NIRS in high TSI condition (> 50% of the physiological normalization) and maximal muscle O_2 flux in fiber bundles measured via high-resolution respirometry on permeabilized fibers. In addition, we showed for the first time that this relationship did not hold in oxygen limiting condition; indeed, $m\dot{V}O_2$ recovery rate constant measured during tissue oxygenation reduced below 50% of the physiological normalization was not associated with any variable describing muscle oxidative capacity in fiber bundles. This latter finding is consistent with Fick's law since $m\dot{V}O_2$ becomes increasingly dependent on DmO_2 as microvascular-to-myocyte PO_2 difference is reduced (see Eq. 1). Therefore, experimental manipulation of TSI through timing and duration of intermittent arterial occlusions provided a new variable, Δk, calculated by the difference in $m\dot{V}O_2$ recovery rate constant between well-oxygenated and poorly-oxygenated experimental conditions. As hypothesized, we found that Δk was associated with capillary-to-fiber ratio in biopsy samples of the same muscle, a primary structural determinant of DmO_2. Thus, the NIRS-derived response measured under conditions of both well-oxygenated and poorly-oxygenated skeletal muscle provided a non-invasive means of assessing both muscle oxidative capacity and muscle diffusing capacity *in vivo*.

Study 2 and 3 were both conducted with the aim to investigate whether skeletal muscle memory occurs in response to repeated high-intensity endurance training interventions interspersed with prolonged detraining period. High-intensity interval training has been used here to serve as endurance training paradigm because, as demonstrated by Barrès and colleagues (2012), high-intensity exercise is more effective in inducing DNA hypomethylation and subsequent increase in gene expression in the mitochondrial biomarker than low-intensity training (Barrès *et al.*, 2012). The underlying

mechanism could be related to the elevated load and intermittent nature of high-intensity interval training, which could mediate the muscle memory effect through epigenetic modifications.

Study 2 was carried out on murine model and was hypothesized that previous high-intensity interval training could facilitate functional and molecular adaptations during retraining in mice. Our results demonstrated that endurance performance measured during graded exercise test on a rodent treadmill was improved in a larger extent after the second exposure to the aerobic stimulus. Moreover, molecular protein involved in the mitochondrial network function and remodeling resulted respond differently upon administration of repeated endurance training. Specifically, confirming previous mitochondrial data in response to resistance training (Lee *et al.*, 2018), adaptations in mitochondrial content and biogenesis during retraining appeared to be facilitated by previous exposure to the training stimulus, showing a greater increase after the second training compared to the effect elicited by the initial intervention although reverted to baseline values during detraining. In addition, during retraining was observed a shift in favor of fission rather than fusion mitochondrial dynamics. The difference in mitochondrial adaptations observed from repeated interventions in the present study paved the way for the presence of memory mechanism affecting muscle aerobic phenotype, suggesting insight into potential aerobic muscle memory to high-intensity endurance training.

Study 3 was conducted in humans and, in order to deepen understanding of the aerobic skeletal muscle memory, aimed to investigate aerobic adaptations at all levels of the entire human organism, from the epigenetic level to the whole-body response to exercise, across repeated exposure to two identical interval training interventions separated by long-term interruption of training. Differently from previous mice study improvement in endurance performance were not different between training and retraining. This observation was reflected by identical response profile of maximal aerobic capacity. Previous human studies characterized by repeated aerobic intervention design with a similar time-course protocol found similar results revealing no difference in oxidative metabolism whole-body adaptations and endurance performance (Simoneau *et al.*, 1987; Del Giudice *et al.*, 2020). Moreover, even for repeated resistance training design, a comparison between human and animal studies showed difference in hypertrophic response with evidence of greater muscle size after retraining than retraining in rodent (Lee *et al.*, 2018; Wen *et al.*, 2021) but similar response in humans (Psilander *et al.*, 2019). A possible explanation could lie in the temporal duration of the intervention in humans, where interventions lasting 2-3 months are not sufficient to complete the adaptive processes induced by the muscle memory mechanism, which start from the epigenetic or transcriptional modifications and through the translational machinery come to an enhanced manifestation of adaptations at whole-body physiological or functional level. However, in the present study some important finding has been detected from molecular and epigenetic analysis. Mitochondrial respiration assessment revealed

that previously high intensity aerobic stimulus was effective in elicit greater improvement in mitochondrial function when subsequently exposed to an identical stimulus after long-term detraining period. The underlying mechanism was observed to lie in epigenetic modifications induced by interval training which led to DNA hypomethylation in the present study. Moreover, two memory profiles were highlighted at epigenetic level characterized by retention of hypomethylation even during the prolonged detraining period. These profiles revealed differentially methylated regions related with genes involved in skeletal muscle metabolic pathways. Our results are in contrast with a previous transcriptomic study where authors, investigating gene expression via RNA sequencing in response to repeated unilateral endurance training, did not found evidence in support to the presence of an aerobic training-induced transcriptomic memory (Lindholm *et al.*, 2016). In addition, even mitochondrial adaptations were not different between the two training interventions (Lindholm *et al.*, 2016). However, in the above study DNA methylation was not investigated and more importantly the exercise paradigm involved was a moderate-intensity endurance training (45 min knee-extension at submaximal intensity). As previously described methylation and gene expression involved in mitochondrial biogenesis are more affected with high-intensity exercise (Barrès *et al.*, 2012). Thereby the lack of evidence of muscle memory in the above-mentioned study may be explained by the absence of specific stimulus to induce epigenetic modifications on mitochondrial transcription factors. Furthermore, the use of the contralateral leg as a control is recognized to be controversial. Training in one leg only can lead to modification in the rest of the body and also in the untrained leg in response to the effect of myokines that are released into the circulation from the muscle tissue of the trained leg and conveyed via vascular and systemic components (Pedersen & Febbraio, 2012). Overall, this third study provides evidence for a mechanism of memory in humans elicited by high-intensity endurance training that initiates at the epigenetic level and extends upstream to affect mitochondrial function. Further genomic and proteomic analyses could elucidate the transcription and translation processes involved in the aerobic muscle memory mechanism connecting epigenetic modification to mitochondrial adaptations.

CHAPTER 7

CONCLUSION

Key findings:

1. Recovery rate constant (k) of muscle oxygen uptake measured by near-infrared spectroscopy reflects muscle oxidative capacity only in well-oxygenated muscle. Δk, the difference in k measured in O_2 limiting and not-limiting conditions, was associated with capillary-to-fiber ratio, a primary structural determinant of muscle oxygen diffusion capacity. Assessment of muscle k and Δk using near-infrared spectroscopy provides a non-invasive window on muscle oxidative and oxygen diffusing capacity.

2. Two repeated interventions of high-intensity interval training induced a greater improvement in aerobic performance after the second exposure to the aerobic training stimulus. This enhanced response appears to be determined by larger expression of mitochondrial biogenesis factors that induced an increase in mitochondrial content, as well as changes mitochondrial dynamics that likely promoted healthier and more functional mitochondria. In conclusion, mitochondria adaptations to a high-intensity interval training intervention are different if the stimulus has been previously encountered, thereby supporting the hypothesis of a mitochondrial memory.

3. Two repeated interventions of interval training interspersed by prolonged training interruption induced different response at epigenetic and mitochondrial level providing evidence of epigenetic memory mechanism in humans. Although physiological adaptions at whole-body level seems not to benefit from repeated interventions, positive effects are evident at cellular level where mitochondrial function is more enhanced after retraining. This finding provides evidence for a mitochondrial muscle memory induced by endurance interval training occurring in the adaptive response of mitochondria. The underlying mechanism lied in epigenetic modifications induced by interval training which led to DNA hypomethylation. Two memory profiles were highlighted at epigenetic level characterized by retention of hypomethylation during long-term detraining period. These profiles revealed were related to genes involved in skeletal muscle metabolic pathways.

Collectively, the results from this thesis provided two important outcomes.
It first provided a novel methodological non-invasive approach to assess *in vivo* oxygen diffusing capacity using near-infrared spectroscopy.
In the second instance, it provided evidence for a skeletal muscle memory mechanism elicited by high-intensity aerobic training that affects muscle aerobic phenotype initiating at the epigenetic level

and extends upstream to affect mitochondrial function and endurance performance. This mechanism has important consequences on the quality of life, since if the stimulus encountered affects positively aerobic adaptations at skeletal muscle level, the organism as a whole may further benefit. This may be beneficial both in terms of sports performance, but also to improve the activities of daily living by promoting health in the elder age with lifelong healthy maintenance.

REFERENCES

Acín-Pérez R, Fernández-Silva P, Peleato ML, Pérez-Martos A & Enriquez JA (2008). Respiratory Active Mitochondrial Supercomplexes. *Mol Cell* **32,** 529–539.

Adami A, Cao R, Porszasz J, Casaburi R & Rossiter HB (2017). Reproducibility of NIRS assessment of muscle oxidative capacity in smokers with and without COPD. *Respir Physiol Neurobiol* **235,** 18–26.

Adami A, Corvino RB, Calmelat RA, Porszasz J, Casaburi R & Rossiter HB (2020). Muscle Oxidative Capacity Is Reduced in Both Upper and Lower Limbs in COPD. *Med Sci Sports Exerc* **52,** 2061–2068.

Adami A & Rossiter HB (2018). Principles, insights, and potential pitfalls of the noninvasive determination of muscle oxidative capacity by near-infrared spectroscopy. *J Appl Physiol* **124,** 245–248.

Adams GR, Hather BM, Baldwin KM & Dudley GA (1993). Skeletal muscle myosin heavy chain composition and resistance training. *J Appl Physiol* **74,** 911–915.

Adhihetty PJ, Irrcher I, Joseph AM, Ljubicic V & Hood DA (2003). Plasticity of skeletal muscle mitochondria in response to contractile activity. *Exp Physiol* **88,** 99–107.

Adhihetty PJ, Ljubicic V, Menzies KJ & Hood DA (2005). Differential susceptibility of subsarcolemmal and intermyofibrillar mitochondria to apoptotic stimuli. *Am J Physiol Cell Physiol*; DOI: 10.1152/AJPCELL.00031.2005.

Akimoto T, Pohnert SC, Li P, Zhang M, Gumbs C, Rosenberg PB, Williams RS & Yan Z (2005). Exercise stimulates Pgc-1alpha transcription in skeletal muscle through activation of the p38 MAPK pathway. *J Biol Chem* **280,** 19587–19593.

Alenghat FJ & Ingber DE (2002). Mechanotransduction: all signals point to cytoskeleton, matrix, and integrins. *Sci STKE*; DOI: 10.1126/STKE.2002.119.PE6.

Alibegovic AC, Sonne MP, Højbjerre L, Bork-Jensen J, Jacobsen S, Nilsson E, Færch K, Hiscock N, Mortensen B, Friedrichsen M, Stallknecht B, Dela F & Vaag A (2010). Insulin resistance induced by physical inactivity is associated with multiple transcriptional changes in skeletal muscle in young men. *Am J Physiol Endocrinol Metab*; DOI: 10.1152/AJPENDO.00590.2009.

Amat R, Planavila A, Chen SL, Iglesias R, Giralt M & Villarroya F (2009). SIRT1 controls the transcription of the peroxisome proliferator-activated receptor-gamma Co-activator-1alpha (PGC-1alpha) gene in skeletal muscle through the PGC-1alpha autoregulatory loop and interaction with MyoD. *J Biol Chem* **284,** 21872–21880.

Amchenkova AA, Bakeeva LE, Chentsov YS, Skulachev VP & Zorov DB (1988). Coupling membranes as energy-transmitting cables. I. Filamentous mitochondria in fibroblasts and

mitochondrial clusters in cardiomyocytes. *J Cell Biol* **107,** 481–495.

American College of Sports Medicine, Riebe D, Ehrman JK, Liguori G & Magal M (2018). *ACSM's guidelines for exercise testing and prescription*, 10th edn. Wolters Kluwer, Philadelphia.

Anastasiadi D, Esteve-Codina A & Piferrer F (2018). Consistent inverse correlation between DNA methylation of the first intron and gene expression across tissues and species. *Epigenetics Chromatin*; DOI: 10.1186/S13072-018-0205-1.

Andersen P & Saltin B (1985). Maximal perfusion of skeletal muscle in man. *J Physiol* **366,** 233–249.

Angleys H & Østergaard L (2020). Krogh's capillary recruitment hypothesis, 100 years on: Is the opening of previously closed capillaries necessary to ensure muscle oxygenation during exercise? *Am J Physiol Heart Circ Physiol* **318,** H425–H447.

Aquilano K, Vigilanza P, Baldelli S, Pagliei B, Rotilio G & Ciriolo MR (2010). Peroxisome proliferator-activated receptor gamma co-activator 1alpha (PGC-1alpha) and sirtuin 1 (SIRT1) reside in mitochondria: possible direct function in mitochondrial biogenesis. *J Biol Chem* **285,** 21590–21599.

Arbab-Zadeh A, Perhonen M, Howden E, Peshock RM, Zhang R, Adams-Huet B, Haykowsky MJ & Levine BD (2014). Cardiac remodeling in response to 1 year of intensive endurance training. *Circulation* **130,** 2152–2161.

Aschenbach WG, Sakamoto K & Goodyear LJ (2004). 5' adenosine monophosphate-activated protein kinase, metabolism and exercise. *Sports Med* **34,** 91–103.

Axelrod CL, Fealy CE, Mulya A & Kirwan JP (2019). Exercise training remodels human skeletal muscle mitochondrial fission and fusion machinery towards a pro-elongation phenotype. *Acta Physiol (Oxf)*; DOI: 10.1111/APHA.13216.

Baar K (2014). Nutrition and the adaptation to endurance training. *Sport Med* **44,** 5–12.

Baar K & Esser K (1999). Phosphorylation of p70(S6k) correlates with increased skeletal muscle mass following resistance exercise. *Am J Physiol*; DOI: 10.1152/AJPCELL.1999.276.1.C120.

Baertschi B & Gyger M (2011). Ethical Considerations in Mouse Experiments. *Curr Protoc Mouse Biol*; DOI: 10.1002/9780470942390.MO100161.

Baggish AL, Wang F, Weiner RB, Elinoff JM, Tournoux F, Boland A, Picard MH, Hutter AM & Wood MJ (2008). Training-specific changes in cardiac structure and function: a prospective and longitudinal assessment of competitive athletes. *J Appl Physiol* **104,** 1121–1128.

Bakeeva LE, Chentsov YS & Skulachev VP (1978). Mitochondrial framework (reticulum mitochondriale) in rat diaphragm muscle. *Biochim Biophys Acta* **501,** 349–369.

Baker MJ, Frazier AE, Gulbis JM & Ryan MT (2007). Mitochondrial protein-import machinery:

correlating structure with function. *Trends Cell Biol* **17,** 456–464.

Baldwin KM, Klinkerfuss GH, Terjung RL, Molé PA & Holloszy JO (1972). Respiratory capacity of white, red, and intermediate muscle: adaptative response to exercise. *Am J Physiol* **222,** 373–378.

Ball MP, Li JB, Gao Y, Lee JH, Leproust EM, Park IH, Xie B, Daley GQ & Church GM (2009). Targeted and genome-scale strategies reveal gene-body methylation signatures in human cells. *Nat Biotechnol* **27,** 361–368.

Barbieri E & Sestili P (2012). Reactive oxygen species in skeletal muscle signaling. *J Signal Transduct* **2012,** 1–17.

Barrès R, Osler ME, Yan J, Rune A, Fritz T, Caidahl K, Krook A & Zierath JR (2009). Non-CpG methylation of the PGC-1alpha promoter through DNMT3B controls mitochondrial density. *Cell Metab* **10,** 189–198.

Barrès R, Yan J, Egan B, Treebak JT, Rasmussen M, Fritz T, Caidahl K, Krook A, O'Gorman DJ & Zierath JR (2012). Acute exercise remodels promoter methylation in human skeletal muscle. *Cell Metab* **15,** 405–411.

Bassel-Duby R & Olson EN (2006). Signaling pathways in skeletal muscle remodeling. *Annu Rev Biochem* **75,** 19–37.

Bassett DR (2002). Scientific contributions of A. V. Hill: exercise physiology pioneer. *J Appl Physiol* **93,** 1567–1582.

Beaver WL, Wasserman K & Whipp BJ (1986). A new method for detecting anaerobic threshold by gas exchange. *J Appl Physiol* **60,** 2020–2027.

Bebout DE, Hogan MC, Hempleman SC & Wagner PD (1993). Effects of training and immobilization on VO2 and DO2 in dog gastrocnemius muscle in situ. *J Appl Physiol* **74,** 1697–1703.

Beever AT, Tripp TR, Zhang J & MacInnis MJ (2020). NIRS-derived skeletal muscle oxidative capacity is correlated with aerobic fitness and independent of sex. *J Appl Physiol* **129,** 558–568.

Benziane B, Burton TJ, Scanlan B, Galuska D, Canny BJ, Chibalin A V., Zierath JR & Stepto NK (2008). Divergent cell signaling after short-term intensified endurance training in human skeletal muscle. *Am J Physiol Endocrinol Metab*; DOI: 10.1152/AJPENDO.90428.2008.

Bergeron R, Ren JM, Cadman KS, Moore IK, Perret P, Pypaert M, Young LH, Semenkovich CF & Shulman GI (2001). Chronic activation of AMP kinase results in NRF-1 activation and mitochondrial biogenesis. *Am J Physiol Endocrinol Metab*; DOI: 10.1152/AJPENDO.2001.281.6.E1340.

Bickel CS, Slade J, Mahoney E, Haddad F, Dudley GA & Adams GR (2005). Time course of

molecular responses of human skeletal muscle to acute bouts of resistance exercise. *J Appl Physiol* **98,** 482–488.

Bird AP (1986). CpG-rich islands and the function of DNA methylation. *Nature* **321,** 209–213.

Bishop DJ, Botella J, Genders AJ, Lee MJC, Saner NJ, Kuang J, Yan X & Granata C (2019). High-Intensity Exercise and Mitochondrial Biogenesis: Current Controversies and Future Research Directions. *Physiology (Bethesda)* **34,** 56–70.

Bishop DJ, Granata C & Eynon N (2014*a*). Can we optimise the exercise training prescription to maximise improvements in mitochondria function and content? *Biochim Biophys Acta* **1840,** 1266–1275.

Bishop DJ, Granata C & Eynon N (2014*b*). Can we optimise the exercise training prescription to maximise improvements in mitochondria function and content? *Biochim Biophys Acta* **1840,** 1266–1275.

Blackstone C & Chang CR (2011). Mitochondria unite to survive. *Nat Cell Biol* **13,** 521–522.

Bleck CKE, Kim Y, Willingham TB & Glancy B (2018). Subcellular connectomic analyses of energy networks in striated muscle. *Nat Commun*; DOI: 10.1038/S41467-018-07676-Y.

Blei ML, Conley KE, Odderson IR, Esselman PC & Kushmerick MJ (1993). Individual variation in contractile cost and recovery in a human skeletal muscle. *Proc Natl Acad Sci U S A* **90,** 7396–7400.

Blocquiaux S, Ramaekers M, Thienen R Van, Nielens H, Delecluse C, Bock K De & Thomis M (2022). Recurrent training rejuvenates and enhances transcriptome and methylome responses in young and older human muscle. *JCSM Rapid Commun* **5,** 10–32.

Bogdanović O & Veenstra GJC (2009). DNA methylation and methyl-CpG binding proteins: developmental requirements and function. *Chromosoma* **118,** 549–565.

Bonne TC, Doucende G, Flück D, Jacobs RA, Nordsborg NB, Robach P, Walther G & Lundby C (2014). Phlebotomy eliminates the maximal cardiac output response to six weeks of exercise training. *Am J Physiol Regul Integr Comp Physiol*; DOI: 10.1152/AJPREGU.00028.2014.

Booth FW & Thomason DB (1991). Molecular and cellular adaptation of muscle in response to exercise: perspectives of various models. *Physiol Rev* **71,** 541–585.

Borg G (1982). Ratings of Perceived Exertion and Heart Rates During Short-Term Cycle Exercise and Their Use in a New Cycling Strength Test. *Int J Sports Med* **3,** 153–158.

Bouchard C, Lesage R, Lortie G, Simoneau JA, Hamel P, Boulay MR, Pérusse L, Thériault G & Leblanc C (1986). Aerobic performance in brothers, dizygotic and monozygotic twins. *Med Sci Sports Exerc* **18,** 639–646.

Boushel R, Gnaiger E, Calbet JAL, Gonzalez-Alonso J, Wright-Paradis C, Sondergaard H, Ara I,

Helge JW & Saltin B (2011). Muscle mitochondrial capacity exceeds maximal oxygen delivery in humans. *Mitochondrion* **11,** 303–307.

Brand MD & Nicholls DG (2011). Assessing mitochondrial dysfunction in cells. *Biochem J* **435,** 297–312.

Brand MD, Pamplona R, Portero-Otín M, Requena JR, Roebuck SJ, Buckingham JA, Clapham JC & Cadenas S (2002). Oxidative damage and phospholipid fatty acyl composition in skeletal muscle mitochondria from mice underexpressing or overexpressing uncoupling protein 3. *Biochem J* **368,** 597.

Brenet F, Moh M, Funk P, Feierstein E, Viale AJ, Socci ND & Scandura JM (2011). DNA methylation of the first exon is tightly linked to transcriptional silencing. *PLoS One*; DOI: 10.1371/JOURNAL.PONE.0014524.

Breuer ME, Koopman WJ, Koene S, Nooteboom M, Rodenburg RJ, Willems PH & Smeitink JAM (2013). The role of mitochondrial OXPHOS dysfunction in the development of neurologic diseases. *Neurobiol Dis* **51,** 27–34.

Brocca L, McPhee JS, Longa E, Canepari M, Seynnes O, De Vito G, Pellegrino MA, Narici M & Bottinelli R (2017). Structure and function of human muscle fibres and muscle proteome in physically active older men. *J Physiol* **595,** 4823.

Brown MD, Jeal S, Bryant J & Gamble J (2001). Modifications of microvascular filtration capacity in human limbs by training and electrical stimulation. *Acta Physiol Scand* **173,** 359–368.

Bruusgaard JC, Johansen IB, Egner IM, Rana ZA & Gundersen K (2010). Myonuclei acquired by overload exercise precede hypertrophy and are not lost on detraining. *Proc Natl Acad Sci U S A* **107,** 15111–15116.

Buchheit M & Laursen PB (2013). High-intensity interval training, solutions to the programming puzzle: Part I: cardiopulmonary emphasis. *Sports Med* **43,** 313–338.

Burgomaster KA, Heigenhauser GJF & Gibala MJ (2006). Effect of short-term sprint interval training on human skeletal muscle carbohydrate metabolism during exercise and time-trial performance. *J Appl Physiol* **100,** 2041–2047.

Burgomaster KA, Howarth KR, Phillips SM, Rakobowchuk M, Macdonald MJ, Mcgee SL & Gibala MJ (2008). Similar metabolic adaptations during exercise after low volume sprint interval and traditional endurance training in humans. *J Physiol* **586,** 151–160.

Burgomaster KA, Hughes SC, Heigenhauser GJF, Bradwell SN & Gibala MJ (2005). Six sessions of sprint interval training increases muscle oxidative potential and cycle endurance capacity in humans. *J Appl Physiol* **98,** 1985–1990.

Buso A, Comelli M, Picco R, Isola M, Magnesa B, Pišot R, Rittweger J, Salvadego D, Šimunič B,

Grassi B & Mavelli I (2019). Mitochondrial adaptations in elderly and young men skeletal muscle following 2 weeks of bed rest and rehabilitation. *Front Physiol*; DOI: 10.3389/FPHYS.2019.00474/PDF.

Cadenas S, Echtay KS, Harper JA, Jekabsons MB, Buckingham JA, Grau E, Abuin A, Chapman H, Clapham JC & Brand MD (2002). The basal proton conductance of skeletal muscle mitochondria from transgenic mice overexpressing or lacking uncoupling protein-3. *J Biol Chem* **277,** 2773–2778.

Calbet JAL, Lundby C, Sander M, Robach P, Saltin B & Boushel R (2006). Effects of ATP-induced leg vasodilation on VO2 peak and leg O2 extraction during maximal exercise in humans. *Am J Physiol Regul Integr Comp Physiol*; DOI: 10.1152/AJPREGU.00746.2005.

Calvo JA, Daniels TG, Wang X, Paul A, Lin J, Spiegelman BM, Stevenson SC & Rangwala SM (2008). Muscle-specific expression of PPARgamma coactivator-1alpha improves exercise performance and increases peak oxygen uptake. *J Appl Physiol* **104,** 1304–1312.

Calvo SE, Clauser KR & Mootha VK (2016). MitoCarta2.0: an updated inventory of mammalian mitochondrial proteins. *Nucleic Acids Res* **44,** D1251–D1257.

Cannavino J, Brocca L, Sandri M, Bottinelli R & Pellegrino MA (2014). PGC1-α over-expression prevents metabolic alterations and soleus muscle atrophy in hindlimb unloaded mice. *J Physiol* **592,** 4575–4589.

Cantó C, Gerhart-Hines Z, Feige JN, Lagouge M, Noriega L, Milne JC, Elliott PJ, Puigserver P & Auwerx J (2009). AMPK regulates energy expenditure by modulating NAD+ metabolism and SIRT1 activity. *Nature* **458,** 1056–1060.

Carrero P, Okamoto K, Coumailleau P, O'Brien S, Tanaka H & Poellinger L (2000). Redox-regulated recruitment of the transcriptional coactivators CREB-binding protein and SRC-1 to hypoxia-inducible factor 1alpha. *Mol Cell Biol* **20,** 402–415.

Cereghetti GM, Stangherlin A, Martins De Brito O, Chang CR, Blackstone C, Bernardi P & Scorrano L (2008). Dephosphorylation by calcineurin regulates translocation of Drp1 to mitochondria. *Proc Natl Acad Sci U S A* **105,** 15803–15808.

Chan DC (2006). Mitochondria: dynamic organelles in disease, aging, and development. *Cell* **125,** 1241–1252.

Chan DC (2012). Fusion and fission: interlinked processes critical for mitochondrial health. *Annu Rev Genet* **46,** 265–287.

Chance B & Williams GR (1955). Respiratory enzymes in oxidative phosphorylation. IV. The respiratory chain. *J Biol Chem* **217,** 429–438.

Chang CR & Blackstone C (2007). Cyclic AMP-dependent protein kinase phosphorylation of Drp1

regulates its GTPase activity and mitochondrial morphology. *J Biol Chem* **282,** 21583–21587.

Charloux A, Lonsdorfer-Wolf E, Richard R, Lampert E, Oswald-Mammosser M, Mettauer B, Geny B & Lonsdorfer J (2000). A new impedance cardiograph device for the non-invasive evaluation of cardiac output at rest and during exercise: comparison with the "direct" Fick method. *Eur J Appl Physiol* **82,** 313–320.

Chen CCW, Erlich AT, Crilly MJ & Hood DA (2018*a*). Parkin is required for exercise-induced mitophagy in muscle: impact of aging. *Am J Physiol Endocrinol Metab* **315,** E404–E415.

Chen CCW, Erlich AT & Hood DA (2018*b*). Role of Parkin and endurance training on mitochondrial turnover in skeletal muscle. *Skelet Muscle*; DOI: 10.1186/S13395-018-0157-Y.

Chen H, Chomyn A & Chan DC (2005). Disruption of fusion results in mitochondrial heterogeneity and dysfunction. *J Biol Chem* **280,** 26185–26192.

Chen H, Vermulst M, Wang YE, Chomyn A, Prolla TA, McCaffery JM & Chan DC (2010). Mitochondrial fusion is required for mtDNA stability in skeletal muscle and tolerance of mtDNA mutations. *Cell* **141,** 280–289.

Chen ZP, McConell GK, Michell BJ, Snow RJ, Canny BJ & Kemp BE (2000). AMPK signaling in contracting human skeletal muscle: acetyl-CoA carboxylase and NO synthase phosphorylation. *Am J Physiol Endocrinol Metab*; DOI: 10.1152/AJPENDO.2000.279.5.E1202.

Chi MMY, Hintz CS, Coyle EF, Martin WH, Ivy JL, Nemeth PM, Holloszy JO & Lowry OH (1983). Effects of detraining on enzymes of energy metabolism in individual human muscle fibers. *Am J Physiol*; DOI: 10.1152/AJPCELL.1983.244.3.C276.

Chin ER (2004). The role of calcium and calcium/calmodulin-dependent kinases in skeletal muscle plasticity and mitochondrial biogenesis. *Proc Nutr Soc* **63,** 279–286.

Chin ER (2010). Intracellular Ca2+ signaling in skeletal muscle: decoding a complex message. *Exerc Sport Sci Rev* **38,** 76–85.

Chung S et al. (2018). Commentaries on Viewpoint: Principles, insights, and potential pitfalls of the noninvasive determination of muscle oxidative capacity by near-infrared spectroscopy. *J Appl Physiol* **124,** 254–255.

Clanton TL, Hogan MC & Gladden LB (2013). Regulation of cellular gas exchange, oxygen sensing, and metabolic control. *Compr Physiol* **3,** 1135–1190.

Clark SA, Chen ZP, Murphy KT, Aughey RJ, McKenna MJ, Kemp BE & Hawley JA (2004). Intensified exercise training does not alter AMPK signaling in human skeletal muscle. *Am J Physiol Endocrinol Metab*; DOI: 10.1152/AJPENDO.00462.2003.

Clayton DA (2000). Transcription and replication of mitochondrial DNA. *Hum Reprod* **15 Suppl 2,** 11–17.

Cochran AJR, Percival ME, Tricarico S, Little JP, Cermak N, Gillen JB, Tarnopolsky MA & Gibala MJ (2014). Intermittent and continuous high-intensity exercise training induce similar acute but different chronic muscle adaptations. *Exp Physiol* **99,** 782–791.

Coffey VG & Hawley JA (2007). The molecular bases of training adaptation. *Sports Med* **37,** 737–763.

Cogliati S, Frezza C, Soriano ME, Varanita T, Quintana-Cabrera R, Corrado M, Cipolat S, Costa V, Casarin A, Gomes LC, Perales-Clemente E, Salviati L, Fernandez-Silva P, Enriquez JA & Scorrano L (2013). Mitochondrial cristae shape determines respiratory chain supercomplexes assembly and respiratory efficiency. *Cell* **155,** 160–171.

Cogswell AM, Stevens RJ & Hood DA (1993). Properties of skeletal muscle mitochondria isolated from subsarcolemmal and intermyofibrillar regions. *Am J Physiol*; DOI: 10.1152/AJPCELL.1993.264.2.C383.

Combes A, Dekerle J, Webborn N, Watt P, Bougault V & Daussin FN (2015). Exercise-induced metabolic fluctuations influence AMPK, p38-MAPK and CaMKII phosphorylation in human skeletal muscle. *Physiol Rep*; DOI: 10.14814/PHY2.12462.

Costill D, Fink W, Hargreaves M, King D, Thomas R & Fielding R (1985). Metabolic characteristics of skeletal muscle during detraining from competitive swimming - PubMed. *Med Sci Sport Exerc*339–343.

Coyle EF, Hemmert MK & Coggan AR (1986). Effects of detraining on cardiovascular responses to exercise: role of blood volume. *J Appl Physiol* **60,** 95–99.

Coyle EF, Martin WH, Bloomfield SA, Lowry OH & Holloszy JO (1985). Effects of detraining on responses to submaximal exercise. *J Appl Physiol* **59,** 853–859.

Coyle EF, Martin WH, Sinacore DR, Joyner MJ, Hagberg JM & Holloszy JO (1984). Time course of loss of adaptations after stopping prolonged intense endurance training. *J Appl Physiol* **57,** 1857–1864.

Cribbs JT & Strack S (2007). Reversible phosphorylation of Drp1 by cyclic AMP-dependent protein kinase and calcineurin regulates mitochondrial fission and cell death. *EMBO Rep* **8,** 939–944.

Crow MT & Kushmerick MJ (1982). Chemical energetics of slow- and fast-twitch muscles of the mouse. *J Gen Physiol* **79,** 147–166.

Cullinane E, Sady S, Vadeboncoeur L, Burke M & Thompson P (1986). Cardiac size and VO2max do not decrease after short-term exercise cessation - PubMed. *Med Sci Sport Exerc*420–424.

Daussin FN, Ponsot E, Dufour SP, Lonsdorfer-Wolf E, Doutreleau S, Geny B, Piquard F & Richard R (2007). Improvement of VO2max by cardiac output and oxygen extraction adaptation during intermittent versus continuous endurance training. *Eur J Appl Physiol* **101,** 377–383.

Daussin FN, Zoll J, Ponsot E, Dufour SP, Doutreleau S, Lonsdorfer E, Ventura-Clapier R, Mettauer B, Piquard F, Geny B & Richard R (2008). Training at high exercise intensity promotes qualitative adaptations of mitochondrial function in human skeletal muscle. *J Appl Physiol* **104,** 1436–1441.

Denham J, Marques FZ, Bruns EL, O'Brien BJ & Charchar FJ (2016). Epigenetic changes in leukocytes after 8 weeks of resistance exercise training. *Eur J Appl Physiol* **116,** 1245–1253.

Dimauro I, Scalabrin M, Fantini C, Grazioli E, Beltran Valls MR, Mercatelli N, Parisi A, Sabatini S, Di Luigi L & Caporossi D (2016). Resistance training and redox homeostasis: Correlation with age-associated genomic changes. *Redox Biol* **10,** 34–44.

Doerrier C, Garcia-Souza LF, Krumschnabel G, Wohlfarter Y, Mészáros AT & Gnaiger E (2018). High-Resolution FluoRespirometry and OXPHOS Protocols for Human Cells, Permeabilized Fibers from Small Biopsies of Muscle, and Isolated Mitochondria. *Methods Mol Biol* **1782,** 31–70.

Dominy JE, Lee Y, Gerhart-Hines Z & Puigserver P (2010). Nutrient-dependent regulation of PGC-1alpha's acetylation state and metabolic function through the enzymatic activities of Sirt1/GCN5. *Biochim Biophys Acta* **1804,** 1676–1683.

Drinkwater BL & Horvath SM (1972). Detraining effects on young women. *Med Sci Sports* **4,** 91–95.

Du P, Zhang X, Huang CC, Jafari N, Kibbe WA, Hou L & Lin SM (2010). Comparison of Beta-value and M-value methods for quantifying methylation levels by microarray analysis. *BMC Bioinformatics*; DOI: 10.1186/1471-2105-11-587.

Duan G & Walther D (2015). The roles of post-translational modifications in the context of protein interaction networks. *PLoS Comput Biol*; DOI: 10.1371/JOURNAL.PCBI.1004049.

Dunn SE, Burns JL & Michel RN (1999). Calcineurin is required for skeletal muscle hypertrophy. *J Biol Chem* **274,** 21908–21912.

Eberharter A & Becker PB (2002). Histone acetylation: a switch between repressive and permissive chromatin. Second in review series on chromatin dynamics. *EMBO Rep* **3,** 224–229.

Eden S & Cedar H (1994). Role of DNA methylation in the regulation of transcription. *Curr Opin Genet Dev* **4,** 255–259.

Eftestøl E, Psilander N, Cumming KT, Juvkam I, Ekblom M, Sunding K, Wernbom M, Holmberg HC, Ekblom B, Bruusgaard JC, Raastad T & Gundersen K (2020). Muscle memory: are myonuclei ever lost? *https://doi.org/101152/japplphysiol007612019* **128,** 456–457.

Egan B, Carson BP, Garcia-Roves PM, Chibalin A V., Sarsfield FM, Barron N, McCaffrey N, Moyna NM, Zierath JR & O'Gorman DJ (2010). Exercise intensity-dependent regulation of peroxisome

proliferator-activated receptor coactivator-1 mRNA abundance is associated with differential activation of upstream signalling kinases in human skeletal muscle. *J Physiol* **588,** 1779–1790.

Egan B, Dowling P, O'Connor PL, Henry M, Meleady P, Zierath JR & O'Gorman DJ (2011*a*). 2-D DIGE analysis of the mitochondrial proteome from human skeletal muscle reveals time course-dependent remodelling in response to 14 consecutive days of endurance exercise training. *Proteomics* **11,** 1413–1428.

Egan B & Zierath JR (2013). Exercise metabolism and the molecular regulation of skeletal muscle adaptation. *Cell Metab* **17,** 162–184.

Egan DF, Shackelford DB, Mihaylova MM, Gelino S, Kohnz RA, Mair W, Vasquez DS, Joshi A, Gwinn DM, Taylor R, Asara JM, Fitzpatrick J, Dillin A, Viollet B, Kundu M, Hansen M & Shaw RJ (2011*b*). Phosphorylation of ULK1 (hATG1) by AMP-activated protein kinase connects energy sensing to mitophagy. *Science* **331,** 456–461.

Egner IM, Bruusgaard JC, Eftestøl E & Gundersen K (2013). A cellular memory mechanism aids overload hypertrophy in muscle long after an episodic exposure to anabolic steroids. *J Physiol* **591,** 6221–6230.

Erickson ML, Ryan TE, Young HJ & McCully KK (2013). Near-infrared assessments of skeletal muscle oxidative capacity in persons with spinal cord injury. *Eur J Appl Physiol* **113,** 2275–2283.

Erickson ML, Seigler N, Mckie KT, Mccully KK & Harris RA (2015). Skeletal muscle oxidative capacity in patients with cystic fibrosis. *Exp Physiol* **100,** 545–552.

Erlich AT, Brownlee DM, Beyfuss K & Hood DA (2018). Exercise induces TFEB expression and activity in skeletal muscle in a PGC-1α-dependent manner. *Am J Physiol Cell Physiol* **314,** C62–C72.

Federspiel WJ & Popel AS (1986). A theoretical analysis of the effect of the particulate nature of blood on oxygen release in capillaries. *Microvasc Res* **32,** 164–189.

Ferrari M, Mottola L & Quaresima V (2004). Principles, techniques, and limitations of near infrared spectroscopy. *Can J Appl Physiol* **29,** 463–487.

Ferreira R, Vitorino R, Alves RMP, Appell HJ, Powers SK, Duarte JA & Amado F (2010). Subsarcolemmal and intermyofibrillar mitochondria proteome differences disclose functional specializations in skeletal muscle. *Proteomics* **10,** 3142–3154.

Flück M & Hoppeler H (2003). Molecular basis of skeletal muscle plasticity--from gene to form and function. *Rev Physiol Biochem Pharmacol* **146,** 159–216.

Formenti F et al. (2010). Regulation of human metabolism by hypoxia-inducible factor. *Proc Natl Acad Sci U S A* **107,** 12722–12727.

Frank M, Duvezin-Caubet S, Koob S, Occhipinti A, Jagasia R, Petcherski A, Ruonala MO, Priault M, Salin B & Reichert AS (2012). Mitophagy is triggered by mild oxidative stress in a mitochondrial fission dependent manner. *Biochim Biophys Acta* **1823,** 2297–2310.

Freyssenet D, Irrcher I, Connor MK, Di Carlo M & Hood DA (2004). Calcium-regulated changes in mitochondrial phenotype in skeletal muscle cells. *Am J Physiol Cell Physiol*; DOI: 10.1152/AJPCELL.00418.2003.

Fulco M, Cen Y, Zhao P, Hoffman EP, McBurney MW, Sauve AA & Sartorelli V (2008). Glucose restriction inhibits skeletal myoblast differentiation by activating SIRT1 through AMPK-mediated regulation of Nampt. *Dev Cell* **14,** 661–673.

Gaitanos GC, Williams C, Boobis LH & Brooks S (1993). Human muscle metabolism during intermittent maximal exercise. *J Appl Physiol* **75,** 712–719.

Gan Z, Fu T, Kelly DP & Vega RB (2018). Skeletal muscle mitochondrial remodeling in exercise and diseases. *Cell Res* **28,** 969–980.

Gauthier GF & Padykula HA (1966). Cytological studies of fiber types in skeletal muscle. A comparative study of the mammalian diaphragm. *J Cell Biol* **28,** 333–354.

Gavin TP, Drew JL, Kubik CJ, Pofahl WE & Hickner RC (2007). Acute resistance exercise increases skeletal muscle angiogenic growth factor expression. *Acta Physiol (Oxf)* **191,** 139–146.

Geisler S, Holmström KM, Skujat D, Fiesel FC, Rothfuss OC, Kahle PJ & Springer W (2010). PINK1/Parkin-mediated mitophagy is dependent on VDAC1 and p62/SQSTM1. *Nat Cell Biol* **12,** 119–131.

Gerhart-Hines Z, Rodgers JT, Bare O, Lerin C, Kim SH, Mostoslavsky R, Alt FW, Wu Z & Puigserver P (2007). Metabolic control of muscle mitochondrial function and fatty acid oxidation through SIRT1/PGC-1alpha. *EMBO J* **26,** 1913–1923.

Gibala MJ, Bostad W & McCarthy DG (2019). Physiological adaptations to interval training to promote endurance. *Curr Opin Physiol* **10,** 180–184.

Gibala MJ, Gillen JB & Percival ME (2014). Physiological and health-related adaptations to low-volume interval training: influences of nutrition and sex. *Sports Med* **44 Suppl 2,** 127–137.

Gibala MJ & Jones AM (2013). Physiological and performance adaptations to high-intensity interval training. *Nestle Nutr Inst Workshop Ser* **76,** 51–60.

Gibala MJ, Little JP, van Essen M, Wilkin GP, Burgomaster KA, Safdar A, Raha S & Tarnopolsky MA (2006). Short-term sprint interval versus traditional endurance training: Similar initial adaptations in human skeletal muscle and exercise performance. *J Physiol* **575,** 901–911.

Gibala MJ, MacLean DA, Graham TE & Saltin B (1998). Tricarboxylic acid cycle intermediate pool size and estimated cycle flux in human muscle during exercise. *Am J Physiol*; DOI:

10.1152/AJPENDO.1998.275.2.E235.

Gibala MJ, McGee SL, Garnham AP, Howlett KF, Snow RJ & Hargreaves M (2009). Brief intense interval exercise activates AMPK and p38 MAPK signaling and increases the expression of PGC-1α in human skeletal muscle. *J Appl Physiol* **106,** 929–934.

Gifford CA et al. (2013). Transcriptional and epigenetic dynamics during specification of human embryonic stem cells. *Cell* **153,** 1149–1163.

Del Giudice M, Bonafiglia JT, Islam H, Preobrazenski N, Amato A & Gurd BJ (2020). Investigating the reproducibility of maximal oxygen uptake responses to high-intensity interval training. *J Sci Med Sport* **23,** 94–99.

Glancy B, Hartnell LM, Combs CA, Femnou A, Sun J, Murphy E, Subramaniam S & Balaban RS (2018). Power Grid Protection of the Muscle Mitochondrial Reticulum. *Cell Rep* **23,** 2832.

Glancy B, Hartnell LM, Malide D, Yu ZX, Combs CA, Connelly PS, Subramaniam S & Balaban RS (2015). Mitochondrial reticulum for cellular energy distribution in muscle. *Nature* **523,** 617–620.

Glancy B, Hsu LY, Dao L, Bakalar M, French S, Chess DJ, Taylor JL, Picard M, Aponte A, Daniels MP, Esfahani S, Cushman S & Balaban RS (2014). In vivo microscopy reveals extensive embedding of capillaries within the sarcolemma of skeletal muscle fibers. *Microcirculation* **21,** 131–147.

Gleyzer N, Vercauteren K & Scarpulla RC (2005). Control of mitochondrial transcription specificity factors (TFB1M and TFB2M) by nuclear respiratory factors (NRF-1 and NRF-2) and PGC-1 family coactivators. *Mol Cell Biol* **25,** 1354–1366.

Gnaiger E (2009). Capacity of oxidative phosphorylation in human skeletal muscle New perspectives of mitochondrial physiology. *Int J Biochem Cell Biol* **41,** 1837–1845.

Goffart S & Wiesner RJ (2003). Regulation and co-ordination of nuclear gene expression during mitochondrial biogenesis. *Exp Physiol* **88,** 33–40.

Gollnick PD, Karlsson J, Piehl K & Saltin B (1974). Selective glycogen depletion in skeletal muscle fibres of man following sustained contractions. *J Physiol* **241,** 59–67.

Gomes LC, Benedetto G Di & Scorrano L (2011). During autophagy mitochondria elongate, are spared from degradation and sustain cell viability. *Nat Cell Biol* **13,** 589–598.

Gouspillou G, Godin R, Piquereau J, Picard M, Mofarrahi M, Mathew J, Purves-Smith FM, Sgarioto N, Hepple RT, Burelle Y & Hussain SNA (2018). Protective role of Parkin in skeletal muscle contractile and mitochondrial function. *J Physiol* **596,** 2565–2579.

Granata C, Jamnick NA & Bishop DJ (2018). Training-Induced Changes in Mitochondrial Content and Respiratory Function in Human Skeletal Muscle. *Sport Med* **48,** 1809–1828.

Granata C, Oliveira RSF, Little JP & Bishop DJ (2020). Forty high-intensity interval training sessions blunt exercise-induced changes in the nuclear protein content of PGC-1α and p53 in human skeletal muscle. *Am J Physiol - Endocrinol Metab* **318,** E224–E236.

Granata C, Oliveira RSF, Little JP, Renner K & Bishop DJ (2016*a*). Mitochondrial adaptations to high-volume exercise training are rapidly reversed after a reduction in training volume in human skeletal muscle. *FASEB J* **30,** 3413–3423.

Granata C, Oliveira RSF, Little JP, Renner K & Bishop DJ (2016*b*). Training intensity modulates changes in PGC-1α and p53 protein content and mitochondrial respiration, but not markers of mitochondrial content in human skeletal muscle. *FASEB J* **30,** 959–970.

Grassi B, Porcelli S & Marzorati M (2019). Translational Medicine: Exercise Physiology Applied to Metabolic Myopathies. *Med Sci Sports Exerc* **51,** 2183–2192.

Grassi B, Porcelli S & Marzorati M (2020). Metabolic Myopathies: "Human Knockout" Models and Translational Medicine. *Front Physiol*; DOI: 10.3389/FPHYS.2020.00350/PDF.

Grassi B & Quaresima V (2016). Near-infrared spectroscopy and skeletal muscle oxidative function in vivo in health and disease: a review from an exercise physiology perspective. *J Biomed Opt* **21,** 091313.

Green HJ, Helyar R, Ball-Burnett M, Kowalchuk N, Symon S & Farrance B (1992). Metabolic adaptations to training precede changes in muscle mitochondrial capacity. *J Appl Physiol* **72,** 484–491.

Greggio C, Jha P, Kulkarni SS, Lagarrigue S, Broskey NT, Boutant M, Wang X, Conde Alonso S, Ofori E, Auwerx J, Cantó C & Amati F (2017). Enhanced Respiratory Chain Supercomplex Formation in Response to Exercise in Human Skeletal Muscle. *Cell Metab* **25,** 301–311.

Groebe K & Thews G (1986). Theoretical analysis of oxygen supply to contracted skeletal muscle. *Adv Exp Med Biol* **200,** 495–514.

Groebe K & Thews G (1990). Calculated intra- and extracellular PO2 gradients in heavily working red muscle. *Am J Physiol*; DOI: 10.1152/AJPHEART.1990.259.1.H84.

Gundersen K (2016). Muscle memory and a new cellular model for muscle atrophy and hypertrophy. *J Exp Biol* **219,** 235–242.

Gurd BJ (2011). Deacetylation of PGC-1α by SIRT1: importance for skeletal muscle function and exercise-induced mitochondrial biogenesis. *Appl Physiol Nutr Metab* **36,** 589–597.

Hamaoka T, Iwane H, Shimomitsu T, Katsumura T, Murase N, Nishio S, Osada T, Kurosawa Y & Chance B (1996). Noninvasive measures of oxidative metabolism on working human muscles by near-infrared spectroscopy. *J Appl Physiol* **81,** 1410–1417.

Hamaoka T & McCully KK (2019). Review of early development of near-infrared spectroscopy and

recent advancement of studies on muscle oxygenation and oxidative metabolism. *J Physiol Sci* **69,** 799–811.

Handschin C, Rhee J, Lin J, Tarr PT & Spiegelman BM (2003). An autoregulatory loop controls peroxisome proliferator-activated receptor gamma coactivator 1alpha expression in muscle. *Proc Natl Acad Sci U S A* **100,** 7111–7116.

Hanneman SK (2008). Design, analysis, and interpretation of method-comparison studies. *AACN Adv Crit Care* **19,** 223–234.

Hardie DG (2007). AMP-activated/SNF1 protein kinases: conserved guardians of cellular energy. *Nat Rev Mol Cell Biol* **8,** 774–785.

Hardie DG & Sakamoto K (2006). AMPK: a key sensor of fuel and energy status in skeletal muscle. *Physiology (Bethesda)* **21,** 48–60.

Harp MA, McCully KK, Moldavskiy M & Backus D (2016). Skeletal muscle mitochondrial capacity in people with multiple sclerosis. *Mult Scler J - Exp Transl Clin*; DOI: 10.1177/2055217316678020.

Haseler LJ, Hogan MC & Richardson RS (1999). Skeletal muscle phosphocreatine recovery in exercise-trained humans is dependent on O2 availability. *J Appl Physiol* **86,** 2013–2018.

Haseler LJ, Lin AP & Richardson RS (2004). Skeletal muscle oxidative metabolism in sedentary humans: 31P-MRS assessment of O2 supply and demand limitations. *J Appl Physiol* **97,** 1077–1081.

Hawley J & Burke L (1998). *Peak performance : training and nutritional strategies for sport*.

Hawley JA (2002). Adaptations of skeletal muscle to prolonged, intense endurance training. *Clin Exp Pharmacol Physiol* **29,** 218–222.

Hawley JA, Hargreaves M, Joyner MJ & Zierath JR (2014). Integrative biology of exercise. *Cell* **159,** 738–749.

Hawley JA & Zierath JR (2004). Integration of metabolic and mitogenic signal transduction in skeletal muscle. *Exerc Sport Sci Rev* **32,** 4–8.

Hellsten Y, Nyberg M, Jensen LG & Mortensen SP (2012). Vasodilator interactions in skeletal muscle blood flow regulation. *J Physiol* **590,** 6297–6305.

Henneman E (1957). Relation between size of neurons and their susceptibility to discharge. *Science* **126,** 1345–1347.

Henríquez-Olguín C, Renani LB, Arab-Ceschia L, Raun SH, Bhatia A, Li Z, Knudsen JR, Holmdahl R & Jensen TE (2019). Adaptations to high-intensity interval training in skeletal muscle require NADPH oxidase 2. *Redox Biol*; DOI: 10.1016/J.REDOX.2019.101188.

Henze K & Martin W (2003). Essence of mitochondria. *Nature* **426,** 127–128.

Hepple RT, Hogan MC, Stary C, Bebout DE, Mathieu-Costello O & Wagner PD (2000). Structural basis of muscle O(2) diffusing capacity: evidence from muscle function in situ. *J Appl Physiol* **88,** 560–566.

Heusch P, Canton M, Aker S, Van De Sand A, Konietzka I, Rassaf T, Menazza S, Brodde OE, Di Lisa F, Heusch G & Schulz R (2010). The contribution of reactive oxygen species and p38 mitogen-activated protein kinase to myofilament oxidation and progression of heart failure in rabbits. *Br J Pharmacol* **160,** 1408–1416.

Hirschey MD et al. (2010). SIRT3 regulates mitochondrial fatty-acid oxidation by reversible enzyme deacetylation. *Nature* **464,** 121–125.

Holloszy JO (1967*a*). Biochemical adaptations in muscle. Effects of exercise on mitochondrial oxygen uptake and respiratory enzyme activity in skeletal muscle. *J Biol Chem* **242,** 2278–2282.

Holloszy JO (1967*b*). Biochemical Adaptations in Muscle: Effects of exercise on mitochondrial oxygen uptake and respiratory enzyme activity in skeletal muscle. *J Biol Chem* **242,** 2278–2282.

Holloszy JO & Coyle EF (1984). Adaptations of skeletal muscle to endurance exercise and their metabolic consequences. *J Appl Physiol* **56,** 831–838.

Holloszy JO, Rennie MJ, Hickson RC, Conlee RK & Hagberg JM (1977). Physiological consequences of the biochemical adaptations to endurance exercise. *Ann N Y Acad Sci* **301,** 440–450.

Holmes BF, Kurth-Kraczek EJ & Winder WW (1999). Chronic activation of 5'-AMP-activated protein kinase increases GLUT-4, hexokinase, and glycogen in muscle. *J Appl Physiol* **87,** 1990–1995.

Honig CR, Gayeski TE, Federspiel W, Clark A & Clark P (1984). Muscle O2 gradients from hemoglobin to cytochrome: new concepts, new complexities. *Adv Exp Med Biol* **169,** 23–38.

Hood DA (2001). Invited Review: contractile activity-induced mitochondrial biogenesis in skeletal muscle. *J Appl Physiol* **90,** 1137–1157.

Hood DA, Irrcher I, Ljubicic V & Joseph AM (2006). Coordination of metabolic plasticity in skeletal muscle. *J Exp Biol* **209,** 2265–2275.

Hood DA, Memme JM, Oliveira AN & Triolo M (2019). Maintenance of Skeletal Muscle Mitochondria in Health, Exercise, and Aging. *Annu Rev Physiol* **81,** 19–41.

Hood DA, Uguccioni G, Vainshtein A & D'souza D (2011*a*). Mechanisms of exercise-induced mitochondrial biogenesis in skeletal muscle: implications for health and disease. *Compr Physiol* **1,** 1119–1134.

Hood MS, Little JP, Tarnopolsky MA, Myslik F & Gibala MJ (2011*b*). Low-volume interval training improves muscle oxidative capacity in sedentary adults. *Med Sci Sports Exerc* **43,** 1849–1856.

Hoppeler H (1986). Exercise-induced ultrastructural changes in skeletal muscle. *Int J Sports Med* **7,** 187–204.

Hoppeler H, Baum O, Lurman G & Mueller M (2011). Molecular mechanisms of muscle plasticity with exercise. *Compr Physiol* **1,** 1383–1412.

Hoppeler H, Howald H, Conley K, Lindstedt SL, Claassen H, Vock P & Weibel ER (1985). Endurance training in humans: aerobic capacity and structure of skeletal muscle. *J Appl Physiol* **59,** 320–327.

Hoppeler H, Lüthi P, Claassen H, Weibel ER & Howald H (1973). The ultrastructure of the normal human skeletal muscle. A morphometric analysis on untrained men, women and well-trained orienteers. *Pflugers Arch* **344,** 217–232.

Hoppeler H, Mathieu O, Weibel ER, Krauer R, Lindstedt SL & Taylor CR (1981). Design of the mammalian respiratory system. VIII Capillaries in skeletal muscles. *Respir Physiol* **44,** 129–150.

Houmard JA, Hortobagyi T, Johns RA, Bruno NJ, Nute CC, Shinebarger MH & Welborn J (1992). Effect of short-term training cessation on performance measures in distance runners. *Int J Sports Med* **13,** 572–576.

Houmard JA, Tyndall GL, Midyette JB, Hickey MS, Dolan PL, Gavigan KE, Weidner ML & Dohm GL (1996). Effect of reduced training and training cessation on insulin action and muscle GLUT-4. *J Appl Physiol* **81,** 1162–1168.

Houston ME, Bentzen H & Larsen H (1979). Interrelationships between skeletal muscle adaptations and performance as studied by detraining and retraining. *Acta Physiol Scand* **105,** 163–170.

Howald H, Hoppeler H, Claassen H, Mathieu O & Straub R (1985). Influences of endurance training on the ultrastructural composition of the different muscle fiber types in humans. *Pflugers Arch* **403,** 369–376.

Howlett RA, Parolin ML, Dyck DJ, Hultman E, Jones NL, Heigenhauser GJF & Spriet LL (1998). Regulation of skeletal muscle glycogen phosphorylase and PDH at varying exercise power outputs. *Am J Physiol*; DOI: 10.1152/AJPREGU.1998.275.2.R418.

Hughson RL (2009). Oxygen uptake kinetics: historical perspective and future directions. *Appl Physiol Nutr Metab* **34,** 840–850.

Hunt JEA, Galea D, Tufft G, Bunce D & Ferguson RA (2013). Time course of regional vascular adaptations to low load resistance training with blood flow restriction. *J Appl Physiol* **115,** 403–411.

Hüttemann M, Lee I & Malek MH (2012). (-)-Epicatechin maintains endurance training adaptation in mice after 14 days of detraining. *FASEB J* **26,** 1413–1422.

Ingalls CP (2004). Nature vs. nurture: can exercise really alter fiber type composition in human skeletal muscle? *J Appl Physiol* **97,** 1591–1592.

Irizarry RA, Ladd-Acosta C, Wen B, Wu Z, Montano C, Onyango P, Cui H, Gabo K, Rongione M, Webster M, Ji H, Potash JB, Sabunciyan S & Feinberg AP (2009). The human colon cancer methylome shows similar hypo- and hypermethylation at conserved tissue-specific CpG island shores. *Nat Genet* **41,** 178–186.

Irrcher I, Adhihetty PJ, Joseph AM, Ljubicic V & Hood DA (2003). Regulation of mitochondrial biogenesis in muscle by endurance exercise. *Sport Med* **33,** 783–793.

Islam H, Bonafiglia JT, Del Giudice M, Pathmarajan R, Simpson CA, Quadrilatero J & Gurd BJ (2021). Repeatability of training-induced skeletal muscle adaptations in active young males. *J Sci Med Sport* **24,** 494–498.

Ito S, Dalessio AC, Taranova O V., Hong K, Sowers LC & Zhang Y (2010). Role of Tet proteins in 5mC to 5hmC conversion, ES-cell self-renewal and inner cell mass specification. *Nature* **466,** 1129–1133.

Izquierdo M, Ibáñez J, Häkkinen K, Kraemer WJ, Ruesta M & Gorostiaga EM (2004). Maximal strength and power, muscle mass, endurance and serum hormones in weightlifters and road cyclists. *J Sports Sci* **22,** 465–478.

Jacobs RA, Flück D, Bonne TC, Bürgi S, Christensen PM, Toigo M & Lundby C (2013). Improvements in exercise performance with high-intensity interval training coincide with an increase in skeletal muscle mitochondrial content and function. *J Appl Physiol* **115,** 785–793.

Jacobs RA & Lundby C (2013). Mitochondria express enhanced quality as well as quantity in association with aerobic fitness across recreationally active individuals up to elite athletes. *J Appl Physiol* **114,** 344–350.

Jin C, Li M, Ouyang Y, Tan Z & Jiang Y (2017). MiR-424 functions as a tumor suppressor in glioma cells and is down-regulated by DNA methylation. *J Neurooncol* **133,** 247–255.

Joffe M, Savage N & Isaacs H (1983). Respiratory activities of subsarcolemmal and intermyofibrillar mitochondrial populations isolated from denervated and control rat soleus muscles. *Comp Biochem Physiol B* **76,** 783–787.

Jones PL, Veenstra GJC, Wade PA, Vermaak D, Kass SU, Landsberger N, Strouboulis J & Wolffe AP (1998). Methylated DNA and MeCP2 recruit histone deacetylase to repress transcription. *Nat Genet* **19,** 187–191.

Jornayvaz FR & Shulman GI (2010). Regulation of mitochondrial biogenesis. *Essays Biochem* **47,** 69–84.

Joseph AM, Joanisse DR, Baillot RG & Hood DA (2012). Mitochondrial dysregulation in the

pathogenesis of diabetes: potential for mitochondrial biogenesis-mediated interventions. *Exp Diabetes Res*; DOI: 10.1155/2012/642038.

Ju J sun, Jeon S il, Park J young, Lee J young, Lee S cheol, Cho K jung & Jeong J moon (2016). Autophagy plays a role in skeletal muscle mitochondrial biogenesis in an endurance exercise-trained condition. *J Physiol Sci* **66,** 417–430.

Ju JS, Varadhachary AS, Miller SE & Weihl CC (2010). Quantitation of "autophagic flux" in mature skeletal muscle. *Autophagy* **6,** 929–935.

Kahn BB, Alquier T, Carling D & Hardie DG (2005). AMP-activated protein kinase: ancient energy gauge provides clues to modern understanding of metabolism. *Cell Metab* **1,** 15–25.

Kalliokoski KK, Oikonen V, Takala TO, Sipilä H, Knuuti J & Nuutila P (2001). Enhanced oxygen extraction and reduced flow heterogeneity in exercising muscle in endurance-trained men. *Am J Physiol Endocrinol Metab*; DOI: 10.1152/AJPENDO.2001.280.6.E1015.

Kanehisa M, Furumichi M, Tanabe M, Sato Y & Morishima K (2017). KEGG: new perspectives on genomes, pathways, diseases and drugs. *Nucleic Acids Res* **45,** D353–D361.

Kanehisa M & Goto S (2000). KEGG: kyoto encyclopedia of genes and genomes. *Nucleic Acids Res* **28,** 27–30.

Kanehisa M, Sato Y, Kawashima M, Furumichi M & Tanabe M (2016). KEGG as a reference resource for gene and protein annotation. *Nucleic Acids Res* **44,** D457–D462.

Kang C, Goodman CA, Hornberger TA & Ji LL (2015). PGC-1α overexpression by in vivo transfection attenuates mitochondrial deterioration of skeletal muscle caused by immobilization. *FASEB J* **29,** 4092–4106.

Kanki T, Ohgaki K, Gaspari M, Gustafsson CM, Fukuoh A, Sasaki N, Hamasaki N & Kang D (2004). Architectural role of mitochondrial transcription factor A in maintenance of human mitochondrial DNA. *Mol Cell Biol* **24,** 9823–9834.

Kemp GJ, Taylor DJ & Radda GK (1993). Control of phosphocreatine resynthesis during recovery from exercise in human skeletal muscle. *NMR Biomed* **6,** 66–72.

Kent JA & Fitzgerald LF (2016). In vivo mitochondrial function in aging skeletal muscle: capacity, flux, and patterns of use. *J Appl Physiol* **121,** 996–1003.

Kim Y & Hood DA (2017). Regulation of the autophagy system during chronic contractile activity-induced muscle adaptations. *Physiol Rep*; DOI: 10.14814/PHY2.13307.

Kim Y, Triolo M, Erlich AT & Hood DA (2019). Regulation of autophagic and mitophagic flux during chronic contractile activity-induced muscle adaptations. *Pflugers Arch* **471,** 431–440.

Klausen K, Andersen LB & Pelle I (1981). Adaptive changes in work capacity, skeletal muscle capillarization and enzyme levels during training and detraining. *Acta Physiol Scand* **113,** 9–16.

Klausen K, Secher NH, Clausen JP, Hartling O & Trap-Jensen J (1982). Central and regional circulatory adaptations to one-leg training. *J Appl Physiol* **52,** 976–983.

Koga S, Rossiter HB, Heinonen I, Musch TI & Poole DC (2014). Dynamic heterogeneity of exercising muscle blood flow and O2 utilization. *Med Sci Sports Exerc* **46,** 860–876.

Korshunov SS, Skulachev VP & Starkov AA (1997). High protonic potential actuates a mechanism of production of reactive oxygen species in mitochondria. *FEBS Lett* **416,** 15–18.

Koves TR, Noland RC, Bates AL, Henes ST, Muoio DM & Cortright RN (2005). Subsarcolemmal and intermyofibrillar mitochondria play distinct roles in regulating skeletal muscle fatty acid metabolism. *Am J Physiol Cell Physiol*; DOI: 10.1152/AJPCELL.00391.2004.

Krieger DA, Tate CA, McMillin-Wood J & Booth FW (1980). Populations of rat skeletal muscle mitochondria after exercise and immobilization. *J Appl Physiol* **48,** 23–28.

Krustrup P, Jones AM, Wilkerson DP, Calbet JAL & Bangsbo J (2009). Muscular and pulmonary O2 uptake kinetics during moderate- and high-intensity sub-maximal knee-extensor exercise in humans. *J Physiol* **587,** 1843–1856.

Kuznetsov A V., Kunz WS, Saks V, Usson Y, Mazat JP, Letellier T, Gellerich FN & Margreiter R (2003). Cryopreservation of mitochondria and mitochondrial function in cardiac and skeletal muscle fibers. *Anal Biochem* **319,** 296–303.

Kwa FAA & Jackson DE (2018). Manipulating the epigenome for the treatment of disorders with thrombotic complications. *Drug Discov Today* **23,** 719–726.

Labbé K, Murley A & Nunnari J (2014). Determinants and functions of mitochondrial behavior. *Annu Rev Cell Dev Biol* **30,** 357–391.

Lacour JR & Denis C (1984). Detraining Effects on Aerobic Capacity. *Med Sci Sports Exerc* **17,** 230–237.

Lagouge M, Argmann C, Gerhart-Hines Z, Meziane H, Lerin C, Daussin F, Messadeq N, Milne J, Lambert P, Elliott P, Geny B, Laakso M, Puigserver P & Auwerx J (2006). Resveratrol improves mitochondrial function and protects against metabolic disease by activating SIRT1 and PGC-1alpha. *Cell* **127,** 1109–1122.

Lamarra N, Whipp BJ, Ward SA & Wasserman K (1987). Effect of interbreath fluctuations on characterizing exercise gas exchange kinetics. *J Appl Physiol* **62,** 2003–2012.

Lan F, Cacicedo JM, Ruderman N & Ido Y (2008). SIRT1 modulation of the acetylation status, cytosolic localization, and activity of LKB1. Possible role in AMP-activated protein kinase activation. *J Biol Chem* **283,** 27628–27635.

Lapuente-Brun E, Moreno-Loshuertos R, Aciń-Pérez R, Latorre-Pellicer A, Colaś C, Balsa E, Perales-Clemente E, Quirós PM, Calvo E, Rodríguez-Hernández MA, Navas P, Cruz R,

Carracedo Á, Loṕez-Otín C, Peŕez-Martos A, Fernańdez-Silva P, Fernańdez-Vizarra E & Enríquez JA (2013). Supercomplex assembly determines electron flux in the mitochondrial electron transport chain. *Science* **340,** 1567–1570.

Layec G, Haseler LJ & Richardson RS (2013). Reduced muscle oxidative capacity is independent of O2 availability in elderly people. *Age (Dordr)* **35,** 1183–1192.

Lazzer S, Salvadego D, Porcelli S, Rejc E, Agosti F, Sartorio A & Grassi B (2013). Skeletal muscle oxygen uptake in obese patients: functional evaluation by knee-extension exercise. *Eur J Appl Physiol* **113,** 2125–2132.

Lee CH, Olson P & Evans RM (2003). Minireview: lipid metabolism, metabolic diseases, and peroxisome proliferator-activated receptors. *Endocrinology* **144,** 2201–2207.

Lee H, Kim K, Kim B, Shin J, Rajan S, Wu J, Chen X, Brown MD, Lee S & Park JY (2018). A cellular mechanism of muscle memory facilitates mitochondrial remodelling following resistance training. *J Physiol* **596,** 4413–4426.

Leick L, Fentz J, Biensø RS, Knudsen JG, Jeppesen J, Kiens B, Wojtaszewski JFP & Pilegaard H (2010). PGC-1{alpha} is required for AICAR-induced expression of GLUT4 and mitochondrial proteins in mouse skeletal muscle. *Am J Physiol Endocrinol Metab*; DOI: 10.1152/AJPENDO.00648.2009.

Lindholm ME, Giacomello S, Werne Solnestam B, Fischer H, Huss M, Kjellqvist S & Sundberg CJ (2016). The Impact of Endurance Training on Human Skeletal Muscle Memory, Global Isoform Expression and Novel Transcripts. *PLoS Genet*; DOI: 10.1371/JOURNAL.PGEN.1006294.

Lindholm ME, Marabita F, Gomez-Cabrero D, Rundqvist H, Ekström TJ, Tegnér J & Sundberg CJ (2014). An integrative analysis reveals coordinated reprogramming of the epigenome and the transcriptome in human skeletal muscle after training. *Epigenetics* **9,** 1557–1569.

Lira VA, Okutsu M, Zhang M, Greene NP, Laker RC, Breen DS, Hoehn KL & Yan Z (2013*a*). Autophagy is required for exercise training-induced skeletal muscle adaptation and improvement of physical performance. *FASEB J* **27,** 4184–4193.

Lira VA, Okutsu M, Zhang M, Greene NP, Laker RC, Breen DS, Hoehn KL & Yan Z (2013*b*). Autophagy is required for exercise training-induced skeletal muscle adaptation and improvement of physical performance. *FASEB J* **27,** 4184–4193.

Lister R, Pelizzola M, Dowen RH, Hawkins RD, Hon G, Tonti-Filippini J, Nery JR, Lee L, Ye Z, Ngo QM, Edsall L, Antosiewicz-Bourget J, Stewart R, Ruotti V, Millar AH, Thomson JA, Ren B & Ecker JR (2009). Human DNA methylomes at base resolution show widespread epigenomic differences. *Nature* **462,** 315–322.

Little JP, Gillen JB, Percival ME, Safdar A, Tarnopolsky MA, Punthakee Z, Jung ME & Gibala MJ

(2011*a*). Low-volume high-intensity interval training reduces hyperglycemia and increases muscle mitochondrial capacity in patients with type 2 diabetes. *J Appl Physiol* **111,** 1554–1560.

Little JP, Safdar A, Benton CR & Wright DC (2011*b*). Skeletal muscle and beyond: the role of exercise as a mediator of systemic mitochondrial biogenesis. *Appl Physiol Nutr Metab* **36,** 598–607.

Little JP, Safdar A, Wilkin GP, Tarnopolsky MA & Gibala MJ (2010). A practical model of low-volume high-intensity interval training induces mitochondrial biogenesis in human skeletal muscle: potential mechanisms. *J Physiol* **588,** 1011–1022.

Ljubicic V, Adhihetty PJ & Hood DA (2004). Role of UCP3 in state 4 respiration during contractile activity-induced mitochondrial biogenesis. *J Appl Physiol* **97,** 976–983.

Ljubicic V, Joseph AM, Adhihetty PJ, Huang JH, Saleem A, Uguccioni G & Hood DA (2009). Molecular basis for an attenuated mitochondrial adaptive plasticity in aged skeletal muscle. *Aging (Albany NY)* **1,** 818–830.

Ljubicic V, Joseph AM, Saleem A, Uguccioni G, Collu-Marchese M, Lai RYJ, Nguyen LMD & Hood DA (2010). Transcriptional and post-transcriptional regulation of mitochondrial biogenesis in skeletal muscle: Effects of exercise and aging. *Biochim Biophys Acta - Gen Subj* **1800,** 223–234.

Van Loon LJC, Greenhaff PL, Constantin-Teodosiu D, Saris WHM & Wagenmakers AJM (2001). The effects of increasing exercise intensity on muscle fuel utilisation in humans. *J Physiol* **536,** 295–304.

Losón OC, Song Z, Chen H & Chan DC (2013). Fis1, Mff, MiD49, and MiD51 mediate Drp1 recruitment in mitochondrial fission. *Mol Biol Cell* **24,** 659–667.

Lowell BB & Spiegelman BM (2000). Towards a molecular understanding of adaptive thermogenesis. *Nature* **404,** 652–660.

Lowry OH, Rosebrough NJ, Farr AL & Randall RJ (1951). Protein measurement with the Folin phenol reagent. *J Biol Chem* **193,** 265–275.

Lujambio A & Lowe SW (2012). The microcosmos of cancer. *Nature* **482,** 347–355.

Lundby C & Jacobs RA (2016*a*). Adaptations of skeletal muscle mitochondria to exercise training. *Exp Physiol* **101,** 17–22.

Lundby C & Jacobs RA (2016*b*). Adaptations of skeletal muscle mitochondria to exercise training. *Exp Physiol* **101,** 17–22.

Lundby C & Montero D (2015). CrossTalk opposing view: Diffusion limitation of O2 from microvessels into muscle does not contribute to the limitation of V̇O2 max. *J Physiol* **593,** 3759–3761.

Maasar MF, Turner DC, Gorski PP, Seaborne RA, Strauss JA, Shepherd SO, Cocks M, Pillon NJ, Zierath JR, Hulton AT, Drust B & Sharples AP (2021). The Comparative Methylome and Transcriptome After Change of Direction Compared to Straight Line Running Exercise in Human Skeletal Muscle. *Front Physiol*; DOI: 10.3389/FPHYS.2021.619447.

MacInnis MJ & Gibala MJ (2017). Physiological adaptations to interval training and the role of exercise intensity. *J Physiol* **595,** 2915–2930.

MacInnis MJ, Zacharewicz E, Martin BJ, Haikalis ME, Skelly LE, Tarnopolsky MA, Murphy RM & Gibala MJ (2017). Superior mitochondrial adaptations in human skeletal muscle after interval compared to continuous single-leg cycling matched for total work. *J Physiol* **595,** 2955–2968.

Madsen K, Pedersen PK, Djurhuus MS & Klitgaard NA (1993). Effects of detraining on endurance capacity and metabolic changes during prolonged exhaustive exercise. *J Appl Physiol* **75,** 1444–1451.

Mahler M (1985). First-order kinetics of muscle oxygen consumption, and an equivalent proportionality between QO2 and phosphorylcreatine level. Implications for the control of respiration. *J Gen Physiol* **86,** 135–165.

Mahoney DJ, Parise G, Melov S, Safdar A & Tarnopolsky MA (2005). Analysis of global mRNA expression in human skeletal muscle during recovery from endurance exercise. *FASEB J* **19,** 1498–1500.

Mairbäurl H (2013). Red blood cells in sports: effects of exercise and training on oxygen supply by red blood cells. *Front Physiol*; DOI: 10.3389/FPHYS.2013.00332.

Maksimovic J, Gordon L & Oshlack A (2012). SWAN: Subset-quantile within array normalization for illumina infinium HumanMethylation450 BeadChips. *Genome Biol*; DOI: 10.1186/GB-2012-13-6-R44.

Maksimovic J, Phipson B & Oshlack A (2017). A cross-package Bioconductor workflow for analysing methylation array data. *F1000Research*; DOI: 10.12688/F1000RESEARCH.8839.3/DOI.

Malek MH & Olfert IM (2009). Global deletion of thrombospondin-1 increases cardiac and skeletal muscle capillarity and exercise capacity in mice. *Exp Physiol* **94,** 749–760.

Malek MH, Olfert IM & Esposito F (2010). Detraining losses of skeletal muscle capillarization are associated with vascular endothelial growth factor protein expression in rats. *Exp Physiol* **95,** 359–368.

Martin WH, Coyle EF, Bloomfield SA & Ehsani AA (1986). Effects of physical deconditioning after intense endurance training on left ventricular dimensions and stroke volume. *J Am Coll Cardiol* **7,** 982–989.

Mason SD, Howlett RA, Kim MJ, Olfert IM, Hogan MC, McNulty W, Hickey RP, Wagner PD, Kahn CR, Giordano FJ & Johnson RS (2004). Loss of skeletal muscle HIF-1alpha results in altered exercise endurance. *PLoS Biol*; DOI: 10.1371/JOURNAL.PBIO.0020288.

Mathieu-Costello O, Ellis CG, Potter RF, MacDonald IC & Groom AC (1991). Muscle capillary-to-fiber perimeter ratio: morphometry. *Am J Physiol*; DOI: 10.1152/AJPHEART.1991.261.5.H1617.

Mathieu-Costello O, Potter RF, Ellis CG & Groom AC (1988). Capillary configuration and fiber shortening in muscles of the rat hindlimb: correlation between corrosion casts and stereological measurements. *Microvasc Res* **36,** 40–55.

Mathieu-Costello O, Suarez RK & Hochachka PW (1992). Capillary-to-fiber geometry and mitochondrial density in hummingbird flight muscle. *Respir Physiol* **89,** 113–132.

Matsuda N, Sato S, Shiba K, Okatsu K, Saisho K, Gautier CA, Sou YS, Saiki S, Kawajiri S, Sato F, Kimura M, Komatsu M, Hattori N & Tanaka K (2010). PINK1 stabilized by mitochondrial depolarization recruits Parkin to damaged mitochondria and activates latent Parkin for mitophagy. *J Cell Biol* **189,** 211–221.

McCoy M, Proietto J & Hargreaves M (1994). Effect of detraining on GLUT-4 protein in human skeletal muscle. *J Appl Physiol* **77,** 1532–1536.

McGee SL & Hargreaves M (2011). Histone modifications and exercise adaptations. *J Appl Physiol* **110,** 258–263.

McMullan RC, Ferris MT, Bell TA, Menachery VD, Baric RS, Hua K, Pomp D, Smith-Ryan AE & de Villena FPM (2018). CC002/Unc females are mouse models of exercise-induced paradoxical fat response. *Physiol Rep*; DOI: 10.14814/PHY2.13716.

Melser S, Chatelain EH, Lavie J, Mahfouf W, Jose C, Obre E, Goorden S, Priault M, Elgersma Y, Rezvani HR, Rossignol R & Bénard G (2013). Rheb regulates mitophagy induced by mitochondrial energetic status. *Cell Metab* **17,** 719–730.

Memme JM, Erlich AT, Phukan G & Hood DA (2021). Exercise and mitochondrial health. *J Physiol* **599,** 803–817.

Menshikova E V., Ritov VB, Toledo FGS, Ferrell RE, Goodpaster BH & Kelley DE (2005). Effects of weight loss and physical activity on skeletal muscle mitochondrial function in obesity. *Am J Physiol Endocrinol Metab*; DOI: 10.1152/AJPENDO.00322.2004.

Metcalfe RS, Koumanov F, Ruffino JS, Stokes KA, Holman GD, Thompson D & Vollaard NBJ (2015). Physiological and molecular responses to an acute bout of reduced-exertion high-intensity interval training (REHIT). *Eur J Appl Physiol* **115,** 2321–2334.

Meyer RA (1988). A linear model of muscle respiration explains monoexponential phosphocreatine

changes. *Am J Physiol*; DOI: 10.1152/AJPCELL.1988.254.4.C548.

Michel RN, Dunn SE & Chin ER (2004). Calcineurin and skeletal muscle growth. *Proc Nutr Soc* **63,** 341–349.

Mikines KJ, Sonne B, Tronier B & Galbo H (1989). Effects of acute exercise and detraining on insulin action in trained men. *J Appl Physiol* **66,** 704–711.

Milanović Z, Sporiš G & Weston M (2015). Effectiveness of High-Intensity Interval Training (HIT) and Continuous Endurance Training for VO2max Improvements: A Systematic Review and Meta-Analysis of Controlled Trials. *Sports Med* **45,** 1469–1481.

Minguez P, Parca L, Diella F, Mende DR, Kumar R, Helmer-Citterich M, Gavin AC, Van Noort V & Bork P (2012). Deciphering a global network of functionally associated post-translational modifications. *Mol Syst Biol*; DOI: 10.1038/MSB.2012.31.

Mishra P, Carelli V, Manfredi G & Chan DC (2014). Proteolytic cleavage of Opa1 stimulates mitochondrial inner membrane fusion and couples fusion to oxidative phosphorylation. *Cell Metab* **19,** 630–641.

Mishra P & Chan DC (2016). Metabolic regulation of mitochondrial dynamics. *J Cell Biol* **212,** 379–387.

Mitchell P (1961). Coupling of phosphorylation to electron and hydrogen transfer by a chemi-osmotic type of mechanism. *Nature* **191,** 144–148.

Mitchell P (1966). Chemiosmotic coupling in oxidative and photosynthetic phosphorylation. *Biol Rev Camb Philos Soc* **41,** 445–502.

Montero D, Cathomen A, Jacobs RA, Flück D, de Leur J, Keiser S, Bonne T, Kirk N, Lundby AK & Lundby C (2015*a*). Haematological rather than skeletal muscle adaptations contribute to the increase in peak oxygen uptake induced by moderate endurance training. *J Physiol* **593,** 4677–4688.

Montero D, Diaz-Cañestro C & Lundby C (2015*b*). Endurance Training and V˙O2max: Role of Maximal Cardiac Output and Oxygen Extraction. *Med Sci Sports Exerc* **47,** 2024–2033.

Montero D & Lundby C (2017). Refuting the myth of non-response to exercise training: "non-responders" do respond to higher dose of training. *J Physiol* **595,** 3377–3387.

Moore RL, Thacker EM, Kelley GA, Musch TI, Sinoway LI, Foster VL & Dickinson AL (1987). Effect of training/detraining on submaximal exercise responses in humans. *J Appl Physiol* **63,** 1719–1724.

Motobe M, Murase N, Osada T, Homma T, Ueda C, Nagasawa T, Kitahara A, Ichimura S, Kurosawa Y, Katsumura T, Hoshika A & Hamaoka T (2004). Noninvasive monitoring of deterioration in skeletal muscle function with forearm cast immobilization and the prevention of deterioration.

Dyn Med **3,** 1–11.

Mourier A, Motori E, Brandt T, Lagouge M, Atanassov I, Galinier A, Rappl G, Brodesser S, Hultenby K, Dieterich C & Larsson NG (2015). Mitofusin 2 is required to maintain mitochondrial coenzyme Q levels. *J Cell Biol* **208,** 429–442.

Mujika I & Padilla S (2000). Detraining: loss of training-induced physiological and performance adaptations. Part I: short term insufficient training stimulus. *Sports Med* **30,** 79–87.

Mujika I & Padilla S (2001). Cardiorespiratory and metabolic characteristics of detraining in humans. *Med Sci Sports Exerc* **33,** 413–421.

Müller W (1976). Subsarcolemmal mitochondria and capillarization of soleus muscle fibers in young rats subjected to an endurance training. *Cell Tissue Res 1976 1743* **174,** 367–389.

Murach KA, Dungan CM, Dupont-Versteegden EE, McCarthy JJ & Peterson CA (2019). "muscle memory" not mediated by myonuclear number? Secondary analysis of human detraining data. *J Appl Physiol* **127,** 1814–1816.

Murach KA, Mobley CB, Zdunek CJ, Frick KK, Jones SR, McCarthy JJ, Peterson CA & Dungan CM (2020). Muscle memory: myonuclear accretion, maintenance, morphology, and miRNA levels with training and detraining in adult mice. *J Cachexia Sarcopenia Muscle* **11,** 1705–1722.

Murias JM, Kowalchuk JM & Paterson DH (2010). Time course and mechanisms of adaptations in cardiorespiratory fitness with endurance training in older and young men. *J Appl Physiol* **108,** 621–627.

Musarò A, McCullagh KJA, Naya FJ, Olson EN & Rosenthal N (1999). IGF-1 induces skeletal myocyte hypertrophy through calcineurin in association with GATA-2 and NF-ATc1. *Nature* **400,** 581–585.

Narendra DP, Jin SM, Tanaka A, Suen DF, Gautier CA, Shen J, Cookson MR & Youle RJ (2010). PINK1 is selectively stabilized on impaired mitochondria to activate Parkin. *PLoS Biol*; DOI: 10.1371/JOURNAL.PBIO.1000298.

Naya FJ, Mercer B, Shelton J, Richardson JA, Williams RS & Olson EN (2000). Stimulation of slow skeletal muscle fiber gene expression by calcineurin in vivo. *J Biol Chem* **275,** 4545–4548.

Nemoto S, Fergusson MM & Finkel T (2005). SIRT1 functionally interacts with the metabolic regulator and transcriptional coactivator PGC-1{alpha}. *J Biol Chem* **280,** 16456–16460.

Neufer P, Costill D, Fielding R, Flynn M & Kirwan J (1987). Effect of reduced training on muscular strength and endurance in competitive swimmers - PubMed. *Med Sci Sports Exerc* **5,** 486–490.

Nielsen J, Gejl KD, Hey-Mogensen M, Holmberg HC, Suetta C, Krustrup P, Elemans CPH & Ørtenblad N (2017). Plasticity in mitochondrial cristae density allows metabolic capacity modulation in human skeletal muscle. *J Physiol* **595,** 2839–2847.

Nitert MD et al. (2012). Impact of an exercise intervention on DNA methylation in skeletal muscle from first-degree relatives of patients with type 2 diabetes. *Diabetes* **61,** 3322–3332.

Oberkofler H, Esterbauer H, Linnemayr V, Donny Strosberg A, Krempler F & Patsch W (2002). Peroxisome proliferator-activated receptor (PPAR) gamma coactivator-1 recruitment regulates PPAR subtype specificity. *J Biol Chem* **277,** 16750–16757.

Oliveira AN & Hood DA (2019). Exercise is mitochondrial medicine for muscle. *Sport Med Heal Sci* **1,** 11–18.

Orang AV, Safaralizadeh R & Kazemzadeh-Bavili M (2014). Mechanisms of miRNA-Mediated Gene Regulation from Common Downregulation to mRNA-Specific Upregulation. *Int J Genomics*; DOI: 10.1155/2014/970607.

Ørom UA, Nielsen FC & Lund AH (2008). MicroRNA-10a binds the 5'UTR of ribosomal protein mRNAs and enhances their translation. *Mol Cell* **30,** 460–471.

Paganini AT, Foley JM & Meyer RA (1997). Linear dependence of muscle phosphocreatine kinetics on oxidative capacity. *Am J Physiol*; DOI: 10.1152/AJPCELL.1997.272.2.C501.

Palmer JW, Tandler B & Hoppel CL (1977). Biochemical properties of subsarcolemmal and interfibrillar mitochondria isolated from rat cardiac muscle. *J Biol Chem* **252,** 8731–8739.

Palmer JW, Tandler B & Hoppel CL (1985). Biochemical differences between subsarcolemmal and interfibrillar mitochondria from rat cardiac muscle: effects of procedural manipulations. *Arch Biochem Biophys* **236,** 691–702.

Parsons SA, Milla DP, Wilkins BJ, Bueno OF, Tsika GL, Neilson JR, Liberatore CM, Yutzey KE, Crabtree GR, Tsika RW & Molkentin JD (2004). Genetic loss of calcineurin blocks mechanical overload-induced skeletal muscle fiber type switching but not hypertrophy. *J Biol Chem* **279,** 26192–26200.

Pavlik G, Bachl N, Wollein W, Lángfy G & Prokop L (1986). Resting echocardiographic parameters after cessation of regular endurance training. *Int J Sports Med* **7,** 226–231.

Pedersen BK & Febbraio MA (2012). Muscles, exercise and obesity: skeletal muscle as a secretory organ. *Nat Rev Endocrinol* **8,** 457–465.

Perry CGR, Kane DA, Lanza IR & Neufer PD (2013). Methods for assessing mitochondrial function in diabetes. *Diabetes* **62,** 1041–1053.

Perry CGR, Kane DA, Lin C Te, Kozy R, Cathey BL, Lark DS, Kane CL, Brophy PM, Gavin TP, Anderson EJ & Neufer PD (2011). Inhibiting myosin-ATPase reveals a dynamic range of mitochondrial respiratory control in skeletal muscle. *Biochem J* **437,** 215–222.

Perry CGR, Lally J, Holloway GP, Heigenhauser GJF, Bonen A & Spriet LL (2010*a*). Repeated transient mRNA bursts precede increases in transcriptional and mitochondrial proteins during

training in human skeletal muscle. *J Physiol* **588,** 4795–4810.

Perry CGR, Lally J, Holloway GP, Heigenhauser GJF, Bonen A & Spriet LL (2010*b*). Repeated transient mRNA bursts precede increases in transcriptional and mitochondrial proteins during training in human skeletal muscle. *J Physiol* **588,** 4795.

Perseghin G, Price TB, Petersen KF, Roden M, Cline GW, Gerow K, Rothman DL & Shulman GI (1996). Increased glucose transport-phosphorylation and muscle glycogen synthesis after exercise training in insulin-resistant subjects. *N Engl J Med* **335,** 1357–1362.

Pesta D & Gnaiger E (2012). High-resolution respirometry: OXPHOS protocols for human cells and permeabilized fibers from small biopsies of human muscle. *Methods Mol Biol* **810,** 25–58.

Petrosillo G, Ruggiero FM & Paradies G (2003). Role of reactive oxygen species and cardiolipin in the release of cytochrome c from mitochondria. *FASEB J* **17,** 2202–2208.

Pfanner N & Geissler A (2001). Versatility of the mitochondrial protein import machinery. *Nat Rev Mol Cell Biol* **2,** 339–349.

Picard M, Azuelos I, Jung B, Giordano C, Matecki S, Hussain S, White K, Li T, Liang F, Benedetti A, Gentil BJ, Burelle Y & Petrof BJ (2015). Mechanical ventilation triggers abnormal mitochondrial dynamics and morphology in the diaphragm. *J Appl Physiol* **118,** 1161–1171.

Picard M, Gentil BJ, McManus MJ, White K, Louis KS, Gartside SE, Wallace DC & Turnbull DM (2013*a*). Acute exercise remodels mitochondrial membrane interactions in mouse skeletal muscle. *J Appl Physiol* **115,** 1562–1571.

Picard M, Wallace DC & Burelle Y (2016). The rise of mitochondria in medicine. *Mitochondrion* **30,** 105–116.

Picard M, White K & Turnbull DM (2013*b*). Mitochondrial morphology, topology, and membrane interactions in skeletal muscle: a quantitative three-dimensional electron microscopy study. *J Appl Physiol* **114,** 161–171.

Pidsley R, Zotenko E, Peters TJ, Lawrence MG, Risbridger GP, Molloy P, Van Djik S, Muhlhausler B, Stirzaker C & Clark SJ (2016). Critical evaluation of the Illumina MethylationEPIC BeadChip microarray for whole-genome DNA methylation profiling. *Genome Biol*; DOI: 10.1186/S13059-016-1066-1.

Pilegaard H, Ordway GA, Saltin B & Neufer PD (2000). Transcriptional regulation of gene expression in human skeletal muscle during recovery from exercise. *Am J Physiol Endocrinol Metab*; DOI: 10.1152/AJPENDO.2000.279.4.E806.

Pilegaard H, Saltin B & Neufer DP (2003). Exercise induces transient transcriptional activation of the PGC-1alpha gene in human skeletal muscle. *J Physiol* **546,** 851–858.

Pillon NJ, Gabriel BM, Dollet L, Smith JAB, Sardón Puig L, Botella J, Bishop DJ, Krook A & Zierath

JR (2020). Transcriptomic profiling of skeletal muscle adaptations to exercise and inactivity. *Nat Commun*; DOI: 10.1038/S41467-019-13869-W.

Pilotto AM, Adami A, Mazzolari R, Brocca L, Crea E, Zuccarelli L, Pellegrino MA, Bottinelli R, Grassi B, Rossiter HB & Porcelli S (2022). Near-infrared spectroscopy estimation of combined skeletal muscle oxidative capacity and O 2 diffusion capacity in humans. *J Physiol*; DOI: 10.1113/JP283267.

Pivarnik JM & Senay LC (1986). Effects of exercise detraining and deacclimation to the heat on plasma volume dynamics. *Eur J Appl Physiol Occup Physiol* **55,** 222–228.

Podolsky RJ & Schoenberg M (1983). Force Generation and Shortening in Skeletal Muscle. *Compr Physiol*173–187.

Poole DC (2019). Edward F. Adolph Distinguished Lecture. Contemporary model of muscle microcirculation: gateway to function and dysfunction. *J Appl Physiol* **127,** 1012–1033.

Poole DC, Kano Y, Koga S & Musch TI (2021). August Krogh: Muscle capillary function and oxygen delivery. *Comp Biochem Physiol A Mol Integr Physiol*; DOI: 10.1016/J.CBPA.2020.110852.

Poole DC, Musch TI & Colburn TD (2022). Oxygen flux from capillary to mitochondria: integration of contemporary discoveries. *Eur J Appl Physiol* **122,** 7–28.

Poole DC, Pittman RN, Musch TI & Østergaard L (2020). August Krogh's theory of muscle microvascular control and oxygen delivery: a paradigm shift based on new data. *J Physiol* **598,** 4473–4507.

Poole DC, Richardson RS, Haykowsky MJ, Hirai DM & Musch TI (2018). Exercise limitations in heart failure with reduced and preserved ejection fraction. *J Appl Physiol* **124,** 208–224.

Powers SK, Criswell D, Lawler J, Li Li Ji, Martin D, Herb RA & Dudley G (1994). Influence of exercise and fiber type on antioxidant enzyme activity in rat skeletal muscle. *Am J Physiol*; DOI: 10.1152/AJPREGU.1994.266.2.R375.

Psilander N, Eftestøl E, Cumming KT, Juvkam I, Ekblom MM, Sunding K, Wernbom M, Holmberg HC, Ekblom B, Bruusgaard JC, Raastad T & Gundersen K (2019). Effects of training, detraining, and retraining on strength, hypertrophy, and myonuclear number in human skeletal muscle. *J Appl Physiol* **126,** 1636–1645.

Rambold AS, Kostelecky B, Elia N & Lippincott-Schwartz J (2011). Tubular network formation protects mitochondria from autophagosomal degradation during nutrient starvation. *Proc Natl Acad Sci U S A* **108,** 10190–10195.

Raney MA & Turcotte LP (2008). Evidence for the involvement of CaMKII and AMPK in Ca2+-dependent signaling pathways regulating FA uptake and oxidation in contracting rodent muscle. *J Appl Physiol* **104,** 1366–1373.

Rasmussen BB & Winder WW (1997). Effect of exercise intensity on skeletal muscle malonyl-CoA and acetyl-CoA carboxylase. *J Appl Physiol* **83,** 1104–1109.

Ready AE & Quinney HA (1982). Alterations in anaerobic threshold as the result of endurance training and detraining. *Med Sci Sports Exerc* **14,** 292–296.

Richard R, Lonsdorfer-Wolf E, Charloux A, Doutreleau S, Buchheit M, Oswald-Mammosser M, Lampert E, Mettauer B, Geny B & Lonsdorfer J (2001). Non-invasive cardiac output evaluation during a maximal progressive exercise test, using a new impedance cardiograph device. *Eur J Appl Physiol* **85,** 202–207.

Richardson RS, Grassi B, Gavin TP, Haseler LJ, Tagore K, Roca J & Wagner PD (1999). Evidence of O2 supply-dependent V̇O(2max) in the exercise-trained human quadriceps. *J Appl Physiol* **86,** 1048–1053.

Richardson RS, Knight DR, Poole DC, Kurdak SS, Hogan MC, Grassi B & Wagner PD (1995*a*). Determinants of maximal exercise VO2 during single leg knee-extensor exercise in humans. *Am J Physiol*; DOI: 10.1152/AJPHEART.1995.268.4.H1453.

Richardson RS, Noyszewski EA, Kendrick KF, Leigh JS & Wagner PD (1995*b*). Myoglobin O2 desaturation during exercise. Evidence of limited O2 transport. *J Clin Invest* **96,** 1916–1926.

Robach P, Bonne T, Flück D, Bürgi S, Toigo M, Jacobs RA & Lundby C (2014). Hypoxic training: effect on mitochondrial function and aerobic performance in hypoxia. *Med Sci Sports Exerc* **46,** 1936–1945.

Robinson MM, Dasari S, Konopka AR, Johnson ML, Manjunatha S, Esponda RR, Carter RE, Lanza IR & Nair KS (2017). Enhanced Protein Translation Underlies Improved Metabolic and Physical Adaptations to Different Exercise Training Modes in Young and Old Humans. *Cell Metab* **25,** 581–592.

Roca J, Agusti AGN, Alonso A, Poole DC, Viegas C, Barbera JA, Rodriguez-Roisin R, Ferrer A & Wagner PD (1992). Effects of training on muscle O2 transport at VO2max. *J Appl Physiol* **73,** 1067–1076.

Roca J, Hogan MC, Story D, Bebout DE, Haab P, Gonzalez R, Ueno O & Wagner PD (1989). Evidence for tissue diffusion limitation of VO2max in normal humans. *J Appl Physiol* **67,** 291–299.

Rodgers JT, Lerin C, Haas W, Gygi SP, Spiegelman BM & Puigserver P (2005). Nutrient control of glucose homeostasis through a complex of PGC-1alpha and SIRT1. *Nature* **434,** 113–118.

Romanul FCA (1964). Distribution of Capillaries in Relation to Oxidative Metabolism of Skeletal Muscle Fibres. *Nat 1964 2014916* **201,** 307–308.

Romanul FCA (1965). CAPILLARY SUPPLY AND METABOLISM OF MUSCLE FIBERS. *Arch*

Neurol **12,** 497–509.

Romijn JA, Coyle EF, Sidossis LS, Gastaldelli A, Horowitz JF, Endert E & Wolfe RR (1993). Regulation of endogenous fat and carbohydrate metabolism in relation to exercise intensity and duration. *Am J Physiol*; DOI: 10.1152/AJPENDO.1993.265.3.E380.

Rose AJ & Hargreaves M (2003). Exercise increases Ca2+-calmodulin-dependent protein kinase II activity in human skeletal muscle. *J Physiol* **553,** 303–309.

Rose AJ, Kiens B & Richter EA (2006). Ca2+-calmodulin-dependent protein kinase expression and signalling in skeletal muscle during exercise. *J Physiol* **574,** 889–903.

Rossiter HB (2011). Exercise: Kinetic considerations for gas exchange. *Compr Physiol* **1,** 203–244.

Rothstein EC, Carroll S, Combs CA, Jobsis PD & Balaban RS (2005). Skeletal Muscle NAD(P)H Two-Photon Fluorescence Microscopy In Vivo: Topology and Optical Inner Filters. *Biophys J* **88,** 2165–2176.

Rowlands DS et al. (2014). Multi-Omic integrated networks connect dna methylation and mirna with skeletal muscle plasticity to chronic exercise in type 2 diabetic obesity. *Physiol Genomics* **46,** 747–765.

Rundqvist HC, Montelius A, Osterlund T, Norman B, Esbjornsson M & Jansson E (2019). Acute sprint exercise transcriptome in human skeletal muscle. *PLoS One*; DOI: 10.1371/JOURNAL.PONE.0223024.

Ruple BA, Godwin JS, Mesquita PHC, Osburn SC, Vann CG, Lamb DA, Sexton CL, Candow DG, Forbes SC, Frugé AD, Kavazis AN, Young KC, Seaborne RA, Sharples AP & Roberts MD (2021). Resistance training rejuvenates the mitochondrial methylome in aged human skeletal muscle. *FASEB J*; DOI: 10.1096/FJ.202100873RR.

Ryan MT & Hoogenraad NJ (2007). Mitochondrial-nuclear communications. *Annu Rev Biochem* **76,** 701–722.

Ryan TE, Brizendine JT & McCully KK (2013*a*). A comparison of exercise type and intensity on the noninvasive assessment of skeletal muscle mitochondrial function using near-infrared spectroscopy. *J Appl Physiol* **114,** 230–237.

Ryan TE, Brophy P, Lin C Te, Hickner RC & Neufer PD (2014). Assessment of in vivo skeletal muscle mitochondrial respiratory capacity in humans by near-infrared spectroscopy: a comparison with in situ measurements. *J Physiol* **592,** 3231–3241.

Ryan TE, Erickson ML, Brizendine JT, Young HJ & McCully KK (2012). Noninvasive evaluation of skeletal muscle mitochondrial capacity with near-infrared spectroscopy: correcting for blood volume changes. *J Appl Physiol* **113,** 175–183.

Ryan TE, Southern WM, Reynolds MA & McCully KK (2013*b*). A cross-validation of near-infrared

spectroscopy measurements of skeletal muscle oxidative capacity with phosphorus magnetic resonance spectroscopy. *J Appl Physiol* **115,** 1757–1766.

Sabag A, Little JP & Johnson NA (2022). Low-volume high-intensity interval training for cardiometabolic health. *J Physiol* **600,** 1013–1026.

Sakamoto K & Goodyear LJ (2002). Invited review: intracellular signaling in contracting skeletal muscle. *J Appl Physiol* **93,** 369–383.

Sakuma K, Nishikawa J, Nakao R, Watanabe K, Totsuka T, Nakano H, Sano M & Yasuhara M (2003). Calcineurin is a potent regulator for skeletal muscle regeneration by association with NFATc1 and GATA-2. *Acta Neuropathol* **105,** 271–280.

Sale DG (1987). Influence of exercise and training on motor unit activation. *Exerc Sport Sci Rev* **15,** 95–151.

Saltin B (1985). Hemodynamic adaptations to exercise. *Am J Cardiol*; DOI: 10.1016/0002-9149(85)91054-9.

Saltin B & Astrand PO (1967). Maximal oxygen uptake in athletes. *J Appl Physiol* **23,** 353–358.

Saltin B & Gollnick PD (1983). Skeletal Muscle Adaptability: Significance for Metabolism and Performance. *Compr Physiol*555–631.

Salvadego D, Keramidas ME, Brocca L, Domenis R, Mavelli I, Rittweger J, Eiken O, Mekjavic IB & Grassi B (2016). Separate and combined effects of a 10-d exposure to hypoxia and inactivity on oxidative function in vivo and mitochondrial respiration ex vivo in humans. *J Appl Physiol* **121,** 154–163.

Salvadego D, Keramidas ME, Kölegård R, Brocca L, Lazzer S, Mavelli I, Rittweger J, Eiken O, Mekjavic IB & Grassi B (2018). PlanHab*: hypoxia does not worsen the impairment of skeletal muscle oxidative function induced by bed rest alone. *J Physiol* **596,** 3341–3355.

Scarpulla RC (2002). Transcriptional activators and coactivators in the nuclear control of mitochondrial function in mammalian cells. *Gene* **286,** 81–89.

Scarpulla RC (2006). Nuclear control of respiratory gene expression in mammalian cells. *J Cell Biochem* **97,** 673–683.

Scribbans TD, Edgett BA, Vorobej K, Mitchell AS, Joanisse SD, Matusiak JBL, Parise G, Quadrilatero J & Gurd BJ (2014). Fibre-specific responses to endurance and low volume high intensity interval training: striking similarities in acute and chronic adaptation. *PLoS One*; DOI: 10.1371/JOURNAL.PONE.0098119.

Seaborne RA & Sharples AP (2020). The Interplay Between Exercise Metabolism, Epigenetics, and Skeletal Muscle Remodeling. *Exerc Sport Sci Rev* **48,** 188–200.

Seaborne RA, Strauss J, Cocks M, Shepherd S, O'brien TD, van Someren KA, Bell PG, Murgatroyd

C, Morton JP, Stewart CE, Mein CA & Sharples AP (2018*a*). Methylome of human skeletal muscle after acute & chronic resistance exercise training, detraining & retraining. *Sci Data*; DOI: 10.1038/sdata.2018.213.

Seaborne RA, Strauss J, Cocks M, Shepherd S, O'Brien TD, Van Someren KA, Bell PG, Murgatroyd C, Morton JP, Stewart CE & Sharples AP (2018*b*). Human Skeletal Muscle Possesses an Epigenetic Memory of Hypertrophy. *Sci Rep* **8,** 1–17.

Selbach M, Schwanhäusser B, Thierfelder N, Fang Z, Khanin R & Rajewsky N (2008). Widespread changes in protein synthesis induced by microRNAs. *Nature* **455,** 58–63.

Shao L, Chen Z, Peng D, Soutto M, Zhu S, Bates A, Zhang S & El-Rifai W (2018). Methylation of the HOXA10 Promoter Directs miR-196b-5p-Dependent Cell Proliferation and Invasion of Gastric Cancer Cells. *Mol Cancer Res* **16,** 696–706.

Sharples AP, Hughes DC, Deane CS, Saini A, Selman C & Stewart CE (2015). Longevity and skeletal muscle mass: the role of IGF signalling, the sirtuins, dietary restriction and protein intake. *Aging Cell* **14,** 511–523.

Sharples AP, Polydorou I, Hughes DC, Owens DJ, Hughes TM & Stewart CE (2016*a*). Skeletal muscle cells possess a "memory" of acute early life TNF-α exposure: role of epigenetic adaptation. *Biogerontology* **17,** 603–617.

Sharples AP & Seaborne RA (2019). Exercise and DNA methylation in skeletal muscle. In *Sports, Exercise, and Nutritional Genomics: Current Status and Future Directions*, ed. Barh D & Ahmetov II, pp. 211–229. Academic Press.

Sharples AP, Seaborne RA & Turner DC (2022). Epigenetics of exercise. In *Molecular Exercise Physiology: An Introduction*, 2nd edn., ed. Sharples AP, Morton JP & Wackerhage H. Routledge.

Sharples AP, Stewart CE & Seaborne RA (2016*b*). Does skeletal muscle have an 'epi'-memory? The role of epigenetics in nutritional programming, metabolic disease, aging and exercise. *Aging Cell* **15,** 603–616.

Shutt T, Geoffrion M, Milne R & McBride HM (2012). The intracellular redox state is a core determinant of mitochondrial fusion. *EMBO Rep* **13,** 909–915.

Simoneau JA, Lortie G, Boulay MR, Marcotte M, Thibault MC & Bouchard C (1987). Effects of two high-intensity intermittent training programs interspaced by detraining on human skeletal muscle and performance. *Eur J Appl Physiol Occup Physiol* **56,** 516–521.

Sjøgaard G (1984). Changes in Skeletal Muscles Capillarity and Enzyme Activity with Training and Detraining. **17,** 202–214.

Skulachev VP (2001). Mitochondrial filaments and clusters as intracellular power-transmitting

cables. *Trends Biochem Sci* **26,** 23–29.

Smith BK, Mukai K, Lally JS, Maher AC, Gurd BJ, Heigenhauser GJF, Spriet LL & Holloway GP (2013). AMP-activated protein kinase is required for exercise-induced peroxisome proliferator-activated receptor co-activator 1 translocation to subsarcolemmal mitochondria in skeletal muscle. *J Physiol* **591,** 1551–1561.

Smith MA & Reid MB (2006). Redox modulation of contractile function in respiratory and limb skeletal muscle. *Respir Physiol Neurobiol* **151,** 229–241.

Snijders T, Aussieker T, Holwerda A, Parise G, van Loon LJC & Verdijk LB (2020). The concept of skeletal muscle memory: Evidence from animal and human studies. *Acta Physiol*; DOI: 10.1111/apha.13465.

Soriano FX, Liesa M, Bach D, Chan DC, Palacín M & Zorzano A (2006). Evidence for a mitochondrial regulatory pathway defined by peroxisome proliferator-activated receptor-gamma coactivator-1 alpha, estrogen-related receptor-alpha, and mitofusin 2. *Diabetes* **55,** 1783–1791.

Sousa JS, D'Imprima E & Vonck J (2018). Mitochondrial Respiratory Chain Complexes. *Subcell Biochem* **87,** 167–227.

Spina RJ, Chi MMY, Hopkins MG, Nemeth PM, Lowry OH & Holloszy JO (1996). Mitochondrial enzymes increase in muscle in response to 7-10 days of cycle exercise. *J Appl Physiol* **80,** 2250–2254.

Spinazzi M, Casarin A, Pertegato V, Salviati L & Angelini C (2012). Assessment of mitochondrial respiratory chain enzymatic activities on tissues and cultured cells. *Nat Protoc* **7,** 1235–1246.

Spinelli JB & Haigis MC (2018). The multifaceted contributions of mitochondria to cellular metabolism. *Nat Cell Biol* **20,** 745–754.

Srere PA (1969). Citrate synthase: EC 4.1.3.7. Citrate oxaloacetate-lyase (CoA-acetylating)]. *Methods Enzymol* **13,** 3–11.

Stephens NA, Brouwers B, Eroshkin AM, Yi F, Cornnell HH, Meyer C, Goodpaster BH, Pratley RE, Smith SR & Sparks LM (2018). Exercise Response Variations in Skeletal Muscle PCr Recovery Rate and Insulin Sensitivity Relate to Muscle Epigenomic Profiles in Individuals With Type 2 Diabetes. *Diabetes Care* **41,** 2245–2254.

Sultana RN, Sabag A, Keating SE & Johnson NA (2019). The Effect of Low-Volume High-Intensity Interval Training on Body Composition and Cardiorespiratory Fitness: A Systematic Review and Meta-Analysis. *Sports Med* **49,** 1687–1721.

Tahiliani M, Koh KP, Shen Y, Pastor WA, Bandukwala H, Brudno Y, Agarwal S, Iyer LM, Liu DR, Aravind L & Rao A (2009). Conversion of 5-methylcytosine to 5-hydroxymethylcytosine in mammalian DNA by MLL partner TET1. *Science* **324,** 930–935.

Takahashi M & Hood DA (1996). Protein import into subsarcolemmal and intermyofibrillar skeletal muscle mitochondria. Differential import regulation in distinct subcellular regions. *J Biol Chem* **271,** 27285–27291.

Talanian JL, Galloway SDR, Heigenhauser GJF, Bonen A & Spriet LL (2007). Two weeks of high-intensity aerobic interval training increases the capacity for fat oxidation during exercise in women. *J Appl Physiol* **102,** 1439–1447.

Talanian JL, Holloway GP, Snook LA, Heigenhauser GJF, Bonen A & Spriet LL (2010). Exercise training increases sarcolemmal and mitochondrial fatty acid transport proteins in human skeletal muscle. *Am J Physiol Endocrinol Metab*; DOI: 10.1152/AJPENDO.00073.2010.

Talanian JL, Tunstall RJ, Watt MJ, Duong M, Perry CGR, Steinberg GR, Kemp BE, Heigenhauser GJF & Spriet LL (2006). Adrenergic regulation of HSL serine phosphorylation and activity in human skeletal muscle during the onset of exercise. *Am J Physiol Regul Integr Comp Physiol*; DOI: 10.1152/AJPREGU.00130.2006.

Talmadge RJ, Otis JS, Rittler MR, Garcia ND, Spencer SR, Lees SJ & Naya FJ (2004). Calcineurin activation influences muscle phenotype in a muscle-specific fashion. *BMC Cell Biol*; DOI: 10.1186/1471-2121-5-28.

Tang BL (2016). Sirt1 and the Mitochondria. *Mol Cells* **39,** 87–95.

Tanida I, Ueno T & Kominami E (2004). LC3 conjugation system in mammalian autophagy. *Int J Biochem Cell Biol* **36,** 2503–2518.

Taylor CT (2008). Mitochondria and cellular oxygen sensing in the HIF pathway. *Biochem J* **409,** 19–26.

Taylor JL, Holland DJ, Spathis JG, Beetham KS, Wisløff U, Keating SE & Coombes JS (2019). Guidelines for the delivery and monitoring of high intensity interval training in clinical populations. *Prog Cardiovasc Dis* **62,** 140–146.

Thompson PD, Cullinane EM, Eshleman R, Sady SP & Herbert PN (1984). The effects of caloric restriction or exercise cessation on the serum lipid and lipoprotein concentrations of endurance athletes. *Metabolism* **33,** 943–950.

Toyama EQ, Herzig S, Courchet J, Lewis TL, Losón OC, Hellberg K, Young NP, Chen H, Polleux F, Chan DC & Shaw RJ (2016). Metabolism. AMP-activated protein kinase mediates mitochondrial fission in response to energy stress. *Science* **351,** 275–281.

Trasler J, Deng L, Melnyk S, Pogribny I, Hiou-Tim F, Sibani S, Oakes C, Li E, James SJ & Rozen R (2003). Impact of Dnmt1 deficiency, with and without low folate diets, on tumor numbers and DNA methylation in Min mice. *Carcinogenesis* **24,** 39–45.

Tremblay A, Simoneau JA & Bouchard C (1994). Impact of exercise intensity on body fatness and

skeletal muscle metabolism. *Metabolism* **43,** 814–818.

Triolo M & Hood DA (2019). Mitochondrial breakdown in skeletal muscle and the emerging role of the lysosomes. *Arch Biochem Biophys* **661,** 66–73.

Turner DC et al. (2020). DNA methylation across the genome in aged human skeletal muscle tissue and muscle-derived cells: the role of HOX genes and physical activity. *Sci Rep*; DOI: 10.1038/s41598-020-72730-z.

Turner DC, Seaborne RA & Sharples AP (2019). Comparative Transcriptome and Methylome Analysis in Human Skeletal Muscle Anabolism, Hypertrophy and Epigenetic Memory. *Sci Rep*; DOI: 10.1038/s41598-019-40787-0.

Vainshtein A & Hood DA (2016). The regulation of autophagy during exercise in skeletal muscle. *J Appl Physiol* **120,** 664–673.

Vega RB, Huss JM & Kelly DP (2000). The coactivator PGC-1 cooperates with peroxisome proliferator-activated receptor alpha in transcriptional control of nuclear genes encoding mitochondrial fatty acid oxidation enzymes. *Mol Cell Biol* **20,** 1868–1876.

Vincent AE, White K, Davey T, Philips J, Ogden RT, Lawess C, Warren C, Hall MG, Ng YS, Falkous G, Holden T, Deehan D, Taylor RW, Turnbull DM & Picard M (2019). Quantitative 3D Mapping of the Human Skeletal Muscle Mitochondrial Network. *Cell Rep* **26,** 996-1009.e4.

Vollestad NK & Blom PCS (1985). Effect of varying exercise intensity on glycogen depletion in human muscle fibres. *Acta Physiol Scand* **125,** 395–405.

Vukovich MD, Arciero PJ, Kohrt WM, Racette SB, Hansen PA & Holloszy JO (1996). Changes in insulin action and GLUT-4 with 6 days of inactivity in endurance runners. *J Appl Physiol* **80,** 240–244.

Vyas S, Zaganjor E & Haigis MC (2016). Mitochondria and Cancer. *Cell* **166,** 555–566.

Wagner PD (1992). Gas exchange and peripheral diffusion limitation. *Med Sci Sports Exerc* **24,** 54–58.

Wagner PD (1995). Limitations of oxygen transport to the cell Background and present knowledge. *Intensive Care Med* **21,** 391–398.

Wagner PD (2000). Diffusive resistance to O2 transport in muscle. *Acta Physiol Scand* **168,** 609–614.

Walter G, Vandenborne K, McCully KK & Leigh JS (1997). Noninvasive measurement of phosphocreatine recovery kinetics in single human muscles. *Am J Physiol*; DOI: 10.1152/AJPCELL.1997.272.2.C525.

Wang JS, Jen CJ & Chen HI (1997). Effects of chronic exercise and deconditioning on platelet function in women. *J Appl Physiol* **83,** 2080–2085.

Wei H, Liu L & Chen Q (2015). Selective removal of mitochondria via mitophagy: distinct pathways for different mitochondrial stresses. *Biochim Biophys Acta* **1853,** 2784–2790.

Wen Y, Dungan CM, Mobley CB, Valentino T, von Walden F & Murach KA (2021). Nucleus Type-Specific DNA Methylomics Reveals Epigenetic "Memory" of Prior Adaptation in Skeletal Muscle. *Funct (Oxford, England)*; DOI: 10.1093/FUNCTION/ZQAB038.

Weston M, Taylor KL, Batterham AM & Hopkins WG (2014). Effects of low-volume high-intensity interval training (HIT) on fitness in adults: a meta-analysis of controlled and non-controlled trials. *Sports Med* **44,** 1005–1017.

Whipp B & Rossiter H (2005). The kinetics of oxygen uptake: physiological inferences from the parameters. In *Oxygen Uptake Kinetics in Sport, Exercise and Medicine*, ed. Jones AM & Poole DC, pp. 62–94. Routledge, Oxon, UK.

Whipp BJ, Davis JA, Torres F & Wasserman K (1981). A test to determine parameters of aerobic function during exercise. *J Appl Physiol* **50,** 217–221.

Whipp BJ, Ward SA & Rossiter HB (2005). Pulmonary O2 uptake during exercise: Conflating muscular and cardiovascular responses. *Med Sci Sports Exerc* **37,** 1574–1585.

Wibom R, Hultman E, Johansson M, Matherei K, Constantin-Teodosiu D & Schantz PG (1992). Adaptation of mitochondrial ATP production in human skeletal muscle to endurance training and detraining. *J Appl Physiol* **73,** 2004–2010.

Widrick JJ, Stelzer JE, Shoepe TC & Garner DP (2002). Functional properties of human muscle fibers after short-term resistance exercise training. *Am J Physiol Regul Integr Comp Physiol*; DOI: 10.1152/AJPREGU.00120.2002.

Wiedemann N, Frazier AE & Pfanner N (2004). The Protein Import Machinery of Mitochondria. *J Biol Chem* **279,** 14473–14476.

Wilber RL & Moffatt RJ (1994). Physiological and Biochemical Consequences of Detraining in... : The Journal of Strength & Conditioning Research. *J Strenght Cond Res* **8,** 110–124.

Williams CJ et al. (2019). A multi-center comparison of VO2peak trainability between interval training and moderate intensity continuous training. *Front Physiol*; DOI: 10.3389/FPHYS.2019.00019/PDF.

Willingham TB, Ajayi PT & Glancy B (2021). Subcellular Specialization of Mitochondrial Form and Function in Skeletal Muscle Cells. *Front Cell Dev Biol* **9,** 1–9.

Willingham TB & McCully KK (2017). In vivo assessment of mitochondrial dysfunction in clinical populations using near-infrared spectroscopy. *Front Physiol*; DOI: 10.3389/FPHYS.2017.00689/PDF.

Willingham TB, Zhang Y, Andreoni A, Knutson JR, Lee DY & Glancy B (2019). MitoRACE:

evaluating mitochondrial function in vivo and in single cells with subcellular resolution using multiphoton NADH autofluorescence. *J Physiol* **597,** 5411–5428.

Wojtaszewski JFP, Nielsen P, Hansen BF, Richter EA & Kiens B (2000). Isoform-specific and exercise intensity-dependent activation of 5'-AMP-activated protein kinase in human skeletal muscle. *J Physiol* **528 Pt 1,** 221–226.

Wright DC, Geiger PC, Han DH, Jones TE & Holloszy JO (2007*a*). Calcium induces increases in peroxisome proliferator-activated receptor γ coactivator-1α and mitochondrial biogenesis by a pathway leading to p38 mitogen-activated protein kinase activation. *J Biol Chem* **282,** 18793–18799.

Wright DC, Han DH, Garcia-Roves PM, Geiger PC, Jones TE & Holloszy JO (2007*b*). Exercise-induced mitochondrial biogenesis begins before the increase in muscle PGC-1alpha expression. *J Biol Chem* **282,** 194–199.

Wright DC, Hucker KA, Holloszy JO & Han DH (2004). Ca2+ and AMPK both mediate stimulation of glucose transport by muscle contractions. *Diabetes* **53,** 330–335.

Wu H, Naya FJ, McKinsey TA, Mercer B, Shelton JM, Chin ER, Simard AR, Michel RN, Bassel-Duby R, Olson EN & Williams RS (2000). MEF2 responds to multiple calcium-regulated signals in the control of skeletal muscle fiber type. *EMBO J* **19,** 1963–1973.

Wu Z, Puigserver P, Andersson U, Zhang C, Adelmant G, Mootha V, Troy A, Cinti S, Lowell B, Scarpulla RC & Spiegelman BM (1999). Mechanisms controlling mitochondrial biogenesis and respiration through the thermogenic coactivator PGC-1. *Cell* **98,** 115–124.

Wüst RCI, van der Laarse WJ & Rossiter HB (2013). On-off asymmetries in oxygen consumption kinetics of single Xenopus laevis skeletal muscle fibres suggest higher-order control. *J Physiol* **591,** 731–744.

Wüst RCI, Myers DS, Stones R, Benoist D, Robinson PA, Boyle JP, Peers C, White E & Rossiter HB (2012). Regional skeletal muscle remodeling and mitochondrial dysfunction in right ventricular heart failure. *Am J Physiol Heart Circ Physiol*; DOI: 10.1152/AJPHEART.00653.2011.

Yang Y, Creer A, Jemiolo B & Trappe S (2005). Time course of myogenic and metabolic gene expression in response to acute exercise in human skeletal muscle. *J Appl Physiol* **98,** 1745–1752.

Yu M, Stepto NK, Chibalin A V., Fryer LGD, Carling D, Krook A, Hawley JA & Zierath JR (2003). Metabolic and mitogenic signal transduction in human skeletal muscle after intense cycling exercise. *J Physiol* **546,** 327–335.

Zacharewicz E, Lamon S & Russell AP (2013). MicroRNAs in skeletal muscle and their regulation

with exercise, ageing, and disease. *Front Physiol*; DOI: 10.3389/FPHYS.2013.00266.

Zierath JR & Hawley JA (2004). Skeletal muscle fiber type: influence on contractile and metabolic properties. *PLoS Biol*; DOI: 10.1371/JOURNAL.PBIO.0020348.

Zuccarelli L, Baldassarre G, Magnesa B, Degano C, Comelli M, Gasparini M, Manferdelli G, Marzorati M, Mavelli I, Pilotto A, Porcelli S, Rasica L, Šimunič B, Pišot R, Narici M & Grassi B (2021). Peripheral impairments of oxidative metabolism after a 10-day bed rest are upstream of mitochondrial respiration. *J Physiol* **599,** 4813–4829.

Zuccarelli L, Do Nascimento Salvador PC, Del Torto A, Fiorentino R & Grassi B (2020). Skeletal muscle V̇o 2 kinetics by the NIRS repeated occlusions method during the recovery from cycle ergometer exercise. *J Appl Physiol* **128,** 534–544.